Signalisation calcique et physiologie cellulaire

Pascal Mariot

Université Des Sciences et Technologies de Lille

Année 2003

N° Ordre 408

Présentation des travaux en vue de l'obtention du diplôme
d'Habilitation à Diriger les Recherches

« Signalisation calcique et physiologie cellulaire »

le 17 décembre 2003

par

Pascal MARIOT

Laboratoire de Physiologie Cellulaire
INSERM EMI0228

Devant le jury composé de :

Dr Jean-Marc Israël, directeur de recherche CNRS, Bordeaux, rapporteur

Dr Philippe Lory, directeur de Recherche INSERM, Montpellier, rapporteur

Dr Patrice Mollard, directeur de Recherche CNRS, Montpellier, rapporteur

Dr Hubert Vaudry, directeur de Recherche INSERM, Rouen, examinateur

Professeur N. Pervarskaya, USTL, directeur de recherche

Sommaire

A Myriam et Antoine,

Je remercie vivement les Drs Jean-Marc Israel, Philippe Lory, Patrice Mollard et Hubert Vaudry d'avoir accepté de participer à ce jury.

Je remercie sincèrement le professeur NataliaPrevarskaya qui m'a accueilli en 1997 et m'a permis de m'intégrer à son unité.

Enfin, je remercie tous mes collègues et amis du laboratoire.

Curriculum Vitae

Pascal MARIOT

né le 10 janvier 1966 à Pithiviers (45)

Marié, un enfant

Adresse personnelle :

29 rue Charles Ronsse, sentier du Rosier Blanc, 59493 Villeneuve d'Ascq

Tél : 03-20-34-10-13

Situation actuelle :

Maître de Conférences à l'Université des Sciences et technologies de Lille

Laboratoire de Physiologie Cellulaire, INSERM EMI 0228, Bâtiment SN3, USTL

Tél : 03-20-43-40-77

Pascal.Mariot@univ-lille1.fr

Cursus universitaire :

1989 : Diplôme d'Etudes Approfondies de Neurosciences, Université de Bordeaux II.

1993 : Doctorat d'Université de Neurosciences et Pharmacologie, Université de Bordeaux II.

1993-1996 : Stage post-doctoral. Department of Physiology, University College London.

1996-1997 : Stage post-doctoral. Département de Physiologie et Pharmacologie. Université Catholique de Louvain, Faculté de Médecine de Bruxelles.

1997-1999 : ATER. Université des Sciences et Technologies de Lille. Laboratoire de Physiologie Cellulaire.

1999-Aujourd'hui : Maître de Conférences à l'USTL. Laboratoire de Physiologie Cellulaire.

Publications

1. Dufy B, Mollard P, Taupignon A, Sartor P, Guérineau N, Mariot P, Dufy-Barbe-L (1990) Mechanisms of action of various neuropeptides on anterior pituitary cells. Electrophysiologic and microspectrofluorometric approach. Ann-Endocrinol-Paris.; 51(3-4): 130-2

2. Bresson L, Fahmi M, Sartor P, Mariot P, Dufy-Barbe L (1991) Stimulation of calcium intake by growth-hormone-releasing-hormone in GH3 cells. C-R-Seances-Soc-Biol-Fil.; 185 : 218-23

3. Vacher P, Mariot P, Dufy-Barbe L, Nikolics K, Seeburg P.H, Kerdelhue B, Dufy B (1991) The GnRH-associated peptide reduces calcium entry in prolactin secreting cells. Endocrinology 128 : 285-294

4. Mariot P, Sartor P, Audin J, Dufy B (1991) Intracellular pH in individual pituitary cells : measurement with a dual emission pH indicator. Life Sciences 48 : 245-252

5. Bouali-Benazzouz R, Mariot P, Audy M-C, Sartor P, Bonnin M, Dufy B (1993) GnRH-induced changes of pHi in pituitary gonadotrophs : influence of estradiol. Endocrinology 132 : 855-861

6. Mariot P, Dufy B, Audy M-C, Sartor P(1993) Biphasic changes in intracellular pH (pHi) induced by thyrotropin-releasing hormone in pituitary cells. Endocrinology 132 : 846-854

7. Corcuff J-B, Guérineau NC, Mariot P, Lussier BT, Mollard-P (1993) Multiple cytosolic calcium signals and membrane electrical events evoked in single arginine vasopressin-stimulated corticotrophs. J-Biol-Chem. 268 : 22313-21

8. Mariot P, O'Sullivan AJ, Brown AM, Tatham PER. (1996) RhoGDI Inhibits exocytosis in mast cells. EMBO-Journal. 15 : 6476-6482

9. Sato Y, Mariot P, Detimary P, Gilon P, Henquin J-C (1998) Inhibitors of protein phospatase 1 and 2A inhibit insulin secretion by decreasing the magnitude and the efficacy of the Ca^{2+} signal in pancreatic B cells. Brit.J.Pharmacol. 123 : 97-105

10. Mariot P, Gilon P, Nenquin M, Henquin J-C (1998) Tolbutamide and Diazoxide influence insulin secretion by changing the concentration not the action of cytoplasmic Ca^{2+} in B cells. Diabetes. 47 : 365-373

11. Skryma R, Mariot P, Bourhis XL, Coppenolle FV, Shuba Y, Vanden Abeele F, Legrand G, Humez S, Boilly B, Prevarskaya N. (2000) Store depletion and store-operated Ca^{2+} current in human prostate cancer LNCaP cells: involvement in apoptosis. J Physiol. 527 : 71-83.

12. Mariot P, Prevarskaya N, Roudbaraki MM, Fen Le Bourhis X, Van Coppenolle F, Skryma R (2000) Evidence of functional ryanodine receptor involved in apoptosis of prostate cancer (LNCaP) cells. Prostate. 43: 205-214.

13. Legrand G, Humez S, Slomianny C, Dewailly E, Abeele FV, Mariot P, Wuytack F, Prevarskaya N. (2001) Ca^{2+} pools and cell growth. Evidence for sarcoendoplasmic Ca^{2+}-ATPases 2B involvement in human prostate cancer cell growth control. J. Biol. Chem. 276 : 47608-47614.

14. Mariot P, Vanoverberghe K, Lalevée N, Rossier MF, Prevarskaya N (2002) Overexpression of an α1H (Ca_v3.2) T-type calcium channel during neuroendocrine differentiation of human prostate cancer cells. J. Biol. Chem. 277 : 10824-10833

15. Vanoverberghe K, Mariot P, Vanden Abeele F, Delcourt P, Parys JB, Prevarskaya N.(2003) Mechanisms of ATP-induced calcium signaling and growth arrest in human prostate cancer cells. Cell Calcium. 34 : 75-85.

16. Vanden Abeele F, Shuba Y, Roudbaraki M, Lemonnier L, Vanoverberghe K, Mariot P, Skryma R, Prevarakaya N (2003) Store-operated Ca^{2+} channels in prostate cancer epithelial cells : function, regulation and role in carcinogenesis. Cell Calcium 33 : 357-373

17. Vanoverberghe K,Vanden-Abeele F, Mariot P, Lepage G, Bonnal JL, Mauroy B, Shuba Y, Skryma R, Prevarskaya N (2003) Ca^{2+} homeostasis and apoptotic resistance of neuroendocrine-diffentiated prostate cancer cells. Cell Death and Differentiation (révisions mineures).

18. Vanoverberghe K, Slommiany C, Mariot P, Prevarskaya N (2003) Cytoskeleton reorganization in neuroendocrine cells leads to modulation of calcium homeostasis. soumis à Biochem.J.

Activités d'Enseignement et de Formation

Activités d'enseignement

Mes activités principales d'enseignement ont été effectuées dans le cadre des postes suivants occupés à l'Université de Lille1 :

- **ATER de septembre 1997 à septembre 1999**
- **Maître de Conférences d'octobre 1999 à aujourd'hui**

Depuis septembre 1997, les activités d'enseignement que j'ai exercées se résument de la manière suivante :

Travaux pratiques :

- **DEUG : Module de physiologie cellulaire.** Etude de l'activité électrique nerveuse, de l'activité contractile.
- **Licence de Biologie Cellulaire et Physiologie :** Module de Physiologie des grandes fonctions. Régulation cardiovasculaire, respiration, excrétion.
- **Maîtrise de Sciences Naturelles :** Module de Physiologie des grandes fonctions.
- **Maîtrise de Biologie Cellulaire et Physiologie :** initiation à l'imagerie de fluorescence (TER)
- **DESS :** initiation à l'imagerie de fluorescence cellulaire

Travaux dirigés :

- **DEUG :** Module de physiologie cellulaire. Etude des échanges ioniques membranaires, de l'activité électrique nerveuse.
- **Maîtrise de Sciences Naturelles :** Module de Physiologie des grandes fonctions.

Cours et séminaires :

- **DEUG :** Module de physiologie cellulaire. Les transports membranaires
- **Maîtrise de Biologie Cellulaire et Physiologie** : Canalopathie de la cellule B du pancréas
- **DEA et DESS :** Mesure de l'exocytose dans les cellules sécrétrices.
- **Prepa Agreg et Prepa CAPES :** participation aux cours et leçons

Activités de formation à la recherche

Encadrement d'étudiants

1998-1999

Co-encadrement d'une étudiante en DEA Biologie-Santé (Karine Vanoverberghe).

Titre du mémoire de DEA: "**Régulation du calcium intracellulaire dans les cellules cancéreuses prostatiques humaines et son implication dans l'apoptose**"

1999-2003

Co-encadrement avec le Professeur N. Prevarskaya d'une étudiante en doctorat Biologie-Santé (Karine Vanoverberghe).

Titre de la thèse de Doctorat soutenue le 9 juillet 2003 : "**Etude de l'altération de l'homéostasie calcique dans l'arrêt de croissance et la différenciation neuroendocrine des cellules cancéreuses prostatiques humaines**"

2003-aujourd'hui : Co-encadrement d'un étudiant en DEA Biologie-Santé (Florian Gakiere)

Titre du mémoire de DEA: "**Régulation et implication du canal calcique de type T dans la physiopathologie des cellules prostatiques**"

1999-aujourd'hui :

Encadrement d'étudiants en BTS Biotechnologie (Sylvain Larouche et Fabienne Allenne, Lycée Valentine Labbé)

Juin-septembre 2002 : Encadrement d'un étudiant en DEUG pour un stage de patch-clamp (Alexis Bavancoff)

Encadrement de chercheurs dans le cadre de stages de formations permanentes

Octobre 1989. Encadrement du stage de formation permanente du CNRS/INSERM,

" *techniques électrophysiologiques et spectrofluorimétriques d'étude des cellules endocrines excitables* "

Mars 1992. Encadrement du stage de formation permanente organisé par Biotechnica,

" *Utilisation des sondes fluorescentes intracellulaires : photométrie - imagerie* "

Activités de Recherche

Préambule

Mon parcours scientifique, commencé en 1988 à Bordeaux dans l'unité de Neurophysiologie CNRS URA1200 dirigée à l'époque par le Dr Bernard Dufy, se caractérise par des fils conducteurs que l'on peut suivre tout au long de ces années. Ces fils d'Ariane sont : calcium, sécrétion et cellule neuroendocrine. Quand on regarde de plus près, on s'aperçoit que ces fils sont interrompus à chaque fin de cycle, et de cycles il y en eut quatre jusqu'à présent. Si lors des études doctorales effectuées à Bordeaux, les trois mot-clés étaient réunis, deux se sont perdus en chemin (calcium et cellule neuroendocrine) lors de mon premier stage post-doctoral à University College London. Je m'intéressais alors à l'exocytose non calcium-dépendante de cellules non-neuroendocrines possédant toutefois une voie de sécrétion régulée : les mastocytes. Le second stage post-doctoral effectué à l'Université Catholique de Louvain fut caractérisé par un retour aux origines ; le calcium dans le couplage stimulation-sécrétion dans les cellules β du pancréas. Enfin, mon arrivée à Lille fut marquée par la disparition des cellules neuroendocrines reconverties pour des raisons thématiques en cellules épithéliales prostatiques exocrines. Finalement, par un coup du sort « différenciateur », ces cellules prostatiques banalement épithéliales se sont mises à exprimer lors de leur cancérisation des marqueurs neuroendocrines beaucoup plus nobles que de simples cytokératines ! Le calcium, lui, est resté fidèle à son poste, ou à ses postes, puisqu'il a eu la prétention avec l'évolution de vouloir tout contrôler dans la cellule, de leur vie et leur mort, et qu'ainsi je l'ai retrouvé au coin de la paillasse donnant le feu vert à l'apoptose, à la prolifération ou à la différenciation cellulaire.

Comme ces fils conducteurs ne sont pas constants dans toutes les études intégrées dans ce manuscrit, bien qu'ils soient toujours présents en filigrane, j'ai préféré présenter ces travaux de manière linéaire, c'est à dire illustrer un parcours plutôt qu'une thématique. Pour cette raison, j'ai délibérément écarté l'idée d'écrire une introduction détaillée et d'une conclusion générale, qui n'auraient pas de sens au vu des différences de thématiques le long de mon parcours. En guise d'introduction, je ferai une description rapide des mécanismes d'homéostasie calcique et du rôle du calcium dans certains aspects de la physiologie cellulaire. De plus, j'ai essayé quand cela était possible, de remettre des données anciennes dans le contexte d'aujourd'hui et de discuter certains de mes résultats d'alors au vu de la littérature actuelle et notamment des découvertes des processus moléculaires impliqués.

Introduction

Afin de situer de manière générale mon parcours dans une thématique, je rappellerai brièvement dans ce chapitre les mécanismes de régulation de la concentration calcique dans les cellules eucaryotes, et je présenterai le rôle du calcium dans le couplage stimulation-sécrétion et dans la régulation de la croissance cellulaire.

I. Les mécanismes de transport de calcium dans la cellule eucaryote

La cellule eucaryote utilise le calcium comme second messager central dans la quasi-totalité de ses fonctions (Berridge et al 1998). Le rôle du calcium dans la physiologie est connu depuis environ 120 ans grâce aux expériences initiatrices de S.Ringer qui ont permis de montrer que la contraction cardiaque nécessitait du calcium (Ringer 1883). Le calcium a été montré par la suite indispensable au couplage excitation-contraction, non seulement du muscle cardiaque mais également du muscle lisse (Stiles 1903). Il faut préciser que, lors d'expériences fondatrices, Ringer remarqua que le muscle squelettique, au contraire du muscle cardiaque, était capable de se contracter pendant plusieurs heures en absence de calcium extracellulaire (Ringer and Buxton 1887). En dépit de cette relative et apparente indépendance vis-à-vis du calcium, des études ultérieures ont montré que l'injection de calcium dans des fibres squelettiques entraînait de manière réversible la contraction de la fibre musculaire (Keil and Sichel, 1936).

On sait aujourd'hui que les cellules eucaryotes, d'une manière générale, peuvent puiser dans deux sources différentes de calcium en fonction de leurs besoins : 1) le milieu extracellulaire fortement concentré en calcium (ordre du mM) et d'un volume quasiment infini en regard du volume cellulaire, et 2) les organites intracellulaires plus limités mais également capables d'accumuler de grandes quantités de calcium (calcium total de l'ordre du mM, calcium libre de l'ordre de 100 µM). La concentration en calcium libre (qui est le paramètre important car c'est le calcium libre qui est immédiatement disponible et utilisable par les protéines calcium-dépendantes) dépend de la concentration en calcium total, des tampons calciques cellulaires et des mécanismes de transport de part et d'autre des différents compartiments. Grâce à ces différents mécanismes, la concentration en calcium libre cytosolique est maintenue dans une limite très étroite au repos (environ 100 nM), qui est susceptible d'augmenter fortement lors d'une stimulation (plusieurs centaines de nM dans l'ensemble du cytosol, voire plusieurs dizaines de micromolaires très localement).

En ce qui concerne les mécanismes de transports, on peut les sub-diviser en deux grandes catégories, les mécanismes ON participant à une augmentation de calcium cytosolique et les

mécanismes OFF ramenant le calcium libre cytosolique à des concentrations de repos (Berridge et al 2000).

I.I. Les mécanismes participant à l'augmentation du calcium cytosolique

Comme indiqué préalablement, la cellule peut puiser dans deux grandes sources de calcium, le milieu ambiant et le milieu contenu dans les organites intracellulaires. Ceci est possible grâce à des transports membranaires de la membrane plasmique et de la membrane des organites.

A) Canaux calciques de la membrane plasmique

Les canaux calciques de la membrane plasmique sont subdivisés en plusieurs sous-familles notamment en fonction du stimulus qui déclenche leur ouverture, de leurs propriétés cinétiques, et de leurs spécificités ioniques et pharmacologiques. On distingue ainsi des canaux VOC ou VDCC (pour Voltage-Operated Calcium Channel ou Voltage-Dependent Calcium Channel), des canaux ROC (pour Receptor-Operated Channel), des canaux SMOC (pour Second Messenger-Operated Channel) et des canaux SOC (pour Store-Operated Channel). Ces familles sont distinguées à partir de données électrophysiologiques sur des principes biophysiques et pharmacologiques. Depuis une quinzaine d'années, les progrès de la biologie moléculaire ont permis de cloner, d'exprimer et de caractériser de nombreuses familles de canaux calciques. Ceci a abouti à d'autres classifications de canaux calciques, qui, si elles sont concordantes dans certains cas avec les classifications bio-physico-pharmacologiques, peuvent être dans d'autres cas plus difficiles à accorder avec les données de l'électrophysiologie. Ceci est certainement dû à la méconnaissance actuelle des structures quaternaires que prennent les sous-unités formant le pore des canaux (homo ou hétéro-tétramérisation par exemple) et des sous-unités régulatrices potentielles des sous-unités pores.

1) Les canaux calciques voltage-dépendants (VDCC)

Les canaux calciques voltage-dépendants ont été identifiés pour la première fois par Fatt et Katz en 1953 sur le muscle squelettique de crustacé.

Les canaux VDCC furent initialement distingués en canaux à haut seuil et canaux à bas seuil, c'est à dire s'activant pour de fortes dépolarisations (haut seuil) ou de faibles dépolarisations (bas seuil). Il est vite apparu que le courant dû à l'activité de ces mêmes canaux était maintenu pour les

canaux à haut seuil, le courant ne s'inactivant que lentement dans le temps, alors que les canaux à bas seuil présentaient une inactivation rapide dans le temps et une faible conductance. Cette classification haut seuil/bas seuil se superposa donc à une distinction entre canaux (ou courants) L (pour Long-Lasting) et T (pour Transient ou Tiny en référence à la conductance). Telle était la situation vers le milieu des années 80 (Carbone et Lux 1984, Armstrong et Matteson 1985). A partir de cette date commença d'une part un travail de caractérisation électrophysiologique approfondi de ces canaux qui permit, sur la base de propriétés pharmacologiques, d'identifier un canal à haut seuil (comme les canaux L) mais qui s'inactive à des potentiels très négatifs (comme les canaux T) (Nowicky et al, 1985), canal qui fut classé de type N (pour Neuronal ou Neither, ni T ni L). La famille des canaux VDCC s'allongea encore par la suite pour aboutir à la classification actuelle comprenant 6 membres, L, N, P (pour cellules de Purkinje où il a été découvert initialement, Llinas et al 1989), Q (produit d'épissage du même gène que P et donc appelé Q, la lettre après P, Zhang et al 1993), R (pour Resistant (aux bloquants) Randall et Tsien 1995) et T le seul canal LVA (pour revue voir Randall et Benham 1999), (voir table 1).

A partir de la fin des années 80, un travail de clonage important aboutit au séquençage des sous-unités formant le canal calcique du muscle squelettique, le canal calcique de type L sensible aux dihydropyridines. La première sous-unité identifiée fut la sous-unité formant le pore, la sous-unité alpha1 de 165 kD (Tanabe et al 1987) puis des sous-unités accessoires (ou régulatrices), de type beta (55 kD), alpha2 (130 kD) liée à la sous-unité delta (28 kD), et gamma (32 kD), furent clonées (Ruth et al 1989, Ellis et al 1988, Jay et al 1990). Ces travaux ont abouti à une représentation schématique idéalisée du canal calcique voltage-dépendant telle qu'elle est illustrée dans la figure 1.

La sous-unité $\alpha 1$ formant le pore est constituée de 4 domaines (de I à IV) constitués chacun de 6 segments transmembranaires (de S1 à S6) et une boucle P délimitant la bouche interne du canal entre les segments S5 et S6 de chaque domaine. Les propriétés principales de canal perméant au calcium, de sensibilité au voltage, d'activation et d'inactivation, de cinétique et de dépendance pharmacologique notamment aux dihydropyridines, aux benzodiazépines et aux phenylalkylamines, sont dépendantes en grande partie (mais pas exclusivement) de la sous-unité alpha1 (voir Shorofsky et Balke 2001 pour revue).

	Canaux L	Canaux N	Canaux P	Canaux Q	Canaux R	Canaux T
Propriété Biophysiques						
Activation	**HVA**	**HVA**	**HVA**	**HVA**	**HVA**	**LVA**
Inactivation (τ à −100 mV)	**Lente**	**Interm. (100 ms)**	**Lente**	**Intermédiaire**	**Rapide (30 msec)**	**Rapide (20 msec)**
Inactivation $V_{0.5}$	**-25 mV**	**-60 mV**	**-25 mV**	**-60 mV**	**-75 mV**	**-60 à -80 mV**
Inactivation Ca^{2+}-dpte	**oui**	**oui**	**Non**	**ND**	**ND**	**Non**
Déactivation (τ à -80 mV)	**rapide (< 200 µs)**	**rapide (< 200 µs)**	**rapide (< 200 µs)**	**rapide (< 200 µs)**	**rapide (< 200 µs)**	**lente (~ 2 msec)**
Perméabilité						
PBa^{2+}/PCa^{2+}	**~2**	**~2**	**~2**	**ND**	**~1.3**	**~1**
sensibilité au Cd^{2+} (IC_{50})	**forte (1 µM)**	**forte (1 µM)**	**forte (1 µM)**	**forte**	**forte (1 µM)**	**faible (> 50 µM)**
blocage par Ni^{2+} (IC_{50})	**faible (~ 230 µM)**	**faible (~ 270 µM)**	**Interm. (90 µM)**	**ND**	**forte (~ 50 µM)**	**Var. (1-100 µM)**
Pharmacologie						
agonistes DHP	**Potentialisation**	**0**	**0**	**0**	**0**	**0**
antagonistes DHP	**Inhibition**	**0**	**0**	**0**	**0**	**0**
w-CTx-GVIA	**0**	**Inhibition**	**0**	**0**	**0**	**0**
w-Aga-IVA (IC_{50})	**0**	**0**	**Inhibition (1 nM)**	**Inhibit. (100 nM)**	**0**	**0**
w-Aga-IIIA (IC_{50})	**Inhibition (1 nM)**	**Inhibition (1 nM)**	**partielle (0.5 nM)**	**Inhibition**	**partielle (3 nM)**	**0**
sensibilité au mibefradil (IC_{50})	**faible**	**faible**	**faible**	**faible**	**faible**	**forte (0.5-5 µM)**

Table 1 : propriétés biophysiques et pharmacologiques des canaux calciques voltage-dépendants
D'après Randall 1998

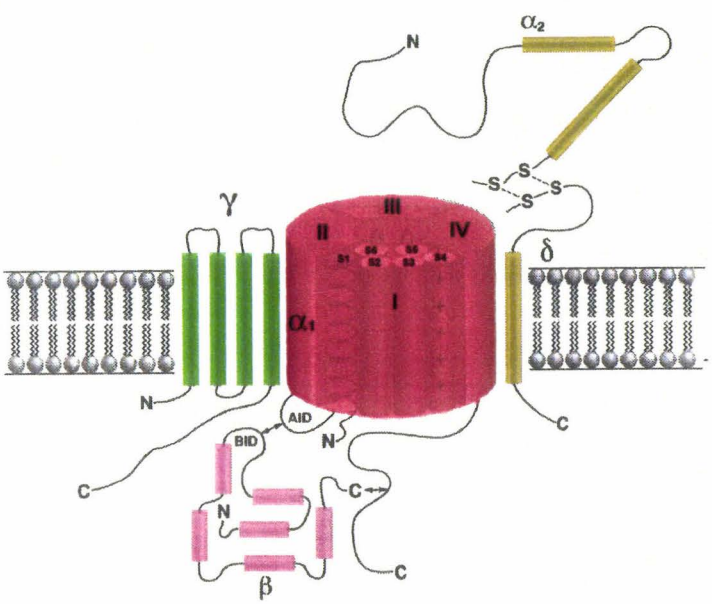

Figure 1 : Structure quaternaire des canaux calciques voltage-dépendants. Les canaux VDCC possèdent une sous-unité pore (α1) susceptible d'être régulée par trois sous-unités accessoires (β, γ,α2–δ).
D'après Randall et Benham (1999)

A l'heure actuelle, 10 sous-unités α1 (C, D, S, F, A, B, E, G, H, I) (Starr et al 1991, Joutel et al 1993, Soong et al 1993, Williams et al 1992, Strom et al 1998, Hogan et al 1994, Mori et al 1991, Schultz et al 1993, Cribbs et al 1998, Lee et al 1999, Klockner et al 1999) 4 sous-unités β (1–4) (voir Arikkath et Campbell 2003), 8 sous-unités γ (1-8) (Powers et al 1993, Letts et al 1998, Chu et al 2001, Burgess et al 2001, et 4 sous-unités α2δ (1-4) (Klugbauer et al 1999, Gao et al 2000, Qin et al 2002) ont été clonées, sans compter les isoformes résultant de produits d'épissage (voir Arikkath et Campbell 2003). L'expression des sous-unités α1 dans des ovocytes ou des cellules de mammifères a permis de rapprocher la classification biophysique avec la classification moléculaire. Les sous-unités α1 C, D, S, et F, lorsqu'elles sont étudiées dans des systèmes d'expression, possèdent les propriétés électrophysiologiques des canaux de type L, les sous-unités α1 B, A et E possèderaient les propriétés des canaux N, P/Q (les canaux P et Q étant des produits d'épissage du même gène α1A) et R, respectivement. Enfin, les sous-unités α1 G, H et I formeraient le canal T fonctionnel.

Evidemment, s'il existe actuellement une certaine unanimité pour accorder les classifications moléculaires avec les classifications biophysiques, concernant la sous-unité α1, les propriétés du canal calcique sont modulées par la présence de sous-unités régulatrices (voir Arikkath et Campbell 2003). Cependant, si on commence à entrevoir comment les sous-unités régulatrices modulent l'activité du canal dans des systèmes d'expression ou grâce aux souris mutantes, la composition des canaux natifs de différents types (L, N, P/Q, R et T) dans les différents tissus est en revanche mal connue. Le modèle le mieux connu est certainement le canal calcique sensible aux dihydropyridines (canal DHP-R pour récepteur aux dihydropyridines) constitué des sous-unités α1S, β1, γ1 et α2δ1. La sous-unité β est la seule sous-unité totalement cytosolique du canal et s'associe grâce à un segment peptidique appelé BID (beta interaction domain) avec la sous-unité α1 au niveau d'un segment AID (pour alpha interaction domain) (Pragnell et al 1994). Les différentes sous-unités régulatrices interviennent pour leur part dans le trafic membranaire et l'adressage correct de α1 (pour α2δ1, β1-4), augmentent l'amplitude du courant calcique (α2δ1-4, β1-4), modulent les propriétés cinétiques d'activation et/ou d'inactivation (α2δ1, β1-4, γ1-3), ou jouent un rôle inhibiteur entraînant une réduction du courant (γ 1, 2, 6, 7) (Arikkath et Campbell 2003). Actuellement, bien que la sous-unité α1 soit capable à elle seule d'exprimer une activité de canal calcique, il est généralement considéré que celle-ci s'associe avec des sous-unités régulatrices pour former un canal fonctionnel, au moins pour les canaux L, N, P/Q et R. En revanche, en ce qui concerne les canaux T, il est généralement admis que le canal T natif est constitué uniquement de la sous-unité α1 (Randall et Benham 1999) bien que certains travaux montrent que les sous-unités α2δ

et β1b augmentent le courant calcique porté par la sous-unité α1G, sans doute en facilitant l'incorporation de l'expression de la sous-unité pore dans la membrane (Dolphin et al 1999).

Certains de ces canaux peuvent s'associer à d'autres protéines (Walker et De Ward 1998), notamment des protéines membranaires (protéines Gβγ, syntaxine, canal RyR, triadine) et ainsi créer des micro ou nano-domaines calciques au sein desquels le calcium peut augmenter de manière très importante et très localisée et permettre ainsi d'activer des mécanismes dans des compartiments très précis de la cellule.

Les canaux calciques voltage-dépendants jouent des rôles fondamentaux dans de multiples aspects de la physiologie cellulaire, dans le couplage excitation-contraction (canal calcique de type L), le couplage excitation-sécrétion et la neurotransmission (canal L, N, P/Q), le contrôle de l'activité pacemaker (canal T) ou le cycle cellulaire. Nous préciserons certains de ces aspects plus loin dans le manuscrit.

2) Les canaux calciques non voltage-dépendants

Cette famille très large de canaux regroupe des canaux activés par d'autres stimuli que les variations de potentiels membranaires avec d'une part les canaux chimio-dépendants qui comprennent les ROC (activés par un ligand) et les SMOC (activés par un second messager) et d'autre part les canaux SOC (activés par la déplétion des stocks intracellulaires). Ces canaux, d'une manière générale, ont une plus faible sélectivité pour le calcium par rapport aux autres cations (K^+, Na^+) que les canaux VOC, et sont donc classés par commodité dans une seule catégorie.

2.1. Les canaux chimio-dépendants

Les canaux ROC comprennent notamment les récepteurs à l'acétylcholine (nicotinique), à la sérotonine ($5HT_3$), au GABA ($GABA_A$), à la glycine (GlyR), au glutamate (NMDA, AMPA, kainate) et les récepteurs purinergiques P2x (voir Hille 2001). Tous ces ROC ne sont pas spécifiques aux cations puisque les canaux $GABA_A$, et GlyR sont des canaux anioniques. La topologie (nombre de sous-unités impliquées et nombre de segments transmembranaires) de ces récepteurs n'est pas toujours connue dans le détail et diffère selon le ligand. Les récepteurs nicotinique, $5HT_3$, $GABA_A$ et GlyR sont supposés former des pentamères à partir de sous-unités possédant chacunes 4 segments transmembranaires. Le récepteur à l'ATP (P2X) semble posséder 2

segments transmembranaires et une région P. Les récepteurs AMPA et NMDA possèdent 4 sous-unités. Les ROC forment donc un groupe hétérogène de canaux qui peuvent laisser passer le calcium dans certaines circonstances (notamment les récepteurs-canaux au glutamate et à l'ATP) et qui jouent notamment un rôle important dans les phénomènes de transmissions synaptiques rapides en contribuant par exemple, en ce qui concerne les récepteurs au glutamate, aux mécanismes de plasticité synaptique impliqués dans l'apprentissage et la mémoire (Madden 2002).

Les SMOC sont exprimés aussi bien dans les cellules excitables que dans les cellules non-excitables et sont activés par différents second messagers (inositol 1,4,5 trisphosphate (IP3), inositol 1,3,4,5 tétrakisphosphate (IP4), GMP cyclique, et calcium) et vont être recrutés lors de l'action d'un agoniste sur un récepteur couplé à une protéine G (voir Clementi et Meldolesi 1996).

2.2. Les canaux SOC

Le SOC ou entrée capacitative de calcium, dont l'existence fut proposée par Putney en 1986, est un mécanisme d'influx calcique observé dans la quasi-totalité des cellules non-excitables et dans une moindre mesure dans certaines cellules excitables qui permet à la cellule de faire entrer du calcium de l'extérieur suite à la vidange de calcium des réserves intracellulaires (voir Putney et al 2001). La déplétion des stocks calciques intracellulaires peut-être induite de différentes manières, activation des récepteurs à l'inositol 1,4,5 trisphophate (IP3R) (Putney 1986), des récepteurs à la ryanodine (RyR) (Bennett et al 1998) ou grâce par exemple à un blocage pharmacologique des Ca^{2+}ATPases du réticulum endoplasmique (RE) (thapsigargine ou acide cyclopiazonique) ou encore en utilisant une perfusion intracellulaire de chélateurs calciques (BAPTA). Un courant membranaire activé par la déplétion du calcium du RE a été mesuré pour la première fois par Hoth et Penner (1992) dans des mastocytes en réponse à la dialyse cellulaire avec de l'IP3, de l'EGTA ou du BAPTA (des chélateurs calciques). Ce courant fut nommé CRAC pour calcium-release-activated calcium channel (Hoth et Penner 1992).

La nature moléculaire des SOC est actuellement une question très débattue et la situation est beaucoup moins claire qu'elle ne l'est pour les canaux VOC par exemple. Il semblerait fortement que les SOC soient constitués de canaux TRP (pour Transient Receptor Potential) qui forment une superfamille de canaux identifiés grâce au clonage moléculaire. Il n'est pas question ici de donner une classification précise ainsi que les propriétés de chacun des TRP. Je rappellerai brièvement que le premier gène codant pour un TRP fut initialement caractérisé chez la drosophile comme un gène impliqué dans la transduction du message visuel (Hardie et Mincke 1992). Les drosophiles mutantes

pour TRP montraient une altération de l'entrée calcique induite par la lumière et d'autre part la structure prédite des protéines TRP était proche des canaux calciques connus alors (pour revue voir Montell et al 2002). La superfamille des TRP comprend plus de 20 canaux répartis en trois sous-familles : les TRPV (pour vanilloid), TRPC (pour canonical) et TRPM (pour melastatin), TRPN (qui comprennent des domaines ankyrine en N-terminal) et TRPP (pour PDK : polycystin kidney disease) (Montell 2003, Birnbaumer et al 2003). Ces canaux sont caractérisés par des sélectivités ioniques et des mécanismes d'activation différents. Un des enjeux des études portant sur les TRP est d'accorder une classification biophysique ou pharmacologique (SOC) avec une classification moléculaire (TRP) et notamment de déterminer quel TRP, si c'est un TRP, est responsable du SOC.

L'autre enjeu important dans l'étude des SOC réside dans leur mécanisme d'activation qui est encore controversé et plusieurs hypothèses semblent plausibles (figure 2):

1) l'hypothèse de l'intervention d'un facteur diffusible de couplage entre les réserves calciques et les canaux membranaires a été émise par Putney (1990). Ce CIF (pour Calcium influx factor) a été ensuite mis en évidence expérimentalement par Randriamampita et Tsien (1993) en utilisant des extraits cellulaires de cellules Jurkat préalablement stimulées. Des extraits de levures *pmr1* génétiquement déficientes en SERCA et par conséquent déplétées en calcium au niveau de leur organelles intracellulaires, ont permis de montrer la présence d'un CIF dans ces extraits qui provoquaient une entrée capacitative dans des Ovocytes de Xénope, des cellules Jurkat ou des cellules vasculaires musculaires (Csutora et al 1999, Trepakova et al 2003). Différentes tentatives de caractérisation du CIF furent menées et à l'heure actuelle, plusieurs molécules de couplage ont été proposées : l'acide 5,6-epoxyeicosatrienoique un métabolite de l'acide arachidonique produit *via* la voie de la cytochrome P450 monooxygénase (Rzigalinksi et al 1999), la sphingosine1-phosphate (Itagaki et Hauser 2003), voire un produit du métabolisme de l'IP3, l'IP4 (Luckoff et Clapham 1992).

2) l'hypothèse d'une insertion vésiculaire par exocytose de nouveaux canaux SOC a été également proposée. Les arguments les plus convaincants pour un tel mécanisme sont l'inhibition du SOC par la toxine botulique A (qui inhibe l'exocytose) ou par l'expression de mutants inactifs d'une protéine SNARE impliquée dans l'exocytose, SNAP-25 (Yao et al 1999) et par la stabilisation du cytosquelette grâce à des agents polymérisants de l'actine-F tels que la jasplakinolide (Patterson et al 1999) ou l'expression de protéines G monomériques RhoA, connue pour promouvoir la polymérisation du cytosquelette (Yao et al 1999).

Cependant, d'autres études ont montré que l'inhibition des protéines SNARE ou de la fusion vésiculaire n'entraînait pas de modifications de l'activité SOC (Scott et al 2003). Dans le cadre de ce modèle reste le problème de la transduction du signal entre la vidange des réserves intracellulaires et l'exocytose. Selon Yao et al (1999), un messager diffusible n'est pas impliqué dans le couplage entre vidange calcique et exocytose.

3) l'hypothèse d'un couplage conformationnel entre des protéines de la membrane du RE et la membrane plasmique est sans doute la plus en vogue à l'heure actuelle. Un des premiers à proposer une interaction protéine-protéine entre le RE et la membrane plasmique fut Irvine (1990). Depuis, il a été montré qu'un mécanisme possible consistait en l'interaction de récepteurs IP3 et de canaux de la membrane plasmique de la famille de TRP. Les candidats TRP les plus sérieux du SOC sont actuellement les TRPC et notamment TRPC1 et TRPC3 (voir Putney et al 2001 pour revue). TRPC1 semble être un bon candidat du SOC mais il est probable qu'il nécessite une hétéromultimérisation avec d'autres canaux TRP ou polycystine2 (également un membre de la superfamille des TRP) pour former un SOC fonctionnel (Beech et al 2003). D'autre part, TRPC3 peut être activé de manière IP3 et IP3-R dépendante (Kiselyov et al 1998, 1999). De plus, il a été montré que les récepteurs de type RyR pouvaient activer, *via* un couplage conformationnel, les canaux TRP3 (Kiselyov et al 2000).

4) Enfin, l'hypothèse d'une régulation négative des SOC par le calcium a été émise. Dans cette hypothèse, une diminution de calcium dans les réserves intracellulaires provoquerait une diminution locale de la concentration en calcium sous la membrane plasmique, ce qui permettrait l'activation des canaux SOC (Barritt 1998).

Ces différentes hypothèses ne sont pas exclusives et il est probable d'une part que les mécanismes d'activation du SOC soient différents d'un type cellulaire à un autre et d'autre part intègrent en fait plusieurs de ces possibles voies de transduction. Par exemple, il a été proposé par Xie et al (2002) un modèle de fonctionnement intégrant à la fois l'hypothèse d'un CIF et l'hypothèse de sécrétion. Dans cette hypothèse, l'acide arachidonique produit par la phospholipase A2 suite à la déplétion des réserves calciques serait métabolisé par la cytochrome P450 et transformé en CIF (l'acide 5,6-epoxyeicosatrienoique). La déplétion des réserves calcique provoquerait de plus un déplacement du RE, et donc un rapprochement de la cytochrome P450 (protéine membranaire du RE), vers la membrane plasmique. Les CIF, dont la demi-vie est très

éphémère, produits par la cytochrome P450 seraient ainsi libérés à proximité de leur cible, *i.e.*, les SOC (Xie et al 2002).

B) Canaux calciques intracellulaires

De tous les compartiments intracellulaires, le réticulum endoplasmique (ou sarcoplasmique) est le plus dynamique. Le calcium peut être libéré de sa lumière vers le cytosol grâce à deux familles importantes de récepteurs-canaux : les récepteurs à l'inositol 1, 4, 5 trisphosphate ou IP3-R et les récepteurs à la ryanodine ou RyR. Ces deux familles de canaux possèdent une structure similaire, constituée de 4 sous-unités, un domaine C-terminal où se situent les segments transmembranaires et une boucle cytosolique N-terminale de très grande taille qui forme un vestibule notamment pour la fixation des drogues et les effets régulateurs du calcium (figure 3).

1) Les récepteurs à l'1, 4, 5 IP3

Les récepteurs à l'IP3 sont activés physiologiquement par l'IP3 formé au niveau de la membrane plasmique par les phospholipases C. Ces récepteurs à l'IP3 purifiés forment des canaux calciques fonctionnels lorsqu'ils sont incorporés dans des bicouches et leur activité est effectivement stimulée par l'IP3 (Ferris et al 1989).

Les IP3-R ont été purifiés à partir de différentes sources de tissus tels que muscle lisse, foie, plante...(Suppattapone et al, 1988, Chadwick et al 1990, Maryleitner et al 1995, Dasgupta et al 1997) et clonés initialement à partir du cervelet (Furuichi et al 1989). Ces récepteurs sont trouvés majoritairement dans le réticulum endoplasmique (Bush et al 1994, Pozzan et al 1994) mais également dans d'autres membranes cellulaires tels que les membranes plasmiques (Kuno and Gardner 1987), Golgiennes (Pinton et al 1998), nucléaires (Nicotera et al 1990) ou des vésicules de sécrétion (Yoo 2000).

Au moins trois gènes distincts codant pour des IP3-R ont été clonés (pour revue voir Patel et al 1999). Ces gènes codant pour ces récepteurs partagent une homologie de séquence considérable comprise entre 60 et 70%. Chacun de ces gènes code pour une protéine de 300 kDa environ, protéines qui s'associent entre elles pour former un tétramère. Chacune des sous-unités contient 3 domaines fonctionnellement distincts : un domaine de liaison pour l'IP3 en région N-Terminale, un domaine formant le pore en région C-Terminale et un large domaine de régulation séparant les deux autres.

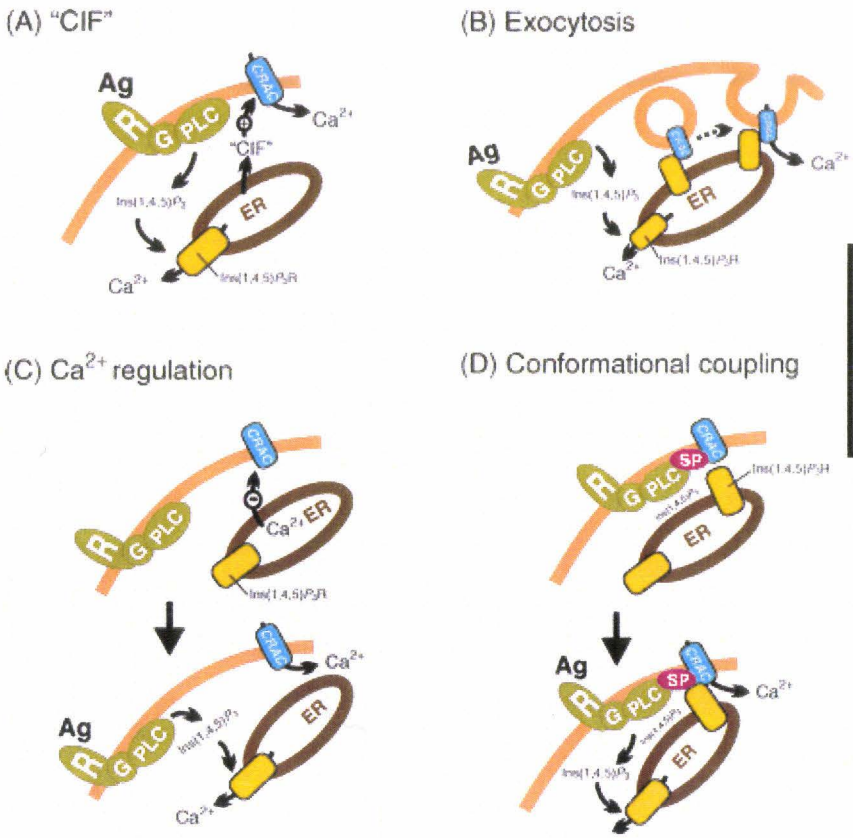

Figure 2 : Mécanismes d'activation possible du SOC.
D'après Putney et al 2001.

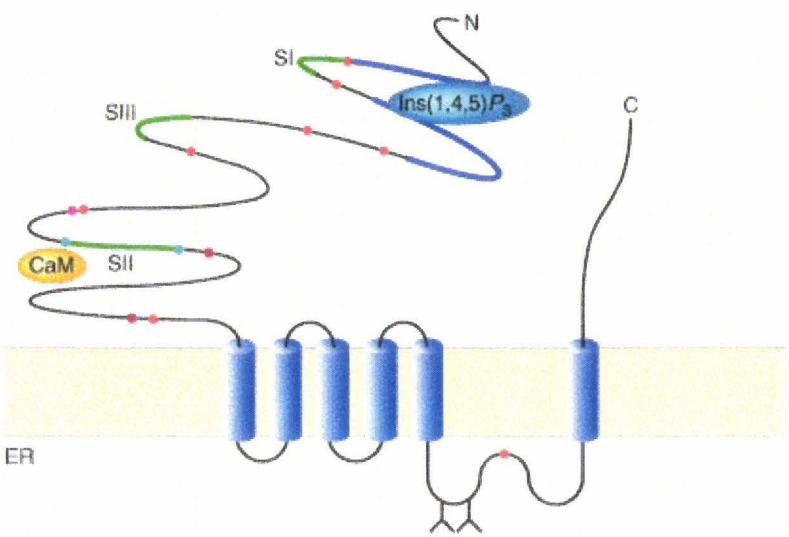

Figure 3 : Récepteur IP3 type I.
D'après Thrower et al (2001).

Le domaine régulateur comprend plusieurs sites potentiels de régulation, des sites de phosphorylations, de fixation de l'ATP, de fixation du calcium. De plus, le récepteur de type I subit un épissage au niveau de plusieurs sites appelés SI, SII, et SIII. Une hétérogénéité supplémentaire est apportée par l'association probable entre les différentes sous-unités sous forme d'hétéro-tétramère. Cette hétérogénéité peut s'observer au niveau tissulaire avec différentes isoformes plus spécifiquement exprimées dans un tissu que dans un autre, comme par exemple le type I au niveau du système nerveux central (pour revue voir Thrower et al 2001). Au niveau sub-cellulaire, il semblerait également que les récepteurs IP3 ne soient pas répartis de manière homogène. Par exemple, dans les cellules acineuses pancréatiques, les récepteurs IP3 sont localisés au niveau apical, là où le signal calcique est initié (Lee et al 1997). Plus précisément, au niveau même du réticulum endoplasmique, il existe une répartition hétérogène des récepteurs (Golovina and Blaustein 1997).

Ces récepteurs possèdent une sensibilité différente à la fois vis-à-vis du ligand principal, l'IP3 mais également vis-à-vis du calcium, qui est un régulateur important du récepteur. Le récepteur de type II est environ 20 fois plus sensible à l'IP3 que le récepteur de type I (EC_{50}=28 nM pour IP3-RII vs 500 nM pour IP3-RI) et 100 fois plus que le récepteur de type III (EC_{50}=3200 nM) (voir Thrower et al 2001). Le récepteur de type I possède pour sa part une propriété spécifique vis-à-vis du calcium par rapport aux autres isoformes car il subit à la fois une activation pour des concentrations relativement faibles de calcium (<300 nM) et une inhibition pour des concentrations de calcium cytoplasmique supérieure à cette valeur. Les autres isoformes sont uniquement activées par des concentrations micromolaires de calcium. Il semblerait que l'inhibition du IP3-RI ne soit pas une propriété intrinsèque de ce canal mais soit due à une inhibition par la calmoduline (Missiaen et al 1999).

Au niveau fonctionnel, les propriétés différentes de ces isoformes en terme de régulation permettent de penser que le type I par exemple, du fait notamment de ses propriétés d'activation et d'inactivation par le calcium est un candidat intéressant pour entretenir les oscillations de calcium répétitives dans des cellules. Le type II, en raison de sa forte sensibilité et de son absence d'inactivation par le calcium, permettrait d'initier un signal calcique rapide et de longue durée pour de faibles concentrations d'IP3. Le type III pour sa part, pourrait engendrer un signal calcique pour de fortes concentrations d'IP3.

Le récepteur à l'IP3 est d'autre part susceptible de s'associer physiquement avec différentes protéines (voir Patel 1999, pour revue). Outre une association avec la protéine accessoire FKBP12, les récepteurs à l'IP3 peuvent se lier avec la calcineurine (peut-être via FKBP12), la calmoduline, des protéines du cytosquelette et de manière tout à fait intéressante avec des canaux calciques membranaires de type *trp* (voir Trebak et al 2003 pour revue). Comme cela a déjà été précisé plus haut, certaines de ces protéines, supposées être à l'origine de l'entrée capacitative ou du SOC (store-operated calcium channel) des cellules non-excitables et notamment TRPC3 (Kielsyov et al 1998) pourraient interagir avec les récepteurs à l'IP3.

2) Les récepteurs à la ryanodine

Ces récepteurs-canaux intracellulaires sont appelés ainsi en raison de leur affinité nanomolaire pour une toxine végétale, la ryanodine. Ces canaux ont été décrits dans les tissus musculaires squelettiques et cardiaques où ils sont particulièrement abondants (Pessah et al 1985, Fleischer et al 1985). Ce sont les plus gros canaux décrits jusqu'à présent. Les extensions cytoplasmiques de ces canaux peuvent être visualisées facilement en microscopie électronique sous forme de pied (foot) s'allongeant entre la membrane du réticulum sarcoplasmique et le membrane plasmique. Il existe actuellement 3 isoformes clonées du récepteur à la ryanodine (RyR1, RyR2, RyR3) (pour revue voir Rossi et Sorrentino 2002). L'isoforme 1 du muscle squelettique est une des protéines clonées les plus volumineuses, chaque monomère possédant plus de 5000 acides aminés. Les deux autres isoformes sont plus spécifiques du cœur (RyR2) et du cerveau et du muscle lisse (RyR3) (McPherson et Campbell, 1993). Ces récepteurs furent initialement considérés comme caractéristiques des cellules excitables puis, avec le clonage de RyR3, il fut établi que les cellules non excitables, épithéliales et endothéliales notamment, exprimaient ce canal et particulièrement l'isoforme 3 (McPherson et Campbell, 1993, Bennett et al 1996).

Les canaux RyR sont les acteurs centraux du couplage excitation-contraction des muscles squelettiques et cardiaques. En fonction du type musculaire, leur mode d'implication est légèrement différent. Dans le muscle squelettique, RyR1 est activé directement lors de l'ouverture du canal calcique DHP-R par un mécanisme de couplage conformationnel sans qu'il y ait nécessairement entrée de calcium par le canal DHP-R (α1S, Lu et Meissner 1994, Leong et McLennan 1998). Dans le tissu musculaire cardiaque, le canal RyR2 est activé par l'entrée de calcium qui a lieu lors de l'ouverture des canaux calciques (α1C) pendant le potentiel d'action. Comme les canaux IP3-R, les RyR sont donc également calcium-dépendants, et leur activation par le calcium permet notamment

le mécanisme de calcium-induced calcium release (Fabiato 1983, Stern 1992), notamment au niveau cardiaque, le récepteur cardiaque (Ryr2) étant plus sensible au calcium que le récepteur squelettique RyR1 (Zimanyi et Pessah 1991).

Contrairement aux IP3-R, le ligand naturel de ces RyR n'est pas connu avec certitude. Un faisceau d'argument met en avant l'ADP ribose cyclique (cADPr) un dérivé cyclique du NAD^+ synthétisé par l'ADP-ribosyl cyclase (Lee et al 1989) comme agoniste naturel des RyR (voir Guse 1999 pour revue). Le cADPr est capable de libérer le calcium des réserves intracellulaires sensibles à la pharmacologie caractéristique des RyR (inhibée par la ryanodine à faible concentration, par le rouge de ruthénium ou la procaine et potentialisée par la caféine et la calcium) ceci dans de nombreux types cellulaires, tels que cellules neuronales ou neuroendocrines, cellules musculaires, cellules exocrines et endocrines pancréatiques, lymphocytes, hépatocytes et cellules végétales (voir Lee 1997 pour revue). En revanche, la production de cADPr en réponse à une activation par un récepteur n'a été montrée que dans peu de systèmes, ce qui limite pour l'instant son rôle éventuel de second messager à un agent modulateur. La formation de cADP à partir de l'ADP-ribosyl cyclase cytosolique peut être stimulée notamment par le monoxyde d'azote (NO) dans des œufs d'oursin ou des cellules clonales médullosurénaliennes PC12 (Gallione et al 1993, Clementi et al 1996). La modulation de l'ADP-ribosyl cyclase membranaire a été rapportée pour la première fois en 1997 (Higashida et al 1997). Il a été montré que la stimulation des récepteurs muscariniques m1 ou m3 permettait l'activation de l'ADP-ribosyl cyclase membranaire alors que celle-ci était inhibée par les récepteurs m2 ou m4. Ces effets étant respectivement sensibles aux toxines cholériques et pertussiques, il a été supposé que des voies de transduction différentes *via* des protéines G différentes pouvaient moduler la production de cADPr (Higashida et al 1997). Les récepteurs RyR (mais aussi les IP3-R) pourraient eux-mêmes être sensibilisés par un autre second messager potentiel également produit par l'ADP-ribosyl cyclase membranaire, le NAADP dont l'existence de récepteurs spécifiques est également proposée (nicotinic acid adenine dinucleotide phosphate) (Cancela et al 2003).

Enfin, d'autres protéines intracellulaires possédant des activités de canaux ont été montrées participer à une libération de calcium des réserves intracellulaires de manière similaire aux canaux IP3-R et RyR, des canaux de la famille des TRP, TRPV1 (Turner et al 2003) et polycystine 2 (Koulen et al 2002).

I.II. Les mécanismes participant à maintenir l'état de repos

Les mécanismes contribuant à maintenir la concentration de calcium dans le cytosol à des valeurs de repos (de l'ordre de 100 nM) sont de plusieurs types ; des transporteurs de la membrane plasmique permettant l'expulsion du calcium vers le milieu ambiant (Ca^{2+}ATPases de la membrane plasmique et échangeur Na/Ca) et des transporteurs intégrés dans les membranes des organites intracellulaires et notamment le réticulum endoplasmique (Ca^{2+} ATPases), permettant l'accumulation de calcium dans ces organites. D'autre part, le RE est supposé posséder des canaux de fuite dont la nature reste toujours élusive (Camello et al 2002) et les mitochondries participent, en capturant le calcium libéré par le RE, au maintien du niveau de calcium cytosolique (Tinel et al 1999). Enfin, les différentes calcium-binding protéines du cytosol (calbindine D28K, parvalbumine ou calretinine, Chard et al 1993, Edmonds et al 2000) et du RE (calréticuline, calnexine, Michalak et al 2002) jouent un rôle important dans la régulation des signaux calciques (amplitude, forme, durée, diffusion, propagation) dans les différents compartiments cellulaires.

Les Ca^{2+} ATPases de la membrane plasmique (PMCA pour plasma membrane Ca^{2+} ATPases) et du réticulum endoplasmique (SERCA pour sarco-endoplasmic reticulum Ca^{2+} ATPases) sont des Ca^{2+} ATPases de type P qui nécessitent un intermédiaire phosphorylé dans la réaction qui transfère le calcium d'un compartiment à une autre. Les PMCA furent mises en évidence pour la première fois dans les érythrocytes (Schatzmann, 1966). Ces pompes qui transfère un ion Ca^{2+} pour l'hydrolyse d'une molécule d'ATP sont ubiquitaires (pour revue voir Carafoli et Brini, 2000). Ces enzymes sont codées par au moins 4 gènes différents (PMCA1-4) et à cause des mécanismes d'épissage, il existe au moins 20 isoformes différentes. Les SERCA permettent le remplissage du RE en transférant 2 ions calcium grâce à l'hydrolyse d'une molécule d'ATP. Trois gènes différents (ATP2A1-A3) au moins codent pour les SERCA (SERCA1-3) chez les vertébrés. Chacune de ces SERCA est susceptible de subir un épissage, la forme la plus ubiquitaire des SERCA étant SERCA2b (Pour revue voir Wuytack et al 2002). Sur un plan pharmacologique, il est possible de distinguer les PMCA des SERCA par l'utilisation d'inhibiteurs sélectifs des SERCA, la thapsigargine, l'acide cyclopiazinique et le 2,5-di-(*tert*-butyl)-1,4-benzohydroquinone. Les SERCA (1 et 2) sont notamment régulées par la phospholambane (PLB), qui diminue l'affinité des SERCA pour le Ca^{2+} cytosolique, cette inhibition étant levée lors de la phosphorylation de PLB par la protéine kinase A (PKA) ou la calcium-calmoduline dependent kinase II (CaMKII) (pour revue voir Wuytack et al 2002).

D'autres Ca^{2+}ATPases appelées pmr1 (plasma membrane related Ca^{2+}ATPases) ont été identifiées dans les levures *Saccharomyces Cerevisiae* (Rudolph et al 1989) et leurs homologues mammaliens ont été clonés (Gunteski-Hamblin et al, 1992). Chez les mammifères, ces protéines également appelées SPCA (pour secretory pathway Ca^{2+}ATPases) sont distribuées au niveau des différents compartiments du Golgi et du réseau trans-golgien (Van Baelen et al 2001, Ton et al 2002), un compartiment acide lui-même en étroite relation avec les autres compartiments acides, lysosomes, endosomes et vésicules de sécrétion. Ces pompes pourraient être responsables de la capture de calcium indépendante de la thapsigargine et donc des SERCA par le Golgi (Pinton et al 1998). Il est à noter que non seulement le Golgi possède des propriétés de stockage de calcium mais qu'il serait également apte à libérer le calcium dans le cytosol de manière IP3-dépendante (Pinton et al 1998), ce qui en ferait un organite de stockage intracellulaire de calcium potentiellement impliqué dans les réponses calciques dynamiques.

I.III. Codage du signal calcique

Le fonctionnement coordonné de ces différents canaux et pompes va donner lieu, selon les cellules et les régions subcellulaires, à des signaux calciques soit généralisés soit localisés, soit transitoires soit maintenus, soit rythmiques soit phasiques. Ainsi, une large classification de ces signaux, comprenant les « spikes » (pics), « transients » (transitoires calciques), les « blips » (« spot » ou point lumineux), les « quarks » (par référence aux quarks de la physique), les « puffs » (bouffées), les « sparks » (étincelles), ou les « waves » (vagues) a-t-elle été progressivement avancée (Berridge et al 2000).

Pour résumer, un signal peut-être extrêmement localisé à la bouche d'un canal, et on considère ce genre de signaux comme un blip ou un quark, selon que le canal soit un IP3-R (blip) ou un RyR (quark). Ces signaux «unitaires» localisés à la bouche des canaux calciques (microdomaines) vont permettre d'activer des cibles spécifiques avant que le signal ne diffuse loin de sa source ou que des mécanismes régénératifs qui propagent le signal à la cellule entière ne soient mis en place. Dans le cas des signaux IP3-R dépendants, la sommation spatio-temporelle de « blips » dus à l'activation de canaux IP3 regroupés par foyers va engendrer des « puffs », signaux d'une durée de l'ordre de la seconde et de plusieurs centaines de nM d'amplitude qui peuvent donner lieu à une vague calcique généralisée à la cellule ou des oscillations rythmiques lors de stimulations neurohormonales (Bootman et al 2001). Certains signaux se limitent à un pôle de la cellule, comme par exemple dans le cas de cellules exocrines pancréatiques où on observe des « spikes » calciques, fortement

sensibles à l'IP3, au niveau du pôle apical (Petersen et al 1999). Dans le cas de cellules excitables musculaires, ont été observés des signaux fortement dépendants de l'activation de récepteurs RyR qui lors de leur activation par les canaux Ca^{2+} sensibles aux dihydropyridines engendrent localement des « quarks (nM) » qui peuvent se sommer en « sparks (µM) » lors de l'activation concomitante de quelques RyR également regroupés par foyers (Niggli 1999). Les « sparks », comme les « puffs » peuvent générer dans la cellule entière une vague calcique généralisée notamment en fonction des concentrations en agonistes et donc en second messagers (IP3, cADPr, NAADP...) et d'autre part en fonction de la nature des seconds messagers impliqués (Cancela et al 2002).

Les cellules excitables émettent généralement des potentiels d'actions spontanées ou déclenchés. Si ces potentiels d'action sont associés à l'ouverture de canaux calciques voltage-dépendants, l'entrée de calcium lors du PA peut entraîner une augmentation rapide de la $[Ca^{2+}]i$ provoquant ainsi un « spike » (pic) ou « transient » (transitoire). Ces transitoires calciques peuvent également permettre l'activation d'une libération de calcium par les canaux IP3-R ou RyR et entraîner ainsi une amplification locale de l'augmentation de calcium par ce mécanisme de « calcium-induced calcium release ». Ce phénomène, s'il est particulièrement important dans l'augmentation de calcium lors des potentiels d'action cardiaques et lors de l'activation des canaux L, n'en est pas moins efficace dans les neurones pour amplifier les signaux calciques intervenant par les canaux N, P/Q.

II. Rôle du calcium dans la physiologie cellulaire

Afin d'illustrer le rôle central du calcium dans la physiologie cellulaire, je donnerai deux exemples principaux de son intervention, 1) dans la neurotransmission ou le couplage stimulation/sécrétion d'une manière générale, 2) dans la régulation génique et notamment les phénomènes de prolifération cellulaire.

II.I. Le couplage stimulation-sécrétion et la notion de calcium-dépendance et de calcium-indépendance

La sécrétion régulée est le mécanisme par lequel les cellules sont capables de libérer, à la demande, des molécules, protéines, amines, acides aminés ou autres, dans le milieu extracellulaire. Ce mécanisme, qui est une des caractéristiques des cellules neuronales (transmission synaptique) et neuroendocrines (libération hormonale) ne leur est pas spécifique puisque les cellules exocrines sécrètent les enzymes digestives ou que des cellules myéloïdes (mastocytes) libèrent des médiateurs de l'inflammation selon ce procédé.

S'il existe des spécificités fonctionnelles et moléculaires de chacun de ces types cellulaires, on peut cependant décrire le mécanisme de libération d'une manière générale selon un schéma assez simple comprenant quelques étapes telles qu'elles sont illustrées sur la figure 4. En commençant par la fin, le mécanisme de libération procède par fusion membranaire lipidique autrement dit par exocytose. Ce mécanisme est réellement le point commun entre tous ces modes de libération, si on excepte la sécrétion des hormones lipidiques (stéroïdes par exemple).

L'exocytose régulée concerne généralement deux populations différentes de compartiments membranaires distingués par leur propriétés morphologiques et fonctionnelles, les vésicules synaptiques, petits compartiments membranaires d'environ 50 nm de diamètre qui fusionnent rapidement avec la membrane plasmique, et les granules de sécrétion, de taille plus importante (supérieure à 100 nm de diamètre), généralement pourvus d'une structure opaque aux électrons en microscopie électronique, le cœur dense, et dont la fusion est plus lente. Ces vésicules et granules, en fusionnant avec la membrane plasmique, vont permettre la libération de neuromédiateurs et neurohormones, respectivement. Un même type cellulaire, par exemple, les cellules β du pancréas, peut posséder ces deux compartiments vésiculaires, l'un servant à la sécrétion régulée d'insuline, l'autre à la libération de GABA (voir figure 4).

La fusion lipidique est la dernière étape du processus sécrétoire. Cette étape est précédée de nombreuses autres étapes depuis la formation des vésicules ou granules au niveau des endosomes ou du Golgi. Toutes ces étapes peuvent être stimulées par différents messagers et entraîner la transition de la vésicule ou du granule d'un stade à un autre. Ces différents stades se répartissent de la manière suivante (voir figure 5) (pour revues voir Südhof 2000, Jahn et al 2003, Augustine 2001, Klenchin et Martin 2000):

1) Une première réserve importante de granules est généralement présente dans le cytoplasme en profondeur de la cellule, mêlée à un réseau de cytosquelette. Ces granules peuvent être recrutés lors de l'étape de translocation ou migration vers la membrane. Cette étape semble nécessiter un remaniement du cytosquelette.

2) Ces granules vont se retrouver ancrés dans la membrane à l'aide d'interactions moléculaires complexes. C'est l'étape de docking ou ancrage (ou encore arrimage). Ainsi, une

deuxième réserve de granules va se retrouver localisée au niveau sous-membranaire et donc plus facilement mobilisable lors d'une stimulation que la première réserve.

3) Ces granules (ou vésicules) ancrés vont ensuite subir une série de modifications biochimiques, caractérisées par des phosphorylations, qui vont rendre les granules compétents pour la dernière étape fusionnelle. Cette étape, nommée « priming » ou amorçage, aboutit à un rapprochement des bicouches entres elles et à une hémifusion des membranes vésiculaires et plasmiques.

4) La dernière étape, la fusion ou l'exocytose proprement dite, va être stimulée par l'arrivée d'un signal calcique, et va entraîner la formation d'un pore de fusion lipidique qui va permettre la libération du contenu vésiculaire vers l'extérieur de la cellule. Cette étape, si elle procède par une fusion des bicouches entre elles, nécessite probablement des structures protéiques qui vont 1) assurer la sensibilité au calcium 2) initier la formation du pore de fusion.

L'étape d'exocytose est suivie par un retraitement membranaire, l'endocytose, que l'on subdivise en deux catégories, l'endocytose *via* les endosomes, mode de retraitement membranaire lent, et le « kiss and run « (voir figure 4 et 5) mode de retraitement excessivement rapide, les vésicules n'ayant pas besoin dans ce cas de repasser par une étape de maturation par les endosomes mais peuvent être directement réemplies avec le neurotransmetteur.

Toutes ces étapes peuvent être la cible de régulations biochimiques qui vont faciliter (ou inhiber) le passage d'un stade à un autre. Le régulateur principal du couplage excitation/sécrétion reste l'ion calcium. Celui est capable dans la quasi-totalité des types cellulaires de stimuler la sécrétion. Comme montré par différentes études, une augmentation de calcium dans des cellules sécrétrices entraîne une sécrétion qui comprend plusieurs phases apparaissant avec des délais et des vitesses différentes. La plupart des études montrent l'existence d'au moins trois phases de sécrétion successives à la suite d'un stimulus calcique, ceci reflétant la stimulation par le calcium de processus biochimiques au niveau des différentes étapes décrites ci-dessus (Neher et Zucker 1993, Kits et Mansvelder 2000).

Un des enjeux majeurs de l'étude du couplage stimulation-sécrétion de ces 10 dernières années fut d'élucider les mécanismes protéiques impliqués dans ces différentes étapes, depuis la translocation des granules depuis le Golgi, jusqu'à la fusion lipidique et notamment les protéines

calcium-dépendantes qui pourraient être les calcium-senseurs de l'exocytose. Une des découvertes majeures fut la caractérisation des protéines participant à la formation du complexe SNARE par l'équipe de J. Rothman (Sollner et al 1993). Les travaux de ce laboratoire ont permis d'identifier les composants majeurs de ce complexe et des protéines qui s'y associent, une ATPase cytosolique : la NSF (N-ethylmaleimide-sensitive fusion protein), les protéines adaptatrices permettant l'association de NSF avec les composants membranaires du complexe : les SNAP (soluble NSF adaptor proteins, comprenant les α, β, et γ SNAP), et enfin les SNAREs eux-mêmes (SNARE pour SNAP receptors). Les SNAREs, que l'on distingue en v-SNARE et t-SNARE en fonction de leur localisation (v pour vésicule et t pour target, c.a.d la membrane plasmique dans le cas de l'exocytose), sont des protéines membranaires qui comprennent trois familles principales : les synaptobrévines (ou VAMP2 pour vesicle-associated membrane protein 2) dans les vésicules et la syntaxine1 et SNAP25, deux protéines de la membrane plasmique. Au début des années 90, la découverte de ces protéines, de leur association lors du processus d'exocytose a abouti, grâce à la découverte des cibles moléculaires des toxines tétaniques et botuliques (les composants du complexe eux-mêmes) par l'équipe de Montecucco (Schiavo et al 1992), à l'hypothèse SNARE, hypothèse selon laquelle le complexe jouerait le rôle d'échafaudage moléculaire entraînant le rapprochement des deux membranes (vésicule et membrane plasmique). Cette hypothèse SNARe est d'autant plus intéressante que les mécanismes moléculaires impliqués sont peu ou prou conservés dans le régne du vivant (Bennett et Scheller 1993) et ne sont pas spécifiques de l'exocytose mais participent aux différentes étapes du trafic intracellulaire membranaire (Galli et al 2002).

Le signal déclenchant le processus final de fusion est l'augmentation de calcium sous-membranaire, pouvant atteindre plus de 100 µM. Cette augmentation a lieu dans les synapses grâce à une entrée de calcium par des canaux calciques voltage-dépendants, notamment de type N, P/Q qui ont été montrés comme étant associés à un complexe moléculaire appelé excisome (voir figure 6) par l'intermédiaire de liaisons avec la syntaxine, la synaptotagmine et SNAP-25 (Atlas 2001). Ces microdomaines ou nanodomaines permettent une stimulation de l'exocytose extrêmement rapide, avec un délai compris entre 0.1 et 1 msec. Le calcium est donc à lui seul capable de déclencher la fusion de granules prêts à fusionner, *i.e,* ayant préalablement subi tous les processus d'amorçage (priming). Le calcium-senseur le plus probable actuellement est la synaptotagmine (Brose et al 1992, Augustine 2001, Jahn et al 2003), une protéine calcium-dépendante qui possède des domaines C2 (A et B) qui lui permettent de lier le calcium et les phospholipides et ainsi d'interagir avec la membrane de manière calcium-dépendante. Des expériences sur des souris knock-out ont notamment permis de montrer que la liaison du calcium sur la synaptotagmine 1 déclenchait la libération synaptique rapide (Fernandez-Chacon et al 2001). Cette protéine a une

calcium-dépendance similaire à celle de l'exocytose (EC50 de l'ordre de 20 μM). Cependant, il ne faut pas négliger dans ce concept de calcium-dépendance de l'exocytose que le calcium va pouvoir agir au niveau des étapes préalables. Par exemple, l'étape de translocation au cours de laquelle s'effectuent des remaniements du cytosquelette est calcium-dépendante. Ceci serait entre autre dû à la phosphorylation de la synapsine, une protéine qui s'associe de manière réversible avec les granules de sécrétion, par la CaMKinase II (Doussau and Augustine 2000). Ceci favoriserait la translocation des granules de sécrétion vers la membrane plasmique. Si les étapes d'amorçage requièrent l'hydrolyse de l'ATP, elles sont également dans une moindre mesure dépendantes du calcium en raison des mécanismes de phosphorylations faisant intervenir des kinases Ca^{2+}-dépendantes (Klenchin et Martin 2000). Ainsi, la PKC qui stimule la sécrétion des cellules PC12 pourrait exercer cette action *via* une phosphorylation de SNAP25 (Nishiszaki et al 1992, Shimazaki et al 1996).

Dans les cellules neuroendocrines, les canaux calciques impliqués dans le couplage stimulation-sécrétion (canaux de type L) ne sont pas nécessairement associés physiquement au complexe moléculaire SNARE mais sont concentrés et co-localisés avec les granules de sécrétion dans des domaines similaires sur le plan fonctionnel à la zone active de la synapse. On peut ainsi de manière arbitraire distinguer des nanodomaines (association physique) et des microdomaines calciques (colocalisation) qui vont définir des vitesses de fusion plus ou moins rapides.

L'exocytose ou la sécrétion d'une manière plus générale est considérée généralement comme calcium-dépendante. Cependant, ce quasi-dogme souffre de quelques exceptions. En effet, certains types cellulaires sont capables, en absence de toute trace de calcium extracellulaire ou cytosolique ($[Ca^{2+}]i < 10$ nM), de sécréter en réponse à un sécrétagogue. C'est notamment le cas des cellules myéloïdes, qui en réponse à une activation pharmacologique des protéines G par exemple du GTP non hydrolysable (GTPγS) dégranulent massivement, même en absence de calcium (Fernandez et al 1984, Gomperts 1990). D'autres types cellulaires et notamment des cellules neuroendocrines telles que des cellules hypophysaires mélanotropes (Okano et al 1993), des cellules chromaffines (Carroll et al 1990) ou des cellules β pancréatiques (Proks et al 1996) sont capables de sécréter en réponse à ce type de stimulus. Ainsi, l'identification des protéines G est-elle devenue un enjeu important dans l'élucidation des mécanismes moléculaires de l'exocytose. Différentes protéines G mono ou multimériques, sur lesquelles nous reviendrons plus tard, ont été postulées comme actrices centrales de la libération neurohormonale.

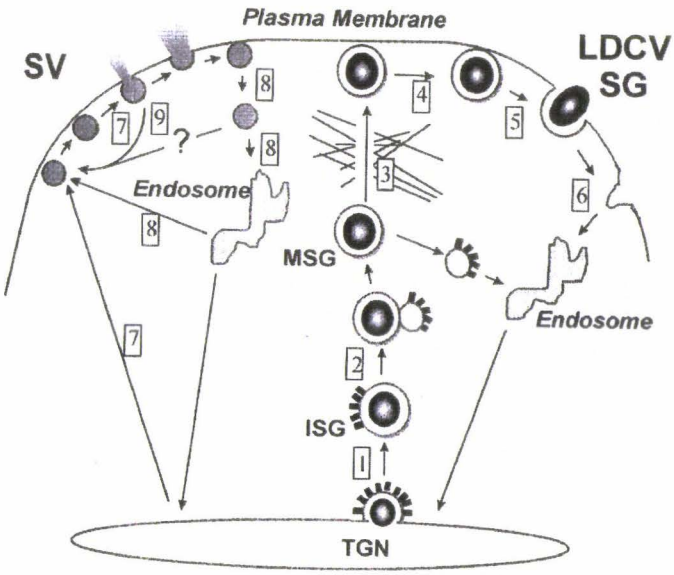

Figure 4 : Voies de sécrétion régulées. Un mécanisme rapide relatif à la fusion des vésicules synaptiques (SV) et à la libération de neurotransmetteurs est illustré sur la partie gauche . Une voie plus lente relative à l'exocytose des granules à cœur dense (LDCV ou SG) et à la libération de neurhormones est schématisé sur la droite.
1 : bourgeonnement du Golgi
2 : maturation des granules
3 : migration
4 : ancrage
5 : amorçage
6 : fusion
7-9 : kiss and run et endocytose

D'après Lang (1999)

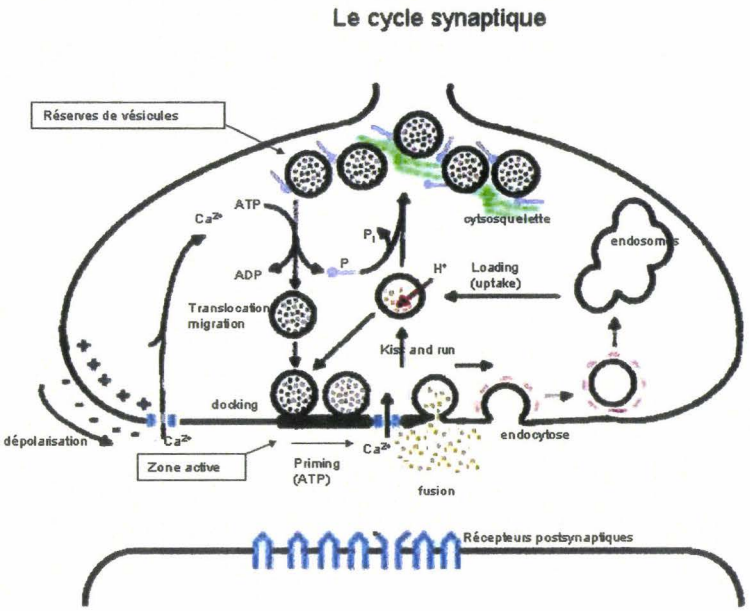

Figure 5 : Le cycle synaptique

II.II. Ca^{2+}, régulation génique, prolifération et apoptose

Il est connu depuis relativement longtemps qu'une augmentation de calcium cytosolique, en utilisant par exemple des ionophores calciques, est capable de stimuler la synthèse de certaines protéines (Wu et al, 1981), et notamment de certaines hormones, *via* une augmentation de la production en ARNm (ainsi, pour compléter le paragraphe précédent, le calcium joue son rôle dans le couplage stimulation-sécrétion jusque dans la stimulation de la transcription). De la même façon, des travaux déjà anciens ont montré que d'une part les cellules tumorales ont une dépendance plus faible au calcium extracellulaire pour leur croissance (Boynton et al 1977) et que d'autre part les ionophores calciques sont capables de stimuler leur prolifération (Jensen et al 1977). Les mécanismes par lesquels le calcium pouvait réguler une expression génique étaient jusqu'à récemment non élucidés. Ces dix dernières années ont permis de lever un peu le voile sur ces mécanismes.

A) Ca^{2+} et expression génique

Les gènes régulés en réponse à un stimulus peuvent être classés en « immediate early gene IEG» (gène précoce) et « late gene » (gène tardif), selon la cinétique (rapide ou lente) et la dépendance vis-à-vis de la synthèse protéique, l'induction de gènes précoces ne nécessitant pas de synthèse protéique.

L'influence du calcium sur l'expression génique a été particulièrement étudiée et il a été montré dans de très élégantes études (Li et al 1998, Dolmetsch et al 1998) que des oscillations de calcium étaient plus efficaces pour stimuler l'expression génique qu'une augmentation soutenue de calcium (pour une variation moyenne identique). D'autre part, ces études ont montré que les facteurs de transcription (NF-AT, NF-κB, et Oct/OAP) n'étaient pas sensibles de la même manière aux oscillations de calcium, les trois étant sensibles à de fortes fréquences alors que seul NF-κB était sensible à de faibles fréquences (Dolmetsch et al 1998). La calcineurine, une phosphatase calcium-dépendante, semble être à l'origine de ces effets. En effet, celle-ci, activée par le calcium, favorise la déphosphorylation de ces facteurs de transcription cytoplasmiques, et entraîne ainsi leur translocation à l'état de complexe avec la calcineurine vers le noyau (Timmerman et al ,1996, Shibasaki et al 1996).

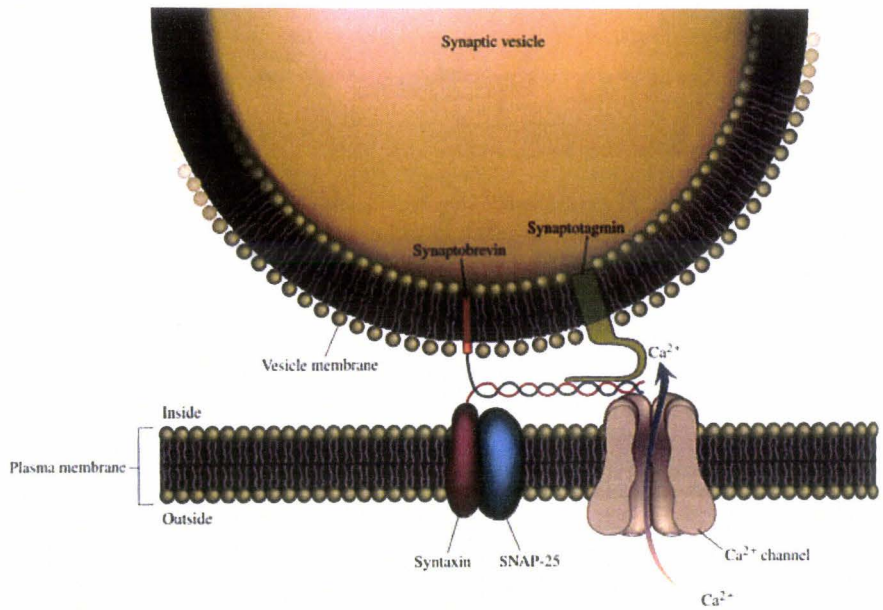

Figure 6 : Complexe SNARE et microdomaines calciques

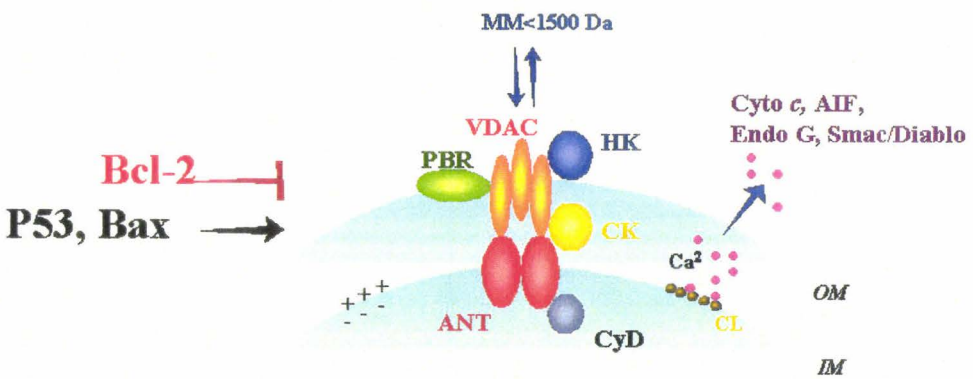

Figure 7 : Le pore de transition de perméabilité mitochondrial

Le calcium, en plus d'activer l'expression génique *via* une phosphatase-Ca^{2+}dépendante, va promouvoir l'expression génique *via* une voie kinase-dépendante, la voie de CRE-CREB (cAMP-responsive element -(binding protein)). CREB est un facteur de transcription nucléaire calcium-dépendant qui peut-être phosphorylé par différentes kinases, cAMP dependent kinases (PKA), calmoduline-dependent kinases (CaM kinases) et la voie des Ras/MAPkinases (voir West et al 2001 pour revue). Son activation par le calcium nécessite sa phosphorylation sur une sérine 133 (Sheng et al 1991). Après sa phosphorylation, CREB recrute une CREB binding protéine (CBP) qui est un coactivateur transcriptionnel. Il a été montré que l'activité de CBP était contrôlée par le calcium nucléaire et impliquait la CamKIV (Chawla et al 1998). Si les CaMK I, II et IV peuvent phosphoryler CREB, la plus importante physiologiquement est ainsi certainement la CaMkinase IV qui est localisée dans le noyau (voir West et al 2001). La concentration en calcium libre dans le noyau jouerait ainsi un rôle important, et différente de celle dans le cytosol, dans les mécanismes d'expression génique, une augmentation de calcium nucléaire permettant l'activation de la voie CRE-CREB alors qu'une augmentation de la concentration en calcium cytosolique entraîne une activation de la voie SRE (serum responsive element) (Hardingham et al 1997). Le Ca^{2+} est de plus capable d'agir directement sur un effecteur nucléaire appelé DREAM (pour downstream regulatory element-antagonist modulator), une protéine possédant 4 domaines liant le calcium de type EF-hand. Ce répresseur transcriptionnel se fixe spécifiquement sur un site DRE (pour Downstream Regulatory Element) jouant le rôle de gène silencer. Lors de l'activation de DREAM par le Ca^{2+}, DREAM ne peut plus se lier à DRE et l'inhibition de la transcription est levée (Carrión et al 1999).

Ainsi, l'élucidation des mécanismes d'homéostasie calcique dans le noyau revêt une importance considérable. A l'heure actuelle, il est toujours débattu comment, et si, le calcium est régulé dans le noyau, certaines études montrant que la concentration calcique dans le noyau suit passivement la concentration cytosolique, le calcium diffusant librement par les pores nucléaires (Lipp et al 1997) alors que d'autres montrent que le noyau possèdent ses propres moyens de régulations (Gerasimenko et al 1995), grâce notamment aux réserves contenues dans l'enveloppe nucléaire et mobilisables par le cADPr ou l'IP3. Il a été montré récemment que les stocks calciques nucléaires possédaient une plus grande sensibilité à l'IP3 que le RE, certainement due à une expression enrichie en IP3-RII dans le noyau par rapport au RE (Leite et al 2003). De plus, des travaux récents montrent qu'il existe une continuité entre le réticulum endoplasmique et l'enveloppe nucléaire sous la forme d'un réseau (réticulum nucléoplasmique). Ce réseau qui s'étend à l'intérieur du noyau, est capable 1) de stocker le calcium, 2) d'exprimer les récepteurs IP3 (type II) et 3) d'initier un signal

calcique nucléaire (avant le signal cytosolique) sous l'action de l'IP3 ou d'un facteur de croissance dans les cellules SKHep1, signal calcique lui-même capable d'induire la translocation de PKCγ de l'espace nucléaire vers l'enveloppe nucléaire (Echevarria et al 2003). Ainsi, ce réseau réticulaire nucléoplasmique pourrait être considéré comme la réserve calcique fonctionnelle du noyau.

B) Ca^{2+} et prolifération cellulaire

La fonction principale du calcium dans le cadre du contrôle de la prolifération cellulaire est d'activer les facteurs de transcription préalablement cités, cytosoliques (NF-AT, NF-kB) ou nucléaires (CREB). D'autres voies de régulation existent néanmoins et notamment au niveau du cycle cellulaire (voir Santella 1998 pour revue). Grâce aux travaux effectués sur les ovocytes ou les oeufs d'oursins, il a été montré que des variations transitoires du calcium cytosolique accompagnent les transitions d'une phase du cycle cellulaire à une autre et plus particulièrement 1) entre la fin la phase G1 et la phase S 2) en G2 avant l'entrée en M 3) pendant la mitose entre la métaphase et l'anaphase et 4) pendant la cytodiérèse (Santella 1998), le passage d'une phase du cycle à une autre étant bloquée par l'injection de chélateur calcique dans les cellules. Il a donc été supposé que les transitoires calciques déclenchaient le passage d'un stade du cycle à un autre (Whitaker et Patel 1990). Ceci doit cependant être minoré par le fait que ce n'est pas nécessairement vrai pour tous les types cellulaires et notamment les cellules de mammifères où par exemple le calcium peut-être impliqué dans la scission de l'enveloppe nucléaire mais pas dans la transition métaphase-anaphase (Kao et al 1990). Les cibles moléculaires du calcium pourraient être les nombreuses protéines impliquées dans la progression du cycle, cyclines ou cycline-dependent kinases. Ainsi, il a été montré que l'activation de la CamKII par une augmentation de calcium aboutit à la phosphorylation de protéines impliquées dans le cycle cellulaire. La CamKII peut ainsi phosphoryler et ainsi activer une tyrosine phosphatase $p54^{cdc25\text{-}c}$ qui va à son tour déphosphoryler et activer la kinase $p34^{CdC2}$, qui associée à la cycline B, est nécessaire au passage de G2 vers M (Patel et al 1999). La CamKII peut également phosphoryler pRB (Retinoblastoma Protein, le produit du gène suppresseur de tumeur Rb1) qui contrôle, au point de restriction, le passage G1/S (Takuwa et al 1993).

Une autre cible pour le calcium dans un rôle régulateur de la prolifération et du cycle cellulaire est constituée par les protéases de type calpaine. Ces protéases sont activées par le calcium, et en présence de calcium permettent la progression dans le cycle (Schollmeyer 1988). D'autre part, leur inhibition arrête la progression du cycle cellulaire. La calpaine serait notamment impliquée dans l'assemblage et le désassemblage des microtubules et la dégradation de la cycline D1 (voir Santella 1998).

Comme le calcium semble jouer un rôle central dans la prolifération, les études destinées à illustrer comment différents mécanismes d'homéostasie calcique sont impliqués dans la croissance cellulaire sont pléthores. En effet, comme le calcium est un ion multifonctionnel, il est nécessaire de comprendre comment il va intervenir sur la prolifération plutôt que sur la différenciation ou la mort cellulaire (voir ci-dessous) par exemple. Un des mécanismes auquel il est le plus souvent fait référence afin d'expliquer cette pluripotentialité du calcium est, un peu pompeusement, appelé le codage spatiotemporel des signaux calciques. En effet, comme cela a déjà été mentionné précédemment, il existe des microdomaines calciques au sein desquels se trouvent les mécanismes d'homéostasie (canaux, pompes, Ca^{2+}-binding protéines) et les cibles calciques. Ces microdomaines vont être évidemment de nature différentes selon l'espace sub-cellulaire et être mis en jeu lors de variations de calcium dans un espace bien précis de la cellule. Le noyau, la membrane plasmique, le réticulum, tous les organites possèdent leurs propres mécanismes d'homéostasie calcique et les variations de calcium dans ces espaces ou même dans des régions plus localisées de ces espaces vont avoir un retentissement bien spécifique sur la physiologie de la cellule. L'exemple des microdomaines synaptiques impliqués dans l'exocytose a déjà été cité mais il est possible de citer également le rôle de microdomaines dans la régulation de l'expression génique. Par exemple, dans les neurones, la transcription de BDNF (brain-derived neurotrophic factor) est activée de manière beaucoup plus efficace par des entrées de calcium par les canaux voltage-dépendants plutôt que par des récepteurs-canaux NMDA (pour des variations de calcium cytosoliques et nucléaires identiques en amplitude et cinétique) (Hardingham et al 1999). Cet effet est du à un recrutement différentiel de CBP sur CREB en fonction du mode d'entrée de calcium dans la cellule. Comme il a été dit plus haut que CREB était activé par des variations de calcium nucléaires, il reste à déterminer comment l'information apportée par les canaux de la membrane plasmique est transmise au niveau nucléaire. Ceci pourrait être due soit à une aptitude différentielle des canaux calciques membranaires à provoquer des variations locales de calcium dans le noyau ou à une association fonctionnelle de molécules de signalisation avec les canaux membranaires (voir West et al 2001 pour revue).

D'autre part, le codage spatio-temporel des signaux calciques, souvent comme précisé plus haut dans le texte, sous forme de variations cycliques (plus efficaces qu'un signal soutenu pour entraîner une réponse physiologique, que ce soit exocytose ou expression génique), nécessite des enzymes capables de décoder des signaux alternatifs. Une enzyme communément citée qui possède ces propriétés de sensibilité temporelle est la CamKinase II. (De Koninck et Schulman 1998).

C) Ca^{2+} et apoptose

Une dérégulation des mécanismes d'homéostasie calcique, et notamment un dépassement de la capacité de la cellule à prendre en charge le calcium (overload), est également impliquée dans les processus de mort cellulaire par nécrose ou apoptose. Historiquement, on sait depuis 25 ans qu'une augmentation de calcium soutenue dans les cellules est délétère (Schanne et al 1979). De plus, une augmentation de calcium stimulée par le ionophore A23187 provoquait une condensation de la chromatine et une fragmentation de l'ADN (Wyllie et al 1981), des indices aujourd'hui acceptés comme marqueurs de l'apoptose. L'apoptose est un mécanisme particulièrement intéressant puisque, contrairement à la nécrose, il n'est ni accidentel ni passif. En effet, la cellule participe activement à sa propre mort en synthétisant ou activant les enzymes nécessaires en réponse à un stimulus spécifique. D'autre part, l'apoptose est impliquée dans le maintien de l'équilibre tissulaire au même titre que la division ou la différenciation, que ce soit lors du développement embryonnaire d'un organe (tissu nerveux par exemple), de son remaniement permanent au cours de la vie de l'individu, ou lors de pathologies (cancer, maladie d'Alzheimer). Les flux calciques capables d'induire l'apoptose sont de différentes natures. Suite aux travaux montrant que l'apoptose était stimulée par des ionophores calciques (Wyllie et al 1981), que l'apoptose induite par les glucocorticoïdes des thymocytes nécessitait une entrée de calcium depuis l'extérieur, et que la fragmentation de l'ADN s'effectuait grâce à une endonucléase dépendante du calcium et du magnésium (Cohen et Duke 1984), il fut proposé que cette endonucléase était un effecteur universel de l'apoptose stimulé par une augmentation de la concentration calcique cytosolique. Il fut ensuite montré que cette étape de dégradation de l'ADN pouvait quelquefois être très tardive voire absente dans le processus apoptotique et que des effecteurs primordiaux de l'apoptose (et notamment de l'apoptose calcium-dépendante) étaient les calpaines (calcium-dépendantes) et les caspases, toutes les deux des cystine-protéases (voir Kass et Orrenius 1999 pour revue, Cohen 1997). Les deux familles existent normalement à l'état de proenzymes qui peuvent être activées grâce à un recrutement dans un complexe moléculaire ou par clivage direct par une autre caspase. Les procaspases, au contraire des calpaines qui sont cytosoliques, existent dans différents compartiments cellulaires, cytosol, mitochondrie et RE (Nakagawa et Yuan 2000).

Ainsi, puisque l'apoptose possède une composante calcium-dépendante, les flux calciques et les compartiments cellulaires impliqués dans l'apoptose sont abondamment étudiés. L'apoptose peut également être stimulée par la libération de calcium du RE via l'activation de récepteurs IP3 ou RyR (voir Hajnócsky et al 2000). Il a été montré par exemple que l'apoptose de lymphocytes était

accompagnée d'une augmentation de l'expression de récepteurs IP3R3, et que l'apoptose induite par des stimuli augmentant la production d'IP3 était inhibée par des antisens contre les récepteurs IP3 ou par l'introduction de délétion dans les récepteurs IP3 (Blackshaw et al 2000, Jarayaman et Marks 1997, Sugarawa et al 1997).

Une libération de calcium des réserves IP3/RyR-dépendantes est donc capable d'induire l'apoptose. Une des questions réitérée par la littérature est de déterminer si cet effet est du : à une augmentation de la concentration calcique dans le cytosol, à la diminution de calcium dans les réserves du RE, ou à la saturation des capacités de capture de calcium des mitochondries (capture du calcium libéré par le RE). Ces différentes hypothèses ont été suggérées et ne sont certainement pas exclusives et laissent supposer l'existence d'effecteurs à ces différents niveaux.

Ces effecteurs agiraient (entre autres) au niveau des protéines de la famille Bcl-2. Ces protéines jouent un rôle central dans l'intégration des signaux pro- et anti-apoptotiques, Bcl-2 et Bcl-xl jouant un rôle anti-apoptotique alors que Bax, Bak, Bid et Bad sont des protéines pro-apoptotiques. Les protéines de cette famille contrôlent les propriétés de perméabilité des membranes intracellulaires et en particulier les flux calciques et vont se transloquer, s'associer ou se dissocier lors de stimuli pro ou anti-apoptotiques (voir Hajnócsky et al 2000). Comme exemple de cibles des signaux calciques cytosoliques, des effecteurs possibles seraient la calcineurine et la calpaine. La calcineurine pourrait provoquer la déphosphorylation et la translocation de Bad vers la mitochondrie, entraînant à ce niveau l'association de Bad avec Bcl-xl, induisant ainsi l'apoptose (Wang et al 1999). La calpaine, une protéase ubiquitaire, été également proposée comme une cible cytosolique du calcium qui est impliquée dans la dégradation de Bid ou de Bax, dont les sous-produits présentent une aptitude importante à stimuler l'apoptose, les sous-produits de Bid par exemple en provoquant une perméabilisation de la membrane mitochondriale externe et la libération de cytochrome C de la mitochondrie (voir Hajnócsky et al 2000).

La déplétion en calcium du RE est potentiellement capable d'induire l'apoptose indépendamment de l'augmentation du calcium cytosolique. Les cibles moléculaires du RE sont les calréticulines ou les calnexines, des protéines chaperons calcium-dépendantes, possiblement impliquées dans le contrôle des processus de synthèse et de maturation protéique. La déplétion des stocks calciques réticulaires pourrait être également détectée par les récepteurs IP3 et RyR (voir Hajnócsky et al 2000). Une caspase du RE (caspase 12) peut être également activée par un stress au niveau du RE, y compris une perturbation de l'homéostasie calcique par des ionophores ou de la thapsigargine et engager ainsi l'apoptose indépendamment de la voie mitochondriale (Nakagawa et

al 2000). Cette caspase 12 pourrait d'autre part être activée par la calpaine et ainsi être sensible aux perturbations de l'homéostasie calcique cytosolique (Nakagawa et Yuan 2000).

La surcharge calcique mitochondriale pourrait être également à l'origine de l'apoptose. La capture de calcium dans la mitochondrie est due au transport de calcium le long de son gradient électrochimique par un uniport mitochondrial à faible affinité. Les mitochondries seraient capables de détecter des variations importantes (10-20 µM) de calcium libéré par des récepteurs IP3 ou RyR situés au niveau de zones de contact très étroites existant entre les mitochondries et le RE. La transmission du signal calcique ici a été assimilée à une transmission quasi-synaptique (du fait de la rapidité, de la directionnalité et de la spécificité de la transmission du signal) (Rizzuto et al 1998, Csórdas et al 1999). La mitochondrie participe donc aux mécanismes d'homéostasie calcique contribuant à rétablir l'état de repos (voir plus haut). Celle-ci peut être dépassée par l'ampleur de la tâche et lorsque la concentration mitochondriale de calcium augmente de manière excessive, le calcium active le PTP mitochondrial, un pore de transition de perméabilité, qui va alors expulser de la mitochondrie vers le cytosol de nombreux facteurs pro-apoptotiques (apotosis-inducing factor (AIF), Smac/Diablo, procaspases, cytochrome C ...), (Crompton 1999) et va provoquer une dépolarisation mitochondriale. Le PTP est un pore non spécifique formé d'un complexe hétéro-multimérique assemblé au contact des membranes internes et externes mitochondriales constitué d'au moins un canal anionique voltage-dépendant (VDAC) dans la membrane externe, une adénine nucléotide translocase (ANT) et la cyclophiline D (CyD) ainsi que d'autres protéines associées ; hexokinase (HK), créatine kinase (CK) et le récepteur aux benzodiazépines périphérique (PBR) (voir figure 7). Le PTP est notamment régulé par les protéines de la famille Bcl-2, Bcl-2 étant capable d'inhiber le pore de transition et ainsi l'expulsion de facteurs pro-apoptotiques (voir Hajnócsky et al 2003). Enfin, le PTP est capable de laisser passer le calcium qui va diffuser selon son gradient électrochimique (surtout selon son gradient de concentration puisque le gradient électrique est considérablement réduit) et quitter la mitochondrie. Une vague calcique peut alors être initiée et être transmise à des mitochondries voisines (Pacher et Hajnócsky, 2000) qui vont pouvoir à leur tour libérer des facteurs pro-apoptotiques.

III. Présentation du travail

Nous avons vu ainsi que le calcium joue un rôle central dans les fonctions physiologiques de la cellule et dans ses altérations. Dans les chapitres qui suivent, j'illustrerai certaines des notions présentées dans l'introduction et, notamment, grâce à des travaux publiés au cours de mes stages

post-doctoraux et depuis mon recrutement à Lille comme ATER puis comme maître de conférences :

1) L'exocytose non-calcium dépendante (article 1)
2) La sécrétion calcium-dépendante et le rôle des canaux calciques voltage-dépendants (articles 2 et 3)
3) Le calcium et la croissance cellulaire (article 4, 5 et 6)
4) Le calcium et la différenciation cellulaire (articles 7 et 8)

Chapitre 1

Le couplage stimulation-sécrétion dans les mastocytes

Travail post-doctoral : 1993-1996

Stage post-doctoral à "University College London, department of Physiology", octobre 1993-septembre 1996

A l'obtention de ma thèse, je suis parti effectuer un stage post-doctoral au département de Physiologie de University College London. Je souhaitais continuer à étudier la régulation de la sécrétion, à laquelle j'avais commencé à m'intéresser pendant la thèse (axée sur le couplage stimulation-sécrétion des cellules hypophysaires), et plus particulièrement son étape ultime, l'exocytose, *i.e.* la régulation du processus de fusion membranaire entre la membrane plasmique et la membrane vésiculaire. J'ai donc décidé d'intégrer le groupe dirigé par le Professeur Bastien Gomperts qui travaillait depuis une dizaine d'année sur le rôle des protéines G dans l'exocytose chez les mastocytes, modèle cellulaire très différent des cellules hypophysaires car non excitable et impliqué dans des réactions allergiques.

Le projet avait pour but de déterminer les protéines impliquées dans les dernières étapes de l'exocytose. Notre stratégie fut d'introduire des protéines dans le cytosol des mastocytes, et d'observer et caractériser leurs effets sur la fusion membranaire grâce à la mesure de la capacité membranaire. La difficulté résidait dans l'introduction des protéines d'intérêt dans le cytosol, de leur laisser le temps d'agir puis de stimuler la sécrétion avec un agent stimulant tel que le GTPγS, analogue non hydrolysable du GTP, qui stimule de façon irréversible les protéines G et l'exocytose dans les mastocytes, comme B.Gomperts l'avait montré antérieurement. Différentes techniques furent envisagées afin de faire pénétrer les protéines exogènes dans les cellules, telles que microinjection, perméabilisation réversible à l'ATP ou double patch. Ces techniques se sont révélées traumatisantes et empêchaient par la suite de pouvoir enregistrer par patch-clamp les cellules microinjectées ou perméabilisées. J'ai mis en place au laboratoire, afin de remédier à ceci, l'utilisation de composés piégés photoactivables (GTPγS piégé) qui sont inactifs et peuvent être activés par un flash ultra-violet (UV). Il fut dans ces conditions possible de faire pénétrer les protéines par patch-clamp dans le cytosol des mastocytes, de laisser les protéines agir pendant plusieurs dizaines de minutes et ensuite d'activer le GTPγS contenu dans les pipettes d'enregistrement (avec la protéine d'intérêt), et de mesurer le processus d'exocytose par mesure électrophysiologique de la capacité membranaire.

Article 1.

RhoGDI inhibits exocytosis in mast cells.

Mariot P, O'Sullivan AJ, Brown AM, Tatham PER. (1996) **EMBO-Journal**. 15 : 6476-6482

I. Position du problème et résultats

Les mastocytes sont un modèle tout à fait intéressant et original pour l'étude de l'exocytose. Ces cellules, qui contiennent dans le cytoplasme environ 900 granules, dégranulent en masse suite à un stimulus. Ces stimuli peuvent être subdivisés en deux catégories. Physiologiquement, celui procède notamment par la fixation du complexe Antigène-IgE sur un récepteur membranaire. L'antigène est généralement un allergène qui peut se fixer sur les IgE qui sont eux-mêmes liés étroitement à des récepteurs membranaires aux immunoglobulines de type IgεRI. En fait, tout ligand étant capable d'induire une oligomérisation des récepteurs IgεRI va agir comme stimulus de l'exocytose et entraîner une dégranulation des mastocytes ou des basophiles. L'oligomérisation va entraîner une cascade d'évènements comprenant une phosphorylation des résidus tyrosine kinase, suivie d'un recrutement de phospholipase C-γ et une production d'IP3 et de DAG, provoquant une augmentation de calcium cytosolique et une activation de la PKC. Pharmacologiquement, il est possible d'induire une dégranulation massive et rapide de ces cellules uniquement en activant la voie des GTP-binding protéines à l'aide par exemple de toxine de guêpes (mastoparan), ou en introduisant des activateurs de ces protéines (GTPγS par exemple) à l'intérieur des cellules (par patch-clamp par exemple). Ces activateurs (des sécrétagogues) activent directement la dégranulation. De plus, il est possible d'induire l'exocytose par une activation des protéines G en absence totale de calcium intracellulaire en utilisant des tampons calciques très puissants. Il a ainsi été supposé l'existence d'une classe de protéines G impliquée de manière directe dans le processus de fusion membranaire : la protéine G_E (Gomperts 1990, Pinxteren et al, 2000, pour revue). Hormis un premier candidat possible identifié comme une potentielle G_E ; la sous-unité Giα3 (Aridor et al 1993), la nature (et la réalité) de ces G_E restait largement élusive. Je me suis ainsi impliqué dans leur caractérisation et me suis notamment intéressé aux petites GTP-binding protéines monomériques de la superfamille des RasGTPases qui comprend plus de 60 membres différents répartis en 5 groupes majeurs : Ras, Rho, Rab, Arf et Ran. Je me suis plus particulièrement intéressé aux GTPases de la famille des RhoGTPases qui comprend les différentes Rac, Rho et CdC42. D'une manière générale, les GTPases fonctionnent comme des interrupteurs régissant, à l'aide d'une

réaction biochimique simple (l'hydrolyse du GTP), des processus biologiques complexes et variés. Ces protéines alternent donc entre deux états dans la cellule : un état actif lié au GTP et un état inactif lié au GDP (voir figure 8). La transition entre ces états est régulée par différentes protéines dont les GDI (Guanine Dissociation Inhibitor qui permettent, en s'associant avec le groupement hydrophobe de la RhoGTPase (groupement prenyl) l'échange entre le cytosol et la membrane des RhoGTPases), les GEF (Guanine nucleotide Exchange Factors qui échange le GDP pour le GTP) et les GAP (GTPase Activating Proteins qui hydrolysent le GTP en GDP) (Etienne-Manneville and Hall, 2002 pour revue).

J'ai démontré qu'une protéine nommée RhoGDI (pour Rho-Guanine Nucleotide Dissociation Inhibitor), qui est une protéine d'environ 23 kD se fixant aux protéines monomériques liant le GTP ("small GTP binding proteins ") de la famille Rho (qui comprend les Rho, Rac et Cdc42), entraînait une inhibition de l'exocytose et de la sécrétion d'hexaminidase, une enzyme sécrétée par les mastocytes. RhoGDI a pour fonction principale de faire alterner les membres de la famille Rho entre l'état soluble cytosolique (lié au RhoGDI, car ces petites protéines G sont très hydrophobes) et membranaire (Rho se lie à la membrane en se dissociant de RhoGDI).

Il a été montré par la suite dans le même modèle cellulaire que les GTPases Rac1, Rac2 et CdC42/G25K étaient capables d'induire la dégranulation des mastocytes (Brown et al , 1998) ou de faciliter la sécrétion calcium-dépendante de cellules neuroendocrines ou la neurotransmission (Doussau et al 2000, Li et al 2003). Les protéines Rho elle-mêmes ne semblent pas impliquées dans l'activation de l'exocytose puisque leur inactivation par ADP-rybosylation par la toxine botulinique C3 n'inhibait pas l'exocytose (Prepens et al, 1996, Mariot et al, observations personnelles).

II. Discussion

Ces résultats montraient l'importance d'un membre de la famille Rho dans la régulation de l'exocytose. Avant d'avancer plusieurs hypothèses pouvant être formulées quant au rôle des protéines de la famille Rho, Rac et CdC42, il faut rappeler l'immense complexité au centre de laquelle se trouve les RhoGTPases. En effet, ces RhoGTPases (au nombre de 20 au moins chez l'homme) sont régulées par pas moins de 60 activateurs (GEF) et 70 inactivateurs (GAP) et possèdent plus de 60 cibles connues ne possédant aucun site consensus. Cette complexité est sans égale pour une GTPase et montre leur importance centrale des régulations cellulaires. Avant de passer au rôle qui nous intéresse en rapport avec le traffic membranaire, il faut préciser que les RhoGTPases sont impliquées dans le contrôle transcriptionnel, la différenciation cellulaire, le cycle cellulaire et l'adhésion cellulaire.

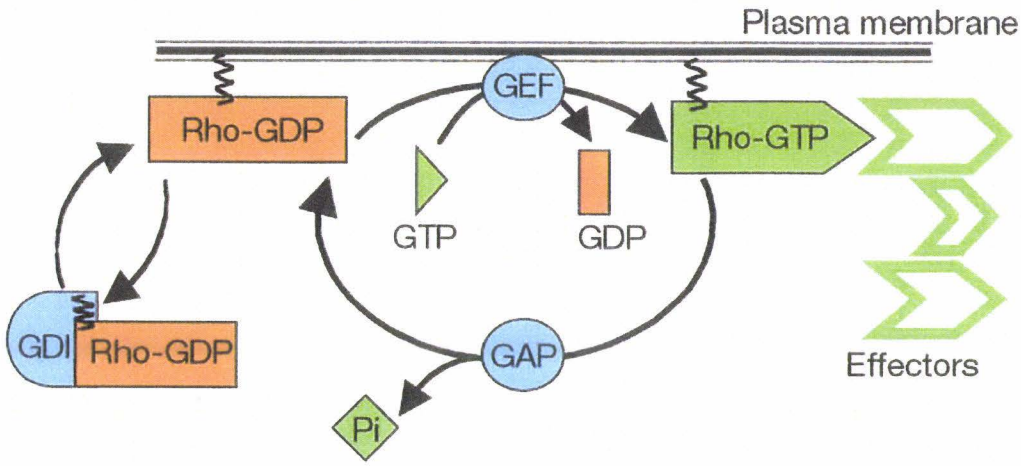

Figure 8 : Cycle des Rho GTPases.
D'après Etienne-Manneville et Hall (2002)

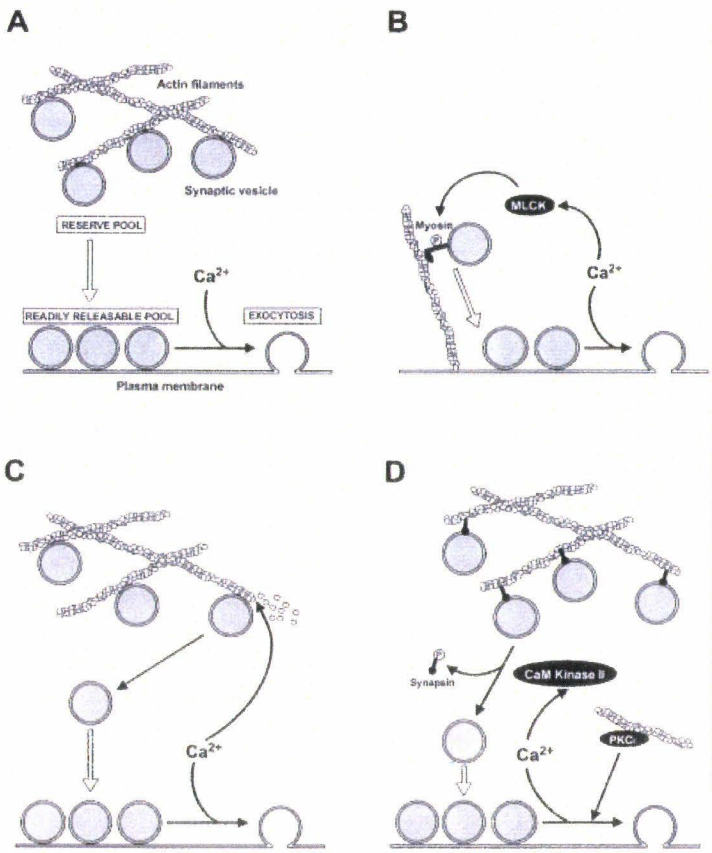

Figure 9 : Mécanismes potentiels d'implication du cytosquelette dans le processus d'exocytose.
Le cytosquelette pourrait jouer un rôle dynamique (A et B) dans lequel ses mouvements (A), ou la phosphorylation (B) de la myosine par la kinase des chaines légères de la myosine (MLCK), pourraient provoquer le déplacement des vésicules.
Dans les modèles C et D, le cytosquelette jouerait un rôle de barrière. Sa dépolymérisation (C), ou le détachement des vésicules des filaments d'actine grâce à la phosphorylation de la synapsine par la CaMkinaseII (D), entraînerait la migration des vésicules vers la membrane plasmique.
D'après Doussau et Augustine (2000).

A. Rôle dans la polymérisation du cytosquelette

Tout d'abord, il est intéressant de noter que les protéines cette famille interviennent dans la régulation de la polymérisation des filaments d'actine. Il est ainsi possible que l'action de RhoGDI sur l'exocytose passe par une action inhibitrice sur le cytosquelette. Il reste évidemment que le rôle du cytosquelette dans l'exocytose, s'il est certain, n'en reste pas moins confus.

D'après des figures de microscopie électronique, il a été montré qu'un réseau subapical d'actine était présent notamment dans les cellules polarisées tells que cellules exocrines. Ces évidences morphologiques laissaient à penser que ce réseau d'actine jouait un rôle de barrière passive aux granules de sécrétion. D'autres hypothèses ont été avancées, notamment un rôle moteur de la contraction des complexes acto-myosine dans le mouvement des vésicules, une facilitation de l'expulsion du contenu granulaire suite à la fusion, ou un rôle de maintien de la structure membranaire au cours de la fusion. Les discordances proviennent notamment de l'inefficacité de la cytochalasine D (un agent dépolymérisant de l'actine F) à bloquer l'exocytose, y compris dans les mastocytes (Norman et al 1994). En revanche, les agents inhibiteurs de la dépolymérisation (jasplakinolide) ou les agents stabilisants (phalloidine) bloquent généralement la sécrétion. Ceci permet de penser que l'exocytose nécessite un remaniement local du cytosquelette. Ce remaniement local pourrait s'accompagner de la formation d'un manteau d'actine à la surface des granules de sécrétion accompagné de la perte d'un marqueur granulaire impliqué dans les étapes de la fusion dépendante du complexe SNARE : la protéine G monomérique Rab3D (Valentijn et al 2000). Un autre argument convaincant concernant le rôle du cytosquelette dans l'exocytose repose sur l'expression sur la membrane vésiculaire de protéines s'associant de manière réversible aux protéines du cytosquelette, la synapsine (Doussau and Augustine 2000), dont la phosphorylation par la CaMKinase II favoriserait la translocation des granules de sécrétion vers la membrane plasmique (voir figure 9).

Les RhoGTPases sont connues pour réguler l'état de polymérisation du cytosquelette (pour revue voir Etienne-Manneville and Hall, 2002). Dans le contexte de la régulation du cytosquelette, les RHoA et B, Rac1 et 2 ainsi que CdC42 ont été les plus étudiées de la famille RhoGTPase. Depuis les premiers travaux axés sur l'étude du rôle des RhoGTPases, datant de 1992, il a été montré que Rho(RhoA) permettait l'assemblage de filaments contractiles d'actine/myosine encore appelés fibres de stress (stress fibers), et que Rac et CdC42 stimulaient la polymérisation de filaments d'actine entraînant la formation de larges protrusions membranaires riches en actine (lamellipodia) pour Rac, et la formation de protrusions cellulaires en forme de doigt (filopodia)

riche en actine pour CdC42. (pour revue voir Etienne-Manneville and Hall, 2002 ; Ridley 2001). L'action des RhoGTPases sur l'actine n'est pas directe mais est médiée par des membres des la famille des protéines WASp/WAVE (Wiskott-Aldrich syndrom protein) qui stimulent le complexe Arp2-3 (actin-related protein) permettant la formation de nouveau filaments d'actine (Machesky and Insall 1999).

Les RhoGTPases, en intervenant notamment sur la polymérisation du cytosquelette, pourraient ainsi participer au traffic membranaire intracellulaire et notamment aux mécanismes d'endo- et d'exocytose (Ridley 2001).

B. Rôle dans la formation de l'exocyste

L'exocyste est un complexe moléculaire impliqué dans une des étapes du traffic membranaire et plus particulièrement de l'exocytose. Vraisemblablement, ce complexe participe aux étapes de targetting (ciblage) et docking (ancrage) au cours de ce processus. Ce complexe est constitué de 8 sous-unités (6 sec protéines et deux sous-unités additionnelles Exo70p et Exo84p, Terbush et al 1996). Les homologues mammaliens de ces 8 sous unités ont été identifiés (Hsu et al 1996). L'exocyste est soumis à une régulation par les RhoGTPases chez la levure (voir Lipschutz and Mostov 2002 pour revue). A l'heure actuelle, s'il n'existe pas de données démontrant une interaction entre l'exocyste mammalien et des RhoGTPases, il n'est cependant possible d'exclure une telle possibilité.

C. Activation de la voie de transduction IP3/calcium

Comme cela a été montré sur des mastocytes, CdC42/Rac pourrait en fait intervenir beaucoup plus tôt dans la chaîne de transduction et, en interagissant avec une PLCγ1, favoriser la production d'IP3 et ainsi augmenter la mobilisation de calcium, ceci entraînant une sécrétion accrue (Hong-Geller and Cerione 2000). Cependant, cet effet ne devrait pas intervenir dans l'action de RhoGDI que nous avons observée dans la mesure où nos expériences étaient menées en présence de fortes concentrations de tampons calciques (10 mM EGTA).

D. Relation avec le complexe SNARE/protéines synaptiques

Il reste une hypothèse intéressante, à savoir que les RhoGTPases pourraient intervenir au niveau du complexe SNARE, complexe moléculaire universellement impliqué dans le processus fusionnel des membranes lipidiques, et des protéines synaptiques associées, hypothèse avancée par certains (Pinxteren et al 2000).

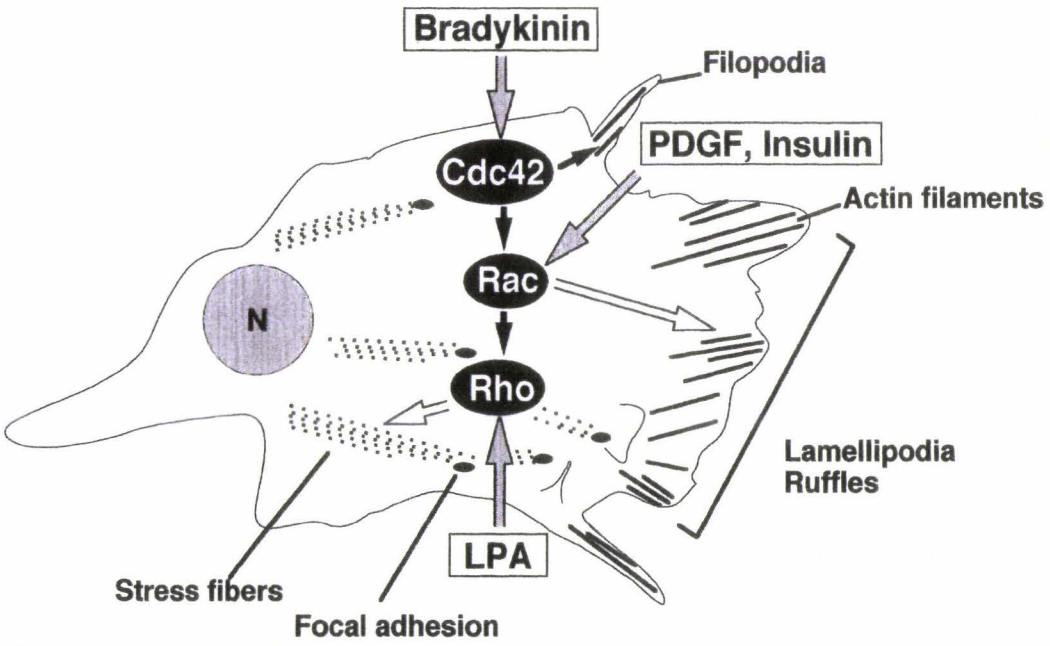

Figure 10 : Rôle des Rho-GTPases dans les mouvements du cytosquelette.
D'après Takai et al (2001).

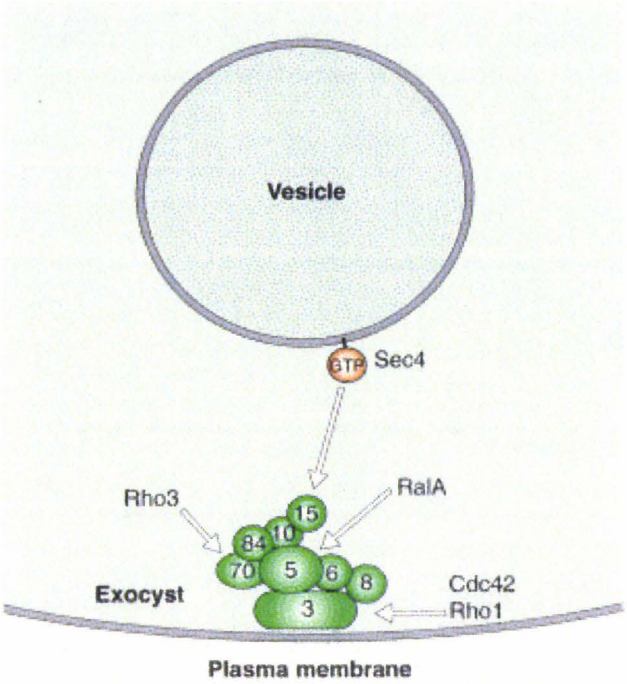

Figure 11 : Structure de l'exocyste.
D'après Lipschutz et Mostov (2002).

Les complexes fusionnels relatifs au processus d'exocytose comprennent de façon minimale la vésicule et les protéines membranaires participant à la formation du complexe SNARE selon l'arrangement minimal décrit dans la figure 6 (et un canal calcique VOC pour les cellules neuronales ou neuroendocrines). De nombreuses autres protéines cytosoliques ou membranaires, dont certaines ont été citées plus haut, participent au processus d'exocytose.

La régulation du complexe SNARE par les RhoGTPases pourrait être directe (association moléculaire avec une des sous-unités du complexe moléculaire) ou indirecte (régulation d'une protéine régulatrice du complexe SNARE). Il a été démontré par exemple que la stimulation de la sécrétion d'insuline des cellules β du pancréas par le mastoparan était médiée, notamment, par une stimulation de l'association de CdC42 avec la syntaxine, une protéine SNARE (Daniel et al, 2002). Une régulation indirecte pourrait illustrée par le fait que Rac active, parmi la longue liste de ses effecteurs, des phosphatidylinositol-phosphate kinase (PI3 kinase, PI-4 5 kinase), et que différentes étapes des processus d'exocytose sont stimulés par les protéines synaptiques qui se lient aux phosphoinositides. Ainsi, la synaptotagmine, possible calcium senseur de l'exocytose, s'associe t'elle avec les phospholipides membranaires de manière calcium-dépendante par l'intermédiaire de ses domaine C2A et C2B ; ou encore la protéine kinase C, potentiellement impliquée dans le processus de priming est-elle dépendante de son association avec les phospholipides membranaires.

Pour résumer, les modes d'action des RhoGTPases peuvent être illustrées selon la figure 12.

Pour terminer ce chapitre, il convient de préciser que, hormis les Rho-GTPases et Giα3 citées plus haut, d'autres candidats potentiels sérieux de G_E ont été identifiés :

1. les sous-unités βγ natives ou recombinantes de protéines G ont été démontrées comme des potentialisateurs de l'exocytose, sinon comme des activateurs (Pinxteren et al 1998)
2. Rab3A et Rab3D ont été supposées jouer un rôle important dans l'exocytose des mastocytes, mais leur rôle semble plutôt se situer en amont de G_E puisqu'il est possible d'activer la dégranulation mastocytaire avec du GTPγS dans des mastocytes exprimant le dominant négatif de Rab3A (Smith et al 1997).
3. Enfin, une autre GTPase a été démontrée comme activatrice de l'exocytose : l'ARF (ADP-rybosylation factor). Cependant, ceci a été démontré dans les lymphocytes (HL60) mais pas dans les mastocytes, mettant en doute son implication « universelle » dans le processus d'exocytose.

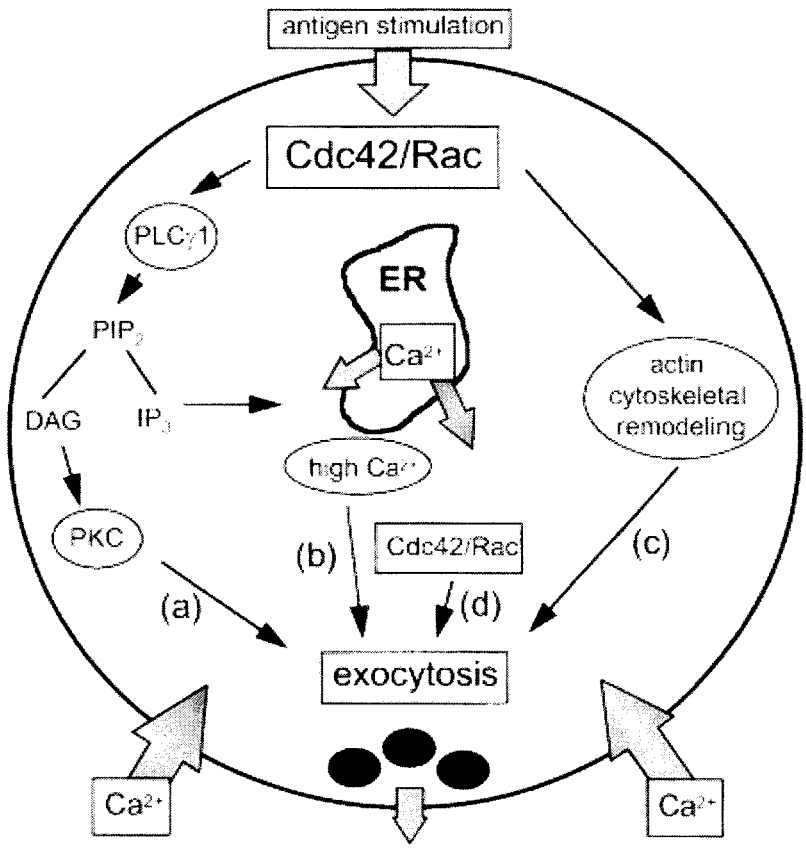

Figure 12 : Modes d'action possibles des Rho-GTPases au cours de l'exocytose.
D'après Hong-Geller and Cerione (2000)

The EMBO Journal vol.15 no.23 pp.6476–6482, 1996

Rho guanine nucleotide dissociation inhibitor protein (RhoGDI) inhibits exocytosis in mast cells

Pascal Mariot, Antony J.O'Sullivan, Anna M.Brown and Peter E.R.Tatham[1]

Department of Physiology, University College London, Rockefeller Building, University Street, London WC1E 6JJ, UK

[1]Corresponding author

Introducing non-hydrolysable analogues of GTP into the cytosolic compartment of mast cells results in exocytotic secretion through the activation of GTP binding proteins. The identity and mechanism of action of these proteins are not established. We have investigated the effects of Rho GDP dissociation inhibitor (RhoGDI) on exocytosis induced by guanosine 5'-*O*-(3-thiotriphosphate) (GTP-γ-S) in rat mast cells, introducing the protein into cells by means of a patch pipette and recording the progress of exocytosis by monitoring cell capacitance. To allow time for the protein to enter the cells and find its correct location, stimulation was provided 5–10 min after patch rupture by photolysing caged GTP-γ-S included in the pipette solution. When bovine RhoGDI was introduced into mast cells, exocytosis was inhibited at concentrations of 200–400 nM for native protein and 800 nM to 8 μM for the recombinant form. Protein denatured by heat or *N*-ethylmaleimide treatment did not inhibit. In permeabilized cells, recombinant RhoGDI increased the rate at which cells lose their ability to respond to GTP-γ-S. These data demonstrate that one or more small GTP binding proteins of the Rho family has a central role in the exocytotic mechanism in mast cells.

Keywords: exocytosis/GTP binding proteins/patch–clamp capacitance

Introduction

Non-hydrolysable analogues of GTP can activate exocytosis when delivered directly to the cytoplasmic compartment of rat peritoneal mast cells (Lillie and Gomperts, 1992) and guinea pig eosinophils (Nüsse *et al.*, 1990) either by membrane permeabilization or through a patch pipette. Under these conditions, there is neither an absolute requirement for the elevation of Ca^{2+}, nor is the presence of ATP essential at the time of stimulation. This is in contrast to other types of regulated secretory cells, such as neurones and many hormone-secreting cells, in which Ca^{2+} is an essential trigger of exocytosis. The mechanism of action and the identity of the GTP binding proteins that are involved in the final steps of the secretory mechanism in mast cells and eosinophils are not yet established, although some evidence exists for the involvement of $G\alpha_{i3}$ (Aridor *et al.*, 1993).

Rat peritoneal mast cells permeabilized by streptolysin O (SL-O) in the presence of guanosine 5'-*O*-(3-thiotriphosphate) (GTP-γ-S) and Ca^{2+} buffered in the micromolar range, can release approaching 100% of their stored products (Howell *et al.*, 1987). However, if this stimulus is provided subsequent to permeabilization, the response is reduced, declining progressively as the cells lose cytosol proteins (Howell *et al.*, 1989). This 'run-down' of secretion has been used as the basis of an assay to test the ability of factors isolated from brain cytosol to support secretion (O'Sullivan *et al.*, 1996). One such factor was identified as the protein Rac1, a GTP binding protein of the Rho family. Rac was shown to support secretion by retarding the run-down of SL-O-permeabilized mast cells, but only when it was provided as a complex with RhoGDI (Rho GDP dissociation inhibitor). In similar experiments, purified RhoGDI provided alone accelerated the run-down of the secretory response after permeabilization (O'Sullivan *et al.*, 1996). RhoGDI interacts with all members of the Rho family and can inhibit GDP release from, and GTP-γ-S binding to, post-translationally processed Rac1 and Rac2 (Ando *et al.*, 1992).

Exocytosis is characterized by the fusion of secretory granule membranes with the cell plasma membrane. Measuring the release of secretory products from permeabilized cells provides, at best, an indirect means of assessing its progress. There is also the risk that, under some conditions, damaged or leaky granules might give rise to release that is not exocytotic. Additionally, permeabilizing agents such as SL-O and digitonin may themselves interfere with the protein and membrane interactions that mediate and characterize exocytosis. A direct method of monitoring exocytosis that provides intracellular access but requires no permeabilizing agent is provided by the whole cell patch–clamp capacitance technique. The progress of exocytosis is followed by monitoring the increase in cell capacitance that occurs as secretory granules fuse with the plasma membrane (Lindau and Neher, 1988; Lindau, 1991). This method also has the advantage that, in contrast to permeabilized cells, the disruption to the plasma membrane caused by a patch pipette is localized to a small region. [For example, a pipette with an outer diameter as large as 4 μm in contact with a mast cell of diameter 13 μm (Helander and Bloom, 1974) will perturb <5% of the total surface.]

When GTP-γ-S is provided through a patch pipette in the whole cell configuration, rat mast cells undergo complete exocytosis, in common with permeabilized cells, and measurements of membrane capacitance (and conductance) have provided evidence of the individual fusion events showing that the release is truly exocytotic (Fernandez *et al.*, 1984). However, in contrast to the permeabilized cells, the response of patched clamped rat mast cells does not decline when the stimulus is provided 15–20 min after achieving the whole cell configuration

(i.e. after patch rupture) (Oberhauser *et al.*, 1992). Under such conditions, thorough dialysis of the cell interior through the single lesion will have taken place (Penner *et al.*, 1987). The persistence of the exocytotic response in rat mast cells in the whole cell configuration provides an opportunity to test the ability of specific proteins to inhibit membrane fusion. Since GTP binding proteins of the Rho family have been implicated in exocytosis (Price *et al.*, 1995; O'Sullivan *et al.*, 1996), we have investigated the effect of RhoGDI by introducing it into rat mast cells through a patch pipette, prior to stimulation with GTP-γ-S, monitoring changes in membrane capacitance as a measure of exocytosis.

Results

Effect of native RhoGDI

We have tested the effect of both the native and recombinant forms of RhoGDI on GTP-γ-S-induced exocytosis in rat mast cells, by including these proteins in the patch pipette solution. To allow time for exogenous proteins to enter the cell and to locate before stimulation, caged GTP-γ-S {guanosine-5′-*O*-(3-thiotriphosphate), 3-*S*-[1-(4,5-dimethoxy-2-nitrophenyl)ethyl]thio ester} was provided in the pipette solution. Cells were then maintained in the whole cell configuration for either 5 or 10 min before brief irradiation with UV light to release the active, non-hydrolysable nucleotide. When no proteins were present in the patch pipette, exocytosis, measured as an increase in cell capacitance (ΔC_m), was always complete within ~10 min of photolysis (completion time = 511 ± 80 s; ΔC_m = 13.2 ± 1.0 pF; mean ± SE, 12 cells). An example is shown in Figure 1A.

RhoGDI protein was isolated from bovine brain as described previously (O'Sullivan *et al.*, 1996). Purification was achieved by a series of chromatographic steps using the run-down bioassay. The final preparation gave a single band, visualized by silver staining, on analysis by SDS–polyacrylamide gel electrophoresis (O'Sullivan *et al.*, 1996). When the purified protein was included in the pipette solution, inhibitory effects were detected when the light pulse was given at either 5 or 10 min after patch rupture. In 6 out of 7 cells stimulated at 5 min, exocytosis was completely inhibited by 10 μg/ml purified RhoGDI. A typical record is shown in Figure 1A. When, under the same conditions, RhoGDI was provided at only 1 μg/ml, it failed to prevent exocytosis in any of the 8 cells studied. An example is shown in Figure 1A (note that although this particular response appears slower and less extensive than the protein-free control, these differences are not statistically significant). To minimize the possibility that the failure of the lower concentration of RhoGDI to inhibit secretion was due to its incomplete diffusion into the cell, the light pulse was delivered at 10 min in all the subsequent experiments. Even so, under these conditions, with RhoGDI present in the pipette at 1 μg/ml, exocytosis still occurred (2 cells). However, at 5–10 μg/ml, a strong inhibition of exocytosis was again observed. A typical record is shown in Figure 1B and the data from 11 cells treated in this way are summarized in Figure 3A ('native RhoGDI'). Of these cells, 10 completely failed to secrete and one cell underwent delayed exocytosis. Boiled

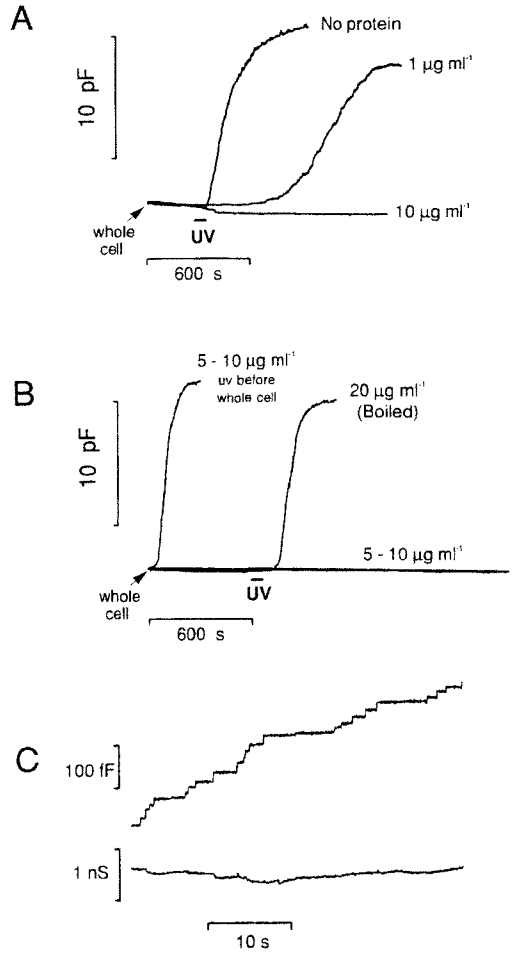

Fig. 1. Exocytosis in mast cells induced by photolysis of caged GTP-γ-S and its inhibition by RhoGDI purified from brain. Mast cells were maintained in the whole cell configuration for either 5 or 10 min, at which time they were exposed to UV illumination for 1 min. The pipette solution (see Materials and methods) included caged GTP-γ-S. (**A**) Examples of relative capacitance changes following stimulation at 5 min. The pipette solution contained no protein or included native RhoGDI at 1 or 10 μg/ml. (**B**) The effect of photoreleasing GTP-γ-S within the patch pipette before patch rupture (left-hand trace) and 10 min after patch rupture when native RhoGDI (5–10 μg/ml) was included in the pipette solution. The effect of heat-denatured protein (20 μg/ml, 'Boiled') upon exocytosis triggered at 10 min is also shown. (**C**) A portion of a capacitance record (cell loaded with 1 μg/ml RhoGDI), plotted at high resolution to show the stepwise increase in capacitance. A simultaneous record of access conductance is shown below.

RhoGDI (20 μg/ml) did not inhibit exocytosis (Figures 1B and 3A).

Alternatively, when 5–10 μg/ml RhoGDI was present in the pipette solution, but the pulse of UV light was applied just before patch rupture (in the cell-attached configuration), secretion commenced immediately. This is illustrated by the trace on the left in Figure 1B. GTP-γ-S was released within the pipette and, since it diffuses rapidly (Pusch and Neher, 1988), it initiated exocytosis before appreciable amounts of protein had entered the cell. This confirms that the cells were secretion competent before protein entry, that the light pulse did not damage them and that the inhibition observed was not caused by any rapidly diffusing substance in the pipette solution. Confirmation that the observed capacitance increases were

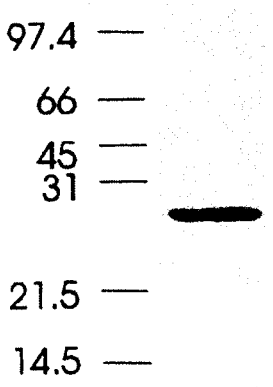

Fig. 2. Purity of recombinant RhoGDI–GST fusion protein. rRhoGDI was prepared as described in Materials and methods and analysed by SDS–PAGE by extraction into standard Laemmli sample buffer (Laemmli, 1970) under denaturing conditions and separation on a 12% gel. Visualization was by silver staining. The protein load was 1.6 μg. The figures indicate relative molecular mass in kDa.

due to exocytosis is provided by examining the capacitance records at high resolution. Part of a record from cells loaded with 1 μg/ml RhoGDI is reproduced in Figure 1C using an expanded scale, revealing the sequence of capacitance steps that indicate individual secretory granules fusing with the plasma membrane. These changes in capacitance are not accompanied by any significant changes in access conductance.

Effects of recombinant RhoGDI

Recombinant bovine RhoGDI–GST fusion protein (rRhoGDI) was expressed in transformed *Escherichia coli* (Hancock and Hall, 1993) and purified. Analysis by SDS–PAGE revealed a single band (Figure 2). Introduction of rRhoGDI into cells revealed inhibitory effects that were not as marked as those of the native protein. Mast cells were loaded with either rRhoGDI, boiled rRhoGDI or *N*-ethylmaleimide (NEM)-treated rRhoGDI and stimulated by photolysis of caged GTP-γ-S as described above. While exocytosis was completely inhibited in some cells, in others reduced or slowed responses were observed. The data summarized in Figures 3 and 4A reflect these three phenomena. In Figure 3A, inhibition manifest as the complete absence of exocytosis is depicted by showing the proportion of cells that responded with an increase in capacitance, however small. In Figures 3B and C and 4A, the characteristics of exocytosis in the responding cells, i.e. those in which exocytosis had not been completely suppressed, are summarized. Figure 3B shows the extents of the capacitance increases and Figure 3C shows the times taken (after stimulation) to reach completion. The inhibitory effect of the native protein (5–10 μg/ml) is much greater than that of the recombinant protein at higher concentrations (Figure 3A). At 100 μg/ml rRhoGDI, exocytosis was prevented in only two out of nine cells. However, the extent of secretion of the seven responding cells was about a half of that of the controls (Figure 3B) and the completion time was 80% longer (Figure 3C). At 200 μg/ml, exocytosis was prevented in 4 out of 7 cells and the secretion time of the three that underwent exocytosis was extended by 74%.

The control experiments are also summarized in Figure

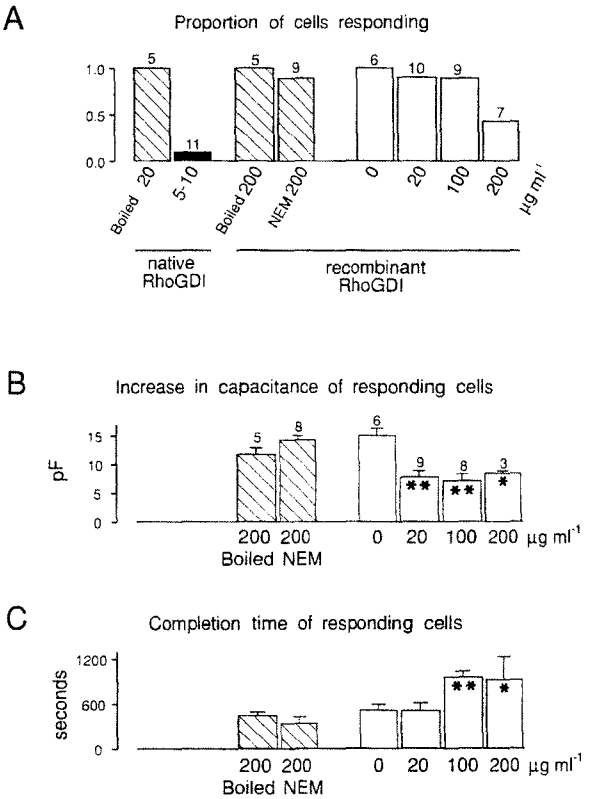

Fig. 3. Inhibition of exocytosis by both native and recombinant RhoGDI. These data summarize the inhibition of exocytosis in three ways. In (**A**) complete suppression of exocytosis is recorded by showing the proportion of cells that responded with any increase in capacitance. The figures above each column indicate the number of cells examined in each category. (**B**) and (**C**) describe the responses of cells in which exocytosis was not completely suppressed. (B) summarizes the extents of the capacitance increases and (C) the time taken to complete exocytosis after stimulation of the responding cells. Data in (B) and (C) are mean ± SE. Numbers of cells are indicated above each column in (B). Significant differences between each set of data and the boiled control are indicated by asterisks. * indicates $P < 0.05$ and ** indicates $P < 0.01$ (Mann–Whitney U test).

3 (hatched bars). When the recombinant protein had been boiled, it failed to inhibit or slow secretion when included at up to 200 μg/ml in the pipette solution. NEM-treated RhoGDI (200 μg/ml) also failed either to reduce or slow secretion.

When rRhoGDI was provided at 20 μg/ml, only one cell out of 10 failed to secrete. However, the progress of exocytosis in the 9 responding cells was quite different from that of the controls. The extent of secretion (Figure 3B) was reduced and, although the time to completion was not different from the controls, the rate of exocytosis was lower especially in the early stages. This is illustrated in Figure 4A where the derivative of averaged capacitance traces during the 200 s following stimulation is shown.

Effect of rRhoGDI on capacitance steps

The slowing effect of rRhoGDI on the progress of exocytosis is also demonstrated by analysis of the step increases in capacitance that characterize individual granule fusions. The distribution of step sizes for cells loaded with rRhoGDI and boiled rRhoGDI do not differ

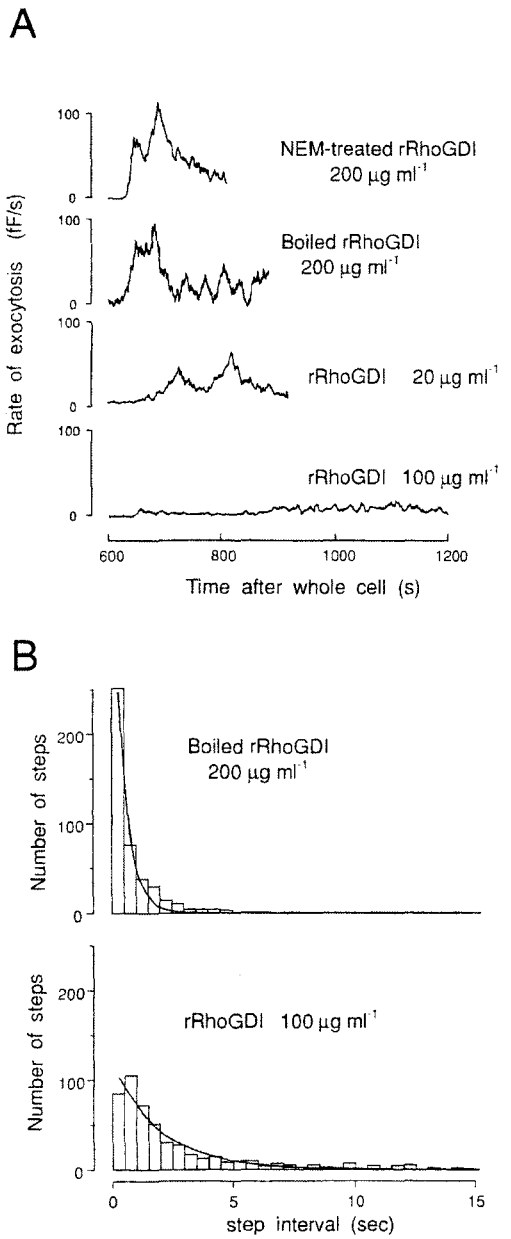

Fig. 4. Effect of rRhoGDI on the progress of exocytosis in responding cells. In (**A**) the rate of exocytosis (the derivative of averaged capacitance records) is plotted against time for cells loaded with either 20 μg/ml (10 cells) or 100 μg/ml (9 cells) rRhoGDI, or with 200 μg/ml NEM-treated rRhoGDI (9 cells) or 200 μg/ml boiled rRhoGDI (5 cells). (**B**) The effect of rRhoGDI upon the timing of capacitance steps. Histograms of the interval between successive steps during the first 30% of each capacitance increase are shown. The curves are single exponential fits (see Materials and methods). For rRhoGDI at 100 μg/ml the time constant of the fitted curve is 2020 ms; for boiled RhoGDI the time constant is 674 ms. Further details are given in Table I.

significantly (data not shown). However, the distribution of interstep times (time between successive events) is quite different for cells loaded with rRhoGDI compared with either of its inactivated forms. Examples of these distributions are shown in Figure 4B. Each histogram was fitted to a single exponential curve and the characteristic time constant was calculated. The results are shown in Table I. The time constant for cells loaded with rRhoGDI at 20 μg/ml was 54% longer than that of the controls, and for cells loaded with rRhoGDI at 100 μg/ml it was longer by a factor of 2.

rRhoGDI accelerates run-down in permeabilized cells

An indication that RhoGDI might be inhibitory to exocytosis was first obtained in experiments with partially responsive mast cells permeabilized by SL-O (O'Sullivan *et al.*, 1996). Acceleration of run-down by the purified protein was observed, beginning as early as 5 min after permeabilization, but the extent of this effect was difficult to assess. This is because the rate at which permeabilized cells run down varies widely from batch to batch and because of the steepness of the run-down curves. Because of its variability and in view of the concern that the run-down phenomenon might be an artefact of the permeabilizing agent SL-O, we have compared the effects of rRhoGDI in patched and SL-O-permeabilized cells. Figure 5A shows the effect of different protein preparations upon mast cells that were permeabilized at time zero and challenged at subsequent times with GTP-γ-S (100 μM) and Ca^{2+} (pCa 5). In the presence of rRhoGDI, the run-down of the response is more rapid. The concentration dependence of the effect on run-down is shown in Figure 5B. The relative cell responsiveness is expressed as the ratio of secretion stimulated by GTP-γ-S 10 min after permeabilization in the presence of boiled rRhoGDI to that with intact protein. The EC_{50} for the acceleration of run-down is in the region of 7 μg/ml. At 20 μg/ml, the concentration at which the effects of the recombinant protein become apparent in patch–clamped cells, the relative responsiveness of the permeabilized cells is at its lowest.

Discussion

To test the effect of an exogenous protein on the mechanism of exocytosis requires its introduction into the cell by a method that does not compromise its ability to undergo membrane fusion. To perfuse the cell interior effectively with a macromolecular solute requires the creation of substantial holes in the plasma membrane. These may be created by permeabilization or by a patch pipette. Because macromolecules diffuse slowly, several minutes may be required for them to accumulate within the cell. During this period, leakage of both low molecular mass solutes and cytosolic proteins occurs from the cell and, in consequence, its ability to respond to a stimulus may diminish with time. For example, rat mast cells permeabilized by SL-O gradually lose their ability to respond to GTP-γ-S over a 20 min period (Howell *et al.*, 1989) (Figure 5A). Patch–clamped rat mast cells, however, do not run down appreciably in the 20 min following patch rupture. The requirements of the patch–clamp technique impose working conditions quite different from those of the permeabilized cell experiments and these may account for the difference in responsiveness. For example, the intracellular solution has different ionic composition and pH (see Materials and methods). Also the electrophysiological experiments were performed at room temperature rather than at 30°C. In addition, the patch–clamped cells were attached to glass coverslips and this may have activated adhesion molecules that interact with intracellular systems such as the cytoskeleton. Finally, the lesions

Table I. Analysis of the distribution of intervals between successive capacitance steps for cells loaded with rRhoGDI

Protein	Concentration (μg/ml)	No. of steps	No. of cells	Time constant (ms)	SE	χ^2	*n*
rRhoGDI	100	515	6	2020	110	1.72	20
rRhoGDI	20	419	5	1040	57	0.48	13
Boiled-rRhoGDI	200	446	5	674	41	3.7	10
NEM-treated rRhoGDI	200	382	5	671	38	0.74	12

χ^2 values refer to goodness of fit and *n* is the number of data points fitted (histogram class intervals, see Materials and methods). The two time constants for cells loaded with rRhoGDI were each significantly different (*t* test, $P < 0.0005$) from either of those observed with cells loaded with inactivated protein.

generated by SL-O are distributed over the whole plasma membrane in contrast to a single hole made by the patch pipette, possibly allowing more leakage from the permeabilized cells. All in all it is clear that there are substantial differences between these two experimental systems. [Note, incidentally, that patch–clamped mast cells from mutant beige mice do run-down, i.e. their ability to respond to (photoreleased) GTP-γ-S is lost within ~5 min; P.Mariot and P.E.R.Tatham, unpublished.] We have taken advantage of the persistence of the exocytotic response in rat mast cells to enable us to load them with exogenous protein, in particular RhoGDI, through a patch pipette, detecting exocytosis by monitoring capacitance. The effect of the loaded protein upon exocytosis was tested by applying a stimulus (photoreleased GTP-γ-S) at up to 10 min after breaking into the cell. In control experiments, the pipette solution contained either inactivated proteins or no protein at all, and uncaging GTP-γ-S resulted in large, rapid capacitance increases, characteristic of full exocytosis. This confirmed that the exocytotic machinery remained intact throughout the loading period. Full exocytosis also occurred promptly when inhibitory protein was not given sufficient time to diffuse into the cell (Figure 1B).

The introduction of bovine RhoGDI, either purified from brain or a recombinant form, has an inhibitory effect upon exocytosis in mast cells. RhoGDI purified from brain is a potent inhibitor (Figure 3A), almost completely suppressing exocytosis at 5–10 μg/ml or 200–400 nM (calculated M_r = 23 421; Fukumoto *et al.*, 1990). The inhibitory effects of this protein are detectable as early as 5 min after patch rupture (Figure 1A). rRhoGDI is also inhibitory, but it is not as effective as the native protein even when provided at a 20-fold higher concentration (up to 200 μg/ml or 8 μM, Figure 3A). The lower efficacy of the recombinant protein compared with its native form may be due to the fact that one or more domains are incorrectly folded. Alternatively, it may lack a post-translational modification, such as a phosphorylation, that is required for its full activity. It has been reported that dephosphorylation of purified RhoGDI reduces the stability of the Rho A–RhoGDI complex (Bourmeyster and Vignais, 1996).

Following previous work, in which native RhoGDI was shown to accelerate run-down in permeabilized mast cells (O'Sullivan *et al.*, 1996), we now show that recombinant RhoGDI has a similar effect and demonstrate its concentration dependence (Figure 5). Detailed concentration–response data are difficult to obtain from patch–clamp experiments. The EC_{50} for inhibition is 7 μg/ml or ~300 nM

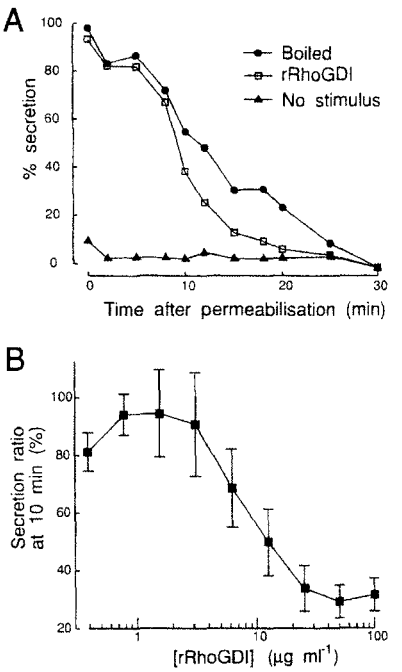

Fig. 5. Effect of rRhoGDI on the run-down of SL-O-permeabilized mast cells. (**A**) Data from cells that were exposed to SL-O at 0°C for 5 min, washed and then brought to 30°C to bring about permeabilization. This was in the presence of 40 μg/ml rRhoGDI. After the indicated times, a stimulus (pCa 5 with GTP-γ-S, 100 μM) was applied and the incubation continued for a further 10 min, at which time the cells were centrifuged and the supernatants assayed for secreted hexosaminidase. Similar data were obtained on three occasions. 'No stimulus' indicates that no GTP-γ-S was provided and the permeabilized cells were maintained at pCa 8 throughout. (**B**) The concentration dependence of the effect of rRhoGDI on the run-down of exocytosis in SL-O-permeabilized mast cells. The data were obtained from cells stimulated 10 min after permeabilization. The ordinate is a measure of cell responsiveness to GTP-γ-S. It is the ratio of the extent of secretion from cells loaded with boiled rRhoGDI to that from cells loaded with intact protein (mean ± SE, n = 3).

(Figure 5B). The lowest concentration at which we have observed consistent effects of this protein in patch–clamped cells is 20 μg/ml. Bearing in mind the considerable dissimilarities between the two experimental systems, these values are comparable and we conclude that the permeabilized cell data provide additional evidence of inhibition by the recombinant protein.

When the capacitance records are examined in more detail to reveal the individual granule fusions that comprise exocytosis, it becomes clear that the slowing of secretion caused by rRhoGDI is due to extended intervals between successive capacitance steps (Figure 4B and Table I). The

distributions of the extended interstep times retain an exponential shape, characteristic of random events occurring with probabilities determined by a Poisson distribution. As expected, the heights of the steps (measures of granule size) and their rise times are not affected by the presence of the protein.

Permeabilized mast cells stimulated by GTP-γ-S and Ca^{2+} at the time of permeabilization undergo an all-or-none response (Hide *et al.*, 1993), and a similar process may occur in patch-clamped mast cells, although we have not attempted to determine this. rRhoGDI decreases not only the rate of exocytosis in our experiments, but also the extent of secretion in individual cells and they cannot therefore be responding in an all-or-none fashion. Whether this is because rRhoGDI removes or inhibits a factor that determines the binary response at the cellular level or is due to the leakage of some other factor remains to be determined.

Since RhoGDI is known to bind to all members of the Rho family (Rho, Rac and Cdc42), it should compete with endogenous binding sites within the cell for all these GTPases. Normalized diffusion rates for the entry of macromolecules through a patch pipette into cells of similar size to rat mast cells have been estimated by Pusch and Neher (1988). Using their equation 18 with an average access conductance of 100 nS, we estimate a time constant for entry of RhoGDI of ~200 s. Several assumptions are made in this calculation, and the actual time constant may lie between 100 and 300 s but, since the stimulus was applied at 600 s in most of our experiments, the RhoGDI concentration in the cytosol should have been close to that in the patch pipette. Within intact cells Rho, Rac and Cdc42 proteins are either attached to membranes where nucleotide exchange can take place only with the assistance of a guanine nucleotide exchange factor or they exist as soluble complexes with endogenous RhoGDI. Since the complexes leak from permeabilized cells (O'Sullivan *et al.*, 1996), they will also wash out from the cells after patch rupture. At the same time, the virtually infinite reservoir of exogenous RhoGDI that is available from the pipette should bind to the membrane-associated Rho proteins effectively extracting them from the cell. Alternatively, the exogenous RhoGDI may compete with the guanine nucleotide exchange factors for these GTPases. Both mechanisms would have consequences not only for secretion, but also for the organization of the cytoskeleton. In summary, these results demonstrate that small GTP binding proteins of the Rho family are essential for exocytosis in mast cells.

Materials and methods

Cells

Rat mast cells were prepared by peritoneal lavage of male Sprague–Dawley rats (300–400 g). For patch-clamp studies, the cells were washed once in a buffer containing 137 mM NaCl, 2.7 mM KCl, 1 mM $MgCl_2$, 1.8 mM $CaCl_2$, 10 mM HEPES pH 7.2 and placed on glass coverslips mounted in plastic Petri dishes. For permeabilized cell experiments, mast cells were purified to >99% purity by centrifugation through a Percoll step as described previously (Tatham and Gomperts, 1990) and suspended in buffer containing 137 mM NaCl, 2.7 mM KCl, 1 mM $MgCl_2$, 20 mM HEPES pH 6.8 and 3 mM Ca.EGTA to maintain pCa 5 or pCa 8 as appropriate.

Capacitance measurements

Membrane capacitance was monitored by the patch-clamp technique using the whole cell configuration and a digital phase detector (Joshi and Fernandez, 1988; Monck *et al.*, 1990; Fidler and Fernandez, 1989). A sinusoidal voltage (830 Hz, 50 mV peak-peak) was applied to the command input of an EPC-7 patch-clamp amplifier at a holding potential of 0 mV. Current amplitude was recorded at two orthogonal phase angles to provide signals proportional to the real and imaginary parts of the admittance. The phase alignment was determined periodically by the phase tracking technique (Fidler and Fernandez, 1996). The real and imaginary components reflected changes in access resistance and capacitance respectively. The pipette solution contained 140 mM potassium glutamate, 10 mM HEPES, 7 mM $MgCl_2$ and 50 μM ATP Mg buffered to pH 7.2 with KOH. K.EGTA and Ca.EGTA were also present to give a total EGTA concentration of 10 mM and pCa 6.7 to pCa 6.3. To stimulate exocytosis, 110 μM caged GTP-γ-S was included in this solution. Pipettes were coated with Sylgard and had resistances of 1–3 MΩ. The mean initial access conductance was 114 ± 3 nS and the mean final access conductance was 84 ± 4.5 nS (SEM, n = 60). The cell membrane resistance (d.c. current) did not change appreciably during capacitance measurements. When proteins were present in the intracellular solution, the tip of the pipette was dipped in protein-free solution for a few seconds before back-filling. For calculations of the extents of the capacitance increases and of the completion times of exocytosis, the end-point was taken as the appearance of a plateau in the capacitance trace or the achievement of a level within 95% of the maximal change. All patch-clamp experiments were carried out at room temperature (20–25°C). Histograms of capacitance step intervals were constructed from data obtained from the initial 30% of the capacitance increase for each cell analysed. Curve fitting to these histograms was performed using 'Origin' (Microcal Software Inc.). Single exponential fits, yielding values of time constant, χ^2 and SE, were obtained by the Levenberg–Marquardt method, weighting each data value statistically ($1/y$).

Photolysis

GTP-γ-S was released by exposing cells loaded with caged GTP-γ-S to a 60 s pulse of light from a high pressure mercury arc lamp (200 W, $\lambda \geq 360$ nm). This light pulse was filtered through water to remove infrared radiation and its intensity was reduced by a neutral density filter (absorbance 0.1). The light was delivered through a fibre optic directed at a region including both the cell and the pipette tip. Caged GTP-γ-S was obtained from Molecular Probes.

Secretion measurements

Cells were permeabilized by SL-O (Murex diagnostics, Dartford Kent) applied to mast cells at ice temperature (1.6 IU/ml). After 5 min, the cells were diluted into buffer containing 137 mM NaCl, 2.7 mM KCl, 1 mM $MgCl_2$, 20 mM PIPES pH 6.8 and 0.1 mM EGTA, and then washed to remove unbound SL-O by centrifugation and resuspension at ice temperature. Permeabilization was started by warming the cells to 30°C. After set periods of time, the cells were stimulated to secrete by transferring 20 μl aliquots to 40 μl of buffer including GTP-γ-S (100 μM final concentration) and Ca.EGTA (3 mM final concentration) to maintain pCa 5 or pCa 8 as appropriate. After a further 10 min incubation at 30°C, the cells were centrifuged and the supernatants assayed for secretion of hexosaminidase as previously described (Gomperts and Tatham, 1992).

Recombinant proteins

RhoGDI–GST fusion protein was expressed in transformed *E.coli* (Hancock and Hall, 1993) obtained from Alan Hall (Laboratory of Molecular Cell Biology, UCL). Bacterial cultures were grown to saturation and challenged with isopropyl-β-thiogalactopyranoside to induce expression. The pelletted bacteria were then resuspended and washed in phosphate-buffered saline (PBS), sonicated on ice and, after centrifugation, the supernatant was removed and mixed with glutathione–agarose beads. These were washed with PBS and then incubated with 20 U/ml of human thrombin at room temperature for 2 h. The supernatant was incubated with *p*-aminobenzamidine agarose beads to remove free thrombin and then dialysed overnight against 10 mM Na–HEPES pH 7.2, 150 mM NaCl. The recombinant protein was quantified using the Bradford assay.

Inactivated proteins

Proteins were heat-denatured by maintaining them at 95°C for 15 min. Recombinant RhoGDI was also inactivated by exposure to NEM (1 mM,

37°C, 30 min). The residual NEM was then neutralized by incubation with dithiothreitol (DTT, 2 mM, 30 min) and the modified protein was passed through a gel filtration column (NAP5) to remove DTT. The final preparation was homogeneous as assessed by anion-exchange chromatography, gel filtration and SDS–PAGE. Inactivation of rRhoGDI was tested by using it to extract GTP binding Rho-related proteins from permeabilized mast cells. Briefly, mast cells were permeabilized by SL-O in the presence of rRhoGDI that had been pre-treated with (or without) NEM. After 25 min, the cells were centrifuged (14000 *g*) and an acetone precipitate of the supernate was prepared. The precipitate was dispersed in standard sample buffer (Laemmli, 1970), subjected to SDS–PAGE, blotted on to nitrocellulose and overlaid with [α-^{32}P]GTP. Autoradiography of the blot then revealed the GTP binding proteins extracted from the cells by both NEM-treated and unmodified RhoGDI. The level of GTP binding obtained using NEM-treated RhoGDI was 28% of the control.

Acknowledgements

We are very grateful to Julio Fernandez for his extensive support and for making capacitance software available to us. We also thank Alan Hall for providing transformed *E.coli*. This work was supported by the Wellcome Trust, (038975/Z/93/Z/1.5/MP/HA and 032639/Z/90/Z1.27/MJM/LEC).

References

Ando,S. *et al.* (1992) Post-translational processing of rac p21s is important both for their interaction with the GDP/GTP exchange proteins and for their activation of NADPH oxidase. *J. Biol. Chem.*, **267**, 25709–25713.

Aridor,M., Rajmilevich,G., Beaven,M.A. and Sagi-Eisenberg,R. (1993) Activation of exocytosis by the heterotrimeric G protein Gi3. *Science*, **262**, 1569–1572.

Bourmeyster,N. and Vignais,P.V. (1996) Phosphorylation of Rho GDI stabilises the Rho A–Rho GDI complex in neutrophil cytosol. *Biochem. Biophys. Res. Commun.*, **218**, 54–60.

Fernandez,J.M., Neher,E. and Gomperts,B.D. (1984) Capacitance measurements reveal stepwise fusion events in degranulating mast cells. *Nature*, **312**, 453–455.

Fidler,N. and Fernandez,J.M. (1989) Phase tracking: an improved phase detection technique for cell membrane capacitance measurements. *Biophys. J.*, **56**, 1153–1162.

Fukumoto,Y., Kaibuchi,K., Hori,Y., Fujioka,H., Araki,S., Ueda,T., Kikuchi,A. and Takai,Y. (1990) Molecular cloning and characterization of a novel type of regulatory protein (GDI) for the rho proteins, ras p21-like small GTP-binding proteins. *Oncogene*, **5**, 1321–1328.

Gomperts,B.D. and Tatham,P.E.R. (1992) Regulated exocytotic secretion from permeabilized cells. *Methods Enzymol.*, **219**, 178–189.

Hancock,J.F. and Hall,A. (1993) A novel role for RhoGDI as an inhibitor of GAP proteins. *EMBO J.*, **12**, 1915–1921.

Helander,H.F. and Bloom,G.D. (1974) Quantitative analysis of mast cell structure. *J. Microsc.*, **100**, 315–321.

Hide,I., Bennett,J.P., Pizzey,A., Boonen,G., Bar-Sagi,D., Gomperts,B.D. and Tatham,P.E.R. (1993) Degranulation of individual mast cells in response to Ca^{2+} and guanine nucleotides: an all-or-none event. *J. Cell Biol.*, **123**, 585–593.

Howell,T.W., Cockcroft,S. and Gomperts,B.D. (1987) Essential synergy between Ca^{2+} and guanine nucleotides in exocytotic secretion from permeabilized mast cells. *J. Cell Biol.*, **105**, 191–197.

Howell,T.W., Kramer,I.M. and Gomperts,B.D. (1989) Protein phosphorylation and the dependence on Ca^{2+} for GTP-γ-S stimulated exocytosis from permeabilized mast cells. *Cell Signalling*, **1**, 157–163.

Joshi,C. and Fernandez,J.M. (1988) Capacitance measurements: an analysis of the phase detector technique used to study exocytosis and endocytosis. *Biophys. J.*, **53**, 885–892.

Laemmli,U.K. (1970) Cleavage of structural proteins during the assembly of the head of bacteriophage T4. *Nature*, **227**, 680–685.

Lillie,T.H.W. and Gomperts,B.D. (1992) Guanine nucleotide is essential, Ca^{2+} is a modulator, in the exocytotic reaction of permeabilized rat mast cells. *Biochem. J.*, **288**, 181–187.

Lindau,M. (1991) Time-resolved capacitance measurements: monitoring exocytosis in single cells. *Q. Rev. Biophys.*, **24**, 75–101.

Lindau,M. and Neher,E. (1988) Patch-clamp techniques for time-resolved capacitance measurements in single cells. *Eur. J. Physiol.*, **411**, 137–146.

Monck,J.R., Alvarez de Toledo,G. and Fernandez,J.M. (1990) Tension in secretory granule membranes causes extensive membrane transfer through the exocytotic fusion pore. *Proc. Natl Acad. Sci. USA*, **87**, 7804–7808.

Nüsse,O., Lindau,M., Cromwell,O., Kay,A.B. and Gomperts,B.D. (1990) Intracellular application of GTP-5′-*O*-(3-thiotriphosphate) induces exocytotic granule fusion in guinea pig eosinophils. *J. Exp. Med.*, **171**, 775–786.

Oberhauser,A.F., Monck,J.R., Balch,W.E. and Fernandez,J.M. (1992) Exocytotic fusion is activated by Rab3a peptides. *Nature*, **360**, 270–273.

O'Sullivan,A.J., Brown,A.M., Freeman,H.N.M. and Gomperts,B.D. (1996) Purification and identification of FOAD-II, a cytosolic protein that regulates secretion in streptolysin-O permeabilized mast cells, as a rac/rhoGDI complex. *Mol. Biol. Cell*, **7**, 397–408.

Penner,R., Pusch,M. and Neher,E. (1987) Washout phenomena in dialyzed mast cells allow discrimination of different steps in stimulus–secretion coupling. *Biosci. Rep.*, **7**, 313–321.

Price,L.S., Norman,J.C., Ridley,A.J. and Koffer,A. (1995) Small GTPases, rac and rho, as regulators of secretion in mast cells. *Curr. Biol.*, **5**, 68–73.

Pusch,M. and Neher,E. (1988) Rates of diffusional exchange between small cells and a measuring patch pipette. *Pflügers Arch.*, **411**, 204–211.

Tatham,P.E.R. and Gomperts,B.D. (1990) Cell permeabilization. In Siddle,K. and Hutton,J.C. (eds.), *Peptide Hormones: A Practical Approach*. IRL Press, Oxford, pp. 257–269.

Received on June 12, 1996; revised on September 4, 1996

Chapitre 2

Le couplage stimulation-sécrétion dans les cellules neuroendocrines pancréatiques

Travail post-doctoral : 1996-1997

Stage post-doctoral à l'Université Catholique de Louvain, département de Physiologie et Pharmacologie, Unité d'endocrinologie et métabolisme, 1996-1997

J'ai ensuite effectué un second stage post-doctoral à l'Université Catholique de Louvain (et financé par l'Université) au département de Physiologie et Pharmacologie, dans l'Unité d'endocrinologie et métabolisme dirigée par le Professeur J-C Henquin qui travaille depuis plusieurs années sur le couplage stimulation-sécrétion dans les cellules β du pancréas qui sécrètent l'insuline. Dans le cadre de ces travaux, j'ai étudié le rôle des phosphatases dans le couplage stimulation-sécrétion **(article 2)** et le mécanisme d'action des sulfonylurées sur les cellules β **(article 3)**.

Article 2.

Inhibitors of protein phosphatase 1 and 2A inhibit insulin secretion by decreasing the magnitude and the efficacy of the Ca^{2+} signal in pancreatic β cells.

Sato Y, Mariot P, Detimary P, Gilon P, Henquin J-C (1998) **Brit.J.Pharmacol.** 123 : 97-105

I. Position du problème et résultats

La sécrétion d'insuline est étroitement dépendante des phénomènes de phosphorylations et déphosphorylations cellulaires. Il est généralement admis que la sécrétion hormonale par les cellules β du pancréas est stimulée par les phénomènes de phosphorylations, provoqués par exemple par une activation des kinases (PKA ou PKC ou autres) ou par une inhibition des phosphatases. Cependant, les études concernant le rôle de ces phosphorylations sur le mécanisme sécrétoire sont relativement contradictoires puisque tandis que certains travaux démontrent une action stimulatrice des phosphorylations sur l'exocytose alors que d'autres prouvent le contraire (pour revue voir Jones and Persaud, 1998).

Nous avons étudié l'action des inhibiteurs des phosphatases 1 et 2A, l'acide okadaique et la calyculine A, sur la sécrétion d'insuline des cellules β du pancréas. Nous avons montré que l'inhibition des phosphatases entraînait :

1) une diminution du calcium intracellulaire, diminution due en partie à une réduction des courants calciques membranaires

2) une inhibition de la sécrétion d'insuline induite par différents agents stimulants des ilôts de Langerhans : le glucose, les sulfonylurées, une dépolarisation potassique ou le kétoisocaproate, inhibition due partiellement à une réduction des courants calciques, ;

3) mais également une diminution de la sécrétion d'insuline liée à une action indépendante de l'entrée de calcium et probablement due à une action à un niveau distal des voies de transduction des différents sécrétagogues.

II. Discussion

Ces résultats, ainsi que d'autres (Ammon et al 1996, Zhang and Kim 1995), montrent que des protéines phosphorylées peuvent exercer une action inhibitrice sur la sécrétion et qu'une déphosphorylation peut être aussi importante dans le processus sécrétoire que les processus de

phosphorylations, qui sont eux notamment impliqués dans l'étape de « priming » ou amorçage des granules de sécrétion, c'est-à-dire l'étape où ils acquièrent la compétence « fusionnelle ». L'identification de ces phosphorylations inhibitrices du processus sécrétoire reste à déterminer. Cependant, certaines pistes existent :

1. La mobilité des vésicules synaptiques est réduite par un traitement à l'acide okadaique (Guatimosim et al 2002). Ceci pourrait se traduire par une diminution de la vitesse d'exocytose des granules d'insuline.
2. Un mécanisme similaire a été montré récemment pour la phosphatase 2B : en effet, la déphosphorylation calcium-dépendante des chaines lourdes de la kinésine, qui permet l'attachement des granules aux microtubules, par les phosphatases 2B (calcineurines), assure le transport des granules le long des microtubules et un réemplissage des réserves de granules sous-membranaires. Ainsi, une inhibition de la PP2B dans ces cellules β du pancréas, entraîne également une diminution de la sécrétion d'insuline glucose-dépendante. Il est à signaler que ce travail montrait que deux autres protéines étaient déphosphorylées de manière calcium-dépendante dans ces cellules (Donelan et al, 2002).
3. Il a été montré que la phosphatase PP2A subissait une translocation du cytosol vers les fractions membranaires lors de la dégranulation mastocytaire et que cette translocation, ainsi que la dégranulation, étaient inhibées par l'acide okadaique (Ludowyke et al 2000). D'autre part, une étude ultérieure a précisé que PP1 et 2A s'associaient transitoirement avec la myosine lors de la dégranulation des mastocytes et que l'inhibition de PP2A inhibait cette dégranulation en provoquant une augmentation de la phosphorylation des chaines légères et lourdes de la myosine (Holst et al 2001).

British Journal of Pharmacology (1998) 123, 97–105

Okadaic acid-induced decrease in the magnitude and efficacy of the Ca^{2+} signal in pancreatic β cells and inhibition of insulin secretion

Yoshihiko Sato, Pascal Mariot, Philippe Detimary, Patrick Gilon & [1]Jean-Claude Henquin

Unité d'Endocrinologie et Métabolisme, University of Louvain Faculty of Medicine, UCL 55.30, Avenue Hippocrate 55, B-1200 Brussels, Belgium

1 Phosphorylation by kinases and dephosphorylation by phosphatases markedly affect the biological activity of proteins involved in stimulus-response coupling. In this study, we have characterized the effects of okadaic acid, an inhibitor of protein phosphatases 1 and 2A, on insulin secretion. Mouse pancreatic islets were preincubated for 60 min in the presence of okadaic acid before their function was studied.

2 Okadaic acid dose-dependently ($IC_{50} \sim 200$ nM) inhibited insulin secretion induced by 15 mM glucose. At 0.5 μM, okadaic acid also inhibited insulin secretion induced by tolbutamide, ketoisocaproate and high K^+, and its effects were not reversed by activation of protein kinases A or C.

3 The inhibition of insulin secretion did not result from an alteration of glucose metabolism (estimated by the fluorescence of endogenous pyridine nucleotides) or a lowering of the ATP/ADP ratio in the islets.

4 Okadaic acid treatment slightly inhibited voltage-dependent Ca^{2+} currents in β cells (perforated patch technique), which diminished the rise in cytoplasmic Ca^{2+} (fura-2 method) that glucose and high K^+ produce in islets. However, this decrease (25%), was insufficient to explain the corresponding inhibition of insulin secretion (90%). Moreover, mobilization of intracellular Ca^{2+} by acetylcholine was barely affected by okadaic acid, whereas the concomitant insulin response was decreased by 85%.

5 Calyculin A, another inhibitor of protein phosphatases 1 and 2A largely mimicked the effects of okadaic acid, whereas 1-norokadaone, an inactive analogue of okadaic acid on phosphatases, did not alter β cell function.

6 In conclusion, okadaic acid inhibits insulin secretion by decreasing the magnitude of the Ca^{2+} signal in β cells and its efficacy on exocytosis. The results suggest that, contrary to current concepts, both phosphorylation and dephosphorylation of certain β cell proteins may be involved in the regulation of insulin secretion.

Keywords: Pancreatic islets; insulin secretion; okadaic acid; calyculin A; protein phosphatase inhibitors; cytoplasmic Ca^{2+}; Ca^{2+} channels

Introduction

Reversible protein phosphorylation is a major mechanism in stimulus-response coupling (Cohen, 1989, Shenolikar, 1994). In many cell types, phosphorylation and dephosphorylation of ionic channels or regulatory intracellular proteins by kinases and phosphatases, respectively, underlie the induction of specific responses by extracellular messengers.

Insulin secretion is primarily stimulated by increases in the plasma concentration of nutrients, in particular glucose, which must be metabolized by pancreatic β cells to promote release of the hormone. This metabolism activates two regulatory pathways. The major one involves closure of adenosine triphosphate (ATP)-sensitive K^+ channels (K^+-ATP channels), membrane depolarization, opening of voltage-dependent Ca^{2+} channels, influx of Ca^{2+} and rise in cytoplasmic Ca^{2+} ($[Ca^{2+}]_i$) which is a triggering signal for exocytosis (Ashcroft & Rorsman, 1989; Henquin, 1994). The second pathway does not involve further changes in $[Ca^{2+}]_i$ but an increase in the efficacy of Ca^{2+} on exocytosis, through an as yet unidentified mechanism (Gembal *et al.*, 1992; 1993; Sato *et al.*, 1992). Insulin secretion is also under strong hormonal and neural control. Acetylcholine, catecholamines, gastro-intestinal hormones are physiological, important modulators of β cells in which they exert their effects by activating membrane receptors coupled to classical transduction pathways (Henquin, 1994; Liang & Matschinsky, 1994).

The rise in $[Ca^{2+}]_i$ with subsequent activation of Ca^{2+} calmodulin-dependent kinases and the receptor-mediated activation of protein kinases A and C lead to phosphorylation of a number of still largely unidentified proteins in islet cells (for reviews see Ashcroft, 1994; Howell *et al.*, 1994). It has generally been held that increased protein-phosphorylation favours exocytosis. As the phosphorylation state is determined by the balance between the phosphorylation and dephosphorylation rates, protein phosphatases might also serve a regulatory role, and their inhibition could be expected to increase insulin secretion. This question has previously been addressed by using okadaic acid (OKA), a membrane permeant inhibitor of protein phosphatases 1 and 2A (PP1 and PP2A) (Bialojan & Takai, 1988; Hardie *et al.*, 1991), but the results are controversial. In β cell lines, OKA was found to increase insulin release slightly and transiently (Haby *et al.*, 1994; Mayer *et al.*, 1994) or to inhibit it (Zhang & Kim, 1995; Ammon *et al.*, 1996). In rat islets, glucose-induced insulin release was strongly impaired by OKA (Tamagawa *et al.*, 1992; Murphy & Jones, 1996). In the present study, we have explored the influence of OKA on various aspects of β cell function and compared its effects to those of 1-norokadaone (NOK) an inactive analogue (Nishiwaki *et al.*, 1990), and calyculin A (CLA), a structurally unrelated inhibitor of PP1 and PP2A (Ishihara *et al.*, 1989). The results showed that OKA inhibits

[1] Author for correspondence.

insulin secretion by decreasing the magnitude of the Ca^{2+} signal and its efficacy on exocytosis.

Methods

Preparation and solutions

All procedures have been approved by the University animal care committee. Islets were isolated by collagenase digestion of the pancreas of fed female NMRI mice (25–30 g), followed by hand-picking. In some experiments the islets were preincubated and then incubated immediately after isolation. In other experiments the islets were prepared aseptically and cultured for 1–2 days in RPMI 1640 medium (Gibco BRL, Paisley, Scotland) containing 10 mM glucose, 10% heat-inactivated foetal calf serum, 100 iu ml^{-1} penicillin and 100 μg ml^{-1} streptomycin. For patch-clamp experiments, the islets were dispersed into single cells with Ca^{2+} free buffer containing 100 μM EGTA and 100 μg ml^{-1} trypsin. The cells were then cultured for 1–2 days.

The medium used for islet isolation and testing was a bicarbonate-buffered solution that contained 120 mM NaCl, 4.8 mM KCl, 2.5 mM $CaCl_2$, 1.2 mM $MgCl_2$ and 24 mM $NaHCO_3$. It was gassed with O_2:CO_2 (94:6) to maintain pH 7.4 and was supplemented with bovine serum albumin (1 mg ml^{-1}). Ca^{2+}-free solutions were prepared by replacing $CaCl_2$ with $MgCl_2$. When the concentration of KCl was increased to 30 mM, that of NaCl was decreased accordingly to maintain isoosmolarity. With the exception of the patch-clamp recordings, which were performed at room temperature, all experiments were carried out at 37°C.

Measurement of insulin secretion

In the first type of experiment (static incubations), freshly isolated islets were preincubated for 60 min in a control medium containing 3 mM glucose before being distributed into batches of three. When the ATP and ADP contents were to be measured simultaneously, the islets were distributed into batches of five. Each batch of islets was then incubated for 60 min in 1 ml of medium containing various concentrations of glucose and test substances. A portion of the medium was withdrawn at the end of the incubation and appropriately diluted for insulin assay. Insulin was measured by a double-antibody radioimmunoassay with rat insulin as the standard (Novo Research Institute, Bagsvaerd, Denmark). In one series, the islets were cultured for 45 h with or without 200 ng ml^{-1} pertussis toxin before their function was tested during incubations.

In another type of experiment (dynamic perifusions), cultured islets were preincubated for 60 min in a control medium containing 10 mM glucose before being placed, in batches of 20–25, in parallel perifusion chambers and perifused at a flow rate of 1.25 ml min^{-1} (Henquin, 1978). Effluent fractions were collected at 1–2 min intervals and insulin was measured as above.

Measurement of islet ATP and ADP

These determinations were made at the end of incubations that also served to study insulin secretion (see above). After the aliquot (0.625 ml) for insulin measurement was taken, the islets were incubated for another 5 min. The tubes were kept at 37°C during the whole procedure. The incubation was then stopped by addition of 0.125 ml of trichloroacetic acid to a final concentration of 5%. The tubes were then treated, and ATP and ADP contents of the islets were measured, as published recently (Detimary *et al.*, 1995).

Measurement of cytoplasmic Ca^{2+}

Cultured islets were loaded with 2 μM fura PE3/AM (Mobitec, Göttingen, Germany) during 120 min of incubation at 37°C in a bicarbonate-buffered solution containing 3 or 10 mM glucose. The islets were then transferred into a temperature-controlled perifusion chamber (Intracell, Royston, Herts, UK) with a bottom made of a coverslip and mounted on the stage of an inverted microscope. The islets were held in place by gentle suction with a glass micropipette. The preparation was perifused at a flow rate of 1.3 ml min^{-1}. The dead space of the system (2 min) has been corrected for in figures and calculations. Perifusion solutions were kept at 38°C in a water bath and the temperature controller ensured a temperature of 37°C (± 0.3°C) in the chamber as monitored by a thermistor placed near the tissue.

The measurements of $[Ca^{2+}]_i$ were performed with the system MagiCal (Applied Imaging, Sunderland, U.K.) as described in detail (Gilon & Henquin, 1992). The tissue was excited at 340 nm and 380 nm. The fluorescence emitted at 510 nm was captured by a CCD video camera (Photonic Science Ltd, Tunbridge Wells, U.K.). From the ratio of the fluorescence at 340 and 380 nm, the concentration of $[Ca^{2+}]_i$ was calculated by comparison with a calibration curve (Gilon & Henquin, 1992).

Measurement of reduced pyridine nucleotide fluorescence

Cultured islets were first preincubated for 60 min at 37°C in control medium containing 3 mM glucose. They were then transferred to the same experimental set-up as for $[Ca^{2+}]_i$ measurements. The reduced forms of NAD and NADP, referred to as NAD(P)H, were excited at 360 nm, and the fluorescence emitted was filtered at 470 nm (Gilon & Henquin, 1992). The changes in fluorescence were expressed as a percentage of basal values by dividing the integrated gray levels at a given time by those obtained during the last min preceding stimulation with 15 mM glucose.

Measurement of Ca^{2+} currents

After culture, dispersed β cells were preincubated for 60 min at 37°C in control medium containing 10 mM glucose without or with 0.5 μM OKA or NOK. Voltage-clamp experiments were performed in the perforated-patch configuration (Horn & Marty, 1988) with an EPC-9 patch-clamp amplifier (HEKA Electronics, Lambrecht/Pfalz, Germany). Membrane currents were recorded with the Pulse 8.05 software (HEKA Electronics). Before storage at a sampling rate of 10 kHz, they were filtered at 3 kHz with a Bessel filter. Voltage-dependent Ca^{2+} currents were corrected for leak currents with a P/n protocol (P/n pulses = 16). Depolarizations of 50 ms duration were applied from a holding potential of −80 mV.

Recordings were carried out at 22°C in an extracellular medium containing (mM) NaCl 125, KCl 4.8, $CaCl_2$ 2.5, $MgCl_2$ 1.2, HEPES 5, glucose 15, tetraethylammonium chloride 10 and tetrodotoxin 0.1 μM. pH and osmolarity were adjusted to 7.4 and 310 mOsmol l^{-1}, respectively. The pipette solution for recording Ca^{2+} currents contained (in mM) CS_2SO_4 76, NaCl 10, KCl 10, $MgCl_2$ 1, HEPES 5 and amphotericin B 0.25 mg ml^{-1}. Osmolarity was adjusted to 290 mOsmol l^{-1} with mannitol (1 g 100 ml^{-1}) and pH was adjusted to 7.25.

Materials

Diazoxide was from Schering-Plough Avondale (Rathdrum, Ireland); okadaic acid (OKA) and calyculin A (CLA) were from Biomol (Hamburg, Germany); 1-norokadaone (NOK) was from Calbiochem (San Diego, CA); ATP, ADP, and all reagents for their measurements were from Boehringer-Mannheim (Mannheim, Germany); dibutyryl (db)-cyclicAMP and α-ketoisocaproate (KIC) were from Aldrich Chemie (Steinheim, Germany); phorbol 12-myristrate 13-acetate (PMA), tolbutamide, tetraethylammonium chloride, acetylcholine chloride (ACh), amphotericin B and pertussis toxin were from Sigma Chemical Co. (St. Louis, MO); tetrodotoxin was from RBI (Natick, MA).

Presentation of results

Results are presented as means ± s.e. for the indicated number of batches of islets. The statistical significance of differences between means was assessed by Student's *t* test for unpaired data when only two groups were compared, or by analysis of variance followed by Dunnett's test for multiple comparisons. Differences were considered significant at $P<0.05$.

Results

Time-dependence of the effects of okadaic acid on insulin secretion

The islets were incubated in a control medium containing 15 mM glucose, i.e. under conditions where the primary mechanism of glucose regulation (at the K^+-ATP channel level) plays the predominant role. They were also incubated in a medium containing 250 μM diazoxide to keep K^+-ATP channels open (Sturgess *et al.*, 1988) and 30 mM K^+ to depolarize the membrane, i.e. under conditions where the second mechanism of glucose regulation can be studied (Gembal *et al.*, 1992). Addition of 0.5 μM OKA to the incubation medium did not significantly affect insulin secretion induced by 15 mM glucose (88 ± 11% of controls, $n=15$) and only slightly inhibited the secretion induced by the combination of 20 mM glucose and high K^+ (75 ± 5% of controls, $n=26$; $P<0.05$). We then observed that the inhibition was larger when the islets were preincubated for 60 min with OKA (Figure 1), and that this inhibition was unaffected by the persistence or omission of OKA during the subsequent incubation. This may be due to a relatively slow permeation of OKA and reflect the time needed to reach an intracellular concentration that completely inhibits phosphatases. Similar observations have been made by others (Ashizawa *et al.*, 1989; Yanagihara *et al.*, 1991; Zhang & Kim, 1995). In all subsequent experiments, therefore, OKA was added to the preincubation medium only.

Concentration-dependence of the effects of okadaic acid on insulin secretion

Preincubation of the islets for 60 min in the presence of various concentrations of OKA resulted in a concentration-dependent inhibition of insulin secretion induced by either 15 mM glucose or the combination of 20 mM glucose and 30 mM K^+ in the presence of diazoxide (Figure 1). The concentration-response curve was similar for both stimuli, with a first significant effect at 50 nM OKA ($P<0.05$), an estimated EC_{50} around 200 nM, and abrogation of secretion by 1 μM OKA (Figure 1). On the basis of these results 0.5 μM OKA was selected for the subsequent experiments.

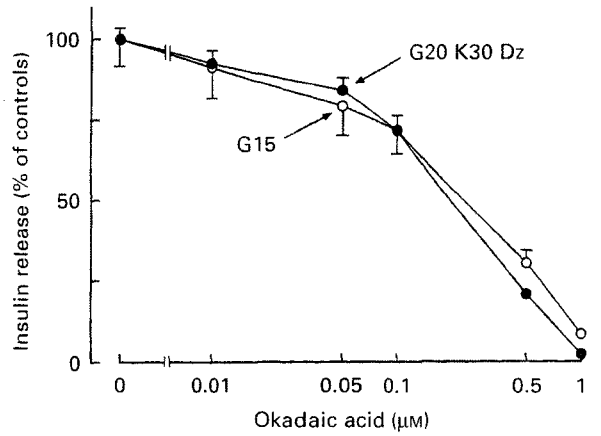

Figure 1 Concentration-dependence of the effects of okadaic acid on insulin release by incubated mouse islets. After isolation the islets were preincubated for 60 min in a medium containing 3 mM glucose and the indicated concentration of okadaic acid. They were then washed and distributed in batches of three in 1 ml of medium containing 15 mM glucose (G15) or 20 mM glucose, 30 mM K^+ and 250 μM diazoxide (G20 K30 Dz). After 60 min of incubation, an aliquot of the medium was taken for insulin assay. Values are means for 20 batches of islets from four separate experiments; vertical lines show s.e.mean. Test values obtained after okadaic acid treatment were expressed as a percentage of control values without okadaic acid in each experiment. Absolute values for these controls were: 3.3 ± 0.4 ng/islet 60 min^{-1} (G15 mM) and 12.9 ± 1.1 ng/islet 60 min^{-1} (G20 K30 Dz).

Comparison of the effects of okadaic acid to those of 1-norokadaone and calyculin A

As shown in Figure 2 (a,c), OKA did not affect basal insulin secretion (3 mM glucose) but inhibited the response to 15 mM glucose or to high K^+ in absence or presence of glucose. In contrast, NOK, an inactive analogue of OKA, was consistently ineffective. CLA, another type of protein phosphatase inhibitor was tested at the single concentration of 10 nM, and was found to inhibit glucose- and high K^+-induced insulin secretion by about 50% (Figure 2a,c).

Influence of okadaic acid on the energy state of the islets

Glucose metabolism and the subsequent changes in β cell energy state are critical events for the stimulation of insulin release by both control pathways (Ashcroft, 1980; Gembal *et al.*, 1993; Henquin, 1994). We, therefore, tested whether they were altered by the protein phosphatase inhibitors. Raising the concentration of glucose from 3 to 15 mM accelerated β cell metabolism, as shown by the marked increase in NAD(P)H fluorescence in the islets (Figure 3). This increase was not impaired when the islets had been treated by OKA or CLA (Figure 3 – inset).

ATP and ADP concentrations were measured in batches of islets from which insulin secretion was also studied (Figure 2, b,d). In a control medium, raising the glucose concentration from 3 to 15 mM increased the ATP/ADP ratio from 2.5 ± 0.1 to 4.0 ± 0.2 ($P<0.01$). In the presence of 30 mM K^+ and diazoxide, the ATP/ADP ratio increased from 2.0 ± 0.1 in the absence of glucose to 3.7 ± 0.1 in the presence of 20 mM glucose ($P<0.01$). These changes are smaller than those we obtained recently because the present measurements were done

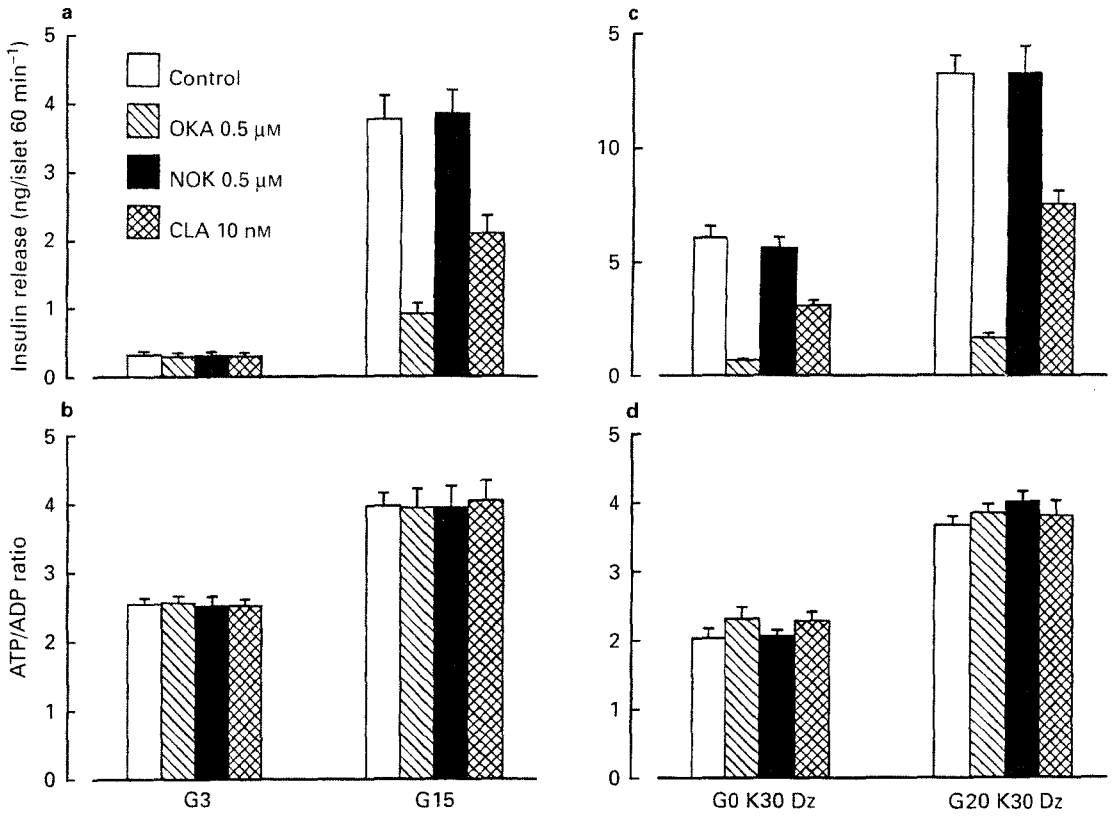

Figure 2 Effects of okadaic acid (OKA), 1-norokadaone (NOK) and calyculin A (CLA) on insulin release (a and c) and the ATP/ADP ratio (b and d) in incubated mouse islets. After isolation the islets were preincubated for 60 min in a medium containing 3 mM glucose alone or with 0.5 μM OKA, 0.5 μM NOK or 10 nM CLA. They were then incubated in the presence of 3(G3) or 15(G15) mM glucose alone, or in a medium with 30 mM K^+, 250 μM diazoxide and 0 or 20 mM glucose. (G0K30Dz and G20K30Dz, respectively). Islet ATP and ADP contents were not measured in all experiments. For insulin release values are means ± s.e.mean for 20 or 30 batches of islets (4–6 separate experiments). For the ATP/ADP ratio, values are means±s.e.mean for 15 batches of islets (3 separate experiments).

in freshly isolated, well granulated islets (Detimary *et al.*, 1995). The important observation is that neither OKA nor CLA affected the ATP/ADP ratio although they inhibited insulin secretion from the same islets (Figure 2).

Effects of okadaic acid and calyculin A on insulin secretion induced by various agents

The next series of experiments was performed to evaluate whether the inhibition of insulin secretion by OKA and CLA could be prevented by agents acting at different steps of stimulus-secretion coupling. Pharmacological closure of K^+-ATP channels by tolbutamide (Sturgess *et al.*, 1988) potentiated glucose-induced insulin release but did not prevent the inhibition by OKA or CLA (Table 1). Both drugs also inhibited insulin secretion induced by ketoisocaproate which is exclusively metabolized in mitochondria. Glucose- and high K^+-induced insulin secretion was potentiated by activation of protein kinase A with dibutyryl cyclicAMP or protein kinase C with PMA (Table 1). However, this activation of the kinases failed to reverse the inhibition by the phosphatase inhibitors. NOK was also tested in some of these experiments and consistently found to be without effect (data not shown).

Taken together the above results indicate that OKA and CLA inhibit the secretory response to agents acting differently. This suggests that the inhibitors of protein phosphatases might affect a common key step of stimulus-secretion coupling. The possible intervention of a G_i-mediated mechanism (Sharp, 1996) was tested by culturing the islets for 45 h with 200 ng ml^{-1} pertussis toxin. This reduced the inhibition of glucose-induced insulin release by 0.1 μM adrenaline from 87±1% to 23±4%, but did not influence the inhibitory effect of 0.5 μM OKA (83±2 and 80±2%; $n=11$). The possible influence of OKA on $[Ca^{2+}]_i$ was next evaluated.

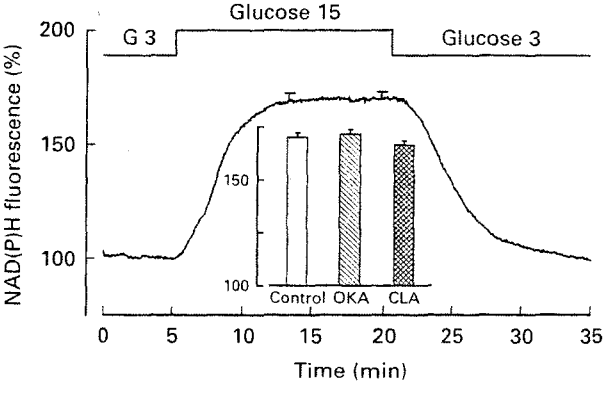

Figure 3 Effects of okadaic acid (OKA) and calyculin A (CLA) on the NAD(P)H fluorescence of glucose-stimulated mouse islets. After isolation the islets were cultured for 1–2 days before being preincubated for 60 min in a medium containing 3 mM glucose and either 0.5 μM OKA or 10 nM CLA. They were then perifused with a medium containing 3 or 15 mM glucose as indicated. CLA was also present in the perifusion medium. The results are expressed as a percentage of the fluorescence recorded in each islet in the presence of 3 mM glucose. The trace shows the response of control islets. The inset shows the mean responses between 15 and 20 min in the 3 groups of islets. Values are means±s.e.mean for 17–19 islets from 4 different cultures.

Table 1 Effects of okadaic acid and calyculin A on insulin release induced by various agents

Line	Test agents	*Insulin release* (ng/islet 60 min^{-1}) Controls	Okadaic acid	Calyculin A
	K 4.8 mM			
1	G15 mM	3.3±0.5	0.7±0.2 (21%)	1.5±0.2 (45%)
2	G15+DbcAMP 0.5 mM	9.5±1.0	2.3±0.4 (24%)	6.4±0.7 (67%)
3	G15+PMA 25 nM	17.9±1.2	3.7±0.5 (21%)	10.8±1.0 (60%)
4	G15+Tolbutamide 100 μM	10.4±1.1	1.3±0.2 (13%)	5.3±0.8 (51%)
5	G3+Ketoisocaproate 10 mM	10.5±1.0	1.5±0.2 (14%)	7.1±0.9 (68%)
	K 30 mM+diazoxide			
6	G20 mM	15.0±1.5	1.8±0.2 (12%)	9.9±1.3 (66%)
7	G20+DbcAMP 0.5 mM	22.2±2.0	3.6±0.4 (16%)	16.4±2.2 (74%)
8	G20+PMA 25 nM	26.7±1.8	5.2±0.7 (19%)	19.1±1.7 (72%)

Freshly isolated islets were preincubated for 60 min in a control medium containing 3 mM glucose (G) alone or with 0.5 μM okadaic acid or 10 nM calyculin A. They were then distributed in batches of three and incubated for 60 min in the presence of the indicated test agents. Values are means±s.e. for 15 batches of islets from at least 3 separate experiments. All values in the presence of okadaic acid or calyculin A are significantly smaller than control values.

Effects of okadaic acid on β cell cytoplasmic Ca^{2+} and Ca^{2+} currents

Stimulation of perifused islets by a rise in the glucose concentration from 3 to 15 mM evoked a biphasic release of insulin (Figure 4a). Both phases were strongly inhibited (~85%) after preincubation of the islets with 0.5 μM OKA. The changes in β cell $[Ca^{2+}]_i$ were measured in individual islets, but the responses were averaged to facilitate comparison with secretion changes. The rise in $[Ca^{2+}]_i$ induced by 15 mM glucose was slightly slower and ~25% smaller ($P<0.01$) in OKA-treated than control islets (Figure 4b). During steady state stimulation with glucose, oscillations of $[Ca^{2+}]_i$ were observed in 83% of control islets and only 59% of OKA-treated islets, and these oscillations were smaller than control ones (Figure 4c). In contrast, NOK affected neither the proportion of islets showing $[Ca^{2+}]_i$ oscillations nor the average $[Ca^{2+}]_i$ rise (Figure 4c).

Glucose-induced changes in $[Ca^{2+}]_i$ result from membrane depolarization secondary to closure of K^+-ATP channels. This indirect mechanism can be short-circuited by raising extracellular K^+ in the presence of diazoxide, which holds K^+-ATP channels open (Sturgess *et al.*, 1988; Gembal *et al.*, 1992). In the absence of glucose, this combination induced a marked rise in $[Ca^{2+}]_i$ that was partially inhibited (~25%) by OKA and CLA, and unaffected by NOK (Figure 5). Similar results were obtained when the experiments were carried out in the presence of 20 mM instead of 0 glucose or at 22°C instead of 37°C (data not shown).

As these results suggested that OKA and CLA inhibit depolarization-induced Ca^{2+} influx in β cells, voltage-dependent Ca^{2+} currents were directly measured (at 22°C) by the perforated patch technique, in the presence of 2.5 mM extracellular Ca^{2+}. Depolarization from a holding potential of −80 mV elicited inward Ca^{2+} currents which became detectable at −40 mV, were maximal at 0 mV and then declined at more positive voltages (Figure 6). Pretreatment of the cells with 0.5 μM OKA inhibited Ca^{2+} currents by ~30%, whereas NOK was without effect. For unknown reasons it proved impossible to form adequate seals with cells pretreated with CLA.

Inhibitory effects of okadaic acid beyond the $[Ca^{2+}]_i$ rise

The above results show that OKA inhibits Ca^{2+} entry in β cells to a much lesser extent than insulin secretion, which raises the possibility that the action of Ca^{2+} is also impaired. This was tested in two ways.

Islets perifused with a medium containing 15 mM glucose and 250 μM diazoxide were stimulated by 30 mM K^+ in the presence of 0.8 mM $CaCl_2$ (Figure 7). This resulted in a rapid increase followed by a stable elevation of $[Ca^{2+}]_i$. A subsequent rise in extracellular Ca^{2+} from 0.8 to 2.5 mM in the presence of high K^+ caused a further increase in $[Ca^{2+}]_i$. These changes were parallel in control and OKA-treated islets, but $[Ca^{2+}]_i$ consistently remained lower in the latter. Insulin secretion occurring under these conditions is shown in Figure 7a. The secretion rate increased stepwise in control islets, but was barely accelerated by high K^+ when the islets had been treated with OKA. It is striking that insulin release was much lower in OKA-treated islets stimulated by 30 mM K^+ and 2.5 mM Ca^{2+} than in control islets stimulated by 30 mM K^+ and 0.8 mM Ca^{2+} although $[Ca^{2+}]_i$ was slightly higher (218±10 nM and 197±8 nM, respectively).

In the absence of extracellular Ca^{2+}, mobilization of intracellular Ca^{2+} by 100 μM acetylcholine evoked a large peak of $[Ca^{2+}]_i$ followed by a small plateau, and triggered a peak of insulin secretion in control islets (Figure 8). Similar changes in $[Ca^{2+}]_i$ were observed in islets pretreated with OKA, but all values were slightly lower than in controls. However, the rise between basal and peak $[Ca^{2+}]_i$ was only 15% smaller in test islets (150 vs 177 nM). On the other hand, the maximum secretion rate was only 2.8 fold the basal rate in OKA-treated islets, as compared with almost 10 fold in control islets (Figure 8).

Discussion

Okadaic acid was found to inhibit insulin secretion from mouse islets in a concentration-dependent manner (IC_{50} ~200 nM). An inhibition of glucose-induced insulin secretion by OKA has also been observed in rat islets (Tamagawa *et al.*, 1992; Murphy & Jones, 1996). The apparently lower sensitivity (~5 fold) of rat islets to OKA inhibition can probably be explained by the fact that the drug was present during incubation only, and not during preincubation as in our study. In the glucose-sensitive INS cell line, an inhibition of glucose-induced insulin release was also observed after preincubation with 1 μM OKA (Zhang & Kim, 1995). The results obtained with the glucose-unresponsive RINm5F cell line are less coherent. OKA was

found to cause a small and transient increase in basal $[Ca^{2+}]_i$ and insulin secretion (Haby *et al.*, 1994; Mayer *et al.*, 1994) or to inhibit K^+ induced $[Ca^{2+}]_i$ rise and insulin secretion (Ammon *et al.*, 1996). These discrepancies may reflect differences between subclones of tumour cells.

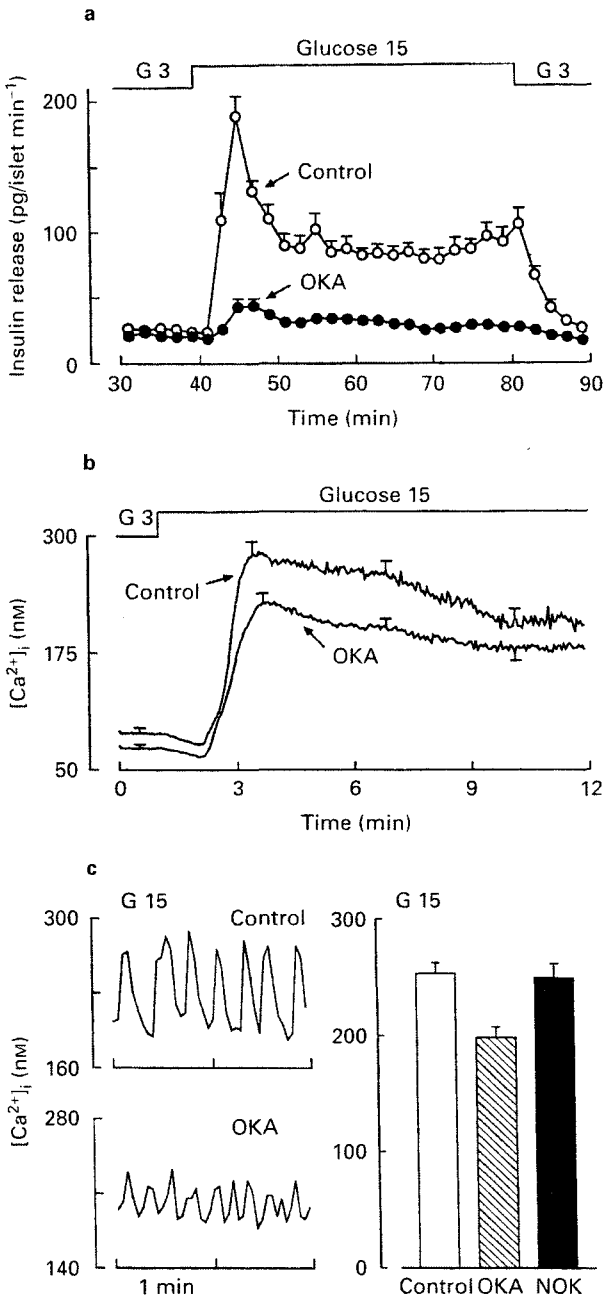

Figure 4 Effects of okadaic acid (OKA) on (a) insulin release and (b and c) $[Ca^{2+}]_i$ in glucose stimulated mouse islets. After isolation, the islets were cultured for 1 day before being preincubated for 60 min in a medium containing 10 mM glucose in the absence of presence of 0.5 μM OKA. When $[Ca^{2+}]_i$ was to be measured, the islets were also loaded with fura PE3 for 120 min. 0.5 μM OKA or 0.5 μM NOK being added during the last 60 min of this preincubation period. The measurements of insulin secretion (batches of 20 islets) and $[Ca^{2+}]_i$ (single islets) were performed in different perifusion systems. The glucose concentration of the medium was raised from 3 to 15 mM as indicated. (a) Shows mean values and s.e.mean (vertical lines) for 6 separate experiments. (b) The time course of the changes in $[Ca^{2+}]_i$ measured in 30 control and OKA-treated islets. (c) On the left are shown representative oscillations in $[Ca^{2+}]_i$ that were recorded in individual control or test islets. The average $[Ca^{2+}]_i$ between 5–7 min of stimulation with 15 mM glucose is shown on the right (means ± s.e.mean for 30 islets from 4 different cultures).

OKA is widely used as a selective inhibitor of PP1 and PP2A (Bialojan & Takai, 1988; Hardie *et al.*, 1991). In cell-free systems, it is more potent on PP2A than PP1 activity (IC_{50} 0.1 and 10 nM, respectively). However, in intact cells concentrations approaching 1 μM must be used because both phosphatases are present at high concentrations (Hardie *et al.*, 1991), and selective inhibition of PP1 and PP2A is not possible (Hardie *et al.*, 1991). PP1 and PP2A are both present in mouse and rat islets (Ämmälä *et al.*, 1994; Murphy & Jones, 1996) together with PP2B (Gagliardino *et al.*, 1991; Murphy & Jones, 1996), which is much less sensitive to OKA (Bialojan & Takai, 1988). PP3, which is also inhibited by OKA, has not been detected in insulin-secreting cells (Sjöholm *et al.*, 1993). In islet and RINm5F cell extracts, PP1/2A activity was inhibited by OKA over the concentration range 0.1 nM – 1 μM (Sjöholm *et al.*, 1993; Ammon *et al.*, 1996; Murphy & Jones, 1996). By contrast, higher concentrations of OKA had to be used to demonstrate increases in the phosphorylation of specific proteins in intact islet cells: 10 μM OKA during incubation only (Persaud *et al.*, 1996) or 1 μM OKA during preincubation (Zhang & Kim, 1995). Our results obtained after preincubation with 0.5 μM OKA can thus reasonably be explained by a slow permeation of the drug and slow inhibition of protein phosphatase activity in intact cells. The lack of effect of 1-norokadaone, a classical inactive control of OKA (Nishiwaki *et al.*, 1990) and the qualitatively similar effects produced by calyculin A, which is structurally unrelated to OKA but also inhibits PP1 and PP2A (Ishihara *et al.*, 1989), also support this proposal. Admittedly, direct measurements of protein phos-

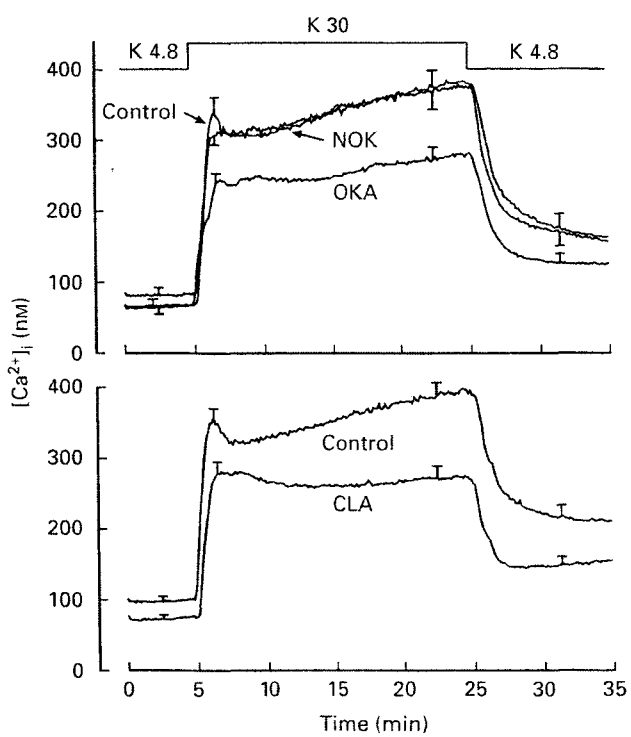

Figure 5 Effects of okadaic acid (OKA), 1-norokadaone (NOK) and calyculin A (CLA) on K^+-induced changes in $[Ca^{2+}]_i$ in perifused mouse islets. After isolation the islets were cultured for 1–2 days before being loaded with fura PE3 for 120 min. The medium contained 3 mM glucose and, for test islets, was supplemented with 0.5 μM OKA, 0.5 μM NOK or 10 nM CLA during the last 60 min. The islets were then perifused with a medium containing no glucose and 250 μM diazoxide. Between 5 and 25 min the K^+ concentration was raised from 4.8 to 30 mM. CLA was also present during the perifusion. Values are means and s.e.mean (vertical lines) for 10 islets from two separate cultures.

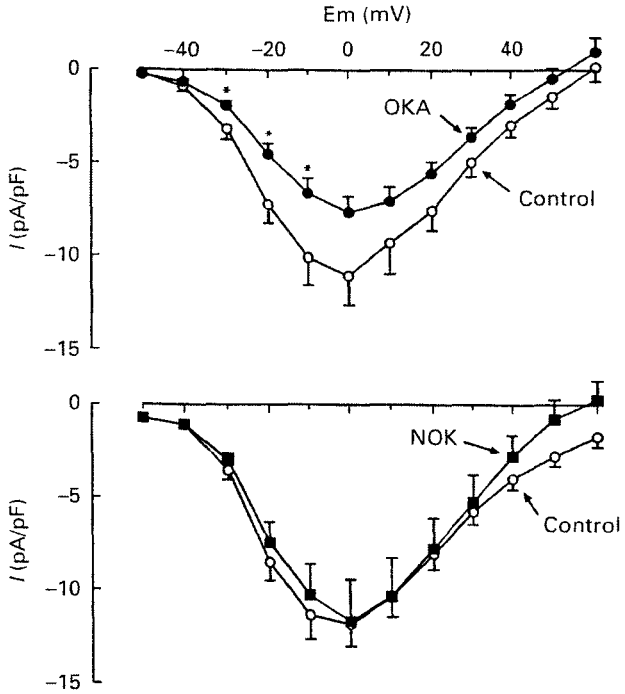

Figure 6 Effects of okadaic acid (OKA) and 1-norokadaone (NOK) on voltage-dependent Ca^{2+} currents in mouse β cells. After isolation the islets were dispersed into single cells which were then cultured for 1–2 days, before being preincubated for 60 min in a medium containing 10 mM glucose and, for test islets, 0.5 μM OKA or 0.5 μM NOK. Ca^{2+} currents were then studied as described in the Methods. Values are means for 11–16 cells from 4 separate cultures; vertical lines show s.e.mean. $^*P<0.05$.

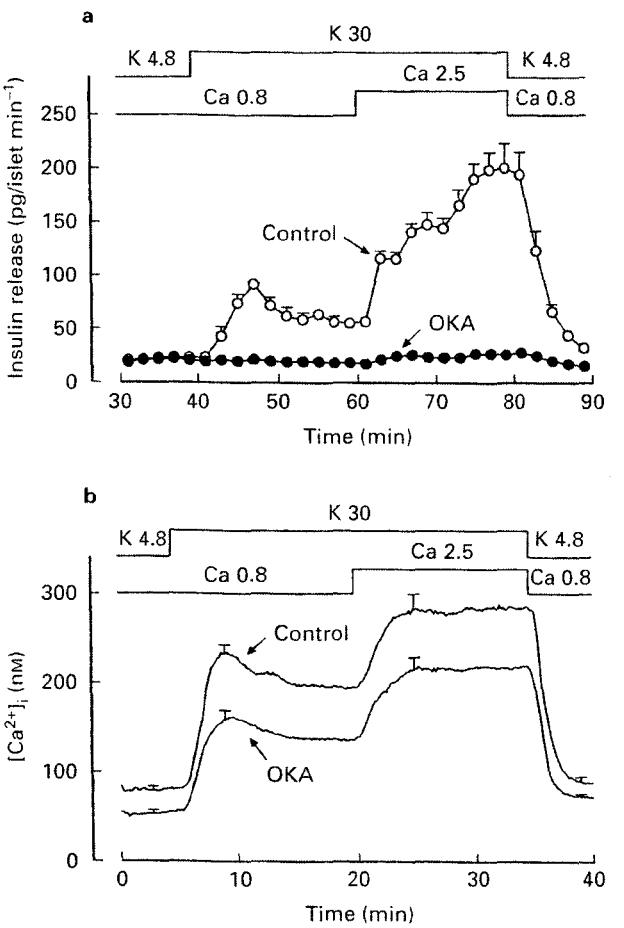

Figure 7 Effects of okadaic acid (OKA) on (a) insulin release and (b) $[Ca^{2+}]_i$ in K^+ stimulated mouse islets. After isolation the islets were cultured for 1 day before being preincubated for 60 min in a medium containing 10 mM glucose without or with 0.5 μM OKA. When $[Ca^{2+}]_i$ was to be measured, the islets were also loaded with fura PE3 for 120 min, OKA being added during the last 60 min of this preincubation period. The measurements of insulin secretion (batches of 20 islets) and $[Ca^{2+}]_i$ (single islets) were performed in different perifusion systems. The perifusion medium contained 15 mM glucose and 250 μM diazoxide throughout, whereas the concentrations of Ca^{2+} and K^+ were changed as indicated. Values are means for 5 experiments of release and for 12 islets from 3 separate cultures for $[Ca^{2+}]_i$; vertical lines show s.e.mean.

phatase activity and protein phosphorylation in intact islets would be necessary to prove it.

In the normal β cell, the response to glucose involves an acceleration of metabolism, an increase in the ATP/ADP ratio, closure of K^+-ATP channels, depolarization of the plasma membrane, activation of voltage-dependent Ca^{2+} channels, influx of Ca^{2+} and a rise in $[Ca^{2+}]_i$ (Ashcroft & Rorsman, 1989; Henquin, 1994). Glucose metabolism, which is exquisitely sensitive to noxious agents, was not impaired in OKA- or CLA-treated islets, as shown by the normal increase in NAD(P)H fluorescence and rise in ATP/ADP ratio. A mere toxic action of the two drugs can thus be excluded. Defects in the closure of K^+-ATP channels and depolarization of the membrane are also unlikely to be involved, because neither direct blockade of the channels with tolbutamide nor depolarization of the membrane with high K^+ in the presence of diazoxide reversed the inhibition of insulin secretion by OKA or CLA.

The first defective step of stimulus-secretion coupling appears to be the influx of Ca^{2+}. Thus, both glucose- and K^+-induced rises in $[Ca^{2+}]_i$ were attenuated in OKA and CLA-treated islets. As Ca^{2+} currents were similarly inhibited after OKA (CLA could not be tested), we suggest that inhibition of PP1 and PP2A eventually impairs Ca^{2+} entry through voltage-dependent Ca^{2+} channels. This is surprising because phosphorylation is generally thought to facilitate Ca^{2+} channel activation (Hescheler *et al.*, 1988; Groschner *et al.*, 1996), including in β cells (Ashcroft & Rorsman, 1989). In agreement with this concept, brief (1–2 min) treatment of mouse β cells with 0.1 μM OKA has been shown to increase Ca^{2+} currents marginally (Ämmälä *et al.*, 1994). However, the same group did not find any acute effects of 1 μM OKA on $[Ca^{2+}]_i$ in intact islets (Zaitsev *et al.*, 1995). It is possible that the difference between these and the present results is explained by the duration of the treatment (short vs long) with OKA. Neither in our experiments (P. Mariot, unpublished results) nor in other studies (Hescheler *et al.*, 1988; Ämmälä *et al.*, 1994) was there any evidence that OKA might be a direct Ca^{2+} channel blocker. It should also be noted that a slight inhibition of Ca^{2+} currents by OKA treatment of intact cells has been observed previously in certain other cell types (Lang *et al.*, 1991; Ward *et al.*, 1991; Groschner *et al.*, 1995).

The 20–25% inhibition of the $[Ca^{2+}]_i$ rise caused by OKA certainly contributes to but cannot entirely explain the almost complete suppression of insulin release. Even when $[Ca^{2+}]_i$ was higher in OKA-treated than control islets (during stimulation with high K^+ and different extracellular Ca^{2+} concentrations), the secretory rate was much lower. Moreover, the peak of insulin release evoked by acetylcholine in the absence of extracellular Ca^{2+} was almost abolished by OKA, although intracellular Ca^{2+} mobilization was only marginally decreased. From these observations we conclude that the efficacy of Ca^{2+} on secretion is decreased after treatment of the islets with OKA.

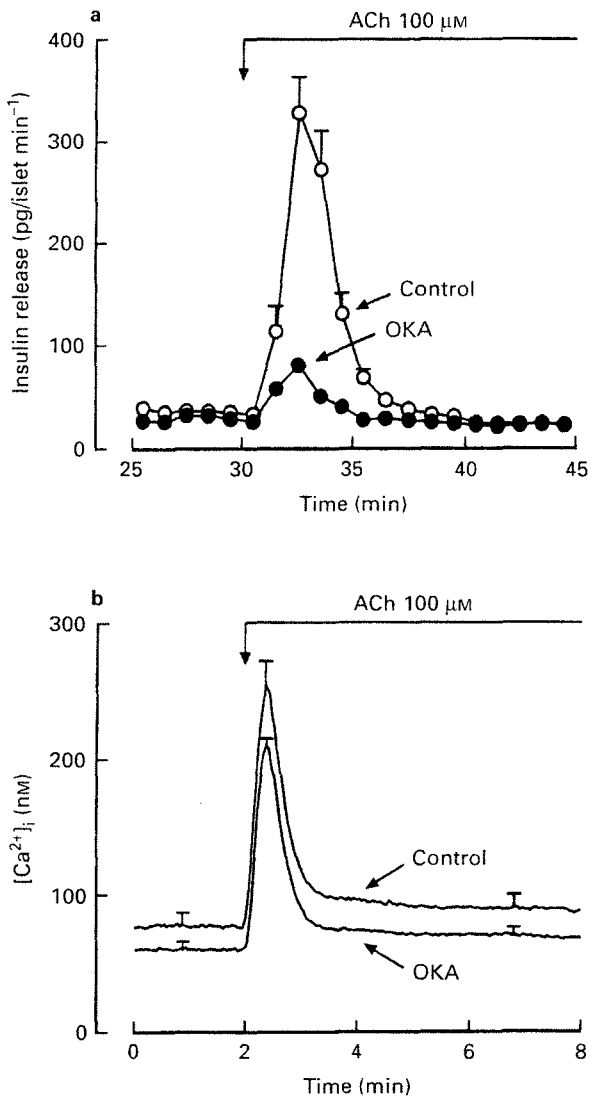

Figure 8 Effects of okadaic acid (OKA) on insulin release and $[Ca^{2+}]_i$ in acetylcholine (ACh)-stimulated mouse islets. After isolation the islets were cultured for 1 day before being preincubated for 60 min in a medium containing 10 mM glucose in the absence or presence of 0.5 μM OKA. When $[Ca^{2+}]_i$ was to be measured, the islets were also loaded with fura PE3 for 120 min, OKA being added during the last 60 min of this preincubation period. The measurements of insulin secretion (batches of 25 islets) and $[Ca^{2+}]_i$ (single islets) were performed in different perifusion systems. The perifusion medium contained 15 mM glucose and was devoid of Ca^{2+}. ACh (100 μM) was added as indicated. Values are means for 6 experiments of release and for 12 islets from 3 separate cultures for $[Ca^{2+}]_i$; vertical lines show s.e.mean.

Two approaches have previously been used to study the effect of OKA on exocytosis of insulin granules. In electrically permeabilized islets, acute application of OKA increased insulin release, but this effect was paradoxical in being observed only in the presence of a non-stimulating concentration of Ca^{2+} (50 nM) while being larger than that of 10 μM free Ca^{2+} (Ratcliff & Jones, 1993). It is unclear whether the proteins whose phosphorylation might be affected by OKA in intact cells are still operative in the model of permeabilized cells. Exocytosis has also been estimated by measuring changes in membrane capacitance in voltage-clamped depolarized β cells. Application of OKA for a few minutes was now found to have no effect on basal exocytosis but to increase the response to Ca^{2+} influx (Ämmälä *et al.*, 1994). However, it should be kept in mind that capacitance measurements evaluate exocytosis of large amounts of insulin granules over a few seconds at the most, whereas direct measurements, like those used here, study release of physiological amounts of insulin over many minutes.

Activation of protein kinases A and C potentiates insulin release at least partly by increasing the efficacy of cytoplasmic Ca^{2+} on the secretory machinery (Ämmälä *et al.*, 1994; Henquin, 1994; Howell *et al.*, 1994). The inhibition of secretion brought about by OKA and CLA could theoretically result from a lesser production of adenosine 3′:5′-cyclic monophosphate (cyclicAMP) or diacylglycerol. This is unlikely because the potentiation of insulin secretion by exogenous cyclicAMP and by a phorbol ester was also impaired by the protein phosphatase inhibitors. OKA exerts a broad spectrum inhibition of insulin secretion that is reminiscent of that of catecholamines, galanin and somatostatin, which act through a pertussis toxin-sensitive G_i-protein (Sharp, 1996). However, pertussis toxin treatment of the islets antagonized the inhibition by adrenaline but did not prevent that by OKA.

Glucose and other nutrients increase the efficacy of Ca^{2+} on insulin secretion (Gembal *et al.*, 1992; 1993; Sato *et al.*, 1992), but the underlying mechanism is still unknown. It does not depend on activation of protein kinases A or C but is correlated with the ATP/ADP ratio (Gembal *et al.*, 1993). The present study suggests that changes in protein phosphatase activity could contribute to this K^+-ATP channel-independent regulation of insulin secretion. Glucose has recently been found to cause a transient increase in PP1-PP2A activity in rat islets (Murphy & Jones, 1996), an effect that could explain the acute increase in acetyl-CoA carboxylase that the sugar produces (Zhang & Kim, 1995). Thus, by preventing dephosphorylation of the enzyme, OKA inhibited its activity in a β cell line (Zhang & Kim, 1995). This may be expected to decrease the level of malonyl-CoA and, therefore, to prevent any rise in cytoplasmic long-chain acyl-CoA esters, which are potential positive modulators of the effect of $[Ca^{2+}]_i$ on insulin secretion (Prentki *et al.*, 1992).

In conclusion, OKA inhibits insulin release by decreasing both the magnitude and the efficacy of the Ca^{2+} signal in β cells. We are not aware of other drugs producing similar effects. If one accepts that the effects of OKA are mediated by an inhibition of protein phosphatases, it appears that the concept of a positive regulation of insulin secretion by protein phosphorylation is an oversimplification. The present study indicates that some phosphorylated proteins might exert an inhibitory action in β cells. Dephosphorylation of certain proteins may be as important as phosphorylation of others to promote optimal Ca^{2+} entry and action. Whether these proteins are distal effector proteins (e.g. Ca^{2+} channels, proteins involved in exocytosis) or enzymes of an upstream cascade of phosphorylations/dephosphorylations remains to be established. Activation of protein kinases certainly plays a positive role but activation of certain phosphatases might also be important at certain steps of stimulus-secretion coupling.

We thank M. Nenquin for editorial assistance. Y. S. is a postdoctoral fellow from Shinshu University and is supported by the Yokoyama Foundation for Clinical Pharmacology, Nagoya. P.G. is Chercheur Qualifié of the Fonds National de la Recherche Scientifique, Brussels. This work was supported by grants 3.4525.94 and LN 9.4592.95 from the Fonds de la Recherche Scientifique Médicale, Brussels, by grant ARC 95/00-188 from the General Direction of Scientific Research of the French Community of Belgium; and by the Fonds S. and J. Pirart from the Belgian Diabetes Association.

References

ÄMMÄLÄ, C., ELIASSON, L., BOKVIST, K., BERGGREN, P.O., HONKANEN, R.E., SJÖHOLM, Å. & RORSMAN, P. (1994). Activation of protein kinases and inhibition of protein phosphatases play a central role in the regulation of exocytosis in the pancreatic B-cells. *Proc. Natl. Acad. Sci. U.S.A.*, **91**, 4343–4347.

AMMON, H.P.T., HEURICH, R.O., KOLB, H.A., LANG, F., SCHAICH, R., DREWS, G. & LEIERS, T. (1996). The phosphatase inhibitor okadaic acid blocks KCl-depolarization-induced rise of cytosolic calcium of rat insulinoma cells (RINm5F). *Naunyn-Schmiedeberg's Arch. Pharmacol.*, **354**, 95–101.

ASHCROFT, S.J.H. (1980). Glucoreceptor mechanisms and the control of insulin release and biosynthesis. *Diabetologia*, **18**, 5–15.

ASHCROFT, S.J.H. (1994). Protein phosphorylation and beta-cell function. *Diabetologia*, **37**, (Suppl. 2), S21–S29.

ASHCROFT, F.M. & RORSMAN, P. (1989). Electrophysiology of the pancreatic β-cell. *Prog. Biophys. Mol. Biol.*, **54**, 87–143.

ASHIZAWA, N., KOBAYASHI, F., TANAKA, Y. & NAKAYAMA, K. (1989). Relaxing action of okadaic acid, a black sponge toxin on the arterial smooth muscle. *Biochem. Biophys. Res. Commun.*, **162**, 971–976.

BIALOJAN, C. & TAKAI, A. (1988). Inhibitory effect of a marine-sponge toxin, okadaic acid, on protein phosphatases. *Biochem. J.*, **256**, 283–290.

COHEN, P. (1989). The structure and regulation of protein phosphatases. *Annu. Rev. Biochem.*, **58**, 453–508.

DETIMARY, P., JONAS, J.C. & HENQUIN, J.C. (1995). Possible links between glucose-induced changes in the energy state of pancreatic B-cells and insulin release: unmasking by decreasing a stable pool of adenine nucleotides in mouse islets. *J. Clin. Invest.*, **96**, 1738–17453.

GAGLIARDINO, J.J., KRINKS, M.H. & GAGLIARDINO, E.E. (1991). Identification of the calmodulin-regulated protein phosphatase, calcineurin, in rat pancreatic islets. *Biochim. Biophys. Acta*, **1091**, 370–373.

GEMBAL, M., DETIMARY, P., GILON, P., GAO, Z.Y. & HENQUIN, J.C. (1993). Mechanisms by which glucose can control insulin release independently from its action on ATP-sensitive K^+ channels in mouse B-cells. *J. Clin. Invest.*, **91**, 871–880.

GEMBAL, M., GILON, P. & HENQUIN, J.C. (1992). Evidence that glucose can control insulin release independently from its action on ATP-sensitive K^+ channels in mouse B-cells. *J. Clin. Invest.*, **89**, 1288–1295.

GROSCHNER, K., SCHUHMANN, K., BAUMGARTNER, W., PASTUSHENKO, V., SCHINDLER, H. & ROMANIN, C. (1995). Basal dephosphorylation controls slow gating of L-type Ca^{2+} channels in human vascular smooth muscle. *FEBS Lett.*, **373**, 30–34.

GROSCHNER, K., SCHUHMANN, K., MIESKES, G., BAUMGARTNER, W. & ROMANIN, C. (1996). A type 2A phosphatase-sensitive phosphorylation site controls modal gating of L-type Ca^{2+} channels in human vascular smooth-muscle cells. *Biochem. J.*, **318**, 513–517.

GILON, P. & HENQUIN, J.C. (1992). Influence of membrane potential changes on cytoplasmic Ca^{2+} concentration in an electrically excitable cell, the insulin-secreting pancreatic B-cell. *J. Biol. Chem.*, **267**, 20713–20720.

HABY, C., LARSSON, O., ISLAM, M.S., AUNIS, D., BERGGREN, P.O. & ZWILLER, J. (1994). Inhibition of serine/threonine protein phosphatases promotes opening of voltage-activated L-type Ca^{2+} channels in insulin secreting cells. *Biochem. J.*, **298**, 341–346.

HARDIE, D.G., HAYSTEAD, T.A.J. & SIM, A.T.R. (1991). Use of okadaic acid to inhibit protein phosphatases in intact cells. *Methods Enzymol.*, **201**, 469–476.

HENQUIN, J.C. (1978). D-glucose inhibits potassium efflux from pancreatic islet cells. *Nature*, **271**, 271–273.

HENQUIN, J.C. (1994). The cell biology of insulin secretion. In *Joslin's Diabetes Mellitus*. ed. Khan, C.R. & Weir, G.C. 13th ed. pp. 56–80. Philadelphia: Lea and Febiger.

HESCHELER, J., MIESKES, G., RÜEGG, J.C., TAKAI, A. & TRAUTWEIN, W. (1988). Effects of a protein phosphatase inhibitor, okadaic acid, on membrane currents of isolated guinea-pig cardiac myocytes. *Pflügers Arch.*, **412**, 248–252.

HORN, R. & MARTY, A. (1988). Muscarinic activation of ionic currents measured by a new whole-cell recording method. *J. Gen. Physiol.*, **92**, 145–159.

HOWELL, S.L., JONES, P.M. & PERSAUD, S.J. (1994). Regulation of insulin secretion: the role of second messengers. *Diabetologia*, **37**, (Suppl. 2), S30–S35.

ISHIHARA, H., MARTIN, B.L., BRAUTIGAN, D.L., KARAKI, H., OZAKI, H., KATO, Y., FUSETANI, N., WATABE, S., HASHIMOTO, K., UEMURA, D. & HARTSHORNE, D.J. (1989). Calyculin A and okadaic acid: inhibitors of protein phosphatase activity. *Biochem. Biophys. Res. Commun.*, **159**, 871–877.

LANG, R.J., OZOLINS, I.Z. & PAUL, R.J. (1991). Effects of okadaic acid and ATPγS on cell length and Ca^{2+}-channel currents recorded in single smooth muscle cells of the guinea-pig taenia caeci. *Br. J. Pharmacol.*, **104**, 331–336.

LIANG, Y. & MATSCHINSKY, F.M. (1994). Mechanisms of action of nonglucose insulin secretagogues. *Annu. Rev. Nutr.*, **14**, 59–81.

MAYER, P., JOCHUM, C., SCHATZ, H. & PFEIFFER, A. (1994). Okadaic acid indicates a major function for protein phosphatases in stimulus-response coupling of RINm5F rat insulinoma cells. *Exp. Clin. Ednocrinol.*, **102**, 313–319.

MURPHY, L.I. & JONES, P.M. (1996). Phospho-serine threonine phosphatases in rat islets of Langerhans: identification and effect on insulin secretion. *Mol. Cell. Endocrinol.*, **117**, 195–202.

NISHIWAKI, S., FUJIKI, H., SUGANUMA, M., FURUYA-SUGIURI, H., MATSUSHIMA, R., LIDA, Y., OJIKA, M., YAMADA, K., UEMURA, D., YASUMOTO, T., SCHMITZ F. & SUGIMURA, T. (1990). Structure-activity relationship within a series of okadaic acid derivatives. *Carcinogenesis*, **11**, 1837–1841.

PERSAUD, S.J., WHEELER-JONES, C.P.D. & JONES, P.M. (1996). The mitogen-activated protein kinase pathway in rat islets of Langerhans: studies on the regulation of insulin secretion. *Biochem. J.*, **313**, 119–124.

PRENTKI, M., VISCHER, S., GLENNON, M.C., REGAZZI, R., DEENEY, J.T. & CORKEY, B.E. (1992). Malonyl-CoA and long chain acyl-CoA esters as metabolic coupling factors in nutrient-induced insulin secretion. *J. Biol. Chem.*, **267**, 5802–5810.

RATCLIFF, H. & JONES, P.M. (1993). Effects of okadaic acid on insulin secretion from rat islets of Langerhans. *Biochim. Biophys. Acta*, **1175**, 188–191.

SATO, Y., AIZAWA, T., KOMATSU, M., OKADA, N. & YAMADA, T. (1992). Dual functional role of membrane depolarization/Ca^{2+} influx in rat pancreatic B-cell. *Diabetes*, **41**, 438–443.

SHARP, G.W.G. (1996). Mechanisms of inhibition of insulin release. *Am. J. Physiol.*, **271**, C1781–C1799.

SHENOLIKAR, S. (1994). Protein serine/threonine phosphatases. New Avenues for cell regulation. *Annu. Rev. Cell. Biol.*, **10**, 55–86.

SJÖHOLM, A., HONKANEN, R.E. & BERGGREN, P.O. (1993). Characterization of serine/threonine protein phosphatases in RINm5F insulinoma cells. *Bioscience Reports*, **13**, 349–358.

STURGESS, N.C., KOZLOWSKI, R.Z., CARRINGTON, C.A., HALES, C.N. & ASHFORD, M.L.J. (1988). Effects of suphonylureas and diazoxide on insulin secretion and nucleotide-sensitive channels in an insulin-secreting cell line. *Br. J. Pharmacol.*, **95**, 83–94.

TAMAGAWA, T., IGUCHI, A., UEMURA, K., MIURA, H., NONOGAKI, K., ISHIGURO, T. & SAKAMOTO, N. (1992). Effects of the protein phosphatase inhibitors okadaic acid and calyculin A on insulin release from rat pancreatic islets. *Endocrinol. Jap.*, **39**, 325–329.

WARD, S.M., VOGALIS, F., BLONDFIELD, D.P., OZAKI, H., FUSETANI, N., UEMURA, D., PUBLICOVER, N.G. & SANDERS, K.M. (1991). Inhibition of electrical slow waves and Ca^{2+} currents of gastric and colonic smooth muscle by phosphatase inhibitors. *Am. J. Physiol.*, **261**, C64–C70.

YANAGIHARA, N., TOYOHIRA, Y., KODA, Y., WADA, A. & IZUMI, F. (1991). Inhibitory effect of okadaic acid on carbachol-evoked secretion of catecholamines in cultured bovine adrenal medullary cells. *Biochem. Biophys. Res. Commun.*, **174**, 77–83.

ZAITSEV, S.V., EFENDIC, S., ARKHAMMAR, P., BERTORELLO, A.M. & BERGGREN, P.O. (1995). Dissociation between changes in cytoplasmic free Ca^{2+} concentration and insulin secretion as evidenced from measurements in mouse single pancreatic islets. *Proc. Natl. Acad. Sci. U.S.A.*, **92**, 9712–9716.

ZHANG, S. & KIM, K.H. (1995). Glucose activation of acetyl-CoA carboxylase in association with insulin secretion in a pancreatic β-cell line. *J. Endocrinol.*, **147**, 33–41.

(Received July 21, 1997
Revised September 22, 1997
Accepted September 29, 1997)

Article 3.

Tolbutamide and Diazoxide influence insulin secretion by changing the concentration not the action of cytoplasmic Ca2+ in β cells.

Mariot P, Gilon P, Nenquin M, Henquin J-C (1998) **Diabetes.** 47 : 365-373

I. Position du problème

Dans le cadre de l'étude du couplage stimulation-sécrétion dans les cellules β du pancréas, j'ai travaillé sur l'action des composés sulfonylurées sur l'exocytose. Il est connu maintenant que ces molécules, du type tolbutamide, agissent en bloquant les courants potassiques sensibles à l'ATP (courant K_{ATP}) en se fixant notamment sur des sites de haute affinité au niveau des sous-unités SUR1 du canal, et permettent ainsi une dépolarisation membranaire entraînant une entrée de calcium dans la cellule et une stimulation de la sécrétion d'insuline. Ces composés sont ainsi couramment utilisés dans la lutte contre le diabète non insulino-dépendant et permettent, en augmentant le taux d'insuline dans le sang, de contrecarrer une hyperglycémie.

Des résultats avaient préalablement montré que le tolbutamide et ses analogues pouvaient stimuler directement la sécrétion d'insuline par une action en aval des canaux K_{ATP}, probablement par une action *via* la protéine kinase C (Eliasson et al 1996). Ces résultats étaient pourtant soumis à controverse puisque des résultats opposés avaient été obtenus par ailleurs (Garcia-Barrado et al, 1996).

II. Résultats et discussion

Le travail que j'ai mené fut d'étudier cet effet distal potentiel des sulfonylurées à l'aide de la mesure de la capacité membranaire sur cellule unique. Mes résultats obtenus sur cellule isolée à l'aide de la mesure de la capacité membranaire, sur ilôts de Langerhans par des mesures de microfluorimétrie du calcium cytosolique et des mesures de sécrétion d'insuline, ont montré que les sulfonylurées n'étaient pas capables de stimuler la sécrétion d'insuline lorsque toute augmentation de calcium cytosolique était bloquée. Ces résultats montraient que les sulfonylurées régulent la sécrétion d'insuline par un effet sur les conductances potassiques seules, et non par un effet distal sur des cibles intracellulaires.

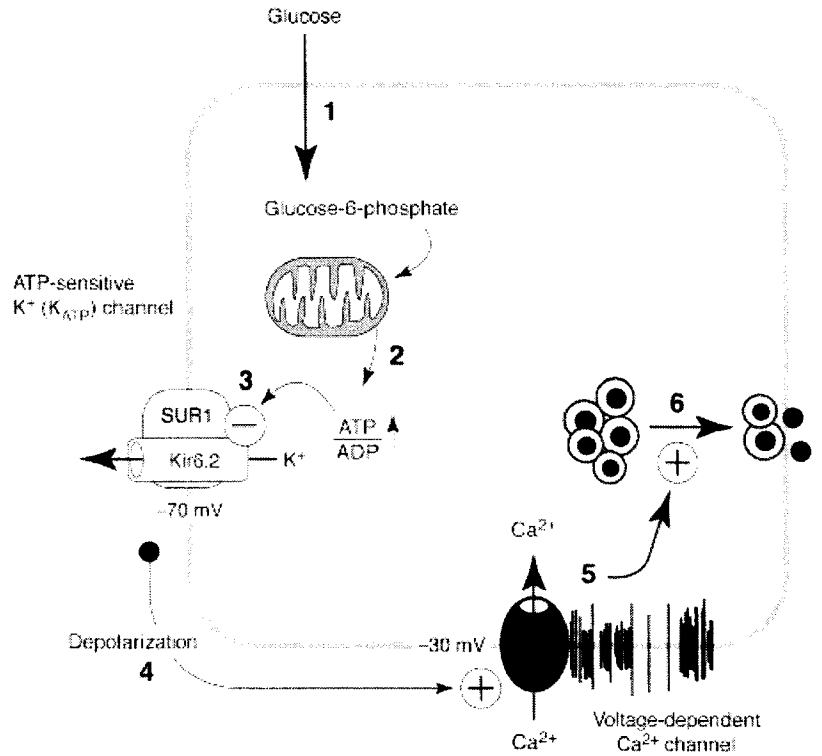

Figure 13 : Mécanisme d'action des sulfonylurées dans le couplage stimulation-sécrétion de la cellule β du pancréas.
D'après Dunne et al (1999)

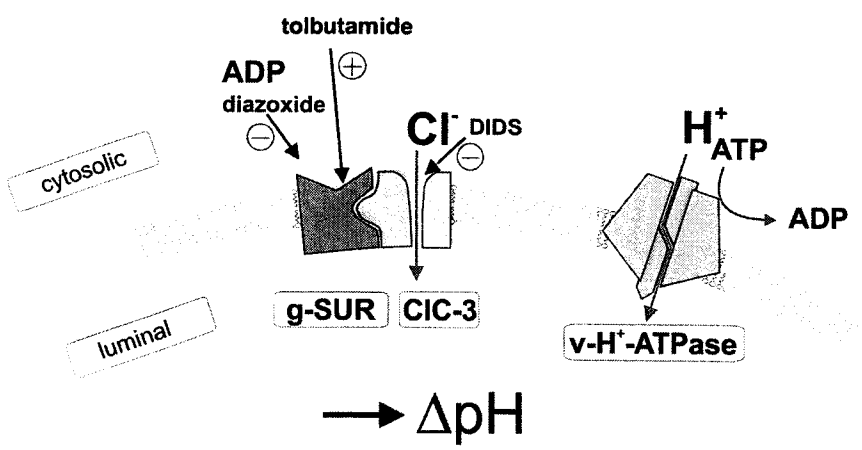

Figure 14 : Mécanisme d'action intracellulaire des sulfonylurées dans le couplage stimulation-sécrétion de la cellule β du pancréas.
D'après Renström et al (2002)

Aujourd'hui, il semblerait que des récepteurs intracellulaires de haute affinité aux sulfonylurées soient probablement démontrés, notamment au niveau des granules de sécrétion (Geng et al. 2003), et qu'une action stimulatrice des sulfonylurées, indépendamment du canal K_{ATP} membranaire, s'effectue *via* ces récepteurs ainsi que *via* des récepteurs mdr-like granulaires (Barg et al 1999, Renström et al 2002 pour revue) ou par une action *via* des récepteurs mitochondriaux (Smith et al 1999).

Les raisons de ces différences de résultats résident probablement dans des différences expérimentales et notamment dans des concentrations en glucose extracellulaire variables entre les différentes études. Ainsi, dans nos études au laboratoire d'endocrinologie dirigé par le professeur J-C Henquin, les ilôts de Langherans ou les cellules β isolées étaient toujours préincubées dans une concentration stimulante de glucose alors que dans d'autres laboratoires (PO Berggren, P. Rorsman), les cellules étaient incubées dans des concentrations non stimulantes de glucose (5 mM). Une étude menée par ces laboratoires (Barg et al 1999) a permis de montrer qu'en passant d'une concentration stimulante de glucose à une concentration non stimulante, le mode d'action intracellulaire des sulfonylurées était révélé certainement à cause des concentrations d'ADP intracellulaires induites par ces traitements. Une concentration importante de glucose diminue les concentrations d'ADP cytosoliques des cellules β et il semblerait que le tolbutamide antagonise l'action inhibitrice de l'ADP sur l'exocytose calcium-dépendante (Renström et al 2002). Le récepteur aux sulfonylurées vésiculaire (g-SUR ou mdr-like de 65 kd) pourrait stimuler la sécrétion d'insuline selon le modèle présenté sur la figure suivante. L'activation d'un canal chlore ClC3 par g-SUR permettrait de stimuler une v-H^+-ATPase vésiculaire, entraînant une acidification granulaire. Cette v-ATPase jouerait le rôle d'enzyme clé dans le processus de priming lors de l'exocytose, l'acidification granulaire entraînant l'acquisition par les granules de la compétence fusionnelle.

D'autre part, ce travail a permis de montrer que l'acétylcholine (Ach), sécrétagogue physiologique important des cellules β, était capable de stimuler la sécrétion d'insuline indépendamment de l'augmentation de calcium cytosolique qu'elle provoque par l'activation de la voie PLC/IP3 puisque l'exocytose (mesurée par mesure de capacitance membranaire) était induite par l'Ach lorsque la $[Ca^{2+}]i$ était maintenue à des concentrations élevées (1 µM) avec des concentrations de tampons calciques (10 mM EGTA) telles que toute variation de calcium était abolie. Ainsi, l'Ach est capable de stimuler la sécrétion d'insuline en augmentant la concentration calcique cytosolique mais également en augmentant l'affinité des cibles cytosoliques.

Tolbutamide and Diazoxide Influence Insulin Secretion by Changing the Concentration but Not the Action of Cytoplasmic Ca^{2+} in β-Cells

Pascal Mariot, Patrick Gilon, Myriam Nenquin, and Jean-Claude Henquin

Sulfonylureas stimulate insulin secretion by blocking ATP-sensitive K^+ channels (K^+-ATP channels) of the β-cell membrane, thereby causing depolarization, Ca^{2+} influx, and rise in cytoplasmic Ca^{2+} concentration ($[Ca^{2+}]_i$), whereas diazoxide inhibits insulin secretion by opening K^+-ATP channels. It has been suggested recently that these drugs also respectively increase and decrease the efficacy of Ca^{2+} on exocytosis. This hypothesis was tested here with intact islets or single β-cells from normal mice. Depolarizing islet cells by raising extracellular K^+ from 4.8 to 15, 30, and 60 mmol/l progressively raised $[Ca^{2+}]_i$ and stimulated insulin secretion. The magnitude of the $[Ca^{2+}]_i$ rise produced by a subsequent addition of 100 μmol/l tolbutamide decreased as the concentration of K^+ was increased. The effect on insulin secretion paralleled that on $[Ca^{2+}]_i$. Similarly, the magnitudes of the $[Ca^{2+}]_i$ drop and of the inhibition of insulin secretion produced by 250 μmol/l diazoxide were inversely related to the concentration of K^+. Either drug was effective on secretion only when it increased or decreased $[Ca^{2+}]_i$. Exocytosis of insulin granules from single, voltage-clamped β-cells was also studied by measuring cell capacitance changes. In the perforated patch configuration, exocytosis was evoked by depolarizing pulses. Addition of tolbutamide to the extracellular medium did not affect the Ca^{2+} current and the resulting change in cell capacitance. In the whole-cell configuration, cell capacitance increased with the concentration of free Ca^{2+} in the solution diffusing from the pipette into the cell. It was markedly potentiated by cAMP, was inhibited by activation of α_2-adrenoceptors with clonidine, and was strongly augmented by acetylcholine. In contrast, tolbutamide was ineffective whether applied intra- or extracellularly, at low or high free Ca^{2+}, and with or without cAMP. Diazoxide also failed to interfere directly with exocytosis. These results indicate that tolbutamide and diazoxide affect insulin secretion by changing the concentration, not the action, of Ca^{2+} in β-cells. *Diabetes* 47:365–373, 1998

From the Unité d'Endocrinologie et Métabolisme, University of Louvain, Brussels, Belgium.

Address correspondence and reprint requests to Dr. J.-C. Henquin, Unité d'Endocrinologie et Métabolisme, UCL 55.30, Avenue Hippocrate 55, B 1200 Brussels, Belgium.

Received for publication 29 August 1997 and accepted in revised form 3 December 1997.

P.M. and P.G. contributed equally to this work.

ACh, acetylcholine; $[Ca^{2+}]_i$, cytoplasmic Ca^{2+} concentration; C_m, cell membrane capacitance; G_a, access conductance; G_m, cell membrane conductance; K^+-ATP channel, ATP-sensitive K^+ channel.

Glucose stimulates insulin secretion by two mechanisms that are respectively dependent and independent of ATP-sensitive K^+ channels (K^+-ATP channels). By closing these channels in the plasma membrane of β-cells, glucose initiates the following sequence of events: membrane depolarization, opening of voltage-dependent Ca^{2+} channels, Ca^{2+} influx, and rise in cytoplasmic Ca^{2+} ($[Ca^{2+}]_i$), which constitutes the triggering signal for exocytosis of insulin granules (1–4). The second mechanism does not involve further changes in $[Ca^{2+}]_i$ but an increase in the efficacy of Ca^{2+} on exocytosis, through as-yet-unidentified pathways (5–7).

Hypoglycemic sulfonylureas remain the only useful drugs to increase a deficient insulin secretion and, therefore, are a cornerstone of the pharmacological treatment of type 2 diabetes (8). They largely mimic the effects of glucose in the generation of the triggering signal (9–11). However, a major difference between both secretagogues is that the closure of K^+-ATP channels by sulfonylureas does not result from changes in β-cell metabolism but from a direct interaction with the sulfonylurea receptor (12,13), which is a subunit of the K^+-ATP channel (14,15). Activation of a Cl^- channel and inhibition of the Na^+ pump might also contribute to the depolarization-mediated rise in $[Ca^{2+}]_i$ brought about by sulfonylureas (10). Recently it has been suggested that sulfonylureas also increase insulin release by a second, very different, mechanism which, like that of glucose, does not involve a rise in $[Ca^{2+}]_i$ but an increase in Ca^{2+} efficacy on exocytosis (16,17).

Diazoxide has long been used to inhibit inappropriate insulin secretion causing hypoglycemia (18). Its major mode of action is the opening of K^+-ATP channels in the β-cell membrane, with repolarization, closure of voltage-dependent Ca^{2+} channels, and lowering of $[Ca^{2+}]_i$ (19–21). However, it has been proposed that diazoxide also decreases the efficacy of Ca^{2+} on exocytosis (16,22).

These proposals that sulfonylureas and diazoxide can influence insulin secretion without necessarily changing $[Ca^{2+}]_i$ in β-cells are based on two types of experiments. First, tolbutamide and glibenclamide were found to increase, whereas diazoxide was found to decrease, insulin release from permeabilized RINm5F or islet cells in which the membrane potential was dissipated and the composition of the intracellular milieu, including $[Ca^{2+}]_i$, was clamped (16). Second, tolbutamide was found to increase and diazoxide to decrease exocytosis of insulin granules estimated by changes in membrane capacitance of voltage-clamped β-cells (17,22).

In contrast with these results, we previously failed to confirm that tolbutamide and glibenclamide are effective secretagogues in permeabilized islet cells and to find evidence that they can increase insulin secretion from intact islets when they do not increase $[Ca^{2+}]_i$ (23).

In this study, we have pursued the investigation of the question for several reasons. First, it is not known whether the newly proposed mechanism of inhibition of insulin secretion by diazoxide also exists in intact cells. Second, it is crucial to know whether sulfonylureas have one or two modes of action and, therefore, whether they may be expected to partially or completely correct defects in glucose regulation of insulin release. Third, identification of a K^+-ATP channel–independent mode of action of sulfonylureas and diazoxide would considerably help in elucidating the second pathway of regulation by glucose. The experiments were performed with normal mouse islets in which the effects of tolbutamide and diazoxide on $[Ca^{2+}]_i$ and insulin secretion were compared. The effects of the drugs on exocytosis were also estimated by recording capacitance changes in single β-cells, the electrophysiological technique that was previously used to identify their novel mode of action (17,22).

RESEARCH DESIGN AND METHODS

Preparation. Islets were isolated by collagenase digestion of the pancreas of fed female NMRI mice (25–30 g), followed by hand-picking. They were then cultured in RPMI 1640 medium (Gibco BRL, Paisley, Scotland, U.K.) containing 10 mmol/l glucose, 10% heat-inactivated fetal calf serum, 100 IU/ml penicillin, and 100 μg/ml streptomycin. For patch-clamp experiments, the islets were dispersed into single cells with a Ca^{2+}-free buffer containing 100 μmol/l EGTA and 100 μg/ml trypsin. The cells were then cultured in the same medium as above. β-Cells make up about 80% of islet cells in normal mice (24) and have a larger diameter (11–14 μm) than do α-cells (8–11 μm) (25). The cells used for the electrophysiological experiments were selected for their large size. From their basal capacitance (~ 6pF) and a specific membrane capacitance of 10 fF/μm^2, one can recalculate that these cells had a diameter of about 13–14 μm.

Solutions. The medium used for islet isolation was a bicarbonate-buffered solution that contained 120 mmol/l NaCl, 4.8 mmol/l KCl, 2.5 mmol/l $CaCl_2$, 1.2 mmol/l $MgCl_2$, and 24 mmol/l $NaHCO_3$. It was gassed with O_2:CO_2 (94:6) to maintain pH 7.4 and was supplemented with bovine serum albumin (1 mg/ml). A similar medium was used for measurements of $[Ca^{2+}]_i$ and insulin secretion. When the concentration of KCl was increased to 15, 30, or 60 mmol/l, that of NaCl was decreased accordingly to maintain iso-osmolarity. When the concentration of $CaCl_2$ was decreased to 0.5 mmol/l, that of $MgCl_2$ was increased from 1.2 to 3.2 mmol/l. Tolbutamide (Sigma, St. Louis, MO) and diazoxide (Schering-Plough Avondale, Rathdrum, Ireland) were added to the medium from stock solutions in NaOH.

For electrophysiological experiments, different types of solutions were used depending on the mode of recording. For whole-cell recordings, the extracellular medium (pH 7.4) contained 145 mmol/l NaCl, 4.8 mmol/l KCl, 3.7 mmol/l $MgCl_2$, 0.1 mmol/l EGTA, 10 mmol/l HEPES, and 20 mmol/l glucose (5 mmol/l in the experiments without cAMP shown in Fig. 4). Under these conditions, only the Ca^{2+} buffer present in the pipette solution can activate secretion; and if there were even a slight inward current, it could not be carried by Ca^{2+}. The pipette solution (pH 7.2) contained 135 mmol/l K-gluconate; 10 mmol/l EGTA; 4 mmol/l $MgCl_2$; 5 mmol/l HEPES; 3 mmol/l ATP; 0 or 0.1 mmol/l GTP; 0, 0.1, or 1 mmol/l cAMP; and 6 or 9 mmol/l $CaCl_2$ (to give 0.2 and 1.25 μmol/l free Ca^{2+}, respectively, as calculated by the software Calc, version 2.2). For perforated-patch recordings, the extracellular medium contained 125 mmol/l NaCl, 20 mmol/l TEA-Cl, 5 mmol/l $CaCl_2$, 1.2 mmol/l $MgCl_2$, 10 mmol/l HEPES, 20 mmol/l glucose, and 2 μmol/l forskolin. The pipette solution contained 76 mmol/l Cs_2SO_4, 35 mmol/l CsCl, 10 mmol/l NaCl, 10 mmol/l KCl, 1 mmol/l $MgCl_2$, and 5 mmol/l HEPES.

Measurements of $[Ca^{2+}]_i$. Islets were cultured on glass coverslips to which they readily attached. After 1–2 days, the coverslip was placed into a bicarbonate medium containing 10 mmol/l glucose and supplemented with 2 μmol/l fura PE3/AM (Teflabs, Austin, TX) for 120 min of incubation at 37°C. Islets loaded with the Ca^{2+} dye were then transferred into a temperature-controlled perifusion chamber (Intracell, Royston, Herts, U.K.) of which the coverslip formed the bottom. The preparation was then perifused at a flow rate of 1.3 ml/min. The solutions were kept at 38°C in a water bath, and a temperature controller ensured a temperature of 37°C (±0.3°C) in the chamber as monitored by a thermistor.

The measurements of $[Ca^{2+}]_i$ were performed with the MagiCal system (Applied Imaging, Sunderland, U.K.) as described in detail (21). The tissue was excited at 340 nm and 380 nm. The fluorescence emitted at 510 nm was captured by a CCD video camera (Photonic Science, Tunbridge Wells, U.K.). From the ratio of the fluorescence at 340 and 380 nm, the concentration of $[Ca^{2+}]_i$ was calculated by comparison with a calibration curve (21).

Measurements of insulin secretion. After 1 day of culture, the islets were preincubated for 60 min at 37°C in a bicarbonate medium containing 10 mmol/l glucose. Batches of 20 islets were then placed in parallel perifusion chambers and perifused at a flow rate of 1.2 ml/min (26). Effluent fractions collected at 2-min intervals were chilled until their insulin content was measured by a double-antibody radioimmunoassay with rat insulin as the standard (Novo Research Institute, Bagsvaerd, Denmark).

Measurements of β-cell membrane capacitance. Patch-clamp experiments were performed at 33°C, in the conventional whole-cell recording configuration or in perforated mode, using an EPC9 patch-clamp amplifier (HEKA Electronics, Lambrecht/Pfalz, Germany). Cultured cells were first preincubated for 30 min in the presence of 10 μmol/l forskolin and then perifused at a rate of 1 ml/min. The bath and pipette solutions were as described above. Patch pipettes were pulled from glass capillaries (Clark Electromedical Instruments, Reading, U.K.) to give a resistance of 2–3 MΩ after coating with Sylgard (Dow Corning, Wiesbaden, Germany) and fire-polishing. For recordings in perforated patch-configuration, pipettes were dipped for a few seconds in the pipette solution free of amphotericin B and then back-filled with the same solution containing 250 μg amphotericin B/ml. Perforation usually occurred progressively, in less than 5 min. The access conductance was considered large enough to begin capacitance measurements when exceeding 30 nS.

To assay exocytosis, membrane capacitance was measured with a technique derived from the phase-sensitive method (27). A 830-Hz sinewave with a peak-to-peak amplitude of 30 mV was applied to the cell under voltage-clamp conditions (–70 mV), and the resulting membrane current was filtered at 3 kHz with a 4-pole Bessel filter. The membrane capacitance (C_m) and conductance (G_m) and the access conductance (G_a) were derived from analysis of the sinusoidal membrane current at two orthogonal phase angles. This was done with the Lockin extension of the Pulse 8.09 software (HEKA Electronics) using the "sine + dc" protocol derived from the method referred to as "computer-aided reconstruction of passive cell parameters" by Lindau and Neher (28,29). The reversal potential of the DC current was assumed to be 0. Protocols of 8 cycles (9.6 ms in total) were applied to the cell every 100 ms. A single value of each membrane parameter (C_m, G_m, and G_a) was computed each cycle; an average value was calculated from the 8 values and eventually sent to the XChart Software (HEKA Electronics). From an initial sampling frequency of 50 kHz for the sinusoidal membrane current, this gave a final frequency acquisition of 10 Hz for capacitance measurements using XChart.

In the perforated mode, exocytosis was triggered by applying voltage steps. Every 2 min, the XChart trace was temporarily interrupted to apply a voltage pulse from Pulse 8.09. This protocol was composed of a control period of 50 ms during which C_m, G_m, and G_a were measured every cycle, a voltage step to 0 mV for 500 ms, and a 1-s period during which C_m, G_m, and G_a were measured every cycle again. This gave a high temporal resolution of C_m, 833 Hz against 10 kHz for the membrane current during the whole protocol. Membrane capacitance increases after depolarization were calculated 1 s after the end of the voltage pulse to avoid contamination by gating charge movements or tail currents. Then measurements with XChart at a low temporal resolution (10 Hz) were automatically resumed. Only traces analyzed from XChart at a low temporal resolution are shown in this study.

In standard whole-cell recording, exocytosis was stimulated by the high concentration of free Ca^{2+} (0.2 or 1.25 μmol/l) in the medium diffusing from the pipette into the cell interior. Measurements of C_m were performed with the above protocol as long as the cell secreted and until C_m reached a plateau.

The exocytotic responses were estimated as maximum changes in cell capacitance (ΔC_m) and, for whole-cell recordings, as rates of capacitance changes (dC_m/dt) calculated during the first min or between 20 and 80% of the C_m variation induced by the stimulus.

Statistical analysis. Results are usually presented as means ± SE. For $[Ca^{2+}]_i$ measurements, recordings were obtained with five or six individual islets from each preparation. The same experiment was repeated with three or four distinct islet preparations. For insulin release, each protocol was tested with islets from six to nine different preparations. For electrophysiological recordings, experiments were repeated on two to four different batches of cells. Results were compared with a paired or unpaired t test, according to the type of experiment.

RESULTS

Effects of tolbutamide on islet $[Ca^{2+}]_i$ and insulin secretion. The experiments were carried out in the presence of variable concentrations of KCl to produce different degrees of β-cell depolarization (30) before stimulation with

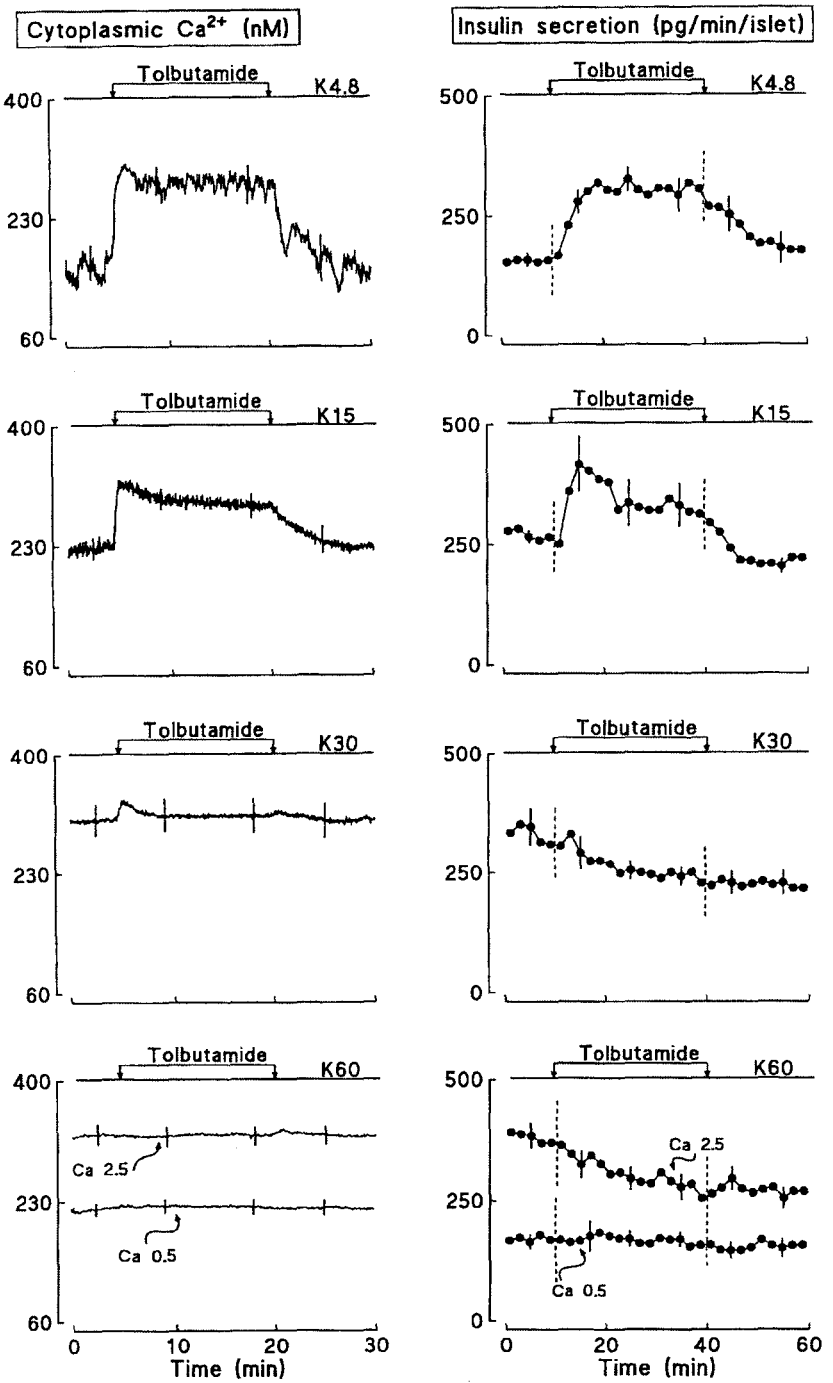

FIG. 1. Effects of tolbutamide on cytoplasmic Ca^{2+} and insulin secretion by perifused mouse islets. The medium contained 15 mmol/l glucose, the indicated concentration of K^+, and 2.5 mmol/l $CaCl_2$ (except in one experimental series of the lower panels). Tolbutamide (100 μmol/l) was added as indicated. Measurements started after an initial equilibration period of 10 ($[Ca^{2+}]_i$) or 30 (insulin) min. Values are means ± SE for 10–22 individual islets ($[Ca^{2+}]_i$) or 6–9 experiments with batches of 20 islets (insulin).

tolbutamide. In a control medium containing 4.8 mmol/l K^+, 15 mmol/l glucose induced oscillations of $[Ca^{2+}]_i$ in the islets (21), which cannot be seen in Fig. 1 (upper left panel) because recordings from different islets have been averaged. Addition of 100 μmol/l tolbutamide caused a rapid and sustained rise in $[Ca^{2+}]_i$ that was completely reversible upon removal of the sulfonylurea. Under these conditions, tolbutamide reversibly doubled glucose-induced insulin secretion (Fig. 1, upper right panel).

When the medium contained 15 instead of 4.8 mmol/l K^+, $[Ca^{2+}]_i$ and insulin secretion were elevated, but tolbutamide remained effective on both $[Ca^{2+}]_i$ and secretion (Fig. 1, mid-

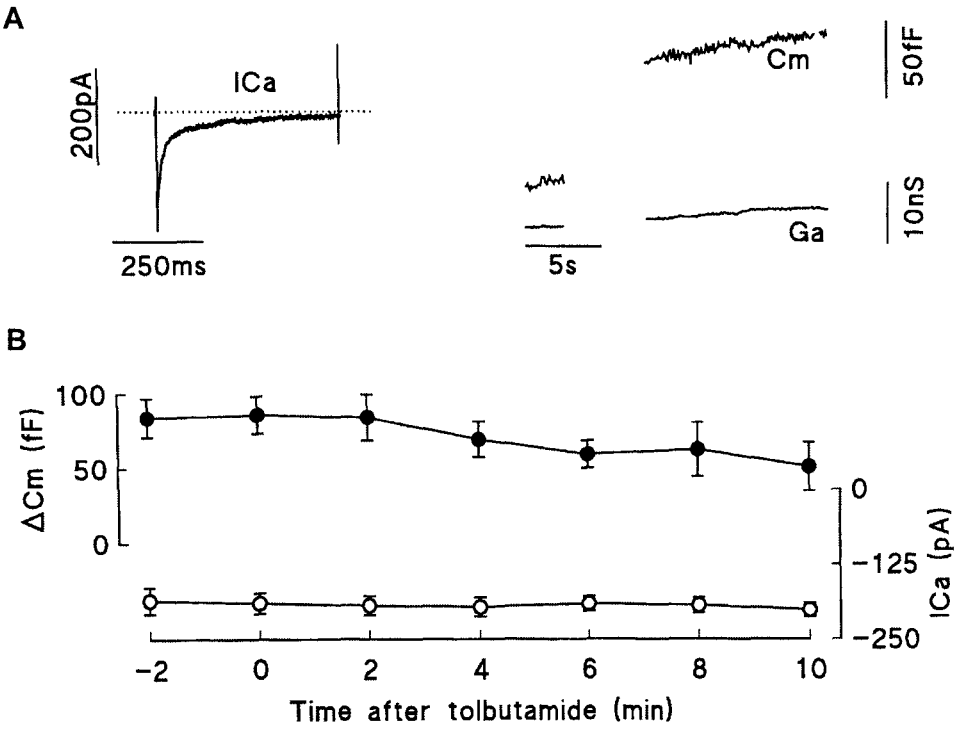

FIG. 2. Ca^{2+} currents and changes in β-cell capacitance evoked by 500-ms depolarizations before and after addition of tolbutamide. *A*: The Ca^{2+} current (ICa), the increase in cell capacitance (C_m), and the lack of change in access conductance (G_a) in a control cell. *B* :The average ICa (at the peak) and average ΔC_m (maximal change from baseline) in response to depolarizations applied in the same cells before and after addition of 100 μmol/l tolbutamide to the medium, which contained 2 μmol/l forskolin throughout. Values are means ± SE for 12 cells, except for min 8 and 10, where n = 10 and 9, respectively.

dle panels). In contrast, tolbutamide only produced a small and transient further rise in $[Ca^{2+}]_i$ and no change in insulin secretion in the presence of 30 mmol/l K^+, and it was completely ineffective in the presence of 60 mmol/l K^+ (Fig. 1, lower panels).

To determine whether this lack of effect is due to membrane depolarization or to high $[Ca^{2+}]_i$, the effects of tolbutamide were also tested in a medium containing 60 mmol/l K^+ and 0.5 instead of 2.5 mmol/l $CaCl_2$ (Fig. 1, lower panels). Under these conditions, both $[Ca^{2+}]_i$ and the insulin secretion rate were between those recorded in the presence of 4.8 and 15 mmol/l K^+, but tolbutamide was again without effect. Similar experiments (n = 7) were also performed in the presence of 0.5 mmol/l dibutyryl cAMP. Control $[Ca^{2+}]_i$ was not affected, but control insulin secretion was increased by ~80% (293 ± 39 vs. 162 ± 16 pg · islet^{-1} · min^{-1}). This, however, did not disclose any effect of tolbutamide (not shown).

Effects of tolbutamide in the presence of meglitinide. Meglitinide, also known as compound HB 699, is the nonsulfonylurea moiety of glibenclamide. It increases insulin secretion by binding to the sulfonylurea receptor and blocking K^+-ATP channels as do tolbutamide and glibenclamide (13,31,32). Repaglinide, a parent compound of meglitinide, has been reported not to possess the second effect of sulfonylureas (33). This means that by virtue of its action on the Ca^{2+} efficacy, tolbutamide should be able to increase insulin secretion in the presence of maximally effective concentrations of meglitinide or repaglinide. In the presence of 15 mmol/l glucose and 4.8 mmol/l K^+, 100 μmol/l meglitinide raised $[Ca^{2+}]_i$ to 306 ± 18 nmol/l (n = 18) and the insulin secretion rate to 294 ± 27 pg · islet^{-1} · min^{-1} (n = 7). Subsequent addition of 100 μmol/l tolbutamide had no effect on $[Ca^{2+}]_i$ and insulin secretion (not shown).

Effects of tolbutamide on β-cell capacitance changes studied in intact β-cells. Whole-cell Ca^{2+} current and cell capacitance were measured using the perforated-patch, whole-cell configuration. The mean basal cell capacitance averaged 6.89 ± 0.31 pF. Under control conditions, 500-ms depolarizations from −70 to 0 mV evoked Ca^{2+} currents of about 200 pA at the peak and capacitance increases that averaged about 80 fF (Fig. 2*A*). When the stimulation was repeated every 2 min up to 10 min after the addition of 100 μmol/l tolbutamide to the bath, the amplitude of the Ca^{2+} current remained fairly stable, and the evoked capacitance change was not significantly affected (Fig. 2*B*). In contrast, the increase in capacitance was tripled after 6 min of treatment with 25 nmol/l phorbol 12-myristate 13-acetate to activate protein kinase C (not shown).

Validation of the whole-cell configuration to study exocytosis by cell capacitance. The mean initial cell capacitance (C_m) recorded upon rupture of the β-cell membrane averaged 6.52 ± 0.13 pF. A progressive increase in C_m followed diffusion into the cell of the pipette solution containing 1.25 μmol/l free Ca^{2+} (Fig. 3*A*). Both the magnitude and the rate of the changes were markedly increased by cAMP (Fig. 3*A*). The nucleotide was therefore present in most of the following experiments. The change in capacitance was clearly smaller when the concentration of free Ca^{2+} was only 0.2 μmol/l, but

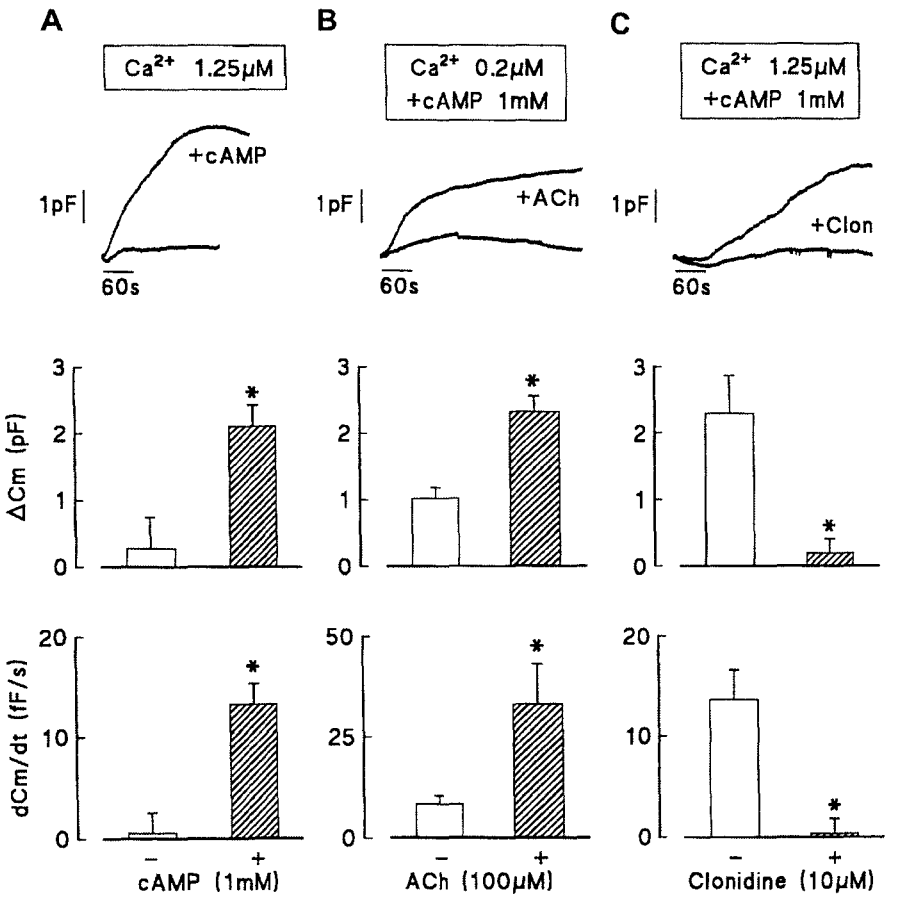

FIG. 3. Influence of cAMP, acetylcholine, and clonidine on the changes in cell capacitance evoked by dialysis of β-cells with 0.2 or 1.25 μmol/l free Ca^{2+}. The upper panels illustrate representative increases in cell capacitance occurring after establishment of the whole-cell recording configuration. cAMP was present in the pipette solution, whereas ACh and clonidine were present in the bath solution (for ~5 min before breaking of the membrane). The middle panels show the average changes in capacitance (ΔC_m), and the lower panels show the average rates of capacitance changes (dC_m/dt) calculated between 20 and 80% of the total change. Values are means ± SE for 10–17 cells. The access conductance (G_a) decreased with time from an average initial value of 119 ± 5 nS to 86 ± 5 nS. A change of G_a within this range of values does not significantly affect calculation of C_m (29).

both its extent and rate were augmented by the presence of 100 μmol/l acetylcholine (ACh) in the extracellular solution (Fig. 3*B*). In contrast, the response evoked by 1.25 μmol/l free Ca^{2+} was strongly inhibited by clonidine (Fig. 3*C*). These results thus show that exocytosis studied with this technique is Ca^{2+} dependent, increased by cAMP, and sensitive to potentiation and inhibition by activation of muscarinic and α_2-adrenergic receptors, respectively.

Effects of tolbutamide on cell capacitance in the presence of 0.2 μmol/l intracellular Ca^{2+}. When β-cells were dialysed with a pipette solution containing 0.2 μmol/l Ca^{2+} and 1 mmol/l cAMP, an increase in cell capacitance averaging about 1 pF was recorded (Fig. 4*A*). The presence of 100 μmol/l tolbutamide in the pipette solution or in the bath solution (which was devoid of $CaCl_2$) had no effect on the maximum change in cell capacitance. The rate of change in cell capacitance (dC_m/dt) was also unaffected by tolbutamide, whether it was calculated between 20 and 80% of the changes (Fig. 4*A*, bottom) or during the 1st min of change: 6.6 ± 1.2, 7.5 ± 1.6, and 6.0 ± 1.6 fF/s for controls, $Tolb_i$, or $Tolb_0$, respectively. Unlike ACh, tolbutamide was also ineffective when added to the bath after the increase in cell capacitance had developed in response to Ca^{2+} and cAMP (Fig. 4*B*, bottom). When the experiments were carried out in the presence of 0.2 μmol/l Ca^{2+} and the absence of cAMP, cell capacitance did not significantly change in the absence or presence of tolbutamide in the pipette (Fig. 4*B*).

Effects of tolbutamide on cell capacitance in the presence of 1.25 μmol/l intracellular Ca^{2+}. In control cells, the maximum increase and the rate of change in cell capacitance evoked by 1.25 μmol/l Ca^{2+} augmented with the concentration of cAMP, but they were not significantly affected by the presence of 100 μmol/l tolbutamide in the pipette solution (Figs. 5*A* and *B*). Addition of tolbutamide to the bath solution was also ineffective under these conditions (data not shown).

Effects of diazoxide on $[Ca^{2+}]_i$ in islet cells and insulin secretion. In the presence of 4.8 mmol/l K^+ and 15 mmol/l glucose, 250 μmol/l diazoxide lowered $[Ca^{2+}]_i$ and the insulin secretion rate to basal levels (Fig. 6, upper panels). Decreases in $[Ca^{2+}]_i$ and insulin secretion were also observed when diazoxide was added to a medium containing 15 or 30 mmol/l K^+. Diazoxide is known to repolarize the β-cell mem-

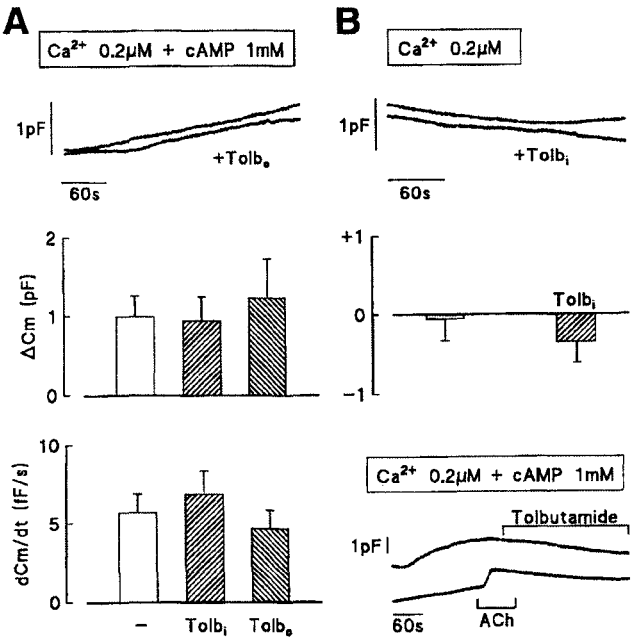

FIG 4. Lack of effect of tolbutamide on the changes in cell capacitance evoked by dialysis of β-cells with 0.2 μmol/l free Ca^{2+} with or without 1 mmol/l cAMP. The upper traces illustrate representative changes in cell capacitance occurring after establishment of the whole-cell recording configuration. Tolbutamide (100 μmol/l) was present either in the bath (To b_0) ~5 min before breaking of the membrane, or in the pipette solution ($Tolb_i$). The other panels show average changes in capacitance and in rate of capacitance changes, as in Fig. 3. Values are means ± SE for 13–18 cells. The bottom right panel illustrates experiments in which 100 μmol/l tolbutamide or 100 μmol/l ACh was added to the bath after establishment of the whole cell-patch. The traces are representative of 7 and 10 cells, respectively.

brane partially under these conditions (5). In contrast, neither $[Ca^{2+}]_i$ nor insulin secretion was affected by diazoxide in the presence of 60 mmol/l K^+, irrespective of the Ca^{2+} concentration in the medium and, hence, of the degree of β-cell stimulation (Fig. 6, lower panels).

Effects of diazoxide on cell capacitance in the presence of 1.25 μmol/l intracellular Ca^{2+}. The presence of 250 μmol/l diazoxide in the pipette solution was without effect on the maximum change (ΔC_m) in cell capacitance evoked by 1.25 μmol/l Ca^{2+} in the presence of 1 mmol/l cAMP (Fig. 5*C*). The rate of change in cell capacitance (dC_m/dt) was also unaffected by diazoxide, whether it was calculated between 20 and 80% of the changes (Fig. 5*C*, bottom) or during the 1st min of change: 12.9 ± 2.7 and 11.9 ± 1.7 fF/s without and with diazoxide, respectively.

DISCUSSION

There is no dispute that K^+-ATP channels are the primary site of action of tolbutamide and diazoxide in β-cells. Their closure and opening eventually increase and decrease $[Ca^{2+}]_i$, leading to stimulation and inhibition of insulin secretion, r espectively The question addressed in this study was whether these drugs also affect secretion by modulating the action of Ca^{2+} on the exocytotic process.

To test the hypothesis, it is essential that $[Ca^{2+}]_i$ remains stable because any change might account for an accompanying change in secretion. This is not easy in intact islets, the use of which is, however, essential to ascertain the physiological relevance of observations made with indirect approaches. When islets are studied in a control medium (4.8 mmol/l K^+, 15 mmol/l glucose), the blockade of K^+-ATP channels by tolbutamide causes depolarization, rise in $[Ca^{2+}]_i$, and stimulation of insulin release (9–12). The latter two events were measured in this study. Raising the concentration of K^+ in the medium to depolarize the β-cell membrane (30) increased control $[Ca^{2+}]_i$ and insulin release, but it caused a parallel attenuation of the effects of tolbutamide on both $[Ca^{2+}]_i$ and secretion. That the eventual abrogation of tolbutamide action on secretion results from an inability to raise $[Ca^{2+}]_i$ was demonstrated by the experiments performed in 60 mmol/l K^+ and 0.5 mmol/l $CaCl_2$. Tolbutamide was inactive in these strongly depolarized islets, although $[Ca^{2+}]_i$ was similar to that of islets that were only partially depolarized by 15 mmol/l K^+ (in the presence of 2.5 mmol/l $CaCl_2$) and in which the drug still raised $[Ca^{2+}]_i$ and secretion.

Exocytosis can be studied at the single-cell level by monitoring changes in cell capacitance (27–29). Because cell capacitance is proportional to cell surface area, and because the latter increases after fusion with secretory vesicles during exocytosis, secretion is detected by increases in cell capacitance. Conversely, endocytosis is followed by decreases in cell capacitance, and the measured changes are the net result of both processes. The technique has already been successfully applied to studies of insulin secretion from single β-cells (34–38).

With the perforated-patch technique, the cell remains intact and exocytosis is triggered by depolarizing pulses that activate Ca^{2+}i nflix through voltage-dependent Ca^{2+} channels. These experiments were carried out in the presence of forskolin because the capacitance changes evoked by Ca^{2+}i nflux are small if cAMP levels are low in β-cells (35,36; P.M., unpublished observations). Under these conditions, depolarizations for 500 ms to 0 mV evoked increases in cell capacitance similar to those reported by others (17,35,36). However, tolbutamide failed to increase the response, which contrasts with the doubling of the response that a similar concentration of the sulfonylurea produced in another study using similar tissue and conditions (17).

Cell capacitance changes can also be measured in the standard whole-cell configuration (37,38). After rupture of the plasma membrane at the tip of the recording pipette, the solution contained in the pipette diffuses within the cell and, if appropriate, stimulates exocytosis. Our results show that cell capacitance increased with the concentration of free Ca^{2+} (38), was markedly potentiated by cAMP, was inhibited by activation of α_2-adrenoceptors with clonidine (39), and was strongly augmented by acetylcholine. In spite of this evidence that our experimental model functions adequately, being able to detect receptor-mediated changes in exocytosis, tolbutamide was again found to be without effect. In a recent study, as yet reported in abstract form only (22), intracellular application of 100 μmol/l tolbutamide did not influence the strong stimulation of exocytosis evoked by 2 μmol/l Ca^{2+} in the presence of cAMP. Our experiments with 1.25 μmol/l Ca^{2+}, two concentrations of cAMP, and intra- or extracellular tolbutamide confirm this lack of effect. However, neither the maximum change in capacitance nor the rate

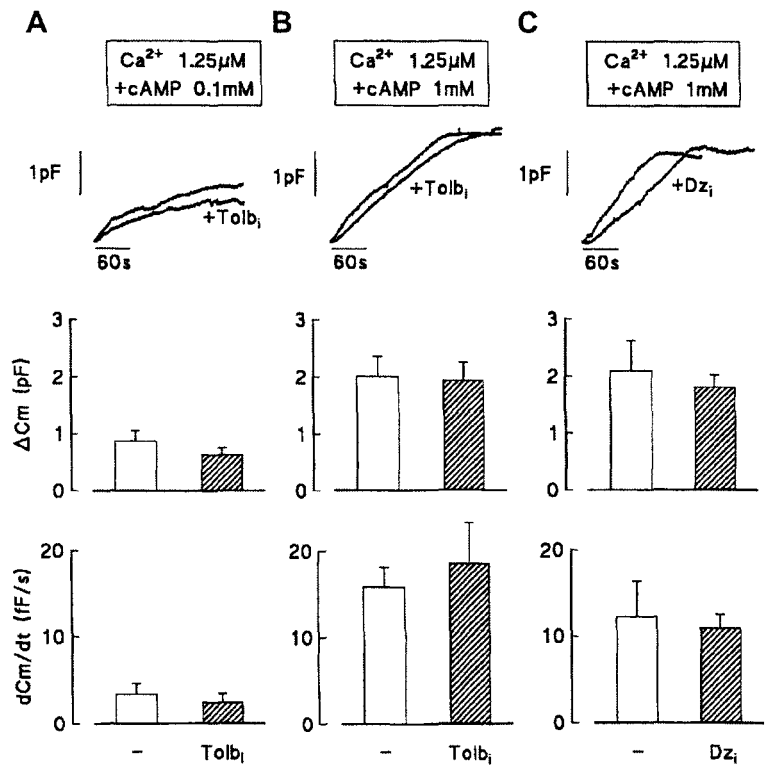

FIG. 5. Lack of effect of tolbutamide and diazoxide on the changes in cell capacitance evoked by dialysis of β-cells with 1.25 μmol/l Ca^{2+} and 0.1 or 1 mmol/l cAMP. The upper traces illustrate representative changes in cell capacitance occurring after establishment of the whole-cell recording configuration. cAMP, tolbutamide (100 μmol/l), and diazoxide (250 μmol/l) were present in the pipette solution ($Tolb_i$, Dz_i). The other panels show average changes in capacitance and rate of capacitance changes, as in Fig. 3. Values are means ± SE for 9–14 cells.

of change was significantly affected by tolbutamide when we tested the drug in the presence of 200 nmol/l Ca^{2+}, without or with cAMP. This contrasts with the report (22) that tolbutamide augmented the initial (~60 s) rate of exocytosis in the presence of 170 nmol/l Ca^{2+}, with or without cAMP. Whether the drug had a net effect on exocytosis (total change in capacitance) was not reported in the abstract (22).

Like those of tolbutamide, the effects of diazoxide on insulin secretion from intact islets have been studied during perifusions with solutions containing various K^+ concentrations. The drug was found to inhibit secretion as long as it also decreased $[Ca^{2+}]_i$ in islet cells. If diazoxide were able to interfere with the action of Ca^{2+} on exocytosis, it should have inhibited insulin secretion in the presence of 60 mmol/l K^+ even when it failed to lower the moderately (0.5 mmol/l extracellular $CaCl_2$) or markedly (2.5 mmol/l extracellular $CaCl_2$) elevated $[Ca^{2+}]_i$. Our measurements of cell capacitance also failed to disclose any direct inhibition of the exocytotic process by diazoxide applied intracellularly. Thus, they disagree with a previous study reporting that diazoxide strongly reduces the rate of capacitance change induced by tolbutamide or Ca^{2+} (22). It should also be borne in mind that many laboratories have reported that, provided glucose is present, high K^+ stimulates a sustained release of insulin from intact islets in the presence of diazoxide (7,40–42). This would not be so if diazoxide had any strong inhibitory action on exocytosis.

What can be the reason for the disparity between the present and previous results (17,22) based on capacitance measurements? With the reservation that few technical details are given in an abstract (22), comparison of both approaches shows the following important similarities and potentially significant differences. The animal species, the recording temperature, and the concentrations of tolbutamide and forskolin were identical, and the concentration of diazoxide was only slightly different (250 vs. 400 μmol/l). Our solutions contained 20 or 5 mmol/l glucose as compared with 5 or 0 mmol/l glucose (17), but this was not found to make any difference in either study. Finally, two different algorithms were used for capacitance measurements. The technique of Eliasson et al. (17) is based on the classic phase-sensitive method (43), whereas ours is based on a modification of this method (28) that has recently proved to be very reliable with the "Pulse-lockin" EPC-9 software that we used (44). Discussion of the respective advantages and limitations of each technique is beyond the scope of this paper, in particular because both approaches have usually been found to yield qualitatively similar results in other systems. We thus have no explanation for the disparity between our results and those of others, but we insist on the fact that our conclusions rely on data obtained with several methodologies.

By using three approaches to study insulin secretion, direct measurements from intact islets perifused for several minutes or from incubated permeabilized islet cells (23) and indirect estimations of exocytosis by recording cell capacitance changes during a few seconds or minutes, we conclude that tolbutamide and diazoxide affect secretion by changing the concentration, not the action, of Ca^{2+} in β-cells. If the latter effect exists, as suggested by others (16,17,22), it must be short-lived and small enough to escape our detection, and it is unlikely to be therapeutically relevant. There is no evidence that sulfonylureas mimic the second mechanism by which glucose stimulates insulin secretion (5–7). This justifies ongoing searches for new drugs acting on β- cd ls

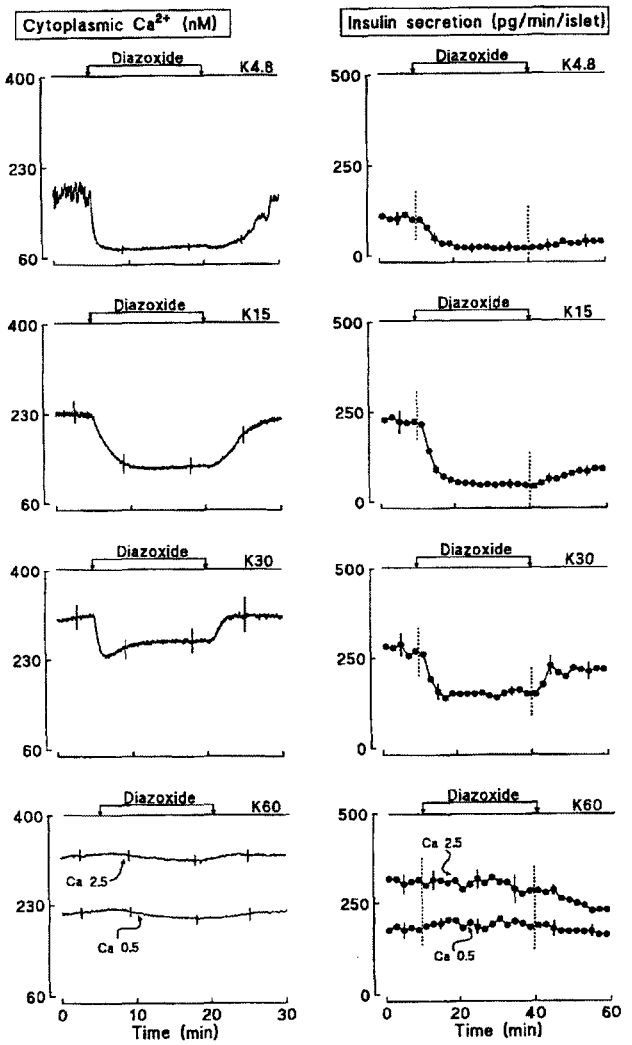

FIG. 6. Effects of diazoxide on cytoplasmic Ca^{2+} and insulin secretion by perifused mouse islets. The medium contained 15 mmol/l glucose, the indicated concentration of K^+, and 2.5 mmol/l $CaCl_2$ (except in one experimental series of the lower panels). Diazoxide (250 µmol/l) was added as indicated. Measurements started after an initial equilibration period of 10 ($[Ca^{2+}]_i$) or 30 (insulin) min. Values are means ± SE for 8–25 individual islets ($[Ca^{2+}]_i$) or 6–9 experiments with batches of 20 islets (insulin).

ACKNOWLEDGMENTS

This work was supported by grants 3.4525.94 and LN 9.4592.95 from the Fonds de la Recherche Scientifique Médicale, Brussels; by grant ARC 95/00-188 from the General Direction of Scientific Research of the French Community of Belgium; and by the Interuniversity Poles of Attraction Programme–Belgian State, Prime Minister's Office–Federal Office for Scientific, Technical and Cultural Affairs. P.G. is Chercheur Qualifié of the Fonds National de la Recherche Scientifique, Brussels.

REFERENCES

1. Henquin JC: The cell biology of insulin secretion. In *The Joslin's Diabetes Mellitus.* 13th ed. Kahn CR, Weir GC, Eds. Philadelphia, Lea and Febiger, 1994, p. 56–80
2. Ashcroft FM, Proks P, Smith PA, Ämmälä C, Bokvist K, Rorsman P: Stimulus-secretion coupling in pancreatic β cells. *J Cell Biochem* 55S:54–65, 1994
3. Wollheim CB, Lang J, Regazzi R: The exocytotic process of insulin secretion and its regulation by Ca^{2+} and G-proteins. *Diabetes Rev* 4:276–297, 1996
4. Cook DL, Taborsky GJ: B-cell function and insulin secretion. In *Ellenberg and Rifkin's Diabetes Mellitus.* 5th ed. Porte D, Sherwin RS, Eds. Stamford, CT, Appleton & Lange, 1997, p. 49–73
5. Gembal M, Gilon P, Henquin JC: Evidence that glucose can control insulin release independently from its action on ATP-sensitive K^+ channels in mouse B-cells. *J Clin Invest* 89:1288–1295, 1992
6. Sato Y, Aizawa T, Komatsu M, Okada N, Yamada T: Dual functional role of membrane depolarization/Ca^{2+} influx in rat pancreatic B-cell. *Diabetes* 41:438–443, 1992
7. Gembal M, Detimary P, Gilon P, Gao ZY, Henquin JC: Mechanisms by which glucose can control insulin release independently from its action on ATP-sensitive K^+ channels in mouse B-cells. *J Clin Invest* 91:871–880, 1993
8. Groop LC: Sulfonylureas in NIDDM. *Diabetes Care* 15:737–754, 1992
9. Henquin JC: Established, unsuspected and novel pharmacological insulin secretagogues. In *New Antidiabetic Drugs.* Bailey CJ, Flatt PR, Eds. London, Smith-Gordon, 1990, p. 93–106
10. Satin LS: New mechanisms for sulfonylurea control of insulin secretion. *Endocrine* 4:191–198, 1996
11. Panten U, Schwanstecher M, Schwanstecher C: Sulfonylurea receptors and mechanism of sulfonylurea action. *Exp Clin Endocrinol* 104:1–9, 1996
12. Nelson DA, Aguilar-Bryan L, Raef H, Boyd AK: Molecular mechanisms of sulphonylurea action in the pancreatic B-cell. In *Nutrient Regulation of Insulin Secretion.* Flatt PR, Ed. London, Portland Press, 1992, p. 319–339
13. Ashcroft SJH, Ashcroft FM: The sulfonylurea receptor. *Biochim Biophys Acta* 1175:45–59, 1992
14. Aguil a-Bryan L, Nichols CG, Wechsler SW, Clement JP IV, Boyd AK III, Gonzalez G, Herrera-Sosa H, Nguy K, Bryan J, Nelson DA: Cloning of the β cell high-affinity sulfonylurea receptor: a regulator of insulin secretion. *S cience* 268:423–426, 1995
15. Inagaki N, Gonoi T, Clement JP IV, Namba N, Inazawa J, Gonzalez G, Aguilar-Bryan L, Seino S, Bryan J: Reconstitution of IKATP: an inward rectifier subunit plus the sulfonylurea receptor. *Science* 270:1166–1170, 1995
16. Flatt PR, Shibier O, Szecowka J, Berggren PO: New perspectives on the actions of sulphonylureas and hyperglycaemic sulphonamides on the pancreatic β-cell. *Diabete Metab* 20:157–162, 1994
17. Eliasson L, Renström E, Ämmälä C, Berggren PO, Bertorello AM, Bokvist K, Chibalin A, Deeney JT, Flatt PR, Gäbel J, Gromada J, Larsson O, Lindström P, Rhodes CJ, Rorsman P: PKC-dependent stimulation of exocytosis by sulfonylureas in pancreatic β cells. *Science* 271:813–815, 1996
18. Marks V, Samols E: Diazoxide therapy of intractable hypoglycemia. *Ann NY Acad Sci* 150:442–454, 1968
19. Henquin JC, Meissner HP: Opposite effects of tolbutamide and diazoxide on $^{86}Rb^+$ fluxes and membrane potential in pancreatic B-cells. *Biochem Pharmacol* 31:1407–1415, 1982
20. Trube G, Rorsman P, Ohno-Shozaku T: Opposite effects of tolbutamide and diazoxide on the ATP-sensitive potassium channel. *Lancet* 2:493–499, 1986
21. Gilon P, Henquin JC: Influence of membrane potential changes on cytoplasmic Ca^{2+} concentration in an electrically excitable cell, the insulin-secreting pancreatic B-cell. *J Biol Chem* 267:20713–20720, 1992
22. Renström E, Rorsman P: Intracellular tolbutamide stimulates calcium-dependent exocytosis in pancreatic B-cells (Abstract). *Diabetologia* 39 (Suppl. 1):A229, 1996
23. Garcia-Barrado MJ, Jonas JC, Gilon P, Henquin JC: Sulphonylureas do not increase insulin secretion by a mechanism other than a rise in cytoplasmic Ca^{2+} in pancreatic B cells. *Eur J Pharmacol* 298:279–286, 1996
24. Hedeskov CJ: Mechanism of glucose-induced insulin secretion. *Physiol Rev* 60:442–509, 1980
25. Pipeleers D: The biosociology of pancreatic B cells. *Diabetologia* 30:277–291, 1987
26. Henquin JC: D-glucose inhibits potassium efflux from pancreatic islet cells. *Nature* 271:271–273, 1978
27. Neher E, Marty A: Discrete changes of cell membrane capacitance observed under conditions of enhanced secretion in bovine adrenal chromaffin cells. *Proc Natl Acad Sci USA* 79:6712–6716, 1982
28. Lindau M, Neher E: Patch-clamp techniques for time-resolved capacitance measurements in single cells. *Pflügers Arch* 411:137–146, 1988
29. Gillis KD: Techniques for membrane capacitance measurements. In *Single-Channel Recording.* Sakman B, Neher E, Eds. New York, Plenum, 1995, p. 155–198
30. Meissner HP, Henquin JC, Preissler M: Potassium dependence of the membrane potential of pancreatic B-cells. *FEBS Lett* 94:87–89, 1978

31. Garrino MG, Schmeer W, Nenquin M, Meissner HP, Henquin JC: Mechanism of the stimulation of insulin release in vitro by HB 699, a benzoic acid derivative similar to the non-sulphonylurea moiety of glibenclamide. *Diabetologia* 28:697–703, 1985
32. Zünkler BJ, Lenzen S, Manner K, Panten U, Trube G: Concentration-dependent effects of tolbutamide, meglitinide, glipizide, glibenclamide and diazoxide on ATP-regulated K^+ currents in pancreatic B-cells. *Naunyn-Schmiedeberg's Arch Pharmacol* 337:225–230, 1988
33. Fuhlendorff J, Carr R, Kofod H, Rorsman P: The mechanism of action of repaglinide differs to sulphonylureas in murine beta cells (Abstract). *Pharmacol Res* 31 (Suppl. 1):32, 1995
34. Gillis KD, Misler S: Single cell assay of exocytosis from pancreatic islet B cells. *Pflügers Arch* 420:121–123, 1992
35. Gillis KD, Misler S: Enhancers of cytosolic cAMP augment depolarization-induced exocytosis from pancreatic B-cells: evidence for effects distal to Ca^{2+} entry. *Pflügers Arch* 424:195–197, 1993
36. Ämmälä C, Ashcroft FM, Rorsman P: Calcium-independent potentiation of insulin release by cyclic AMP in single β-cells. *Nature* 363:356–358, 1993
37. Barnett DW, Misler S: Coupling of exocytosis to depolarization in rat pancreatic islet β cells: effects of Ca^{2+}, Sr^{2+} and Ba^{2+}-containing extracellular solutions. *Pflügers Arch* 430:593–595, 1995
38. Proks P, Eliasson L, Ämmälä C, Rorsman P, Ashcroft FM: Ca^{2+}- and GTP-dependent exocytosis in mouse pancreatic β-cells involves both common and distinct steps. *J Physiol* 496:255–264, 1996
39. Renström E, Ding WG, Bokvist K, Rorsman P: Neurotransmitter-induced inhibition of exocytosis in insulin-secreting β cells by activation of calcineurin. *Neuron* 17:513–522, 1996
40. Taguchi N, Aizawa T, Sato Y, Ishihara F, Hashizume K: Mechanisms of glucose-induced biphasic insulin release: physiological role of adenosine triphosphate-sensitive K^+ channel-independent glucose action. *Endocrinology* 136:3942–3948, 1995
41. Cunningham BA, Deeney JT, Bliss CR, Corkey BE, Tornheim K: Glucose-induced oscillatory insulin secretion in perifused rat pancreatic islets and clonal β-cells (HIT). *Am J Physiol* 271:E702–E710, 1996
42. Zawalich WS, Zawalich KC: Regulation of insulin secretion via ATP-sensitive K^+ channel independent mechanisms: role of phospholipase C. *Am J Physiol* 272:E671–E677, 1997
43. Joshi C, Fernandez JM: Capacitance measurements: an analysis of the phase detector technique used to study exocytosis or endocytosis. *Biophys J* 53:885–892, 1988
44. Gillis KD, Mossner R, Neher E: Protein kinase C enhances exocytosis from chromaffin cells by increasing the size of the readily releasable pool of secretory granules. *Neuron* 16:1209–1220, 1996

Chapitre 3

Homéostasie calcique et cellules prostatiques.

Travaux de recherche actuels : 1997-2003

ATER puis Maître de Conférences, laboratoire de Physiologie Cellulaire, Université des Sciences et Technologies de Lille, 1997-1999

J'ai été recruté en 1997 comme ATER à l'USTL puis comme Maître de Conférences en 1999. Je me suis intégré dans le laboratoire de Physiologie Cellulaire, dirigé par le Professeur N.Prevarskaya. Le projet sur lequel j'ai été recruté concernait l'étude du rôle des mécanismes d'homéostasie calcique dans la physiopathologie de la prostate.

Il est établi que la croissance et le développement de la prostate sont sous contrôle androgénique. Les thérapies actuelles se limitent à diminuer les taux d'androgènes circulants. Malgré leur efficacité temporaire sur les tumeurs, ces traitements se révèlent inopérants à long terme sur l'évolution des carcinomes prostatiques. En effet, à un stade avancé, le cancer de la prostate devient androgéno-indépendant et échappe aux traitements hormonaux. Il est ainsi évident que d'autres facteurs, tels que les facteurs de croissance et les neuropeptides interviennent dans la cancérogenèse de la prostate. Dans d'autres modèles cellulaires, les étapes précoces de la transduction de neuropeptides ou de facteurs de croissance sont caractérisées par l'activation de canaux ioniques. Des études récentes ont montré que ces canaux membranaires et le calcium intracellulaire sont des éléments importants des cascades d'événements conduisant à la prolifération, la différenciation, et l'apoptose. Cependant, il existait peu de données sur l'expression, le fonctionnement, la régulation et le rôle des canaux ioniques dans la prostate humaine lors de la création du laboratoire de Physiologie cellulaire par le Professeur Prevarskaya en 1996.

Ainsi, le projet de recherche du laboratoire s'est orienté particulièrement vers l'étude, d'une part, des mécanismes contrôlant l'homéostasie calcique et le fonctionnement des canaux ioniques au cours du développement des tumeurs de la prostate et d'autre part, de leur régulation par les neuropeptides et les facteurs de croissance.

Dans le cadre de l'étude de la régulation du métabolisme calcique dans les cellules de la prostate humaine, et de son rôle dans les phénomènes de prolifération et d'apoptose, j'ai participé à la caractérisation des mécanismes d'homéostasie calcique et de leur rôle dans la régulation de la croissance (articles **4, 5, 6**), et de la différenciation neuroendocrine (articles **7, 8**) des cellules prostatiques.

Calcium et croissance cellulaire

Article 4.

Store depletion and store-operated calcium current in human prostate cancer cells LNCaP : involvement in apoptosis.

Skryma R, Mariot P, Van Coppenolle F, Le Bourhis X, Boilly B, Schuba Y, Chernevskaya N, Prevarskaya N (2000) **J. Physiol.** 527 : 71-83.

Article 5.

Evidence of functional ryanodine receptors involved in apoptosis of prostate cancer (LNCaP) cells involved in apoptosis.

Mariot P, Prevarskaya N, Roudbaraki MM, Le Bourhis X, Van Coppenolle F, Skryma R (2000) **Prostate** 43 : 205-214.

I. Position du problème et résultats

Afin de déterminer le rôle du calcium dans les processus apoptotiques des cellules cancéreuses androgéno-dépendantes, nous avons tout d'abord caractérisé certains mécanismes d'homéostasie calcique de ces cellules. Nous avons recherché tout d'abord l'existence d'un stock calcique intracellulaire, dans les cellules LNCaP, en utilisant la thapsigargine (TG) qui inhibe sélectivement les Ca^{2+}-ATPases du réticulum endoplasmique (**article 4**). Nous avons ainsi observé que la thapsigargine induit une augmentation du $[Ca^{2+}]i$ grâce à une vidange des réserves de calcium contenu dans le réticulum et à un influx consécutif de Ca^{2+}. En effet, cet influx est inhibé en absence de calcium dans le milieu extracellulaire ou en présence d'inhibiteurs de l'influx du Ca^{2+}: Nickel (Ni^{2+}) et Lanthane (La^{3+}). Comme cette entrée d'ions Ca^{2+} est dépendante du contenu en calcium dans les réserves intracellulaires, elle est dénommée "entrée capacitative" dans d'autres systèmes. Nous avons étudié le rôle de cette entrée capacitative dans l'apoptose de la prostate. Nos résultats montrent que la TG stimule l'apoptose des cellules LNCaP. En revanche, le Ni^{2+} n'inhibe pas l'apoptose induite par un traitement à long terme avec la TG alors qu'il bloque l'augmentation de calcium dans le cytosol. Au contraire, le Ni^{2+}, sans effet par lui-même sur l'apoptose, potentialise l'effet de la TG sur l'apoptose. Ceci montre que ce n'est pas l'augmentation de calcium libre dans le cytosol conséquente à l'entrée capacitative de calcium qui stimule l'apoptose.

Dans **l'article 5**, nous avons étudié l'expression de récepteurs-canaux calciques du RE sensibles à la ryanodine (récepteurs RyR) et leur implication potentielle dans le processus d'apoptose. Nous

avons montré que l'activation de ces récepteurs entraînait une mobilisation de calcium des réserves intracellulaires contenues dans le réticulum endoplasmique et était de plus capable de provoquer une entrée capacitative de calcium dans les cellules LNCaP. Cette étude a permis de démontrer l'existence d'un canal calcique intracellulaire sensible à la ryanodine et fonctionnel dans les cellules non-excitables prostatiques cancéreuses. Nous avons montré par RT-PCR que des récepteurs de type RyR1 (muscle squelettique) et RyR2 (cardiaque) étaient exprimés de manière fonctionnelle dans les cellules LNCaP. D'autre part, nous avons montré que l'activation de ce canal pouvait stimuler le processus de mort cellulaire programmée.

II. Discussion

La libération de calcium des réserves intracellulaires contenues dans le RE a été démontrée comme stimulant l'apoptose dans différents modèles cellulaires.

Deux hypothèses différentes ont été avancées pour expliquer cet effet :

1) l'augmentation de calcium cytosolique (McConkey et al 1988, Martikainen et al 1991, Jiang et al 1994, Furuya et al 1994, Wang et al 1999)
2) la diminution de la concentration en calcium dans le RE (Lam et al 1993, He et al 1997, Bian et al 1997, Soboloff et Berger 2002)

Le rôle d'une entrée capacitative a été démontré dans les cellules non androgéno-dépendantes de la prostate (DU145) par l'équipe d'Isaacs (Furuya et al 1994). Ces derniers ont émis comme hypothèse que le paramètre important dans la stimulation de l'apoptose était la concentration en calcium dans le cytosol. Nos résultats montrent que le mode d'induction de l'apoptose est différent dans les cellules androgéno-dépendantes. Ainsi, la mort cellulaire programmée n'est pas directement dépendante de la concentration en calcium dans le cytosol mais très probablement de la concentration en calcium dans les différentes zones de réserves intracellulaires de la cellule et plus particulièrement le RE. Il est possible que l'état de remplissage des réserves intracellulaires de calcium soit également un facteur important dans la régulation de l'apoptose et qu'une vidange de ces réserves soit un facteur favorisant ou déclenchant la mort cellulaire programmée. Ceci est d'autre part corroboré par le fait que la déplétion des réserves calciques (stimulée par la TG) du RE est beaucoup moins importante dans les cellules transfectées avec la protéine anti-apoptotique bcl-2 (He et al, 1997, Foyouzi-Youssefi et al 2000), ce qui suggère que la protéine bcl-2 joue son rôle protecteur en contrôlant le niveau de calcium dans le RE. D'autre part, nous nous avons montré dans ce travail que l'entrée capacitative SOC, certainement en permettant le remplissage du RE,

permet de contrecarrer l'apoptose induite par la vidange du RE. Nous avons montré ultérieurement (Vanden Abeele et al 2003) que la nature du SOC impliqué est très probablement dépendante de l'expression de deux isoformes de TRP : TRPV6 et TRPC1.

Plusieurs hypothèses peuvent expliquer le rôle de l'état de remplissage du RE dans l'induction de l'apoptose :

1) Le calcium dans la lumière du RE étant nécessaire à la synthèse et à la maturation protéique, la vidange des stocks calciques du RE pourrait provoquer un arrêt de la synthèse, de la maturation, et du transport intracellulaire de certaines protéines.

2) La vidange des réserves calciques du RE pourrait déstabiliser le gel protéine-Ca^{2+} associé à la membrane du RE et provoquer une formation de vésicules et la formation de figures apoptotiques caractéristiques (« blebs »),

3) La vidange du RE provoquerait la libération d'une endonucléase vers le noyau qui serait responsable de la fragmentation de l'ADN,

4) Les contacts quasi-synaptiques entre membrane du RE et membrane mitochondriale, qui permettent à la mitochondrie de capturer très rapidement le calcium libéré par le RE, suggèrent également que la vidange du RE conduit à une surcharge calcique mitochondriale, qui serait responsable de la mort cellulaire (Rizzuto et al 1998, Csórdas et al 1999).

Ces mécanismes ne sont pas nécessairement contradictoires et peuvent être dépendants du type cellulaire impliqué. Ainsi, Soboloff et Berger (2002) montrent qu'une déplétion massive des réserves intracellulaires de calcium induit l'apoptose de mastocytes par des mécanismes différents en fonction du mode d'activation de la vidange. Dans ce modèle cellulaire, la TG induit l'apoptose *via* une surchage calcique mitochondriale et l'econazole *via* une inhibition de la synthèse protéique, les deux provoquant une vidange calcique du RE.

Nous avons également montré que l'activation de récepteurs-canaux calciques intracellulaires, ici des RyR, provoque également la mort cellulaire, dans des proportions moins importantes que celle induite par la TG (4 % vs 70 % au bout de 84 heures de traitement). Les récepteurs RyR ont été également démontrés par d'autres auteurs comme des acteurs majeurs du signal apoptotique. Ainsi, des cellules CHO transfectées avec RyR1 sont sensibles aux agents stimulants des RyR (caffeine, ryanodine) et voient leur mort cellulaire apoptotique induite par ces mêmes agents (Pan et al 2000). La stimulation des récepteurs ryanodine dans des cellules CHO surexprimant RyR2 entraîne également la mort cellulaire (George et al 2003). L'activation de récepteurs IP3 a été également démontrée comme stimulatrice de l'apoptose. Ainsi, la déficience en récepteurs IP3-R1

chez les thymocytes leur confère une résistance à l'apoptose induite par différents stimulis (dexamethasone, rayons ionisants...) (Jayaraman et Marks 1997). De plus, les récepteurs IP3-R3 voient leur expression (protéine et mRNA) augmentée lors de processus apoptotiques, à la fois lors du développement, ou lors de stimulis (activation de récepteurs glutamate de type kainate) dans de multiples modèles cellulaires (neurones, cellules intestinales, et cellules folliculaires) (Blackshaw et al 2000). Il a été également montré, grâce à l'utilisation de cellules déficientes en IP3R1 exprimant une calcineurine A constitutive, que la calcineurine restaurait la sensibilité aux agents proapoptotiques. Ceci suggère que la calcineurine est en aval de la chaine de transduction dans laquelle sont impliqués les récepteurs IP3, et que celle-ci permet la translocation de facteurs de transcription NF-AT vers le noyau et la déphosphorylation de Bad (Jayaraman et al 2000), un facteur pro-apoptotique lorsqu'il est déphosphorylé et associé à Bcl-2 ou Bcl-Xl et antiapoptotique lorsqu'il est phosphorylé (par la kinase Akt notamment) et libéré de Bcl-2/Bcl-Xl (Zha et al 1996). De plus, il a été montré que la stimulation des récepteurs purinergiques, couplés à la voie phospholipase C/IP3 induisait l'apoptose *via* l'activation de récepteurs RyR, ce qui suggère que les récepteurs IP3 et RyR seraient couplés au niveau fonctionnel et participeraient conjointement à l'induction de l'apoptose (George et al 2003). Les récepteurs IP3 ou RyR pourraient de plus jouer le rôle de détecteurs et être sensibles aux concentrations de calcium dans la lumière du RE et ainsi à une déplétion des réserves calciques (Hajnócsky et al 2000).

Nos résultats, en accord avec ceux de Wertz et al (2000), montrent également que la dépendance de l'apoptose vis-à-vis du calcium est différente entre cellules cancéreuses androgéno-dépendantes et androgéno-indépendantes (Furuya et al 1994). La voie de la caspase 9 (une caspase initiatrice), qui peut activer les caspases 7 et 3 (effecteurs) et amplifier le processus de protéolyse, semble être impliquée dans l'action pro-apoptotique de la TG dans les cellules LNCaP (Wertz et Dixit, 2000). Cependant, il a été montré dans d'autres modèles cellulaires qu'une déplétion des réserves intracellulaires provoque un stress au niveau du RE qui entraîne l'activation de la voie de la caspase 12 (une caspase initiatrice) (Nakagawa et al 2000). La voie de la caspase 12 semble être ainsi au centre de la détection d'une vidange calcique du RE alors que la voie de la caspase 9 semble être stimulée par la surcharge calcique mitochondriale. Cependant, comme la caspase 12 peut être activée par les caspases 9 et 7, il est possible que les voie des caspases 9 et 12 soient toutes les deux impliquées dans l'action de la TG (voir figure 15).

Dans les cellules androgéno-indépendantes, l'apoptose est activée par l'entrée de calcium *via* un SOC (Furuya et al 1994). Une des raisons possibles de cette différence réside dans l'expression de la protéine anti-apoptotique Bcl-2. Les cellules prostatiques androgéno-indépendantes cancéreuses (DU145) sont plus résistantes à l'apoptose que les cellules androgéno-dépendantes (LNCaP).

D'autre part, la surexexpression de BCl-2 induit un phénotype androgéno-indépendant (Raffo et al 1995). Il a été montré de plus par notre laboratoire (Vanden Abeele et al 2002) et d'autres (Pinton et al 2000, Foyouzi-Youssefi et al 2000) que la surexpression de BCl-2 induit une diminution des réserves calciques intracellulaires, une diminution de la vidange des réserves en réponse à la TG et une dimunition du SOC. D'autre part, en augmentant l'entrée de calcium, il est possible d'induire l'apoptose dans les cellules LNCaP surexprimant Bcl-2 (Vanden Abeele et al 2002), au contraire des cellules LNCaP androgéno-dépendantes (Skryma et al 2000). Ainsi, Bcl-2, se comportant possiblement comme un canal de fuite au niveau du RE, pourrait protéger les cellules contre un stress du RE, *i.e.* une vidange calcique. Cependant, s'il a été montré que Bcl-2 pouvait se comporter comme un canal ionique dans le RE (Minn et al 1997, Schendel et al 1997), il n'est pas démontré qu'il puisse conduire le calcium.

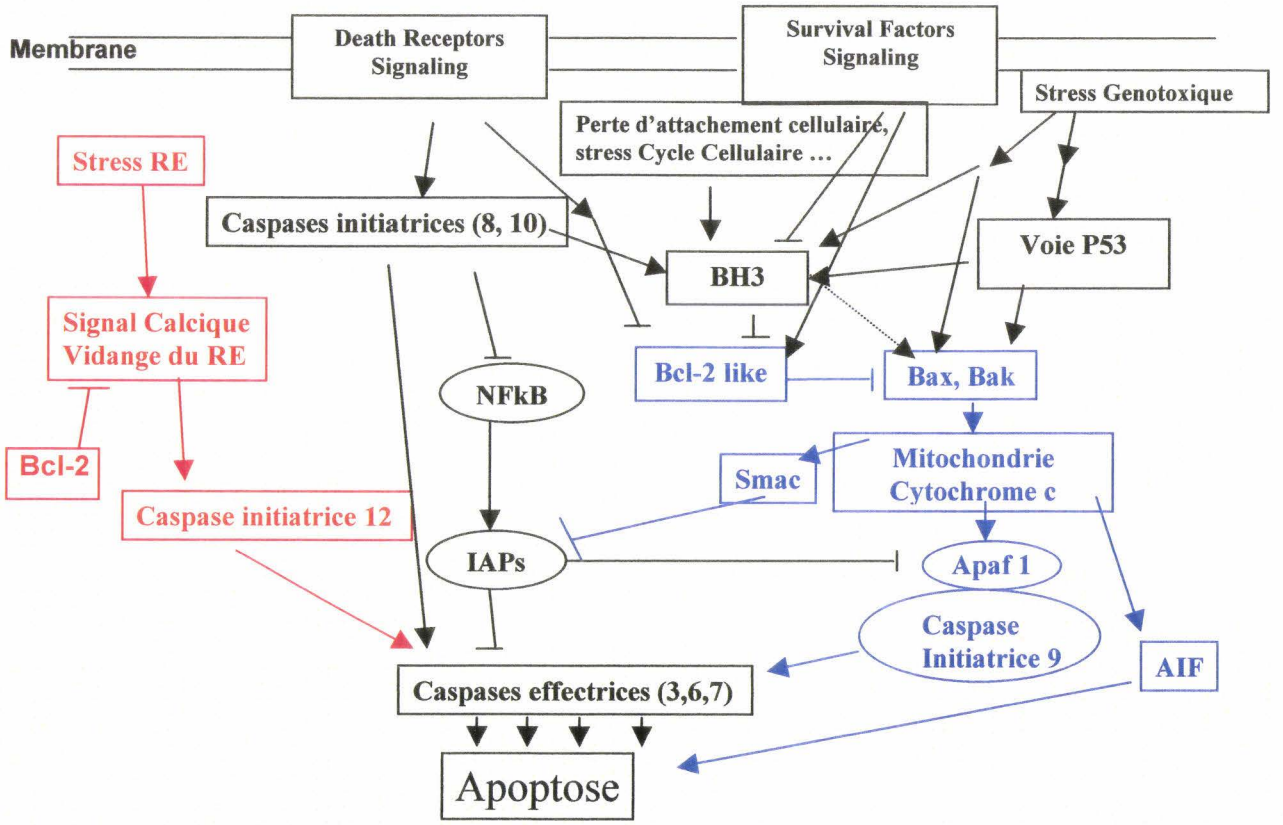

Figure 15 : Principales voies d'induction de l'apoptose

En rouge : voie du RE

En bleu : voie mitochondriale

→ Stimulation

⊣ Inhibition

Store depletion and store-operated Ca^{2+} current in human prostate cancer LNCaP cells: involvement in apoptosis

Roman Skryma, Pascal Mariot, Xuefen Le Bourhis*, Fabien Van Coppenolle, Yaroslav Shuba, Fabien Vanden Abeele, Guillaume Legrand, Sandrine Humez, Benoni Boilly* and Natalia Prevarskaya

*Laboratoire de Physiologie Cellulaire, INSERM EPI-9938 and *Laboratoire de Biologie du Développement, USTL, Villeneuve d'Ascq, France*

(Received 31 January 2000; accepted after revision 18 May 2000)

1. In the present study, we investigated the mechanisms involved in the induction of apoptosis by the Ca^{2+}-ATPase inhibitor thapsigargin (TG), in androgen-sensitive human prostate cancer LNCaP cells.

2. Exposure of fura-2-loaded LNCaP cells to TG in the presence of extracellular calcium produced an increase in intracellular Ca^{2+}, the first phase of which was associated with depletion of intracellular stores and the second one with consecutive extracellular Ca^{2+} entry through plasma membrane, store-operated Ca^{2+} channels (SOCs).

3. For the first time we have identified and characterized the SOC-mediated membrane current (I_{store}) in prostate cells using whole-cell, cell-attached, and perforated patch-clamp techniques, combined with fura-2 microspectrofluorimetric and Ca^{2+}-imaging measurements.

4. I_{store} in LNCaP cells lacked voltage-dependent gating and displayed an inwardly rectifying current–voltage relationship. The unitary conductance of SOCs with 80 mM Ca^{2+} as a charge carrier was estimated at $3{\cdot}2 \pm 0{\cdot}4$ pS. The channel has a high selectivity for Ca^{2+} over monovalent cations and is inhibited by Ni^{2+} (0·5–3 mM) and La^{3+} (1 μM).

5. Treatment of LNCaP cells with TG (0·1 μM) induced apoptosis as judged from morphological changes. Decreasing extracellular free Ca^{2+} to 200 nM or adding 0·5 mM Ni^{2+} enhanced TG-induced apoptosis.

6. The ability of TG to induce apoptosis was not reduced by loading the cells with intracellular Ca^{2+} chelator (BAPTA-AM).

7. These results indicate that in androgen-sensitive prostate cancer cells the depletion of intracellular Ca^{2+} stores may trigger apoptosis but that there is no requirement for the activation of store-activated Ca^{2+} current and sustained Ca^{2+} entry in induction and development of programmed cell death.

Prostate cancer is the second highest cause of cancer death in men (Woolf *et al.* 1995; Parker *et al.* 1997). Androgen withdrawal therapy is commonly used to delay the progression of the disease (Montironi *et al.* 1994). However, prostate cancer under hormonal ablation therapy will in most cases exhibit androgen-independent characteristics and the tumours will continue to progress. The androgen-insensitive prostate cancer cells are characterized by a very low proliferation rate that renders the typical chemotherapy agents ineffective. For this reason, targeting programmed cell death, or apoptosis, may be particularly relevant for prostate cancer therapy.

It has now been established that Ca^{2+} ions are major players in an intracellular signalling system that translates extracellular stimuli into the regulation and control of cellular events leading to programmed cell death (for a review see McConkey & Orrenius, 1997; see also Dowd, 1995; Berridge *et al.* 1998). Increases in intracellular Ca^{2+} concentration ($[Ca^{2+}]_i$) have been shown to trigger apoptosis (Martikainen *et al.* 1991; Juin *et al.* 1998) and numerous apoptosis inducers increase $[Ca^{2+}]_i$ (McConkey *et al.* 1989; Spielberg *et al.* 1991). However, the precise mechanism(s) by which Ca^{2+} ions trigger apoptosis remain poorly understood. Ca^{2+} stores are intracellular compartments characterized by their high intraluminal Ca^{2+} content and their participation in the regulation of $[Ca^{2+}]_i$ through rapid Ca^{2+} accumulation and release (Gill *et al.* 1996; Berridge, 1997). The depletion of Ca^{2+} stores induces a 'Ca^{2+}-refilling mechanism', a plasma membrane Ca^{2+} entry initially called capacitative Ca^{2+} influx by Putney (1986, 1990) or store-operated Ca^{2+} current (I_{store}).

This mechanism has been demonstrated in a variety of non-excitable cells (for review see Parekh & Penner, 1997). Store-operated Ca^{2+} channels (SOCs) have been shown to be involved in controlling many important physiological and physiopathological functions: secretion, gene transcription, cell cycle, proliferation and also apoptosis (Parekh & Penner, 1995; Fanger *et al.* 1995; Berridge, 1995*a*; McConkey & Orrenius, 1997; Santella, 1998). While the implication of Ca^{2+} ions in the induction of apoptosis is now generally accepted, the data concerning the role of store-operated current in this process are rather contradictory and confusing. Two hypotheses have been proposed. The first assumes that apoptosis may be triggered by endoplasmic reticulum (ER) calcium pool depletion without any requirement for the cytosolic Ca^{2+} elevation due to store-operated Ca^{2+} entry (He *et al.* 1997; Bian *et al.* 1997). Moreover, according to this hypothesis the capacitative Ca^{2+} current may be important for optimal ER pool filling and apoptosis inhibition. The second hypothesis, on the contrary, assumes that a sustained elevation in cytosolic Ca^{2+} to a critical level is the initiator of apoptosis (Dowd *et al.* 1992; Furuya *et al.* 1994; Wang *et al.* 1999).

This last hypothesis is based on experiments where apoptosis was induced by the sarco-endoplasmic reticulum Ca^{2+}-ATPase (SERCA pump) inhibitor thapsigargin (TG) in androgen-insensitive human prostate cancer cells from the TSU-Pr1, DU-145 and PC-3 cell lines (Furuya *et al.* 1994; Wang *et al.* 1999). However, nothing is known about apoptosis-inducing Ca^{2+} signalling in androgen-sensitive prostate cancer cells, where the androgen receptor plays a critical role in regulating growth and differentiation. The study of Ca^{2+}-regulating mechanisms involved in apoptosis in androgen-dependent human prostate cancer cells could be of great importance as it was shown by Gong *et al.* (1995) that, in such cells, intracellular calcium is a potent regulator of androgen receptor gene expression. It has been found in this work that the calcium ionophore A23187 and thapsigargin down-regulate steady-state androgen receptor mRNA levels. On the other hand, androgen depletion is known to induce apoptosis in androgen-sensitive cancer cells and this mechanism involves Ca^{2+} signals (Isaacs *et al.* 1992). The transition of prostate cancer cells from androgen sensitivity to androgen insensitivity may also involve modifications in Ca^{2+} homeostasis and, probably, in the functioning of store-operated channels. Membrane current initiated by these channels, assumed to play an essential role in cancer cell apoptosis, has never been characterized using patch-clamp techniques in both androgen-sensitive and -insensitive prostate cells. In view of the fact that abnormalities in this current may give rise to human disorders, it is important to understand how this current is regulated and how it affects prostate cell behaviour.

In this work we identify the mechanism by which thapsigargin induces apoptosis in androgen-sensitive human prostate cancer LNCaP cells. We characterize for the first time the store-operated Ca^{2+} current in prostate cancer cells, using patch-clamp and fluorimetric (fura-2) single-cell techniques. We also show that the depletion of intracellular Ca^{2+} stores in androgen-sensitive prostate cancer cells may trigger apoptosis without the activation of a store-activated Ca^{2+} current or sustained Ca^{2+} entry. Our results provide new information on the link between Ca^{2+} pools and apoptosis of cancer cells, suggesting evidence for a potentially important signalling pathway involved in the transition from hormone-sensitive to hormone-insensitive prostate cancer.

METHODS

Cell lines

LNCaP cells from the American Type Culture Collection were grown in RPMI 1640 (Biowhittaker, Fontenay sous Bois, France) supplemented with 5 mM L-glutamine (Sigma, L'Isle d'Abeau, France) and 10% fetal bovine serum (Seromed, Poly-Labo, Strasbourg, France). The culture medium also contained 50 000 IU l^{-1} penicillin and 50 mg l^{-1} streptomycin. Cells were routinely grown in 50 ml flasks (Nunc) and kept at 37 °C in a humidified incubator in an air–CO_2 (95%–5%) atmosphere. For electrophysiological experiments, the cells were subcultured in Petri dishes (Nunc) coated with polyornithine (5 mg l^{-1}, Sigma) and used after 4–6 days.

Recording solutions

Bath Ringer solution contained (mM): 140 NaCl, 5 KCl, 2 $CaCl_2$, 2 $MgCl_2$, 0·3 Na_2HPO_4, 0·4 KH_2PO_4, 4 $NaHCO_3$, 5 glucose and 10 Hepes (pH 7·3 ± 0·01 with NaOH). In perforated-patch experiments, the recording pipette was filled with an artificial intracellular saline containing (mM): 55 CsCl, 70 Cs_2SO_4, 7 $MgCl_2$, 1 $CaCl_2$, 5 D-glucose and 10 Hepes (pH 7·2 with CsOH) with nystatin (200 μg ml^{-1}). In whole-cell experiments, the recording pipette was filled with an artificial intracellular saline containing (mM): 140 CsCl, 2 $MgCl_2$, 1 $CaCl_2$, 10 EGTA and 5 Hepes (pH 7·3 ± 0·01 with CsOH); osmolarity 290 mosmol l^{-1}. In cell-attached experiments, the pipette solution contained 80 mM $CaCl_2$ as a charge carrier plus (mM): TEA-Cl 30, glucose 5, Hepes 10 and 4,4′-diisothiocyanostilbene-2,2′-disulphonic acid (DIDS) 0·1 (pH 7·3 with TEA-OH). The presence in the pipette of the K^+ channel blocker TEA and the Cl^- channel blocker DIDS ensured maximal suppression of potentially contaminating K^+ and Cl^- single-channel activities. All experiments were performed at room temperature (20–22 °C).

Electrophysiological recording

The electrodes were pulled on a PIP 5 (HEKA, Germany) puller in two stages from borosilicate glass capillaries (1·5 mm in diameter; BBL, WPI, USA) to a tip diameter of 1·5–2·0 μm. The cultures were viewed under phase contrast with an Axiovert 135 (Zeiss, Germany) inverted microscope. Electrodes were positioned with List-Medical (Germany) micromanipulators. Grounding was achieved through a silver chloride-coated silver wire inserted into an agar bridge.

Perforated-patch recordings were performed with 200 μg ml^{-1} nystatin in the pipette, which was first back-filled with normal Ringer solution to allow reliable seal formation. Series resistance had a steady value of 20–100 MΩ. Perforated-patch and whole-cell recordings were carried out using an Axopatch-200B amplifier (Axon Instruments). Stimulus control, as well as data acquisition and processing were carried out with a PC computer (IBM), fitted with a Digidata 1200 series interface, using pCLAMP 6 software

(Axon Instruments, interface and software). The activity of single, store-dependent, plasma membrane Ca^{2+} channels was recorded in the cell-attached configuration using a HEKA PC-9 amplifier. The currents in response to voltage-clamp pulses were low-pass filtered at 1·5 kHz and digitized at 10 kHz. Under such filtering conditions the root mean square noise, σ, was 0·09 pA. The single-channel data were analysed using PulseFit and Origin 5 software. The techniques have previously been described in detail (Skryma *et al.* 1994; Prevarskaya *et al.* 1995).

Data and statistical analysis

Results were expressed as means ± standard deviation where appropriate. Each experiment was repeated several times. Student's *t* test was used for statistical comparison among means and differences, with $P < 0·05$ considered significant.

Fluorescence measurements of $[Ca^{2+}]_i$ with fura-2

For fura-2 measurements, cells were excited alternately at 340 and 380 nm. Emitted fluorescence was long-pass filtered at 510 nm, captured and analysed by a photomultiplier-based system (Photon Technologies International Ltd, Princeton, NJ, USA). $[Ca^{2+}]_i$ was calculated from the ratio of the emitted fluorescence, excited by 340 and 380 nm light, using the Grynkiewicz, Poenie & Tsien equation (Grynkiewicz *et al.* 1985). For microfluorimetric measurements, cells were grown on glass coverslips for at least 3 days before the experiment, loaded for 30 min with the acetoxymethyl ester derivative of the dye (5 μM fura-2 AM), and subsequently washed three times with a dye-free solution.

Determination of apoptosis

Cells were seeded in 8-chamber culture slides (Lab-Tek) in RPMI medium containing 10% fetal calf serum. After 24 h, cells were treated with Ni^{2+} or thapsigargin for varying periods of time. For morphological analysis, at the end of the treatment, cells were fixed with ice-cold methanol for 10 min and washed twice with phosphate-buffered saline (PBS). Cells were then stained with 5 μg ml^{-1} Hoescht 33258 for 10 min at room temperature and mounted in glycergel (DAKO). Nuclear morphology was displayed on an Olympus BH-2 fluorescence microscope (405–435 nm). The percentage of apoptotic cells was determined by counting at least 500 cells in random fields. Apoptosis was also detected by the TUNEL technique (terminal deoxynucleotide transferase-mediated dUTP–biotin nick-end labelling) using an apoptosis detection kit (Boehringer Mannheim). Following the TUNEL reaction, which detects strand breaks, cells were counterstained with 0·1% Methyl Green for 10 min. The free calcium concentration was assayed in solutions used for apoptosis experiments using the fura-2 fluorescence equipment described above. The fluorescence of culture medium containing no added calcium was measured, as was that of chelated serum with EGTA at various concentrations (0·1 and 1 mM) with 5 μM fura-2 pentapotassium salt. Free calcium concentration was found to be 200 and 20 nM in the presence of 0·1 and 1 mM EGTA, respectively. Using serial dilutions, we assumed that the free calcium contamination in the culture medium containing no added calcium and chelated serum was around 5–10 μM. The free calcium concentration of the Ringer solution used for calcium measurements was 1 μM with no added $CaCl_2$ and no EGTA.

It should be noted that the incubation with the high doses (more than 1 mM) of Ni^{2+} was toxic for LNCaP cells (the percentage of cells incorporating Trypan Blue was enhanced by 20 ± 5% after incubation with 1 mM Ni^{2+} for 24 h). As 0·5 mM Ni^{2+} inhibited I_{store} but was not toxic in long-term experiments this concentration was selected as a standard dose for all studies of apoptosis.

Chemicals

All chemicals were bought from Sigma except for fura-2 AM, fura-2 pentapotassium salt, SK&F 96365 and thapsigargin, which were purchased from Calbiochem.

RESULTS

SERCA pump inhibitors induce a biphasic Ca^{2+} rise in LNCaP cells

The $[Ca^{2+}]_i$ resting level of LNCaP cells in a solution containing 2 mM $CaCl_2$ was about 81 ± 7 nM ($n = 103$) and remained stable during the recording for up to 60 min.

A common means of discharging the Ca^{2+} stores is to inhibit SERCA pump activity (Premack *et al.* 1994; Parekh & Penner, 1996). Potent, selective Ca^{2+} pump inhibitors such as thapsigargin (Thastrup *et al.* 1990) or cyclopiazonic acid (CPA; Mason *et al.* 1991) deplete intracellular Ca^{2+} pools and concomitantly promote a sustained capacitative Ca^{2+} entry (Huang & Putney, 1998). This makes Ca^{2+} pump inhibitors useful tools for studying controlled intracellular calcium changes and their consequences in cell physiology.

Exposure of fura-2-loaded LNCaP cells to 0·1 μM thapsigargin in the presence of 2 mM extracellular calcium produced a large initial increase in intracellular Ca^{2+} as a

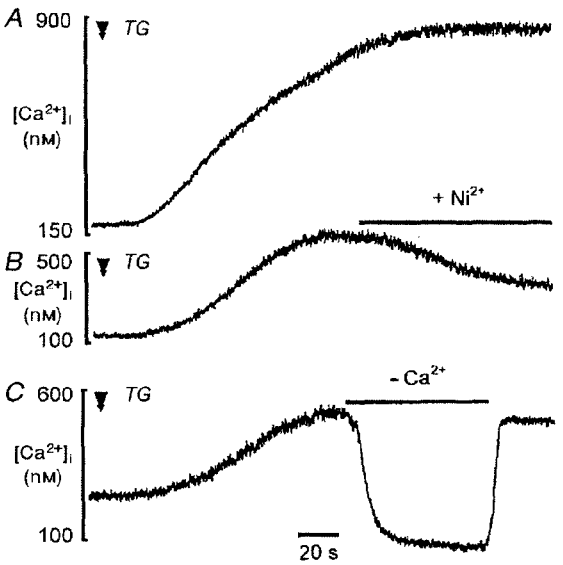

Figure 1. Stimulation of Ca^{2+} influx by thapsigargin in LNCaP cells

A, thapsigargin (0·1 μM) induces an increase in Ca^{2+} in LNCaP cells and stimulates Ca^{2+} release with consecutive Ca^{2+} entry. *B*, the action of thapsigargin (0·1 μM) in Ca^{2+}-containing medium in the presence of Ni^{2+} (3 mM). *C*, dependence of thapsigargin-induced Ca^{2+} influx on extracellular Ca^{2+}. Removing Ca^{2+} from the external medium (measured free Ca^{2+} in these conditions was 1 μM) blocks thapsigargin-stimulated Ca^{2+} entry. Thapsigargin (0·1 μM) was added at the time indicated by arrows. Testing solutions were applied from a puffing pipette during the periods indicated by bars.

result of the depletion of intracellular stores (Fig. 1*A*). This was followed by a sustained plateau, corresponding to a Ca^{2+} influx. This depletion-activated Ca^{2+} entry was confirmed by the fact that 3 mM Ni^{2+} (Fig. 1*B*) and 1 μM La^{3+} (data not shown) blocked the sustained Ca^{2+} rise. Decreasing extracellular free Ca^{2+} concentration to 1 μM by removing $CaCl_2$ from the bath also suppressed Ca^{2+} entry while reintroducing extracellular Ca^{2+} restored Ca^{2+} (Fig. 1*C*).

To ensure that the effects of thapsigargin resulted from its action on intracellular Ca^{2+}-ATPase, we also examined the effects of CPA, a structurally unrelated agent that similarly inhibits the SERCA pump. CPA (10 μM) produced similar effects on $[Ca^{2+}]_i$ to those of thapsigargin, also inducing an initial Ca^{2+} mobilization followed by Ca^{2+} entry (not shown, $n = 11$).

Depletion of intracellular Ca^{2+} stores activates a Ca^{2+} current through store-operated channels

We used the perforated-patch recording technique combined with $[Ca^{2+}]_i$ measurement to compare the kinetics of the $[Ca^{2+}]_i$ increase induced by TG, and the development of the I_{store} Ca^{2+} current. As illustrated in Fig. 2, within 15 ± 6 s, TG stimulated an initial $[Ca^{2+}]_i$ increase due to the mobilization of Ca^{2+} from intracellular stores. An inward current appeared within 25 ± 5 s after TG application ($n = 11$). Decreasing extracellular free Ca^{2+} concentration to 1 μM by removing $CaCl_2$ from the bath inhibited the second phase of the $[Ca^{2+}]_i$ increase induced by TG and the corresponding inward current (Fig. 2*A*, $n = 7$). When Ca^{2+} was added again the sustained plateau was restored and the Ca^{2+} current was induced. I_{store} was also blocked by Ni^{2+} in the range of 0·5–3 mM. However, the rate of blockade was concentration dependent; 3 mM Ni^{2+} completely inhibited the current within 1–2 min whereas 10–15 min were required to completely inhibit the current with 0·5 mM Ni^{2+}. Figure 2*B* demonstrates the effect of TG on $[Ca^{2+}]_i$ and I_{store} in cells incubated in 0·5 mM Ni^{2+} during 15 min where only Ca^{2+} mobilization from intracellular stores was observed without any stimulation of store-operated current. Moreover, when Ni^{2+} was present in the extracellular solution, TG only induced an initial Ca^{2+} rise due to Ca^{2+} mobilization, but I_{store} was not stimulated ($n = 9$, Fig. 2*B*). Likewise, TG induced a monophasic increase in $[Ca^{2+}]_i$ under conditions when extracellular Ca^{2+} was removed from the bath solution (not shown, $n = 7$).

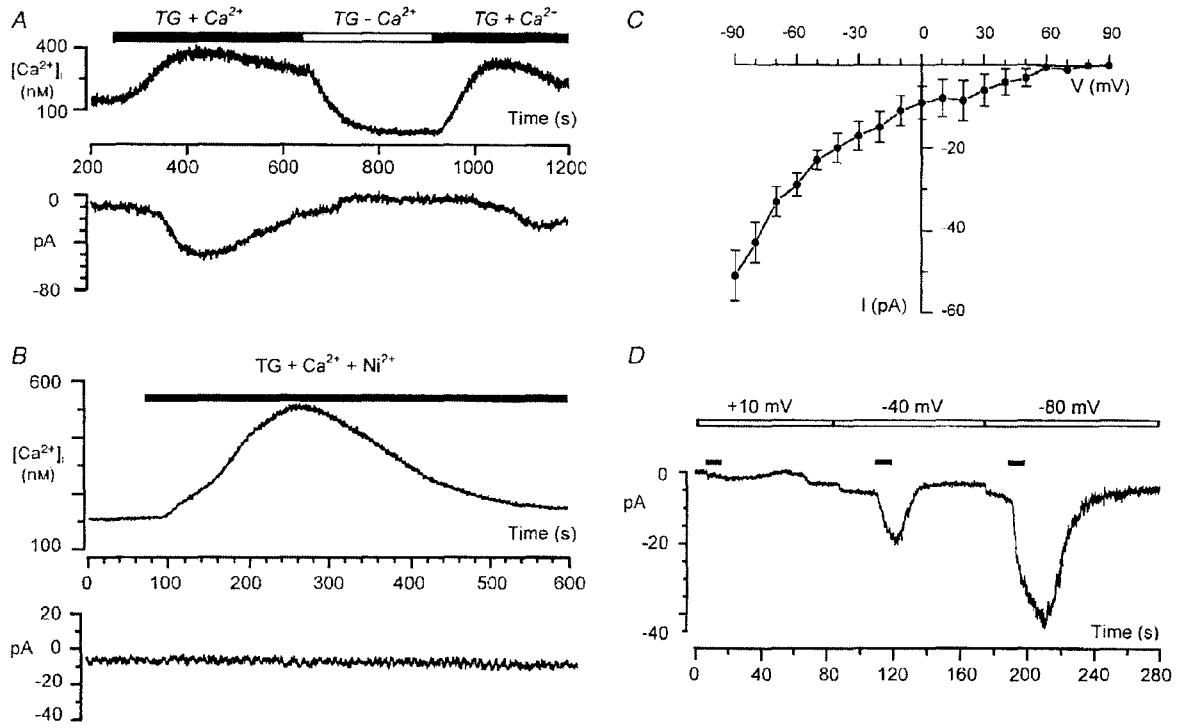

Figure 2. Patch-clamp recordings of store-operated Ca^{2+} current in LNCaP cells

A and *B*, combined perforated-patch and microspectrofluorimetric single-cell recordings of the thapsigargin-activated store-operated Ca^{2+} current at a holding potential of −80 mV. *A*, reversible blockade of Ca^{2+} current by removing Ca^{2+} from external medium (measured free Ca^{2+}, 1 μM). *B*, thapsigargin induces Ca^{2+} mobilization but does not induce store-operated Ca^{2+} current in the presence of 0·5 mM Ni^{2+}. *C*, current–voltage relationship of the store-operated Ca^{2+} current (current is inwardly rectifying and not activated by depolarization). *D*, whole-cell patch-clamp recordings of store-operated Ca^{2+} current at different holding membrane potentials. The horizontal filled bars indicate the episodes of 22 mM $CaCl_2$ application.

We used the whole-cell patch-clamp technique to study the voltage dependence of I_{store} in LNCaP cells. Ca^{2+} stores were emptied by incubating cells with 0·1 μM TG for 15 min in the low free Ca^{2+} (1 μM) bath solution while dialysing the interior of the cell with a strongly buffered Ca^{2+} solution (see Methods). I_{store} was elicited by adding 22 mM $CaCl_2$ to the bath at different holding membrane potentials. An example of such an experiment and its current–voltage (I–V) relationship are shown in Fig. 2*C* and *D*. The store-operated calcium channels in LNCaP cells were non-conducting at very depolarized potentials. In contrast, the current amplitude increased following membrane hyperpolarization and the I–V relationship displayed an inward rectification (Fig. 2*C*).

Changing external Na^+ (replaced by choline) had no significant effect on I_{store} in both whole-cell ($n = 5$) and perforated-patch experiments ($n = 3$). In all cells studied ($n = 7$, perforated-patch combined with fura-2 experiments) I_{store} was also insensitive to one of the suggested capacitative Ca^{2+} current inhibitors, SK&F 96365 (100 μM).

The activity of single store-operated Ca^{2+} channels

The cell-attached patch-clamp configuration was used to study the unitary SOC activity in LNCaP cells. In the presence of 0·1 μM TG in the Ca^{2+}-free bath solution and 80 mM $CaCl_2$ in the pipette, under conditions that ensured inhibition of all membrane currents except those of Ca^{2+}, we recorded a unitary activity in an inward direction that had a resolvable amplitude only at potentials more negative than the resting potential of the cell. In order to examine this type of activity at a broad range of membrane potentials and at the same time measure its I–V relationship, we employed a complex pulse protocol consisting of two steady levels of hyper- and depolarizing potentials connected to each other with a voltage ramp (V_r). The pulse protocol together with the single-channel traces are shown in Fig. 3*A*. In order to construct the I–V relationship, we thoroughly inspected each trace and used the cursor procedure to select those portions of the traces in response to voltage ramps that contained openings of only one channel (overlapping openings and closed states were discarded). Single-channel amplitudes corresponding to each ramp voltage were averaged, then the resulting curve was smoothed and placed in the I–V coordinates (Fig. 3*B*). The resultant I–V plot showed strong rectification in the inward direction. The currents at potentials close to and more positive than the resting potential were beyond the resolution limit, therefore the slope conductance was determined by the linear fit of the I–V plot at potentials of −40 to −120 mV (relative to V_r) where unitary amplitudes could be adequately resolved. This linear fit produced a slope conductance value of 3·2 ± 0·4 pS ($n = 5$).

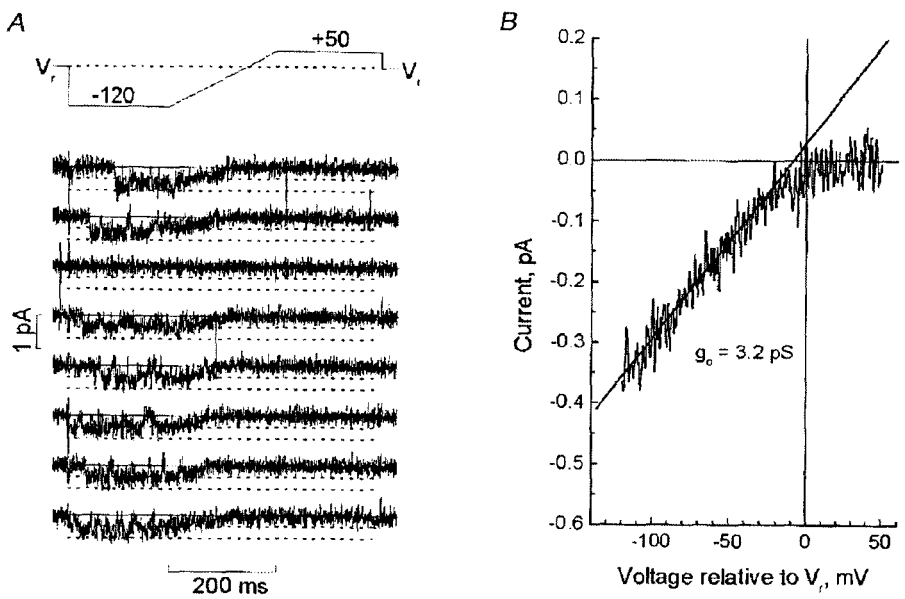

Figure 3. The activity of single store-dependent Ca^{2+} channels

A, single-channel recordings obtained in response to the consecutive application of voltage-clamp pulses (shown in the upper panel, 10 s interpulse interval) to the cell-attached patch in TG-treated LNCaP cells; superimposed continuous lines indicate zero current levels; downward deflection corresponds to the inward current. The recordings presented probably reflect the activity of two store-dependent Ca^{2+} channels. Dotted lines indicate two levels of single-channel amplitudes of −0·35 and −0·7 pA. *B*, the I–V relationship of the single store-dependent Ca^{2+} channel; the I–V plot was constructed from the ramp portions of single-channel recordings by selecting the parts corresponding to the opening of one channel (overlapping openings and closed states were discarded) with subsequent averaging and digital smoothing of the resulting curve to reduce noise; superimposed linear fit provides the value of the slope conductance (g_0) of 3·2 pS.

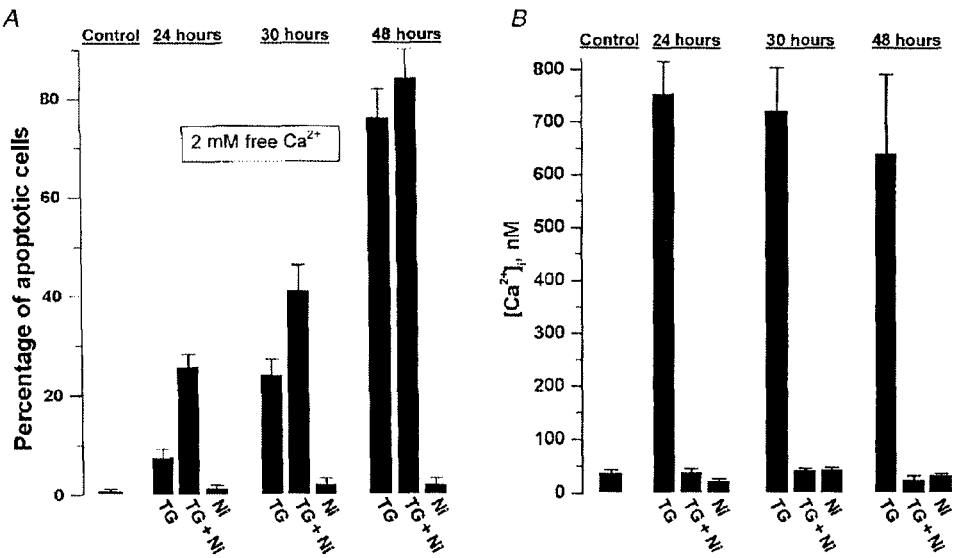

Figure 4. Temporal changes in apoptosis and in the cytosolic Ca^{2+} concentration of the LNCaP cells under physiological conditions of 2 mM extracellular free Ca^{2+}

A, temporal changes in apoptosis of the LNCaP cells (estimated by the number of apoptotic cells) treated with 0·1 μM TG, 0·5 mM Ni^{2+} or 0·1 μM TG combined with 0·5 mM Ni^{2+}. *B*, temporal changes in cytosolic Ca^{2+} concentration of the LNCaP cells treated with 0·1 μM TG, 0·5 mM Ni^{2+} or 0·1 μM TG combined with 0·5 mM Ni^{2+}.

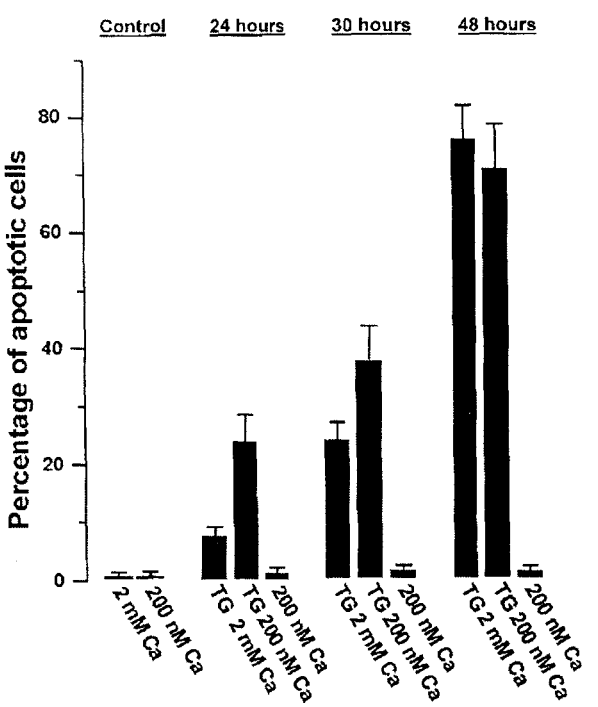

Figure 5. Temporal changes in the apoptosis of LNCaP cells under conditions of low extracellular free Ca^{2+}

Cells were treated with 0·1 μM TG in 2 mM free Ca^{2+}, with 0·1 μM TG in 200 nM free Ca^{2+} or with 200 nM free Ca^{2+} medium.

The following lines of evidence support our notion that the unitary activity described thus far is associated with the activation of single store-dependent, plasma membrane Ca^{2+} channels. (i) This activity was only observed in TG-treated cells; no similar activity was found in the cells under normal conditions. (ii) The activity shows strong inward rectification, typical of Ca^{2+}-selective channels. (iii) Neither K^+ (Skryma *et al.* 1997, 1999) nor Cl^- (Y. M. Shuba, unpublished observation) channels known to be present in LNCaP cells would be capable of producing a similar type of activity under these experimental conditions used. (iv) SOC has no similarity to the TG-independent Ca^{2+}-permeable 23 pS cation channel recently reported by Gutiérrez *et al.* (1999) in LNCaP cells.

Thapsigargin induces apoptosis in LNCaP cells

Hoescht staining was used to determine apoptosis induced by TG treatment. Under control conditions, in the absence of TG, the percentage of apoptotic cells was less than 1%. Typical apoptotic features induced by treatment with 0·1 μM TG for 24 h are shown in Fig. 6*C*. TG-induced apoptosis was also detected by the TUNEL technique (Fig. 7*C*). TG induced apoptosis in a time-dependent manner (Fig. 4*A*), with 7, 24 and 77% of cells reaching apoptosis at 24, 30 and 48 h, respectively.

Sustained elevation of cytosolic Ca^{2+} due to SOC activation is not required for induction of apoptosis by thapsigargin

As it has previously been reported that I_{store} activation, leading to a sustained increase in cytosolic Ca^{2+}, is required for TG-induced apoptosis in androgen-insensitive prostate

cancer cells (Furuya *et al.* 1994), we tested this hypothesis in androgen-sensitive prostate cancer LNCaP cells.

To determine whether the I_{store} in LNCaP cells is important in apoptosis induction by TG, we examined the ability of TG to induce apoptosis under different experimental conditions. In patch-clamp experiments, I_{store} was completely abolished by 0·5 mM Ni^{2+} (Fig. 2*B*). According to the hypothesis stated above, TG-induced apoptosis should decrease in cells treated with 0·5 mM Ni^{2+}. Unexpectedly, TG-induced apoptosis was significantly potentiated by treatment with 0·5 mM Ni^{2+} (Fig. 4*A*) whereas cell treatment with 0·5 mM Ni^{2+} alone did not induce apoptosis in LNCaP cells (Figs 4*A*, 6*B* and 7*B*). This enhancement of cell death was mostly visible after 24 and 30 h (25 *vs.* 7% and 41 *vs.* 24% of apoptotic cells for TG + Ni^{2+} and TG at 24 and 30 h, respectively). It therefore seems that Ni^{2+} does not enhance cell death any further after 48 h treatment (84 *vs.* 77% of apoptotic cells for TG + Ni^{2+} and TG, respectively). Apparently, blocking the store-operated Ca^{2+} current facilitates and accelerates TG-induced apoptosis. Figure 6*D* shows the apoptotic features of LNCaP cells after combined treatment with TG and Ni^{2+} for 24 h. These results were also confirmed by the TUNEL technique. Figure 7 shows the apoptosis detection in LNCaP cells treated with TG (Fig. 7*C*) and with TG combined with Ni^{2+} (Fig. 7*D*) for 24 h. To assess how $[Ca^{2+}]_i$ is affected by these apoptosis-inducing conditions, we compared cytoplasmic Ca^{2+} levels in LNCaP cells after 24, 30 and 48 h treatment with TG, Ni^{2+} and TG combined with Ni^{2+}. $[Ca^{2+}]_i$ remained at high levels throughout the 48 h, and even longer when cells were treated with TG alone, while the $[Ca^{2+}]_i$ level in cells treated with Ni^{2+} or TG combined with Ni^{2+} was almost the same as that of the control (Fig. 4*B*). This indicates that a sustained high level of $[Ca^{2+}]_i$ is not required for induction of apoptosis by TG and its subsequent development.

To confirm that blocking Ca^{2+} influx potentiates rather than inhibits TG-induced apoptosis, we then assessed the influence of decreasing the extracellular Ca^{2+} concentration. The Ca^{2+}-deprived medium contained no added Ca^{2+} and dialysed serum was used to remove Ca^{2+} contaminants (as well as other low molecular weight species) in addition to 0·1 mM EGTA to buffer the free calcium concentration in the extracellular solution (see Methods). This gave a Ca^{2+} concentration of 200 nM. As shown in Fig. 5, the Ca^{2+}-deprived medium potentiated the apoptosis induced by TG in a time-dependent manner without having any action on its own. The potentiation of TG-induced apoptosis due to

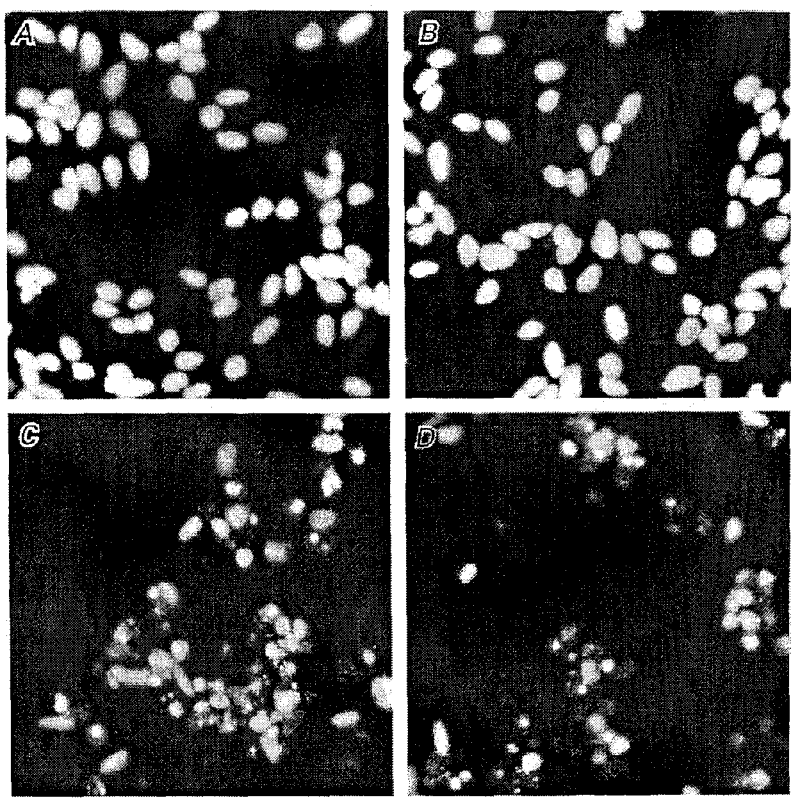

Figure 6. LNCaP prostate cells (staining with 5 μg ml^{-1} Hoescht) undergoing apoptosis due to treatment with thapsigargin

A, control cells; *B*, cells treated with 0·5 mM Ni^{2+} (24 h); *C*, cells treated with 0·1 μM TG (24 h); *D*, cells treated with 0·1 μM TG + 0·5 mM Ni^{2+} (24 h).

decreasing the extracellular calcium was similar to that caused by nickel. Indeed, we observed that TG-induced apoptosis was enhanced by 340% (34 h) and 170% (30 h) by a Ca^{2+}-deprived solution compared with 310% (24 h) and 160% (30 h) by nickel. Reduction to even lower Ca^{2+} levels with 1 mM EGTA (giving 20 nM free Ca^{2+}) in the external medium also led to an enhancement of TG-induced apoptosis. However, in this condition, the Ca^{2+}-deprived medium had an apoptotic action on its own (20, 28 and 88% of apoptotic cells at 24, 30 and 48 h, respectively; data not shown). The effects of Ni^{2+} and low extracellular Ca^{2+} were really due to enhancement of TG-induced cell apoptosis and not due to necrosis. This was confirmed by an increase in the morphological indicators of apoptosis, i.e. the extent of internucleosomal degradation and DNA ladder formation (data not shown). Furthermore, the percentage of cells excluding Trypan Blue was not affected by incubation with 0·5 mM Ni^{2+} or 200 nM free Ca^{2+} medium for more than 72 h.

Transient $[Ca^{2+}]_i$ increase due to depletion of Ca^{2+} stores is not responsible for apoptosis induction by thapsigargin

As thapsigargin is still capable of inducing a rise in $[Ca^{2+}]_i$ in the absence of extracellular Ca^{2+}, due to a passive leak of Ca^{2+} through the ER membrane, we checked whether this initial transient increase in $[Ca^{2+}]_i$ was involved in apoptosis induction. To eliminate the transient rise in $[Ca^{2+}]_i$, LNCaP cells were incubated for 20 min in the presence of 50 μM BAPTA-AM, an intracellular Ca^{2+} chelator, and in the 200 nM free Ca^{2+} medium (with 0·1 mM EGTA). This procedure resulted in sufficient intracellular Ca^{2+} buffering to completely eliminate the transient rise in $[Ca^{2+}]_i$ that occurred when thapsigargin was added to a Ca^{2+}-free medium (not shown). In BAPTA-loaded cells, $[Ca^{2+}]_i$ was 69 ± 9 nM. $[Ca^{2+}]_i$ was 65 ± 7 nM 150 s after TG addition, a concentration not different from that before TG addition. BAPTA-AM treatment for 20 min without TG did not induce apoptosis in LNCaP cells (< 0·1 % of apoptotic cells in control after 48 h and < 0·1 % of apoptotic cells after 48 h following 20 min incubation with BAPTA-AM). The cells were then treated with 0·1 μM TG for 48 h and the percentage of apoptotic cells was compared with that of cells not loaded with BAPTA. The ability of TG to induce apoptosis in LNCaP cells was not reduced by BAPTA loading in these conditions (70 ± 5% apoptotic cells in BAPTA-loaded, TG-treated cells, as compared with 71 ± 8% in TG-treated cells in the 200 nM free Ca^{2+} medium).

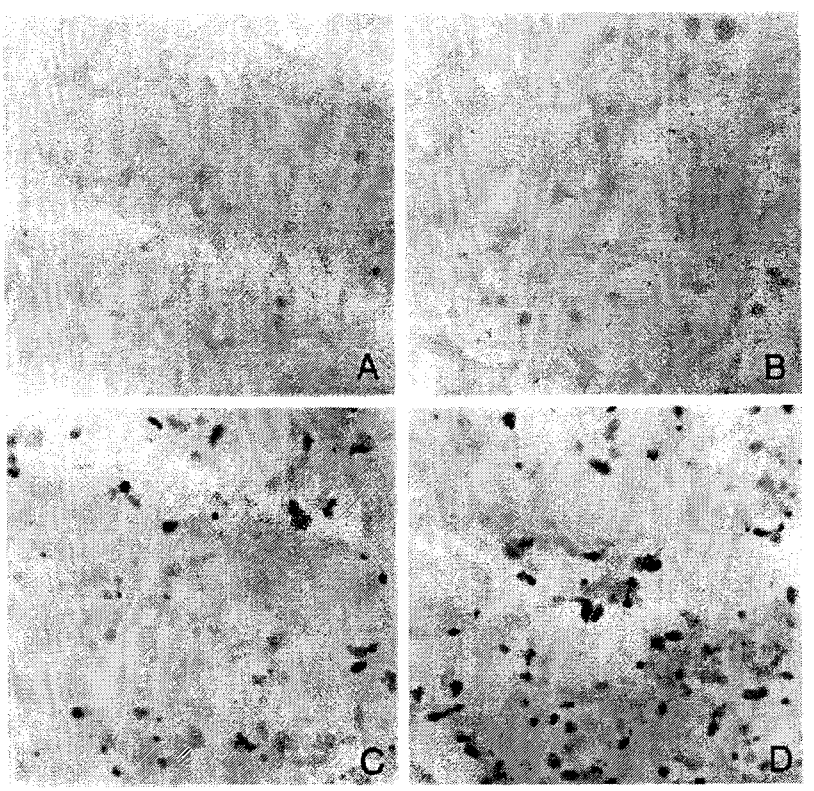

Figure 7. Thapsigargin-induced apoptosis detection in LNCaP prostate cells using the TUNEL technique

A, control cells; *B*, cells treated with 0·5 mM Ni^{2+} (24 h); *C*, cells treated with 0·1 μM TG (24 h); *D*, cells treated with 0·1 μM TG + 0·5 mM Ni^{2+} (24 h).

DISCUSSION

The present study demonstrates that emptying intracellular Ca^{2+} stores by SERCA pump inhibitors stimulates a Ca^{2+} current, I_{store}, through specific store-operated channels (SOCs), in androgen-sensitive human prostate cancer LNCaP cells. These channels are activated by intracellular store depletion, and had not previously been identified and characterized in prostate cells.

The presence of store-operated Ca^{2+} entry has been documented in a large variety of cells, mainly on the basis of measurements of intracellular Ca^{2+} levels after store depletion by thapsigargin. The first electrophysiological demonstration of a store-operated Ca^{2+} current was carried out in mast cells by Hoth & Penner (1992), who called it Ca^{2+} release-activated current (I_{CRAC}). I_{CRAC} is now the best-characterized store-operated Ca^{2+} current. It is known to be activated by depleting intracellular Ca^{2+} stores and has the highest selectivity for Ca^{2+} over other cations (Hoth & Penner, 1992; Zweifach & Lewis, 1993; Berridge, 1995*b*). Recent studies using patch-clamp techniques have now clearly established the existence of a number of store-operated Ca^{2+} currents in several non-excitable cell types, differentiated by their unitary conductance, selectivity and pharmacology (for review see Parekh & Penner, 1997). Regardless of some differences in channel properties, store-operated channels form a family of channels characterized by several specific, common features. The first of these properties consists of current activation by emptying the intracellular calcium stores, using a variety of procedures. In our experiments, I_{store} was identified by emptying intracellular stores using TG. As in basophilic leukaemia (RBL) cells, or Jurkat T cells, I_{store} in LNCaP cells appears to be the critical Ca^{2+} influx pathway as LNCaP cells do not have voltage-activated Ca^{2+} channels (Skryma *et al.* 1997, 1999). The second important property of I_{store} is its characteristic voltage dependence. I_{store} could be considered as a voltage-independent Ca^{2+} current, as it is not gated by membrane voltage changes (Zweifach & Lewis, 1993; Hoth & Penner, 1993). However, once it has been activated by store depletion, I_{store} increases when the membrane potential shifts toward negative values. The current–voltage relationship also shows a pronounced inward rectification at negative voltages (Zweifach & Lewis, 1993; Hoth & Penner, 1993). The I_{store} reversal potential was above +50 mV, as expected for selective Ca^{2+} currents. Changing external Na^+ had no significant effect on I_{store} in LNCaP cells, demonstrating that Na^+ does not permeate the channel in the presence of external Ca^{2+}. I_{store} was inhibited by Ni^{2+} and La^{3+}, thus corresponding to the typical pharmacological profile of store-operated currents in other cells (Schlegel *et al.* 1993; Grudt *et al.* 1996). SK&F 96365, one of the proposed inhibitors of capacitative Ca^{2+} current, did not inhibit I_{store} in LNCaP cells. However, blocking the Ca^{2+} current with this inhibitor is not evidence for capacitative current as it can also block other channels in similar concentrations (Franzius *et al.* 1994).

The unitary conductance of the I_{store} channel was identified as approximately 3·2 pS, which is rather large in comparison with classical I_{CRAC} single-channel conductance, which is usually under 1 pS (Zweifach & Lewis, 1993; Parekh & Penner, 1997). Large single-channel conductances of 2 and 11 pS were also observed for store-operated currents in A431 epidermal cells (Lückhoff & Clapham, 1994) and endothelial cells (Vaca & Kunze, 1995), respectively. However, in our experiments, as in other cell models (Lückhoff & Clapham, 1994), the *I–V* relationship for store-operated channels is non-linear. For a non-linear *I–V* relationship, the slope conductance is a function of potential. When comparing values obtained in different cells it is, therefore, necessary to consider not only specific ionic conditions but also the range of membrane potentials at which they were determined. This makes separating store-operated channels by their single-channel conductance quite a challenging task. Thus the properties of SOC in human cancer prostate LNCaP cells suggest that it belongs to the 'store-operated' channel family, but it may be not the same as classical CRAC.

Our study provides the first direct demonstration and characterization of a store-operated current in prostate cells. SOC characterization could be of great interest in prostate cancer studies as these channels were suggested to be the target of a Ca^{2+}-influx inhibitor, which has been found, in clinical trials, to slow down the growth of certain aggressive cancer cells (Kohn *et al.* 1996). We studied the role of SOCs in TG-induced apoptosis in androgen-sensitive prostate cancer LNCaP cells. TG induces apoptosis in many cell types (Furuya *et al.* 1994; Gill *et al.* 1996; He *et al.* 1997; Bian *et al.* 1997). Based on the changes in Ca^{2+} homeostasis induced by TG, three hypotheses can be proposed to explain the apoptosis induction mechanism. Apoptosis is induced by: (i) a transient increase in $[Ca^{2+}]_i$ due to a passive leak of Ca^{2+} through the ER membrane, (ii) Ca^{2+} pool depletion, or (iii) a sustained rise in cytosolic Ca^{2+} secondary to Ca^{2+} entry through I_{store} channels. In this report we show that neither the transient nor the sustained increase in $[Ca^{2+}]_i$ is required for induction of apoptosis by TG. Our results show first that a sustained increase in $[Ca^{2+}]_i$ via I_{store} activation is not required for TG to induce apoptosis in LNCaP cells because I_{store} inhibition by the 200 nM free Ca^{2+} medium or 0·5 mM Ni^{2+} did not abolish TG-induced apoptosis whereas the TG-increased cytosolic Ca^{2+} concentration was reduced to control values by the incubation in 200 nM free Ca^{2+} or 0·5 mM Ni^{2+}-containing medium. Under these conditions, however, a transient rise in $[Ca^{2+}]_i$ can still occur due to calcium mobilization from internal stores. We strongly buffered $[Ca^{2+}]_i$ by preincubating cells with the Ca^{2+} chelator BAPTA-AM to eliminate the transient rise in $[Ca^{2+}]_i$, while the sustained rise was abolished by the absence of external calcium. This did not inhibit apoptosis induced by TG, suggesting that the transient increase in $[Ca^{2+}]_i$ is not responsible for apoptosis induction. These results, where cytosolic Ca^{2+} is strongly buffered using BAPTA-AM, also exclude another possible consequence of ER depletion that might induce apoptosis: mitochondrial calcium overloading

(Berridge *et al.* 1998; Green & Reed, 1998). These data are consistent with the findings of others on lymphoid cells (Berridge, 1995*a*; Bian *et al.* 1997) and murine hypothalamic cell lines (Wei *et al.* 1998). However, surprisingly, they are in contrast with those described in androgen-insensitive prostate cancer cells (Furuya *et al.* 1994). In these cells, as in thymocytes (Jiang *et al.* 1998), TG-induced apoptosis was inhibited by preincubating cells with BAPTA-AM, or by overexpressing the cytosolic Ca^{2+}-binding protein calbindin. On the basis of these results, a sustained increase in cytosolic Ca^{2+}, mediated by a store-operated Ca^{2+} current, was considered to play a role in apoptosis induction by TG (Furuya *et al.* 1994).

Our results therefore suggest that Ca^{2+} pool depletion, and not an increase in cytosolic Ca^{2+}, induces apoptotic cell death in androgen-sensitive human prostate cancer cells. In addition, our data show that TG-induced apoptosis was enhanced (see Figs 4*A* and 5) by 0·5 mM Ni^{2+} and a low external free Ca^{2+} concentration (200 nM free Ca^{2+}). Therefore, blocking capacitative Ca^{2+} entry potentiates apoptosis induced by TG. This reinforces the hypothesis that Ca^{2+} pool depletion is involved in apoptosis, since an increase in cytosolic Ca^{2+} due to capacitative Ca^{2+} entry (inhibited by Ni^{2+}) would be required for optimal ER pool filling and apoptosis inhibition. It should be noted that decreasing external calcium to very low levels using 1 mM EGTA (20 nM free Ca^{2+}) led to apoptosis on its own. This is certainly due to the inversion of the Ca^{2+} concentration gradient in comparison to physiological conditions (the intracellular Ca^{2+} concentration of LNCaP cells is usually about 100 nM). The intracellular Ca^{2+} stores are depleted in response to the decrease in cytosolic Ca^{2+} concentration (in turn induced by stimulation of the Ca^{2+} pump of the plasma membrane by low extracellular Ca^{2+}). This calcium gradient hypothesis may also be confirmed by the fact that, under low external calcium conditions (200 nM), where values are, however, higher than the intracellular Ca^{2+} concentration (100 nM), apoptosis was not observed in the absence of TG ($< 1\%$ of apoptotic cells at 48 h). Similarly, this does not occur with Ni^{2+} because the Ca^{2+} gradient is not perturbed.

Our data are in agreement with those of Distelhorst and colleagues (He *et al.* 1997) on WEH17.2 lymphoma cells. These authors suggested that ER calcium pool depletion by TG could trigger apoptosis and that overexpression of the Bcl-2 anti-apoptotic protein, which anchors to intracellular membranes, maintains Ca^{2+} homeostasis within the ER, thereby inhibiting apoptosis induction by TG.

The exact mechanism by which calcium pool depletion induces apoptosis is not known. The high levels of Ca^{2+} within the lumen of the ER are essential not only for Ca^{2+} signal transduction, but also for protein synthesis and processing, and cell division (Sambrook, 1990; Koch, 1990; Kuznetsov *et al.* 1992; Gill *et al.* 1996; Jiang *et al.* 1998). Three potential mechanisms by which ER depletion might contribute to apoptosis have been proposed (He *et al.* 1997): (i) depletion of the ER Ca^{2+} pool might destabilize the Ca^{2+}–protein gel and its associated membrane, leading to vesiculation and the formation of apoptotic blebs; (ii) disruption of protein processing and transport within the ER may contribute to TG-induced apoptosis; (iii) TG-induced ER Ca^{2+} pool depletion releases an endonuclease into the nucleus responsible for DNA fragmentation. Thus the decline in ER calcium levels leads to the activation of stress signals that switch on the genes associated with death. Although the importance of intraluminal ER Ca^{2+} storage in apoptosis appears to be evident, other mechanisms depending on extracellular, cytosolic, mitochondrial or nuclear Ca^{2+} have been shown to contribute to apoptosis in a variety of cell models (Dowd, 1995; Marin *et al.* 1996; McConkey & Orrenius, 1997). Therefore, the general applicability of the store-depletion hypothesis is doubtful and the relationship between intracellular Ca^{2+} stores, Bcl-2 and apoptosis may be cell specific.

The reasons why the differences between androgen-dependent and androgen-independent prostate cancer cells are associated with changes in Ca^{2+} store-dependent mechanisms involved in apoptosis remain intriguing. It is known that such progression is also associated with expression of the intracellular membrane protein Bcl-2 (Raffo *et al.* 1995; Chaudhary *et al.* 1999). Bcl-2 expression modulates intracellular signalling and preserves the integrity of the ER Ca^{2+} pool in cells exposed to various apoptosis-inducing stimuli, including cytotoxic Ca^{2+} ionophores, TG and reactive oxygen species (Distelhorst *et al.* 1996; He *et al.* 1997). Moreover, it has been shown that Bcl-2 preserves the ER Ca^{2+} store via an upregulation of calcium pump SERCA gene expression. Bcl-2 may possibly interact with this pump as well (Kuo *et al.* 1998). Interestingly, the androgen-insensitive DU-145 cells do not express Bcl-2, but rather Bcl-X(L) (Shirahama *et al.* 1997), which is poorly expressed in LNCaP cells. Wang *et al.* (1999) have shown that apoptosis induction by TG in DU-145 cells requires an increase in cytoplasmic Ca^{2+} since it activates the Ca^{2+}-activated protein phosphatase calcineurin that was found to dephosphorylate BAD (proapoptotic member of Bcl-2 family), thus enhancing BAD heterodimerization with Bcl-X(L) (but not with Bcl-2) and promoting apoptosis. Another Ca^{2+}-regulating protein, calreticulin (Krause & Michalak, 1997), has been identified in prostate cells (Zhu & Wang, 1999). The expression of this highly conserved intracellular Ca^{2+}-binding protein in the lumen of the endoplasmic reticulum is regulated by androgen (Zhu *et al.* 1998). The downregulation of calreticulin by androgen ablation correlates with apoptosis and the upregulation of calreticulin by androgen replacement in castrated rats correlates with proliferation and differentiation of epithelial cells in the prostate (Zhu *et al.* 1998; Zhu & Wang, 1999). The induction of calreticulin by androgen in prostate organ culture partially resists protein synthesis inhibition,

suggesting that calreticulin is a direct androgen-response gene (Zhu *et al.* 1998). Furthermore, Mery *et al.* (1996) have shown in a mouse L fibroblast cell line that overexpression of calreticulin increases intracellular Ca^{2+} storage and decreases store-operated Ca^{2+} current suggesting an active involvement of calreticulin in intracellular Ca^{2+} pool refilling regulation. Thus, as calreticulin is a major intracellular Ca^{2+}-binding protein involved in Ca^{2+} homeostasis and is regulated by androgens, it could be a promising candidate for mediating androgen regulation of intracellular calcium levels in prostate cells. Thus the differences in Ca^{2+}-dependent apoptosis induction between androgen-dependent and androgen-independent prostate cancer cells may be explained by the differential expression of apoptosis-regulating proteins (Bcl-2, Bcl-X(L), calreticulin).

In summary, we have characterized the Ca^{2+}-regulated mechanisms involved in thapsigargin-induced apoptosis in androgen-sensitive human prostate cancer LNCaP cells. We suggest that a decrease in ER calcium is the major factor in apoptosis induction in these cells; however, direct measurement of the Ca^{2+} concentration in ER lumen would be required to confirm this statement. In contrast to the situation in androgen-insensitive prostate cancer cells, the activation of I_{store}, responsible for ER refilling, and increasing cytosolic Ca^{2+} are not required for TG-induced apoptosis. Further studies are needed to identify the precise Ca^{2+}-regulated mechanisms involved in the progression of prostate cancer cells from androgen dependence to androgen independence.

Berridge, M. J. (1995*a*). Calcium signalling and cell proliferation. *Bioessays* **17**, 491–500.

Berridge, M. J. (1995*b*). Capacitative calcium entry. *Biochemical Journal* **312**, 1–11.

Berridge, M. J. (1997). Elementary and global aspects of calcium signalling. *Journal of Physiology* **499**, 291–306.

Berridge, M. J., Bootman, M. D. & Lipp, P. (1998). Calcium – a life and death signal. *Nature* **935**, 645–648.

Bian, X., Hughes, F. M. Jr, Huang, Y., Cidlowski, J. A. & Putney, J. W. Jr (1997). Roles of cytoplasmic Ca^{2+} and intracellular Ca^{2+} stores in induction and suppression of apoptosis in S49 cells. *American Journal of Physiology* **272**, C1241–1249.

Chaudhary, K. S., Abel, P. D. & Lalani, E. N. (1999). Role of the bcl-2 gene family in prostate cancer progression and its implications for therapeutic intervention. *Environmental Health Perspectives* **107**, 49–57.

Disthelhorst, C. W., Lam, M. & McCormick, T. S. (1996). Bcl-2 inhibits hydrogen peroxide-induced ER Ca^{2+} pool depletion. *Oncogene* **12**, 2051–2055.

Dowd, D. R. (1995). Calcium regulation of apoptosis. *Advances in Second Messenger and Phosphoprotein Research* **30**, 255–279.

Dowd, D. R., McDonald, P. N., Komm, B. S., Haussler, M. R. & Miesfeld, R. (1992). Stable expression of the calbindin-D28K complementary DNA interferes with the apoptotic pathway in lymphocytes. *Molecular Endocrinology* **6**, 1843–1848.

Fanger, C. M., Hoth, M., Crabtree, G. R. & Lewis, R. S. (1995). Characterization of T cell mutants with defects in capacitative calcium entry: genetic evidence for the physiological roles of CRAC channels. *Journal of Cellular Biology* **131**, 655–667.

Franzius, D., Hoth, M. & Penner, R. (1994). Non-specific effects of calcium entry antagonists in mast cells. *Pflügers Archiv* **428**, 433–438.

Furuya, Y., Lundmo, P., Short, A. D., Gill, D. L. & Isaacs, J. T. (1994). The role of calcium, pH, and cell proliferation in the programmed (apoptotic) death of androgen-independent prostatic cancer cells induced by thapsigargin. *Cancer Research* **54**, 6167–6175.

Gill, D. L., Waldron, R. T., Rys-Sikora, K. E., Ufret-Vincenty, C. A., Graber, M. N., Favre, C. J. & Alfonso, A. (1996). Calcium pools, calcium entry, and cell growth. *Bioscience Reports* **16**, 139–157.

Gong, Y., Blok, L. J., Perry, J. E., Lindzeys, J. K. & Tindall, D. J. (1995). Calcium regulation of androgen receptor expression in the human prostate cancer cell line LNCaP. *Endocrinology* **136**, 2172–2178.

Green, D. R. & Reed, J. C. (1998). Mitochondria and apoptosis. *Apoptosis* **281**, 1309–1316.

Grudt, T. J., Usowicz, M. M. & Henderson, G. (1996). Ca^{2+} entry following store depletion in SH-SY5Y neuroblastoma cells. *Molecular Brain Research* **36**, 93–100.

Grynkiewicz, G., Poenie, M. & Tsien, R. Y. (1985). A new generation of Ca^{2+} indicators with greatly improved fluorescence properties. *Journal of Biological Chemistry* **260**, 3440–3450.

Gutiérrez, A. A., Arias J. M., Garcia L., Mas-Oliva, J. & Guerrero-Hernandez, A. (1999). Activation of a Ca^{2+}-permeable cation channel by two different inducers of apoptosis in a human prostatic cancer cell line. *Journal of Physiology* **517**, 95–107.

He, H., Lam, M., McCormick, T. S. & Distelhorst, C. W. (1997). Maintenance of calcium homeostasis in the endoplasmic reticulum by bcl-2. *Journal of Cellular Biology* **138**, 1219–1228.

Hoth, M. & Penner, R. (1992). Depletion of intracellular calcium stores activates a calcium current in mast cells. *Nature* **355**, 353–356.

Hoth, M. & Penner, R. (1993). Calcium release-activated calcium current in rat mast cells. *Journal of Physiology* **465**, 359–386.

Huang, Y. & Putney, J. W. (1998). Relationship between intracellular calcium store depletion and calcium release-activated calcium current in a mast cell line (RBL-1). *Journal of Biological Chemistry* **273**, 19554–19559.

Isaacs, J. T., Lundmo, P. I., Berges, R., Martikainen, P., Kyprianou, N. & English, H. F. (1992). Androgen regulation of programmed death of normal and malignant prostatic cells. *Journal of Andrology* **13**, 457–464.

Jiang, S., Chow, S. C., Nicotera, P. & Orremius, S. (1998). Intracellular Ca^{2+} signals activate apoptosis in thymocytes: studies using the Ca^{2+}-ATPase inhibitor thapsigargin. *Experimental Cellular Research* **212**, 84–92.

Juin, P., Pelletier, M., Oliver, L., Tremblais, K., Grégoire, M., Meflah, K. & Vallette, F. M. (1998). Induction of a caspase-3-like activity by calcium in normal cytosolic extracts triggers nuclear apoptosis in a cell-free system. *Journal of Biological Chemistry* **273**, 17559–17564.

Koch, G. L. E. (1990). The endoplasmic reticulum and calcium storage. *Bioessays* **12**, 527–531.

KOHN, E. C., REED, E., SAROSY, G., CHRISTIAN, M., LINK, C. J., COLE, K., FIGG, W. D., DAVIS, P. A., JACO GOLDSPIEL, B. & LIOTTA, L. A. (1996). Clinical investigation of a cyanotic calcium influx inhibitor in patients with refractory cancers. *Cancer Research* **56**, 569–573.

KRAUSE, K. H. & MICHALAK, M. (1997). Calreticulin. *Cell* **88**, 439–443.

KUO, T. H., KIM, H. R. C., ZHU, L., YU, Y., LIN, H. M. & TSANG, W. (1998). Modulation of endoplasmic reticulum calcium pump by bcl-2. *Oncogen* **17**, 1903–1910.

KUZNETSOV, G., BROSTROM, M. A. & BROSTROM, C. O. (1992). Role of endoplasmic reticular calcium in oligosaccharide processing of alpha 1-antitrypsin. *Journal of Biological Chemistry* **268**, 2001–2008.

LÜCKHOFF, A. & CLAPHAM, D. E. (1994). Calcium channels activated by depletion of internal calcium stores in A431 cells. *Biophysical Journal* **67**, 177–182.

MCCONKEY, D. J., NICOTERA, P., HARTZELL, P., BELLOMS, G., WYLLIE, A. M. & ORREMIUS, S. (1989). Glucocorticoids activate a suicide process in thymocytes through an elevation of cytosolic Ca^{2+} concentration. *Archives of Biochemistry and Biophysics* **269**, 365–370.

MCCONKEY, D. J. & ORRENIUS, S. (1997). The role of calcium in the regulation of apoptosis. *Biochemical and Biophysical Research Communications* **239**, 357–366.

MARIN, M. C., FERNANDEZ, A., BICK, R. J., BRISBAY, S., BUJA, L. M., SNUGGS, M., MCCONKEY, D. J., VON ESCHENBACH, A. C., KEATING, M. J. & MCDONNELL, T. J. (1996). Apoptosis suppression by bcl-2 is correlated with the regulation of nuclear and cytosolic Ca^{2+}. *Oncogen* **12**, 2259–2266.

MARTIKAINEN, P., KYPRIANOU, N., TUCKER, R. W. & ISAACS, J. T. (1991). Programmed death of nonproliferating androgen independent prostatic cancer cells. *Cancer Research* **51**, 4693–4700.

MASON, M. J., GARCIA-RODRIGUEZ, C. & GRINSTEIN, S. (1991). Coupling between intracellular Ca^{2+} stores and the Ca^{2+} permeability of the plasma membrane. Comparison of the effects of thapsigargin, 2,5-di-(tert-butyl)-1,4-hydroquinone, and cyclopiazonic acid in rat thymic lymphocytes. *Journal of Biological Chemistry* **266**, 20856–20862.

MERY, L., MESAELI, N., MICHALAK, M., OPAS, M., LEW, D. P. & KRAUSE, K. H. (1996). Overexpression of calreticulin increases intracellular Ca^{2+} storage and decreases store-operated Ca^{2+} influx. *Journal of Biological Chemistry* **271**, 9332–9339.

MONTIRONI, R., MAGI-GALLUZZI, C., MUZZUNIGRO, G., PRETE, E., POLITO, M. & FABRIS, G. (1994). Effects of combination endocrine treatment on normal prostate, prostatic intraepithelial neoplasia, and prostatic adenocarcinoma. *Journal of Clinical Pathology* **47**, 906–913.

PAREKH, A. B. & PENNER, R. (1995). Activation of store-operated calcium influx at resting $InsP_3$ levels by sensitization of the $InsP_3$ receptor in rat basophilic leukaemia cells. *Journal of Physiology* **489**, 377–382.

PAREKH, A. B. & PENNER, R. (1996). Regulation of store-operated calcium currents in mast cells. *Organellar Ion Channels and Transporters* **51**, 231–239.

PAREKH, A. B. & PENNER, R. (1997). Store depletion and calcium influx. *Physiological Reviews* **77**, 901–929.

PARKER, S. L., TONG, T., BALDEN, S. & WINGO, P. A. (1997). Cancer statistics. *CA Cancer Journal for Clinicians* **47**, 5–27.

PREMACK, B. A., MCDONALD, T. V. & GARDNER, P. (1994). Activation of Ca^{2+} current in Jurkat T cells following the depletion of Ca^{2+} stores by microsomal Ca^{2+}-ATPase inhibitors. *Journal of Immunology* **152**, 5226–5240.

PREVARSKAYA, N., SKRYMA, R., VACHER, P., DANIEL, N., DJIANE, J. & DUFY, B. (1995). Rôle of tyrosine phosphorylation in potassium channel activation. *Journal of Biological Chemistry* **270**, 24292–24299.

PUTNEY, J. W. JR (1986). A model for receptor-regulated calcium entry. *Cell Calcium* **7**, 1–12.

PUTNEY, J. W. JR (1990). Capacitative calcium entry revisited. *Cell Calcium* **11**, 611–624.

RAFFO, A. J., PERLMAN, H., CHEN, M. W., DAY, M. L., STREITMAN, J. S. & BUTTYAN, R. (1995). Overexpression of bcl-2 protects prostate cancer cells from apoptosis *in vitro* and confers resistance to androgen depletion *in vivo*. *Cancer Research* **55**, 4438–4445.

SAMBROOK, J. F. (1990). The involvement of calcium in transport of secretary proteins from the endoplasmic reticulum. *Cell* **61**, 197–199.

SANTELLA, L. (1998). The role of calcium in the cell cycle: facts and hypotheses. *Biochemical and Biophysical Research Communications* **244**, 317–324.

SCHLEGEL, W., MOLLARD, P., DEMAUREX, N., THELER, J. M., CHIAVAROLI, C., GUÉRINEAU, N., VACHER, P., MAYR, G., KRAUSE, K. H., WOLLHEIM, C. B. & LEW P. D. (1993). Calcium signalling: comparison of the role of Ca^{2+} influx in excitable endocrine and non-excitable myeloid cells. *Advances in Second Messenger and Phosphoprotein Research* **28**, 142–152.

SHIRAHAMA, T., SAKAKURA, C., SWEENEY, E. A., OZAWA, M., TAKEMOTO, M., NISHIYAMA, K., OHI, Y. & IGARASHI, Y. (1997). Sphingosine induces apoptosis in androgen-independent human prostatic carcinoma DU-145 cells by suppression of bcl-X(L) gene expression. *FEBS Letters* **407**, 97–100.

SKRYMA, R., PREVARSKAYA, N., VACHER, P. & DUFY, B. (1994). Voltage-dependent ionic conductances in Chinese hamster ovary cells. *American Journal of Physiology* **267**, 544–553.

SKRYMA, R. N., PREVARSKAYA, N. B., DUFY-BARBE, L., ODESSA, M. F., AUDIN, J. & DUFY, B. (1997). Potassium conductance in the androgen-sensitive prostate cancer cell line, LNCaP: involvement in cell proliferation. *The Prostate* **33**, 112–122.

SKRYMA, R. N., VAN COPPENOLLE, F., DUFY-BARBE, L., DUFY, B. & PREVARSKAYA, N. (1999). Characterization of Ca^{2+}-inhibited potassium channels in the LNCaP human prostate cancer cell line. *Receptors and Channels* **6**, 241–253.

SPIELBERG, H., JUNE, C. H., BLAIR O. C., NYSTROM-ROSANDER, C., CEREB, N. & DEEG, H. J. (1991). UV irradiation of lymphocytes triggers an increase in intracellular Ca^{2+} and prevents lectin-stimulated Ca^{2+} mobilization: evidence for UV- and nifedipine-sensitive Ca^{2+} channels. *Experimental Hematology* **19**, 742–748.

THASTRUP, O., CULLEN, P. J., DROBAK, B. K., HANLEY, M. R. & DAWSON, A. P. (1990). Thapsigargin a tumor promoter discharges intracellular Ca^{2+} stores by specific inhibition of the endoplasmic reticulum Ca^{2+}-ATPase. *Proceedings of the National Academy of Sciences of the USA* **87**, 2466–2470.

VACA, L. & KUNZE, D. L. (1995). Depletion of intracellular Ca^{2+} stores activates a Ca^{2+}-selective channel in vascular endothelium. *American Journal of Physiology* **269**, C733–738.

WANG, H.-G., PATHAN, N., ETHELL, I. M., KRAJEWSKI, S., YAMAGUCHI, Y., SHIBASAKI, F., MCKEON, F., BOBO, T., FRANKE, T. F. & REED, J. C. (1999). Ca^{2+}-induced apoptosis through calcineurin dephosphorylation of BAD. *Science* **284**, 339–343.

WEI, H., WEI, W., BREDESEN, D. E. & PERRY, D. C. (1998). Bcl-2 protects against apoptosis in neuronal cell line caused by thapsigargin-induced depletion of intracellular calcium stores. *Journal of Neurochemistry* **70**, 2305–2314.

WOOLF, S. H. (1995). Screening for prostate cancer with prostate specific antigen. An examination of the evidence. *New England Journal of Medicine* **333**, 1401–1405.

ZHU, N. & WANG, Z. (1999). Calreticulin expression is associated with androgen regulation of the sensitivity to calcium ionophore-induced apoptosis in LNCaP prostate cancer cells. *Cancer Research* **59**, 1896–1902.

ZHU, N., PEWITT, E. B., CAI, X., COHN, E. B., LANG, S., CHEN, R. & WANGS, Z. (1998). Calreticulin: an intracellular Ca^{2+}-binding protein abundantly expressed and regulated by androgen in prostatic epithelial cells. *Endocrinology* **139**, 4337–4344.

ZWEIFACH, A. & LEWIS, R. S. (1993). Mitogen-regulated Ca^{2+} current of T lymphocytes is activated by depletion of intracellular Ca^{2+} stores. *Proceedings of the National Academy of Sciences of the USA* **90**, 6295–6299.

Acknowledgements

The authors gratefully acknowledge the technical assistance of Isabelle Servant and Isabelle Spadone. This work was supported by grants from INSERM, Ministère de l'Education Nationale, ARC (Association pour la Recherche Contre le Cancer), Ligue Nationale Contre le Cancer, ARTP (Association pour le Recherche sur les Tumeurs de la Prostate), France. Y. Shuba was supported by INSERM and University of Science and Technology of Lille International Cooperation Programs.

R. Skryma and P. Mariot contributed equally to this work.

Corresponding author

N. Prevarskaya: Laboratoire de Physiologie Cellulaire, INSERM EPI-9938, USTL, Bâtiment SN3, 59655 Villeneuve d'Ascq Cedex, France.

Email: phycel@pop.univ-lille1.fr

Author's permanent address

Y. Shuba: Bogomoletz Institute of Physiology, Bogomoletz Street, 4, Kiev, Ukraine.

The Prostate 43:205–214 (2000)

Evidence of Functional Ryanodine Receptor Involved in Apoptosis of Prostate Cancer (LNCaP) Cells

Pascal Mariot,[1] Natalia Prevarskaya,[1] Morad M. Roudbaraki,[1] Xuefen Le Bourhis,[2] Fabien Van Coppenolle,[1] Karine Vanoverberghe,[1] and Roman Skryma[1]*

[1]*Laboratoire de Physiologie Cellulaire, INSERM EPI 9938, Bâtiment SN3, USTL, Villeneuve d'Ascq, France*

[2]*Laboratoire de Biologie du Développement, USTL, Villeneuve d'Ascq, France*

BACKGROUND. Very little is known about the functional expression and the physiological role of ryanodine receptors in nonexcitable cells, and in prostate cancer cells in particular. Nonetheless, different studies have demonstrated that calcium is a major factor involved in apoptosis. Therefore, the calcium-regulatory mechanisms, such as ryanodine-mediated calcium release, may play a substantial role in the regulation of apoptosis.

METHODS. We assessed the presence of such functional receptors in LNCaP prostate cancer cells, using fluorimetric measurements of intracellular calcium and expression assays of mRNA encoding ryanodine receptors.

RESULTS. We show here that LNCaP cells responded to caffeine, a ryanodine receptor agonist, by mobilizing calcium. Another ryanodine receptor agonist, 4-chloro-*m*-cresol, had a similar effect and promoted calcium release. These effects were inhibited by pretreatment with ryanodine or thapsigargin. In addition to a calcium release, caffeine was able to produce a calcium entry blocked by nickel. We used a reverse transcription-polymerase chain reaction assay to investigate the expression of ryanodine receptors in LNCaP cells. Two types of ryanodine receptor mRNAs were expressed in LNCaP cells: RyR1 and RyR2 mRNAs. Finally, we show that ryanodine receptor activation by caffeine slightly stimulates apoptosis of prostate cancer cells, and that the inhibition of these receptors by ryanodine protects the cells against apoptosis.

CONCLUSIONS. The combination of results showed that LNCaP cells, derived from a human prostate cancer, express functional RyRs able to mobilize Ca^{2+} from intracellular stores and which might control apoptosis. *Prostate 43:205–214, 2000.*

KEY WORDS: **intracellular calcium; ryanodine receptor; apoptosis; prostate**

INTRODUCTION

Ryanodine receptors are a family of intracellular Ca^{2+} channels playing important roles in cellular Ca^{2+} homeostasis. The ryanodine receptor (RyR) and the functional ryanodine-sensitive calcium pool were first described in skeletal and cardiac muscles [1,2], and for some time the expression of these Ca^{2+} channels was believed to be strictly muscle-specific, controlling the excitation-contraction coupling: RyR1 in skeletal and RyR2 in cardiac muscles [3,4]. Ryanodine receptors were then shown to be expressed in other types of excitable cells, including neurons [5,6], neuroendo-

Grant sponsor: INSERM; Grant sponsor: Association pour la Recherche Contre le Cancer, France; Grant sponsor: Ligue Nationale Contre le Cancer; Grant sponsor: Association pour la Recherche sur les Tumeurs de la Prostate; Grant sponsor: Fondation de la Recherche Medicale, France.

M.M.R. is presently at the Laboratory of Cell Pharmacology, Department of Molecular Cell Biology, KUL, Herestraat 49, B-3000 Leuven, Belgium.

P.M and N.P. contributed equally to this work

*Correspondence to: Roman Skryma, Laboratoire de Physiologie Cellulaire, INSERM EPI 9807, Bâtiment SN3, Université des Sciences et Technologies de Lille, 59655 Villeneuve d'Ascq, France.
E-mail: phycel@pop.univ-lille1.fr

Received 12 July 1999; Accepted 31 December 1999

crine cells [7,8], and smooth muscle [5,6]. To date, three members of this ryanodine receptor family have been identified (RyR1, RyR2 and RyR3), initially described in the skeletal muscle, the cardiac muscle, and the brain, respectively.

Ryanodine receptors were thought to be rather specific to excitable cells, where they represented the counterpart of IP3 receptors [9]. However, recent studies showed that some types of nonexcitable cells, where voltage-dependent Ca^{2+} channels are lacking, may also express ryanodine receptors [10]. The results concerning the expression and functional evidence of RyRs in nonexcitable cells are rather contradictory. In hepatocytes, for example, the effects of ryanodine on agonist-induced calcium signals have been demonstrated [11], but RyR mRNA expression has not been detected [5,12]. Larini et al. [13] suggested a ryanodine-like Ca^{2+} channel expression in nonexcitable cells; however, their Western blot analysis of total cell extracts failed to demonstrate the presence of an RYR-band in many cell types except for fibroblasts. A recent study [10] also showed that, while RyR mRNA was very occasionally present in a few nonexcitable cell types, the function of these receptors was not clear, as the agonists of RyRs, such as caffeine and ryanodine, were unable to release Ca^{2+}.

Furthermore, and more importantly, if some role has been ascribed to ryanodine receptors in excitable cells, e.g., its involvement in calcium-induced calcium release and excitation-contraction coupling [14], none has been demonstrated in nonexcitable cells and prostate cancer cells in particular. Nonetheless, different studies have shown that calcium is a major factor involved in apoptosis [15–17]. Therefore, the calcium regulatory mechanisms, such as IP3- or ryanodine-mediated calcium release, may play a substantial part in the regulation of apoptosis. Apoptosis is of prime importance for cancer cells and mostly for prostate cancer cells that proliferate very slowly. Calcium-stores depletion with thapsigargin induces apoptosis in many cell types, and among them, prostate cancer cells [18]. However, which of the intracellular calcium channels is implicated in apoptosis is still not known. Then, the identification of the existence of functional ryanodine receptors in prostate cancer cells would be of great consequence in an understanding of how apoptosis can be regulated.

In this work, using RT-PCR and Fura 2 fluorimetry and imaging, we show evidence of functional RyR in LNCaP prostate cancer cells. mRNAs of RyR1 and RyR2, but not RyR3, were identified in LNCaP cells. These cells do not possess the properties of excitable cells, as they do not express voltage-dependent inward currents, i.e., calcium and/or sodium currents [19]. However, in our experiments, LNCaP cells responded to several ryanodine receptor agonists: caffeine, 4 chloro-*m*-cresol, and ryanodine itself. Moreover, caffeine was able not only to mobilize calcium from a ryanodine-sensitive pool but also to promote calcium entry. We then show that apoptosis is enhanced by the activation of ryanodine receptors in prostate cancer cells and that inhibition of these receptors could protect the cancer cells against apoptosis.

MATERIALS AND METHODS

Chemicals

All chemicals were bought from Sigma Chemical Co. (St. Louis, MO) except for Fura 2/AM, ryanodine, and thapsigargin, which were purchased from Calbiochem France Biochem (Meudon, France).

Cell Culture

LNCaP prostate cancer cells were maintained in culture in RPMI-1640 medium supplemented with 10% fetal calf serum, penicillin (50 IU/ml), and streptomycin (50 μg/ml). Cells were grown in a humidified atmosphere containing 5% CO_2. Prior to fluorescence measurements, they were trypsinized and transferred to glass coverslips. They were used 1–4 days after trypsinization.

Calcium Measurements

The culture medium was replaced by an HBSS (Hank's Balanced Salt Solution) solution containing 142 mM NaCl, 5.6 mM KCl, 1 mM $MgCl_2$, 2 mM $CaCl_2$, 0.34 mM Na_2HPO_4, 0.44 mM KH_2PO_4, 10 mM HEPES, and 5.6 mM glucose. The osmolarity and pH of this solution were adjusted to 310 mOsm and 7.4, respectively. When a calcium-free medium was required, $CaCl_2$ was omitted and replaced by equimolar $MgCl_2$, and 0.1 mM EGTA was used to chelate calcium. Dye loading was achieved by transferring the cells into a standard HBSS solution containing 1 μM Fura 2/AM for 40 min at 37°C, and then rinsing them three times with the same dye-free solution. Intracellular calcium was measured by a photometric system (Photon Technology International, Monmouth Junction, NJ) or an imaging system (Quanticell 900, Applied Imaging, Sunderland, UK). In both cases, the glass coverslip was mounted in a chamber on a Nikon microscope equipped for fluorescence. Fura 2 fluorescence was excited at 340 nm and 380 nm, and the emitted fluorescence was measured above 510 nm using a long-pass filter. The intracellular calcium concentration $[Ca^{2+}]_i$ was derived from the ratio of the fluorescence intensities for each of the excitation wavelengths (F340/F380), and from the equation of Grienkewicz et al. [20]. All recordings were carried out at room tem-

perature. The cells were continuously perfused with the HBSS solution, and chemicals were added via the perfusion system. Two different perfusion systems were used in these experiments: first, a local application system using a glass pipette placed nearby the recorded cell (about 100–200 μm); and second, a whole-chamber perfusion. Kinetics of the calcium changes could be affected by these differences, since a whole-chamber perfusion only gradually modifies the solution surrounding the recorded cells. The flow rate of the whole-chamber perfusion was set to 1 ml/min and the chamber volume was 500 μl. However, even with differences in kinetics, caffeine raised intracellular calcium to the same level using both procedures. Unless specified in the figure legends, traces shown in this article were recorded using whole-chamber perfusion.

As previously shown by Islam et al. [21], we observed that application of caffeine led to small parallel increases of fluorescence at both excitation wavelengths, 340 and 380 nm, giving sometimes a slight decrease of the fluorescence ratio F340/F380. This has been demonstrated to be due to interference of caffeine with Fura 2 [21]. However, these variations at both wavelengths were not significant and did not impede calcium measurements.

RNA Isolation and RT-PCR Analysis

Total RNA from LNCaP cells was isolated by the guanidium thiocyanate-phenol-chloroform extraction procedure [22]. Five micrograms of total RNA were reverse-transcribed into complementary DNA (cDNA) at 42°C, using random hexamer primers (Perkin Elmer, Foster City, CA) and MuLV reverse transcriptase (Perkin Elmer) in a final volume of 20 μl. Then, a 1-μl aliquot was used for the PCR reaction, with RyR primers based on the sequences of the human RyRs. For RyR mRNA detection by RT-PCR, three oligonucleotide primers were synthesized by aligning the previously published RyR1, RyR2, and RyR3 sequences [23–25]. To detect each isoform of RyR mRNA, a reverse primer (RyR1-, RyR2-, and RyR3-specific) (hRyRB) complementary to the common transmembrane domain coding region (5′-TACATCTTCCAGACATAAGA-3′) was combined with either an RyR2-RyR3-specific sense primer (hRyRF1) (5′-GTAACTCACAATGGCAAACAG-3′) or an RyR1-RyR3-specific primer (hRyRF2) (5′-TCAACTTCTTCCGCAAGTTCTACAA-3′) corresponding to the same transmembrane domains. The predicted sizes of the PCR-amplified products were 554 base pairs (bp) and 476 bp, using hRyRF1/hRyRB and hRyRF2/hRyRB, respectively. RNA samples were assayed for DNA contamination by PCR prior reverse transcription. Each sample was amplified by AmpliTaq Gold DNA Polymerase (Perkin Elmer) in an automated thermal cycler (Perkin Elmer GeneAmp PCR System 2400). DNA amplification conditions were the same for both pairs of primers and included an initial denaturation step of 10 min at 95°C (which, at the same time, activated the gold variant of the Taq Polymerase) and 40 cycles of 30 sec at 95°C, 30 sec at 56°C, and 30 sec at 72°C. The RT-PCR samples were electrophoresed on a 2% agarose gel and stained with ethidium bromide (0.5 μg/ml). One microgram of 1 kb Plus DNA ladder (Life Technologies, Merelbeke, Belgium) was also run on agarose gel as a DNA size marker.

Restriction Enzyme Analysis of RT-PCR Products

In order to study the isoform expression of RyRs in LNCaP cells, the RT-PCR products were subjected to restriction enzyme analysis. PCR products precipitated by ethanol, suspended in water, and aliquots were digested by *Hae*III, *Bgl*II, or *Sac*I (Boehringer Mannheim, Brussels, Belgium). For hRyRF1/hRyRB-amplified PCR product, *Hae*III was expected to cut RyR1 (if amplified) into 225-, 168-, 85-, and 38-bp fragments, RyR2 into 301- and 253-bp fragments, and RyR3 into 255-, 253-, and 46-bp fragments. *Sac*I was expected to cut RyR1 only (if amplified), to produce fragments of approximately 295, 213, and 96 bp. *Bgl*II was expected to cut RyR2 only, producing 312- and 242-bp fragments. For RT-PCR products obtained using hRyRF2/hRyRB primers, *Sac*I was expected to cut RyR1 only, producing fragments of 167, 213 and 96 bp. *Bgl*II was expected to cut RyR2 only, into 312- and 164-bp fragments. Digested products were analyzed by electrophoresis on ethidium bromide-stained 2% agarose gel, and 1 kb Plus DNA ladder (Life Technologies, Merelbeke, Belgium) was used as the DNA size marker.

Apoptosis Assay

Cells were fixed in cold methanol (–20°C) for 10 min and washed twice with PBS before staining with 4 μg/ml Hoechst 33258 for 30 min at room temperature in the dark. Cells were then washed with PBS and mounted with coverslips, using glycergel. Apoptotic cells exhibiting condensed and fragmented nuclei were counted under an Olympus-BH2 fluorescent microscope. A minimum of 500–1,000 adherent cells was examined for each case, and the results were expressed as a number of apoptotic cells over the total number of cells counted.

Data Analysis

Results were expressed as mean ± SEM. Plots were produced using Origin 5.0 (Microcal Software, Inc., Northampton, MA).

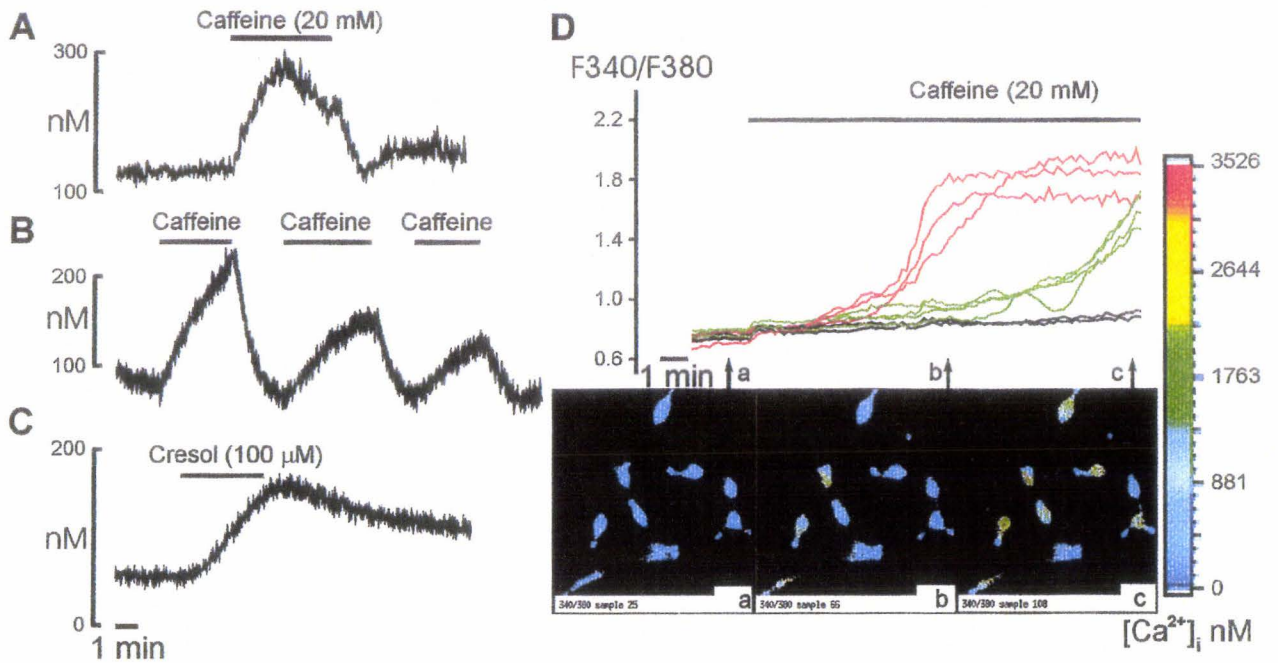

Fig. 1. Fluorescence measurements indicate that ryanodine receptor agonists increase $[Ca^{2+}]i$ in LNCaP cells. Microfluorimetric measurements of calcium $Ca^{2+}i$ (**A–C**) and calcium imaging (**D**) show that the activation of ryanodine sensitive pools using 20 mM caffeine (**A, B, D**) or 100 µM 4-chloro-*m*-cresol (cresol, in **C**) induces a calcium increase.

RESULTS

When LNCaP cells were bathed in a solution containing 2 mM $CaCl_2$, their intracellular calcium was about 76 ± 6 nM (n = 91) and remained stable during the recording (15–60 min). In order to investigate the existence of a ryanodine-sensitive store in LNCaP cells, we first studied how caffeine affected the cytosolic calcium concentration. Figure 1A shows that caffeine induced a rise in $[Ca^{2+}]i$ when applied at 20 mM. Most cells tested (87%, n = 54) responded in a similar pattern. The calcium increased from 87 ± 6 nM to 406 ± 79 nM. This increase could be reproduced several times on the same cell, with a slight decrease in the calcium peak in most cases (Fig. 1B). A similar calcium rise could be mimicked by 100 µM 4-chloro-*m*-cresol (n = 7, Fig. 1C), a potent ryanodine receptor activator [26]. Fura 2 imaging confirmed the increase in intracellular calcium after application of caffeine (Fig. 1D). Calcium imaging showed that the calcium increase kinetics differed from one cell to another, with some cells responding earlier than the others (e.g., the three cells left of b, in Fig. 1D).

We assessed the target of caffeine by pretreating LNCaP cells with ryanodine, which blocks calcium release from ryanodine-sensitive stores when used at high concentrations [27,28]. When ryanodine (10 µM)

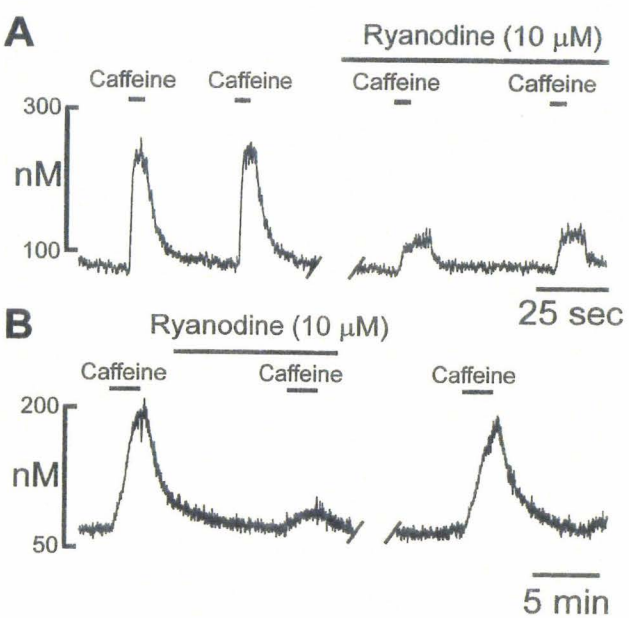

Fig. 2. Caffeine-induced $[Ca^{2+}]i$ increase is inhibited by ryanodine. **A:** Inhibition of caffeine-induced calcium increase by ryanodine (10 µM). Solutions are applied in this experiment using a local application pipette. **B:** Effect of caffeine recovered following the removal of ryanodine. Recordings were interrupted for 3 min in both A and B.

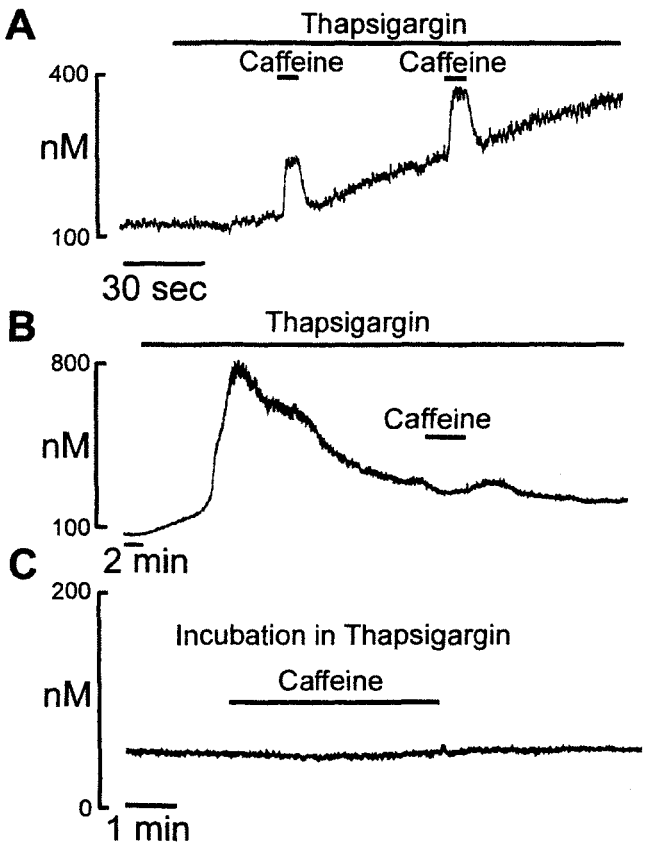

Fig. 3. Caffeine-induced $[Ca^{2+}]i$ increase is gradually abolished by thapsigargin, an inhibitor of endoplasmic reticulum ATPases. Thapsigargin (0.1 μM) induced an increase in $[Ca^{2+}]i$, followed by a gradual return to initial values. Thapsigargin was perfused for different lengths of time before caffeine was applied. Caffeine was applied (**A**) during the calcium increase induced by thapsigargin, (**B**) during the recovery phase, or (**C**) after a complete return to the basal calcium level. In A, solutions were applied with a local application pipette.

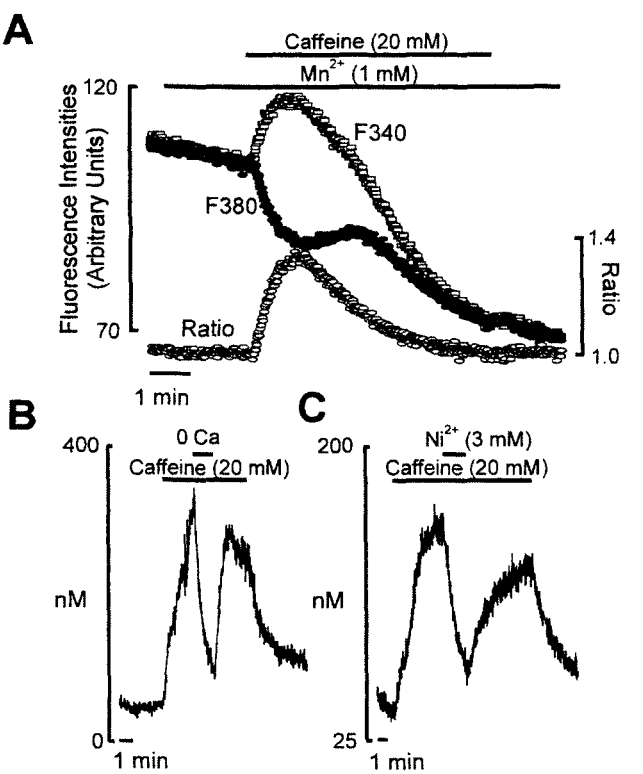

Fig. 4. Caffeine-induced $[Ca^{2+}]i$ increase occurs via a calcium mobilization and a calcium entry. **A:** Manganese quenching experiments under calcium-free conditions showed that caffeine first induced an increase in Fura 2 fluorescence at 340 nm and a decrease at 380 nm, thus indicating a calcium mobilization from internal stores. A rapid decrease in Fura 2 fluorescence was then observed at both wavelengths, showing a quenching of the Fura 2 fluorescence by manganese and indicating manganese entry into the cell. **B:** The calcium rise induced by caffeine was counteracted by an application of calcium-free medium, or (**C**) by 3 mM $NiCl_2$.

was applied before caffeine, the response to caffeine was almost completely abolished (n = 15, Fig. 2A,B). The inhibitory effect of ryanodine was reversible and the response to caffeine recovered (n = 3, Fig. 2B) after 5-min washing in a ryanodine-free medium, indicating that caffeine response was mediated by ryanodine-sensitive receptors.

We used thapsigargin (0.1 μM), a Ca^{2+} ATPase blocker [29], to check whether caffeine mobilized Ca^{2+} ions from intracellular stores. Emptying intracellular calcium stores led to a gradual inhibition of the response to caffeine, indicating a calcium mobilization from internal stores (n = 45). The application of thapsigargin induced a calcium increase up to 800 ± 20 nM, followed by a slow recovery (Fig. 3). Caffeine was still able to induce a rise in $[Ca^{2+}]i$ when applied during the increase in intracellular calcium due to thapsigargin (Fig. 3A). This effect no longer occurred when caffeine was perfused after the calcium peak (Fig. 3B). If thapsigargin was allowed to perfuse the cells long enough, i.e., more than 15 min, the cytosolic calcium concentration eventually returned to resting values, but caffeine was still unable to produce a calcium rise (Fig. 3C).

A calcium-free medium containing 1 mM $MnCl_2$ was used to further determine the origin of the calcium. Under these conditions, a calcium mobilization from internal stores should induce opposite variations on the two wavelengths: an increase in fluorescence intensity at 340 nm and a decrease at 380 nm. On the contrary, if caffeine led to calcium entry, these experimental conditions should produce a manganese entry and the quenching of Fura 2 fluorescence [30]. We observed that caffeine first induced a calcium increase, with opposite variations on the two wavelengths (Fig. 4A). This shows that in the absence of extracellular calcium, caffeine is able to produce a calcium mobilization from internal stores. After this initial phase, a rapid decrease in fluorescence intensity was observed

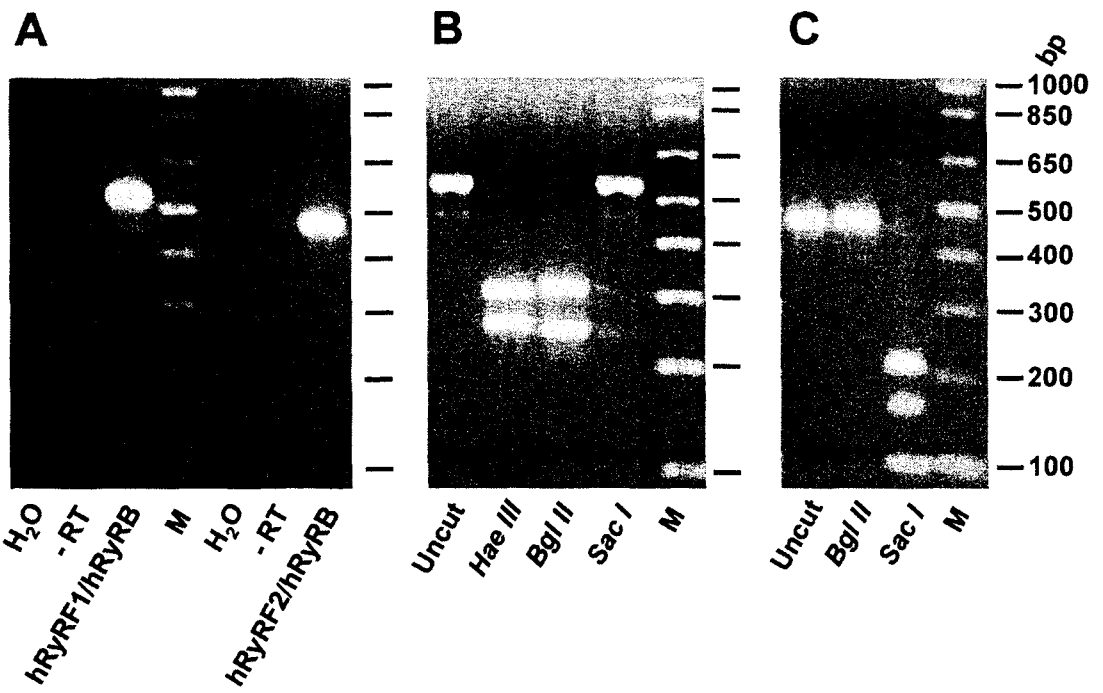

Fig. 5. Expression of RyRs in LNCaP cells. **A:** RT-PCR detection of RyRs in LNCaP cells. RT-PCR was performed with either of the following pairs of primers: hRyRF1/hRyRB or hRyRF2/hRyRB. PCR products of either 554 bp or 476 bp were detected in LNCaP cDNA but not in control reactions containing H_2O (**lane H_2O**) or LNCaP RNA without reverse transcription (**lane −RT**). **B:** Restriction enzyme digest of RyR RT-PCR products obtained using hRyRF1/hRyRB. **C:** Restriction enzyme digest of RyR RT-PCR products obtained using hRyRF2/hRyRB. **Lane M**, size markers.

at both wavelengths, indicating a quenching of Fura 2 fluorescence by manganese entering through plasma membrane channels. This indicated that caffeine was capable of increasing intracellular calcium concentrations via two pathways: calcium mobilization from internal stores, followed by calcium entry. This calcium entry was confirmed by applying a calcium-free medium during the response to caffeine (Fig. 4B). This led to a decrease in $[Ca^{2+}]i$ down to resting levels. Perfusion of $NiCl_2$ (3 mM), shown to inhibit capacitive calcium entry [31], produced a similar effect (Fig. 4C).

We used an RT-PCR assay to study RyR mRNA expression in LNCaP cells. By aligning the previously published RyR sequences, we designed primers to amplify either RyR2 and RyR3 (hRyRF1/hRyRB) or RyR1 and RyR3 (hRyRF2/hRyRB). The pairs of primers generated fragments of the expected sizes of 554 and 476 bp, respectively (Fig. 5A). To determine the isoforms expressed, we performed restriction digests on these PCR products, using specific enzymes for each isoform. The hRyRF1/hRyRB PCR product was completely cut by *Bgl*II (RyR2-specific), giving fragments of 312 and 242 bp, and also by *Hae*III, generating fragments of 301 and 253 bp, corresponding to the restriction profile of RyR2 (Fig. 5B). These observations show the expression of RyR2 but not RyR3 mRNA in LNCaP cells. In order to study the expression of RyR1 mRNA in these cells, we studied the enzyme restriction of the hRyRF2/hRyRB PCR product (amplifying RyR1 and RyR3). The PCR product was completely cut by *Sac*I (RyR1-specific) into 167-, 213-, and 96-bp products (Fig. 5C), showing that RyR1 mRNA was also expressed in these cells. Taken together, these results showed the expression of mRNAs of RyR1 and RyR2, but not RyR3, isoforms in LNCaP cells.

To study the physiological role of RyRs in LNCaP cells, we next assessed the effects of ryanodine receptor activation on apoptosis. Cells were treated with 5 mM caffeine for 48 hr in the presence or absence of 15 μM ryanodine. Figure 6 demonstrates that both untreated and ryanodine-treated cells exhibited a very low apoptotic index (less than 0.1%). By contrast, when the cells were treated with caffeine, about 3.5% of adherent cells were induced into apoptosis. Ryanodine partially inhibited the caffeine-induced apoptosis. These observations suggest that ryanodine-sensitive calcium stores mediate the induction of apoptosis by caffeine.

DISCUSSION

We conclude from these findings that LNCaP prostate cells express functional ryanodine receptors. We showed that caffeine was able to release calcium from

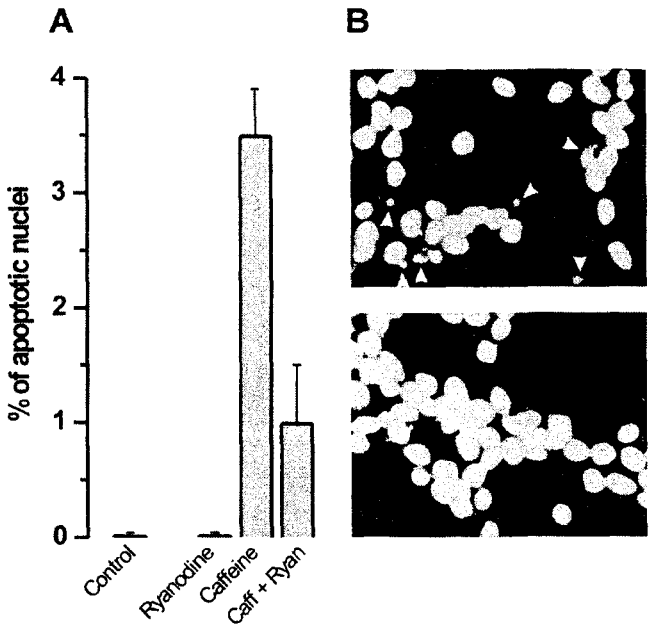

Fig. 6. Effect of ryanodine on induction of apoptosis by caffeine. Cells were seeded in RPMI-1640 medium containing 10% fetal calf serum. Two days later, cells were treated with 5 mM caffeine in the presence or absence of 15 μM ryanodine for 48 hr. Apoptosis was determined as described in Materials and Methods. Shown here are results of a triplicate assay in one experiment, which is representative of two independent experiments. **A:** Histogram showing percent of apoptotic cells in the presence or absence of caffeine and ryanodine. **B:** Fluorescence photographs of cells in the presence of caffeine (**top**), and in the presence of caffeine and ryanodine (**bottom**). Arrowheads indicate apoptotic nuclei.

ryanodine-sensitive intracellular stores in LNCaP cells. Caffeine has also been shown to elevate intracellular calcium in many cell types by other means such as inhibition of K_{ATP} channels, leading to a depolarization and then a calcium influx, or by increasing cAMP through its action on phosphodiesterase or by stimulating a ryanodine receptor-independent calcium influx [21,32]. We show here that the action of caffeine occurs through ryanodine receptors, since a similar calcium rise was reproduced using 4 chloro-*m*-cresol, another ryanodine receptor agonist [26]. Furthermore, this effect was inhibited by ryanodine, an inhibitor of calcium-induced calcium release. In addition, unlike in systems where caffeine produces a calcium entry [21], thapsigargin, a calcium ATPase inhibitor which depletes intracellular calcium stores [29], completely inhibited the calcium rise induced by caffeine in our experiments. Also, in the absence of external calcium (quench experiment, Fig. 4A), caffeine still produced antiparallel variations of the Fura 2 fluorescence, indicating that there is not a strict requirement for extracellular calcium for the initial cytosolic calcium increase. We thus conclude that LNCaP cells, which are nonexcitable, possess intracellular ryanodine-sensitive calcium stores, and that caffeine is able to mobilize these calcium stores.

A recent study showed that ryanodine receptor mRNA could be detected in only 2 of 12 different nonexcitable cell types [10]. However, the function of RyRs in these cells could not be determined, as they did not respond to caffeine. The fact that the response to an IP3 agonist was attenuated by ryanodine led the authors to suggest that stimulation of ryanodine receptors would promote an amplification of the 1,4,5-IP3-induced calcium release. As nonexcitable cells where ryanodine receptors are expressed are usually nonresponsive to caffeine, LNCaP cells appear to be an original cell model. Using an RT-PCR assay, we showed that RyR1 and RyR2 mRNAs were expressed in LNCaP cells. This is rather surprising as, in the few nonexcitable models where RyRs have been detected by RT-PCR, only RyR3 and RyR2 have been identified in epithelial gut cells [33], T lymphocytes [34], HeLa cervix carcinoma [10], and epithelial kidney cells [35]. To our knowledge, the only nonexcitable cells where RyR1 has been shown to be expressed are parotid cells [36].

In excitable cells, besides the well-known role of RyRs in excitation-contraction coupling in muscles [37–39], other functions have been suggested for these receptors, including an involvement in synaptic plasticity [40], as well as regulation of cell proliferation [34]. When present in nonexcitable cells, the function of ryanodine receptors is not clear, as opposed to excitable cells, where they are closely linked to dihydropyridine receptors and respond to plasma membrane depolarization [37] or calcium entry during depolarization [38] by releasing intraluminal calcium into the cytosol. It is nonetheless possible that ryanodine receptors are also implicated in calcium-induced calcium release in nonexcitable cells through a coupling to voltage-independent or ligand-gated Ca^{2+} channels.

In order to define the role of ryanodine receptors in calcium homeostasis in prostate cancer cells, we investigated the relationship between ryanodine receptor activation and another source of calcium, calcium entry through plasma membrane channels. We show here that ryanodine receptor activation by caffeine is closely associated with calcium influx. As there are no voltage-dependent calcium channels in these cells [19], this may be due to a capacitive calcium entry, a "calcium-refilling mechanism" induced by the depletion of calcium stores [41]. This type of calcium entry was first described in mast cells [42] and then in various cell models. It is now considered a typical response of nonexcitable cells to the agents that stimulate the phospholipase C/IP3 pathway, mobilizing Ca^{2+} from internal stores [41]. Capacitive calcium en-

try has also been described in excitable cells [43,44] and has been reported to be activated following ryanodine receptor activation in PC12 cells [45] and muscle cells [46,47]. In our experiments, the calcium influx was able to permeate manganese and was inhibited by nickel (one of the most potent capacitive calcium entry inhibitors) [31]. Our results show that calcium entry, and thus refilling of internal calcium stores, was promoted by the activation of ryanodine-sensitive calcium stores in nonexcitable prostate cancer cells.

We then investigated the role of ryanodine receptors in apoptosis. Calcium has been shown to be involved in apoptosis [15–17], but it is not clear which of the calcium levels in the cytosol and the filling state of the intracellular stores is the important factor implicated. In hormone-independent prostate cancer cells, thapsigargin stimulates apoptosis by a Ca^{2+} mobilization from intracellular pools and a following sustained Ca^{2+} entry [18]. We have also observed in hormone-dependent prostate cancer cells that apoptosis can be triggered by thapsigargin but independently of the capacitative calcium entry (R. Skryma, unpublished findings). We have shown in our experiments that activation of RyRs with caffeine slightly stimulated apoptosis and that this effect was inhibited by ryanodine. By this way, RyRs could modulate apoptosis in prostate cancer cells by regulating the calcium levels in the cytosol or in intracellular stores. In nonexcitable cells, and in cancer cells in particular, growth factors and hormones trigger Ca^{2+} entry through voltage-independent Ca^{2+} channels stimulated by tyrosine or serine/threonine kinase phosphorylation, or stimulate calcium release from IP3-sensitive stores [9,48,49]. This calcium entry or release could in turn activate RyRs by a CICR, Calcium–Induced Calcium Release mechanism and by this way induce apoptosis. The connection between ryanodine-sensitive stores and apoptosis has not yet been demonstrated. If some reports show that caffeine can enhance the cytotoxicity of other drugs, its action was not shown to be dependent on ryanodine receptors [50,51]. On the contrary, the role of IP3 receptors in apoptosis has been better documented [52], and it has been demonstrated that T cells devoid of type 1 IP3 receptors are resistant to the apoptosis induced by various treatments [53]. We show in our experiments that the stimulation of apoptosis by caffeine is relatively low (3.5% of apoptotic cells with caffeine vs. 0.1% in the absence of caffeine). However, one might expect this effect to be large enough to lead to a reduction in cell growth rate. In addition, it must be pointed out that the amount of apoptosis due to caffeine treatment is similar to the percentage of cell death observed in some studies, where cell death was induced by androgen depletion in human prostate cancer cells [54]. We therefore suggest that activation of the other major intracellular calcium receptor, the ryanodine receptor, can also regulate apoptosis in prostate cancer cells.

These results could be of fundamental importance, since the development of prostate tumors can be slowed by inducing apoptosis. Apoptosis may be induced in prostate cells by androgen depletion [55], which is a commonly used therapy. It remains to be determined at that stage if androgen depletion-induced apoptosis involves changes in calcium homeostasis. Furthermore, since the development of prostate cancer is always accompanied in the later stages by the loss of androgen ablation sensitivity due to the presence of androgen-independent cells in the prostate tumor [56], an important issue would be to characterize regulatory mechanisms of ryanodine receptors, and their role in the activation of apoptosis in such androgen-independent cells.

ACKNOWLEDGMENTS

We are grateful to Prof. Carl Denef for allowing us to perform part of the experiments in his Laboratory of Cell Pharmacology, Department of Molecular Cell Biology, Catholic University of Leuven (Leuven, Belgium). We are grateful to I. Servant for excellent technical assistance.

REFERENCES

1. Imagawa T, Nakai J, Takeshima H, Nakasaki Y, Shigekawa M. Purified ryanodine receptor from muscle sarcoplasmic reticulum is the Ca^{2+}-permeable pore of the calcium release channel. J Biol Chem 1987;262:16636–16643.
2. Lai F, Anderson K, Rousseau E, Liu Q, Meissner G. Purification and reconstitution of the calcium release channel from skeletal muscle. Nature 1988;331:315–319.
3. Otsu K, Willard HF, Khanna VK, Zorzat F, Green NM, MacLennan DH. Molecular cloning of cDNA encoding the Ca^{2+} release channel (ryanodine receptor) of rabbit cardiac muscle sarcoplasmic reticulum. J Biol Chem 1990;265:13472–13483.
4. Marks AR, Tempst P, Hwang KS, Taubman MB, Inui M, Chadwick C, Fleischer S, Nadal-Ginard B. Molecular cloning and characterization of the ryanodine receptor junctional channel complex cDNA from skeletal muscle sarcoplasmic reticulum. Proc Natl Acad Sci USA 1989;86:8683–8687.
5. Giannini G, Conti A, Mammarella S, Scrobogna M, Sorrentino V. The ryanodine receptor/calcium channel genes are widely and differentially expressed in murine brain and peripheral tissues. J Cell Biol 1995;128:893–904.
6. Hakamata Y, Nakai J, Takeshima H, Imoto K. Primary structure and distribution of a novel ryanodine receptor/calcium release channel from rabbit brain. FEBS Lett 1992;312:229–235.
7. Islam MS, Rorsman P, Berggren PO. Ca^{2+}-induced Ca^{2+} release in insulin-secreting cells. FEBS Lett 1992;296:287–291.
8. Clementi E, Riccio M, Sciorati C, Nistico G, Meldolesi J. The type 2 ryanodine receptor of neurosecretory PC 12 cells is activated by cyclic ADP-ribose. Role of the nitric oxide/cGMP pathway. J Biol Chem 1996;271:17739–17745.

9. Clapham DE. Calcium signalling. Cell 1995;80:259–268.
10. Bennett DL, Cheek TR, Berridge MJ, De Smedt H, Parys JB, Missiaen L, Bootman MD. Expression and function of ryanodine receptors in nonexcitable cells. J Biol Chem 1996;271:6356–6362.
11. Sanchez-Bueno A, Cobbold PH. Agonist-specifity in the role of Ca^{2+}-induced Ca^{2+} release in hepatocyte Ca^{2+} oscillations. Biochem J 1993;291:169–172.
12. Shoshan-Barmatz V, Pressley TA, Higham S, Kraus-Friedmann N. Characterization of high-affinity ryanodine-binding sites of rat liver endoplasmic reticulum. Differences between liver and skeletal muscle. Biochem J 1991;15:41–46.
13. Larini F, Menegazzi P, Baricordi O, Zorzato F, Treves S. A ryanodine receptor-like Ca^{2+} channel is expressed in nonexcitable cells. Mol Pharmacol 1995;47:21–28.
14. Coronado R, Morrissette J, Sukhareva M, Vaughan DM. Structure and function of ryanodine receptors. Am J Physiol 1994; 266:1485–1504.
15. Berridge MJ. Calcium signalling and cell proliferation. Bioessays 1995;17:491–500.
16. McConkey DJ, Orrenius S. The role of calcium in the regulation of apoptosis. Biochem Biophys Res Commun 1997;239:357–366.
17. Berridge MJ, Bootman MD, Lipp P. Calcium—a life and death signal. Nature 1998;395:645–648.
18. Furuya Y, Lundmo P, Short AD, Gill DL, Isaacs JT. The role of calcium, pH, and cell proliferation in the programmed (apoptotic) death of androgen-independent prostatic cance cells induced by thapsigargin. Cancer Res 1994;54:6167–6175.
19. Skryma R, Prevarskaya N, Dufy-Barbe L, Odessa MF, Audin J, Dufy B. Potassium conductance in the androgen-sensitive prostate cancer cell line, LNCaP: involvement in cell proliferation. Prostate 1997;33:112–122.
20. Grynkiewicz G, Poenie M, Tsien RY. A new generation of Ca^{2+} indicators with greatly improved fluorescence properties. J Biol Chem 1985;260:3440–3450.
21. Islam MS, Larsson O, Nilsson T, Berggren PO. Effects of caffeine in cytoplasmic free Ca^{2+} concentration in pancreatic beta-cells are mediated by interaction with ATP-sensitive K^+ channels and L-type voltage-gated Ca^{2+} channels but not the ryanodine receptor. Biochem J 1995;306:679–686.
22. Chomczynski P, Sacchi N. Single-step methode of RNA isolation by acid guanidium thiocyanate-phenol-chloroform extraction. Anal Biochem 1987;162:156–159.
23. Zorzato F, Fujii J, Otsu K, Phillips M, Green NM, Lai FA, Meissner G, MacLennan DH. Molecular cloning of cDNA encoding human and rabbit forms of the Ca^{2+} release channel (ryanodine receptor) of skeletal muscle sarcoplasmic reticulum. J Biol Chem 1990;265:2244–2256.
24. Tunwell RE, Wickenden C, Bertrand BM, Shevchenko VI, Walsh MB, Allen PD, Lai FA. The human cardiac muscle ryanodine receptor-calcium release channel : identification, primary structure and topological analysis. Biochem J 1996;318:477–487.
25. Leeb T, Brenig B. cDNA cloning and sequencing of the human ryanodine receptor type 3 (RyR3) reveals a novel alternative splice site in the RyR3 gene. FEBS Lett 1998;423:367–370.
26. Hermann-Franck A, Richter R, Sarkozi S, Mohr U, Lehmann-Horn F. 4-chloro-m-cresol, a potent and specific activator of the skeletal muscle ryanodine receptor. Biochim Biophys Acta 1996; 1289:31–40.
27. McPherson PS, Campbell KP: The ryanodine receptor/Ca^{2+} release channel. J Biol Chem 1993;268:13765–13768.
28. Fleischer S, Inui M. Biochemistry and biophysics of excitation-contraction coupling. Annu Rev Biophys Chem 1989;18:333–364.
29. Lytton J, Westlin M, Hanley MR. Thapsigargin inhibits the sarcoplasmic or endoplasmic reticulum Ca-ATPase family of calcium pumps. J Biol Chem 1991;266:17067–17071.
30. Merritt JE, Jacob R, Hallam TJ. Use of manganese to discriminate between calcium influx and mobilization from internal stores in stimulated human neutrophils. J Biol Chem 1989;264: 1522–1527.
31. Schlegel W, Mollard P, Demaurex N, Theler JM, Chiavaroli C, Guerineau N, Vacher P, Mayr G, Krause KH, Wollheim CB. Calcium signalling: comparison of the role of Ca2+ influx in excitable endocrine and non-excitable myeloid cells. Adv Second Messenger Phosphoprotein Res 1993;28:143–152.
32. Ufret-Vincenty CA, Short AD, Alfonso A, Gill DL. A novel Ca^{2+} entry mechanism is turned on during growth arrest induced by Ca^{2+} pool depletion. J Biol Chem 1995;270:26790–26793.
33. Verma V, Carter C, Keable S, Bennett D, Thorn P. Identification and function of type-2 and type-3 ryanodine receptors in gut epithelial cells. Biochem J 1996;319:449–454.
34. Hakamata Y, Nishimura S, Nakai J, Nakashima Y, Kita T, Imoto K. Involvement of the brain type of ryanodine receptor in T-cell proliferation. FEBS Lett 1994;352:206–210.
35. Tunwell REA, Lai FA. Ryanodine receptor expression in the kidney and a non-excitable kidney epithelial cell. J Biol Chem 1996;271:29583–29588.
36. Zhang X, Wen J, Bidasce KR, Besch R Jr, Rubin RP. Ryanodine receptor expression is associated with intracellular Ca^{2+} release in rat parotid acinar cells. Am J Physiol 1997;273:1306–1314.
37. Numa S, Tanabe T, Takeshima H, Mikami A, Niidome T, Nishimura S, Adams BA, Beam KG. Molecular insights into excitation-contraction coupling. Cold Spring Harbor Symp Quant Biol 1990;5:1–7.
38. Stern MD. Theory of excitation-contraction coupling in cardiac muscle. Biophys J 1992;63:497–517.
39. Cheng H, Lederer MR, Xiao RP, Gomez AM, Zhou YY, Ziman B, Spurgeon H, Lakatta EG, Lederer WJ. Excitation-contraction coupling in heart: new insights from Ca^{2+} sparks. Cell Calcium 1996;20:129–140.
40. Chavis P, Fagni L, Lansman JB, Bockaert J. Functional coupling between ryanodine receptors and L-type calcium channels in neurons. Nature 1996;382:719–722.
41. Berridge MJ. Capacitative calcium entry. Biochem J 1995;312:1–11.
42. Hoth M, Penner R. Depletion of intracellular calcium stores activates a calcium current in mast cells. Nature 1992;355:353–356.
43. Miura Y, Henquin JC, Gilon P. Emptying of intracellular Ca^{2+} stores stimulates Ca^{2+} entry in mouse pancreatic beta-cells by both direct and indirect mechanisms. J Physiol, (London) 1997; 503:387–398.
44. Villalobos C, Garcia-Sancho J. Capacitative Ca^{2+} entry contributes to the Ca^{2+} influx induced by thyrotropin-releasing hormone (TRH) in GH3 pituitary cells. Pflugers Arch 1995;430:923–935.
45. Bennett DL, Bootman MD, Berridge MJ, Cheek TR. Ca^{2+} entry into PC 12 cells initiated by ryanodine receptors or inositol 1,4,5-trisphosphate receptors. Biochem J 1998;329:349–357.
46. Wayman CP, Gibson A, McFadzean I. Depletion of either ryanodine- or IP3-sensitive calcium stores activates capacitative calcium entry in mouse anococcygeus smooth muscle cells. Pflugers Arch 1998;435:231–239.
47. Noguera MA, Madrero Y, Ivorra MD, D'Ocon P. Characterization of two different Ca^{2+} entry pathways dependent on depletion of internal Ca^{2+} pools in rat aorta. Naunyn Schmiedebergs Arch Pharmacol 1998;357:92–99.
48. Peppelenbosch MP, Tertoolen LJ, den Hertog J, de Laat SW. Epidermal growth factor activates calcium channels by phospholipase A2/5-lipoxygenase-mediated leukotriene C4 production. Cell 1992;69:295–303.

49. Lovisolo D, Distasi C, Antoniotti S, Munaron L. Mitogens and calcium channels. News Physiol Sci 1997;12:279–285.
50. Takahashi M, Yamamoto Y, Hatori S, Shiozawa M, Suzuki M, Rino Y, Amano T, Imada T. Enhancement of CDDP cytotoxicity by caffeine is characterized by apoptotic cell death. Oncogene Rep 1998;5:53–56.
51. Janss AJ, Levow C, Bernhard EJ, Muschel RJ, McKenna WG, Sutton L, Phillips PC. Caffeine and staurosporine enhance the cytotoxicity of cisplatin and camptothecin in human brain tumor cell lines. Exp Cell Res 1998;25:29–38.
52. Marks AR. Intracellular calcium-release channels: regulators of cell life and death. Am J Physiol 1997;272:597–605.
53. Jayaraman T, Marks AR. T cells deficient in inositol 1,4,5-trisphosphate receptor are resistant to apoptosis. Mol Cell Biol 1997;17:3005–3012.
54. Kyprianou N, English HF, Isaacs JT. Programmed cell death during regression of PC-82 human prostate cancer following androgen ablation. Cancer Res 1990;50:3748–3753.
55. Kyprianou N, Isaacs JT. Activation of programmed cell death in the rat ventral prostate after castration. Endocrinology 1988;122: 552–562.
56. Crawford ED, Eisenberg MA, McLeod DC, Spaulding J, Benson R, Dorr FA, Blumenstein BA, Davis MA, Goodman PJ. A controlled trial of leuprolide with and without flutamide in protastic carcinoma. N Engl J Med 1989;321:419–424.

Article 6.

Mechanisms of ATP-induced calcium signaling and growth arrest in human prostate cancer cells

Vanoverberghe K, Mariot P, Vanden Abeele F, Delcourt P, Parys JB, Prevarskaya N.(2003) **Cell Calcium.** 34 : 75-85.

I. Position du problème et résultats

Le but de ces travaux était de déterminer le rôle des variations de concentration en calcium dans les cellules prostatiques dans l'inhibition de croissance induite par la stimulation des récepteurs purinergiques par l'ATP. Il avait été montré d'une part que l'action d'agonistes purinergiques (*via* des récepteurs P2Y) sur des cellules prostatiques cancéreuses androgéno-indépendantes induisait un arrêt de prolifération (Fang et al 1992). Il était particulièrement important de comprendre le mécanisme d'action de ces agonistes purinergiques car, à ce stade androgéno-indépendant, les cellules cancéreuses prostatiques sont particulièrement agressives et ne sont sensibles à aucun traitement hormonal ou chimiothérapique. D'autre part, nous avions montré dans un travail préalable (Legrand et al 2001) sur des cellules prostatiques cancéreuses que l'action proliférative de facteurs de croissance (type EGF, epidermal growth factor) était dépendante de l'état de remplissage des réserves calciques. Nous avons donc étudié particulièrement le rôle des niveaux de calcium dans le cytosol et le RE dans les processus d'inhibition de prolifération.

La première partie de cet article a consisté à caractériser le mécanisme de transduction impliqué dans la réponse purinergique des cellules prostatiques androgéno-indépendantes DU145. Nous avons ainsi montré que l'action inhibitrice de l'ATP sur la croissance cellulaire était médiée par la voie de la phospholipase C/IP3/PKC. Les récepteurs IP3 impliqués dans la réponse à l'ATP dans les cellules DU145 sont principalement de type 3. D'autre part, nous montrons que l'entrée capacitative induite par l'ATP dépendait de l'activation de la protéine kinase C.

Dans la seconde partie de l'article, nous avons étudié le rôle respectif des variations de calcium dans l'inhibition de croissance des cellules DU145 induite par l'ATP Nous montrons ici que l'augmentation de calcium induite par l'ATP, due à la fois à une mobilisation des réserves intracellulaires et une entrée capacitative, n'est pas nécessaire dans la réponse anti-proliférative. En revanche, nos résultats suggèrent que l'ATP entraîne une diminution de la concentration en calcium libre dans les réserves intracellulaires et que cette vidange pourrait être impliquée dans l'inhibition de la prolifération.

II. Dicussion

Nos résultats montrent que la concentration en calcium libre dans les réserves intracellulaires sensibles à la TG (RE) est impliquée dans le contrôle de la prolifération cellulaire. Comme précisé dans l'introduction, le rôle du calcium dans la prolifération est connu depuis environ 25 ans (Boynton et al 1977, Jensen et al 1977). Certains travaux, incluant les nôtres (Legrand et al 2001), ont montré que l'état de remplissage des réserves du RE était un élément clé de contrôle de la croissance cellulaire (Ghosh et al 1991, Short et al 1993, Waldron, et al 1994). Il a été montré que des traitements à la TG induisait une vidange calcique, une inhibition de la synthèse d'ADN et protéique et une inhibition de la croissance cellulaire dans des lignées de cellules musculaires lisses en culture (Gosh et al 1991). Cet effet était indépendant d'une action sur les transports mitochondriaux. D'autre part, cette action de la TG est antagonisée par un traitement avec de fortes quantités de sérum qui induit un remplissage des stocks calciques du RE, une néo-expression de SERCA2 dans le RE et rétabli un niveau de croissance cellulaire initial (Waldron et al 1994). Nous avons également montré dans les cellules LNCaP que l'action proliférative de facteurs de croissance (EGF) s'exerce notamment *via* une surexpression de SERCA2b et un remplissage des réserves calciques du RE plus important (Legrand et al 2001). Nous montrons ici qu'une stimulation physiologique (purinergique) de récepteurs-canaux intracellulaires provoque une inhibition de la prolifération par une vidange des réserves calciques intracellulaires.

La thapsigargine par elle-même n'induit pas d'inhibition de la prolifération cellulaire dans les cellules DU-145, contrairement aux cellules LNCaP, ce qui laisse suposer des mécanismes différents quant aux rôle du calcium du RE dans le contrôle de la prolifération de ces cellules. Ceci suggère que :

- La vidange des réserves calciques à elle-seule n'est pas suffisante dans les cellules androgéno-indépendantes DU145 pour induire un arrêt de prolifération,
- Que cette vidange est néanmoins un élément indispensable activée par les récepteurs purinergiques dans la chaîne de transduction menant à l'arrêt de prolifération,
- Que la vidange nécessite, pour induire un arrêt de croissance cellulaire, une activation de systèmes de transduction qui ne sont pas stimulés par la TG dans ces cellules,

Une des hypothèses permettant d'expliquer ceci est que la vidange calcique provoquée par l'ATP agit conjointement avec des seconds messagers impliqués dans la réponse ATP, par exemple l'IP3 ou la voie de la protéine kinase C ou les MAP kinases qui sont activés dans d'autres systèmes cellulaires par les récepteurs purinergiques (Soltoff et al 1998, Wilden et al 1998). Il est possible qu'une concomittence temporelle et spatiale de ces signaux (par exemple vidange des réserves calciques et activation des récepteurs IP3) soit nécessaire pour induire un arrêt de prolifération.

Il existe deux hypothèses principales pouvant expliquer l'inhibition de prolifération par une vidange des réserves calciques intracellulaires :

1) les niveaux de calcium dans le RE sont nécessaires à une synthèse et une maturation protéique correcte et une altération des niveaux de calcium dans la lumière du RE va entraîner une altération de ces processus.

2) le calcium dans la lumière du RE contrôle des signaux de transduction impliqués dans la régulation génique.

La deuxième hypothèse est certainement la plus intéressante et plusieurs possibilités peuvent rendre compte d'une action des niveaux de calcium dans le RE sur la transcription de gènes (voir figure 16).

L'induction de l'arrêt de prolifération cellulaire par la vidange des réserves calciques induite par une activation des récepteurs IP3-R pourrait être notamment médiée par une protéine appellée CHERP (pour Calcium Homeostasis Endoplasmic Reticulum Protein). Cette protéine est une protéine intégrale à la membrane du RE et est colocalisée avec les récepteurs IP3 notamment au niveau des régions périnucléaires. Il a été montré que son inhibition, grâce à une stratégie antisens, aboutit à une diminution de la quantité de calcium libéré par des agonistes des récepteurs IP3, à une diminution de la prolifération et à une inhibition de la translocation du facteur de transcription NF-AT du cytosol vers le noyau. CHERP pourrait ainsi être le relais entre la détection du niveau de remplissage des réserves calciques du RE (par les récepteurs IP3 par exemple) et l'activation des facteurs de transcription NF-AT (Laplante et al 2000, O'Rourke et al 2003).

Le niveau de calcium dans le RE peut également affecter les fonctions de calcium-binding protéines, telles que la calréticuline ou les calnexines (pour revue voir Michalak et al 2002). La calréticuline est connue pour jouer un rôle considérable comme protéine tampon de la concentration calcique du RE, capable de réagir à des variations de la concentration de calcium dans la lumière du RE et de moduler l'homéostasie calcique. Cependant, la liaison du calcium sur la calréticuline va également moduler son activité et influencer son interaction avec d'autres protéines calcium-dépendantes. Ainsi, la calréticuline peut jouer un rôle important dans le contrôle de la mort cellulaire et de la prolifération en contrôlant par exemple la disponibilité des ions calcium pour la translocation de NF-AT vers le noyau ou en contrôlant l'activité de la calcineurine, une phosphatase calcium-dépendante impliquée dans le contrôle de l'activité transcriptionnelle (Michalak et al 2002, Guo et al 2002).

Enfin, l'existence d'un réseau réticulaire nucléoplasmique (Echevarria et al 2003) laisse supposer qu'une vidange calcique du RE pourrait être transmise vers les réserves calciques nucléaires et engendrer un signal transcriptionnel grâce à un facteur de transcription nucléaire.

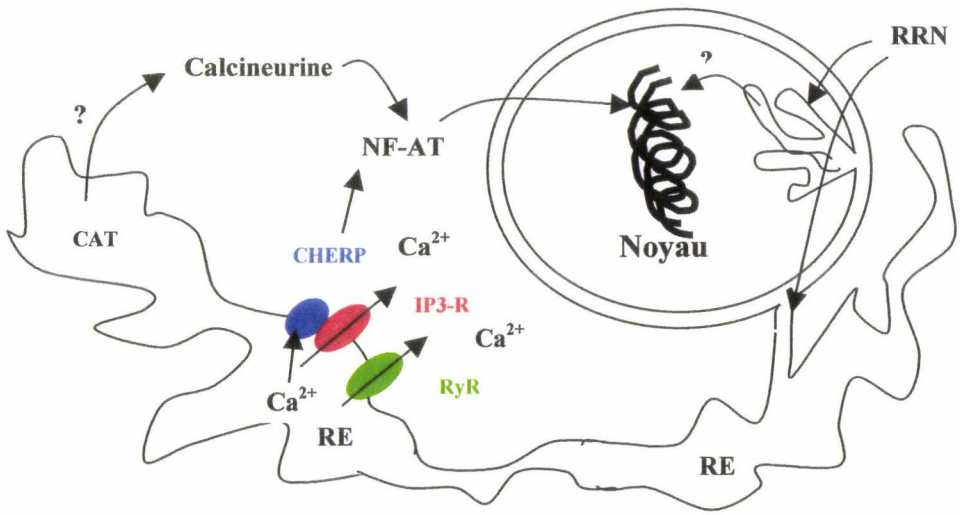

Figure 16 : Possibles voies de régulation de la transcription génique *via* une altération de la concentration en calcium du RE

CAT : calréticuline

RRN : réseau réticulaire nucléosomique

CHURCHILL LIVINGSTONE

Cell Calcium 34 (2003) 75–85

cell calcium

www.elsevier.com/locate/ceca

Mechanisms of ATP-induced calcium signaling and growth arrest in human prostate cancer cells

K. Vanoverberghe[a,1], P. Mariot[a,1], F. Vanden Abeele[a], P. Delcourt[a], J.B. Parys[b], N. Prevarskaya[a,*]

[a] *INSERM EMI 0228, Laboratoire de Physiologie Cellulaire, Bâtiment SN3, Université des Sciences et Technologies de Lille, 59655 Villeneuve d'Ascq Cédex, France*

[b] *Laboratorium voor Fysiologie, Campus Gasthuisberg O/N—K.U. Leuven, B-3000, Leuven, Belgium*

Received 19 November 2002; received in revised form 18 January 2003; accepted 28 January 2003

Abstract

This study investigates the calcium mechanisms involved in growth arrest induced by extracellular ATP in DU-145 androgen-independent human prostate cancer cells. Exposure of DU-145 cells to 100 μM ATP produced an increase in cytoplasmic calcium concentration ($[Ca^{2+}]_i$), due to a mobilization of calcium from the endoplasmic reticulum stores and to subsequent capacitative calcium entry (CCE).

We have shown that this $[Ca^{2+}]_i$ increase occurs after stimulation by ATP of the phospholipase C (PLC) pathway. For the first time, we have identified the inositol 1,4,5-trisphosphate receptor (IP_3R) isoforms expressed in this cell line and have demonstrated a participation of protein kinase C in CCE. Using fluorescence imaging, we have shown that a long-term treatment with ATP leads to a decrease in the intraluminal endoplasmic reticulum calcium concentration as well as in the amount of releasable Ca^{2+}. Modulating extracellular free calcium concentrations indicated that variations in $[Ca^{2+}]_i$ did not affect the ATP-induced growth arrest of DU-145 cells. However, treating cells with 1 nM thapsigargin (TG) to deplete intracellular calcium pools prevented the growth arrest induced by ATP. Altogether, these results indicate that growth arrest induced in DU-145 cells by extracellular ATP is not correlated with an increase in $[Ca^{2+}]_i$ but rather with a decrease in intracellular calcium pool content.

Keywords: Calcium signaling; ATP; Growth arrest

1. Introduction

Due to the constant increase in human life expectancy, prostate cancer is the second leading cause of cancer death in men [1]. Although it has been clearly established that the growth of prostate cells is regulated by androgens [2], antiandrogen therapies in combination with medical or surgical castration [3] are only temporarily effective in most cases. Tumors eventually exhibit androgen-independent characteristics and resume their progression. For this reason, a thorough knowledge of the mechanisms inhibiting the proliferation of human androgen-independent prostate carcinoma cells is particularly useful for prostate cancer therapy.

Indeed, little is known about the factors regulating the growth of androgen-independent prostate cancer cells. In this context, extracellular ATP is considered to be one of the physiological agents that inhibit the growth of several transformed cell lines through interactions with pharmacologically distinct P2 purinergic receptors [4]. The concept that ATP may also function as a direct regulator of cell viability through the activation of P2Y purinoreceptors in the human androgen-independent prostate carcinoma cell lines such as PC3, PC3-M or DU-145, was first suggested by Fang et al. [5] and recently further explored by Janssens and Boeynaems [6]. However, the mechanisms by which ATP acts on androgen-independent prostate carcinoma cell lines have not yet been elucidated.

Calcium ions play a central role in the regulation of many aspects of cell physiology. Control of muscle contraction or neurotransmitter release are obvious examples but calcium homeostasis has been also demonstrated to be implicated in processes such as cancer growth, cell cycle progression [7,8], cell migration [9], angiogenesis [10], apoptosis [11] and proliferation [12].

* Corresponding author. Tel.: +33-3-20-43-40-77; fax: +33-3-20-43-40-66.

E-mail address: Natacha.Prevarskaya@univ-lille1.fr (N. Prevarskaya).

[1] Both of them contributed equally to this work.

0143-4160/03/$ – see front matter © 2003 Elsevier Science Ltd. All rights reserved.
doi:10.1016/S0143-4160(03)00024-1

In order to accommodate so many functions, the mechanisms responsible for generating calcium signals are very diverse. The cell has access to two sources of calcium ions: an infinite supply of external calcium and a more finite internal store sequestered in the endoplasmic reticulum (ER) [13]. Maintenance of a sufficient level of calcium within the ER ($[Ca^{2+}]_{ER}$) is critical for normal cell function. Several studies, including our own, have shown that $[Ca^{2+}]_{ER}$ exerts a profound control over cell growth and progression through the cell cycle [14]. Depletion of the ER Ca^{2+} stores induces growth arrest [8] and may trigger apoptosis [15,16]. On the other hand, calcium release from intracellular stores can produce an influx of extracellular calcium through store-operated Ca^{2+} channels in the plasma membrane, a process named capacitative calcium entry (CCE) [17]. CCE is a major pathway involved in refilling ER Ca^{2+} stores and may play a role in the control of cell cycle progression and apoptosis [16,18].

The importance of calcium homeostasis for malignant cells has been demonstrated by studies showing that antagonists of the phosphoinositide pathway [19] or calcium influx [20] arrest the growth of a variety of tumor cells in culture. Nevertheless, the involvement of calcium in the growth-inhibitory effect of ATP is unclear and no significant links have been established between calcium pools, extracellular calcium, and the ability of cells to progress through the cell cycle under ATP control. The aim of this work was to identify which calcium homeostasis mechanisms altered by extracellular ATP interfere with the proliferation of androgen-insensitive human prostate cancer DU-145 cells. The data presented here show that DU-145 cells predominantly express type 3 inositol 1,4,5-trisphosphate receptors (IP_3Rs) and confirm that the application of extracellular ATP on these cells leads to activation of phosphatidylinositol (PtdIns) turnover and increases in cytosolic calcium concentrations due to calcium release from the endoplasmic reticulum (ER) and the consecutive opening of plasma membrane calcium channels.

Our results illustrate a new mechanism by which ATP inhibits prostate cancer cell growth, correlated to a decrease in intracellular Ca^{2+}-pool content but not with a calcium influx or eventual changes in cytosolic Ca^{2+} concentration $[Ca^{2+}]_i$. These results suggest that intracellular Ca^{2+} store content may play a pivotal role in the control of prostate cancer cell growth by extracellular ATP.

2. Materials and methods

2.1. Cell culture

The human prostatic carcinoma cell line DU-145 was obtained from the American Type Culture Collection (Rockville, MD, USA). Cells were grown in RPMI 1640 with 5% fetal bovine serum (FBS, Deutcher, Brumath, France) at 37 °C in a humidified atmosphere containing 5% CO_2. The media was supplemented with 300 μg/ml L-glutamine, 100 U/ml penicillin and 100 μg/ml streptomycin. Tissue culture media and supplements were obtained from Life Technologies (Life Technologies, Cergy Pontoise, France). Cells were seeded in 75 cm^2 flasks and the growth medium was renewed every other day.

Prior to fluorescence measurements, the cells were removed from the culture flasks with 0.05% trypsin (Life Technologies) and cultured on glass coverslips in the same culture medium. Cells were then used 2–5 days after trypsinization.

2.2. Intracellular calcium imaging

Before each imaging experiment, the culture medium was replaced by a Hank's Balanced Salt Solution (HBSS) containing (in mM): NaCl, 142; KCl, 5.6; $MgCl_2$, 1; $CaCl_2$, 2; Na_2HPO_4, 0.34; KH_2PO_4, 0.44; HEPES, 10; glucose, 5.6; and buffered to pH 7.4 with NaOH. Cells were loaded with fura-2 by exposure to 2 μM fura-2 acetoxymethyl ester (fura-2/AM) in HBSS for 45 min at 37 °C. After incubation, cells were washed three times in the same dye-free solution. Glass coverslips bearing loaded cells were placed in a perfusion chamber on an Olympus IX70 microscope equipped for fluorescence.

Fura-2 fluorescence was alternately excited at 340 and 380 nm using a polychrome II monochromator (TILL Photonics, Germany) and the emitted fluorescence was measured at 510 nm (long-pass filter) using a CCD camera MicroMax 5 MHz (Princeton Instruments, Evry, France). Fluorescence signals were recorded and analyzed using Metafluor software (Universal Imaging). $[Ca^{2+}]_i$ was calculated on-line from the fluorescence ratio (F_{340}/F_{380}) according to the formula derived from Grynkiewicz et al. [21]. All recordings were carried out at 33 °C. Cells were continuously perfused with the HBSS solution (1 ml/min) and chemicals were added via the chamber perfusion system.

2.3. Microinjection

Cells were microinjected using microelectrodes (of about 50 MΩ resistance) filled with either 100 μM fura-2 or fura-2 plus heparin diluted in a saline solution containing (in mM): KCl, 140; $MgCl_2$, 1; HEPES, 5. After impaling the cell, a slight positive pressure (0.1 ml of air) was applied to the microelectrode to eject its content. During microinjection, the cell slightly swelled. The microelectrode was then immediately removed from the cell. Microinjection was controlled under a fluorescent microscope (magnification = 400×). Fura-2 fluorescence was excited at 340 nm and the diffusion of the dye into the cell from injection point was considered as indicative of microinjection success. The quality of the microinjection was assessed by fura-2 imaging performed after a period of rest of 15 min following microinjection. Injected cells were qualified for further experiment if their basal intracellular Ca^{2+} concentration was less than 150 nM (about 50% of the cells).

2.4. Western-blot analysis

DU-145 and control microsomal preparations from RBL-2H3 mucosal mast cells were performed according to earlier published procedures [22]. Microsomes were boiled for 2 min in sample buffer, analyzed on 3–12% Laemmli-type linear gradient gels, transferred to Immobilon-P and probed with isoform-specific antibodies against IP_3R1 (Rbt03), IP_3R2 (Rbt02 and Rbt226) or IP_3R3 (MMAtype3, I31220, Transduction Laboratories, KY, USA, 1/1000) [23]. To analyze simultaneously the different IP_3R isoforms, we used Rbt475, a new developed antibody directed against amino acids 127–141 (KSNKYLTVNKRLPAL) of human IP_3R1. Its epitope is completely conserved between the three mammalian IP_3R isoforms and it recognizes the various IP_3R isoforms with equal affinity [24]. To allow a precise quantification of the immuno-reactive bands, Rbt475 was affinity purified against the peptide. Quantification of the immuno-reactive bands was performed after incubation with secondary antibodies coupled to alkaline phosphatase, detection using Vistra^{TM} ECF (Amersham Pharmacia Biotech, UK) and fluorimaging as described before [22]. After quantification, the relative levels of the various IP_3R isoforms were assessed either by comparison [25] with the levels observed in RBL-2H3 microsomes [26], or directly by comparison of the signals obtained with the affinity-purified Rbt475 antibody for the different molecular weight bands.

2.5. Measurement of in vitro cell growth

Cells were seeded at an initial density of 1×10^3 cells/well in 96-well plates (Poly Labo, Strasbourg, France). After 48 h incubation, cells were cultured in treatment media, as described in Section 3 (day 0). From day 0, the treatment medium was then changed every day for each condition. Cells were harvested on day 4 and cell number was determined by a colorimetric method (CellTiter 96 Aqueous Non-Radioactive Cell Proliferation Assay).

2.6. Direct quantification of $[Ca^{2+}]_{ER}$

DU-145 cells were loaded with 2 μM of the AM-ester derivative of Mag-fura-2 (Mag-fura-2/AM) for 45 min at 37 °C. This compartmentalized fluorescent dye has been successfully used to monitor changes in free Ca^{2+} within the endoplasmic reticulum lumen [27]. After incubation with Mag-fura-2/AM, cells were briefly rinsed in a high K^+ solution (in mM): KCl, 125; NaCl, 25; HEPES, 10; $MgCl_2$, 0.1; pH 7.2. They were then exposed to 5 μg/ml digitonin diluted in the high K^+ solution supplemented with 0.2 mM MgATP for 2 min, with free $[Ca^{2+}]$ clamped to 170 nM using $CaCl_2$/EGTA buffers (0.5 mM $CaCl_2$, 1 mM EGTA; WinMaxc 1.7 software). Following digitonin permeabilization, Mag-fura-2 was localized in the subcellular compartments. Mag-fura-2 fluorescence was measured by ratio imaging, using a Princeton imaging system as described earlier.

2.7. Reagents and chemicals

All chemicals were purchased from Sigma (l'Isle d'Abeau, France) except fura-2/AM (France Biochem, Meudon, France).

2.8. Data analysis and statistics

Results were expressed as mean ± S.E.M. Plots were produced using Origin 5.0 (Microcal Software Inc., Northampton, MA, USA). Statistical analysis was performed using ANOVA tests followed by Tukey–Kramer post-tests.

3. Results

3.1. Basal calcium levels

The cytosolic calcium concentration ($[Ca^{2+}]_i$) in fura-2 loaded DU-145 cells averaged 95 ± 2 nM (n = 448) in the presence of 2 mM external calcium. When calcium was removed from the external saline, $[Ca^{2+}]_i$ slightly decreased to 81 ± 1 nM (n = 446).

3.2. ATP induced an increase in $[Ca^{2+}]_i$ in DU-145 cells

A typical effect of extracellular ATP on $[Ca^{2+}]_i$ in DU-145 cells is illustrated in Fig. 1A. In the presence of external calcium, ATP triggered a calcium increase ($\Delta[Ca^{2+}]$ = 593 ± 36 nM, n = 22) in most cells, which declined after about 15 min to a new basal $[Ca^{2+}]_i$ level. In the absence of extracellular free calcium, the addition of 100 μM ATP induced a single rapid transient increase in $[Ca^{2+}]_i$ ($\Delta[Ca^{2+}]$ = 528 ± 54 nM, n = 42 (Fig. 1B)). Under the same conditions, the Ca^{2+} release evoked by ATP (100 μM) was followed by a series of $[Ca^{2+}]_i$ oscillations in 7% of cells (Fig. 1C). This shows that, in the absence of extracellular calcium, ATP was still able to produce a calcium increase, originating from internal stores.

3.3. Activation of purinergic receptors triggers both Ca^{2+} release from intracellular stores and store-operated entry

A standard experimental protocol [28] was used to study the ATP-induced calcium entry in DU-145 cells. The cells were first bathed with a Ca^{2+}-free buffer and after a period of observation to ensure that the baseline $[Ca^{2+}]_i$ was stable, the cells were then exposed to thapsigargin (TG), a specific irreversible inhibitor of ATP-dependent Ca^{2+} pumps (SERCA) localized in the endoplasmic reticulum (ER) [29]. As a consequence of SERCA pump inhibition, Ca^{2+} was released from ER Ca^{2+} stores into the cytosol via ER Ca^{2+} leak channels, leading to a transient increase in $[Ca^{2+}]_i$. This ER Ca^{2+} store depletion then activated a CCE pathway, leading to a sustained increase in $[Ca^{2+}]_i$ when calcium was readmitted into the external medium. Fig. 2 shows that expo-

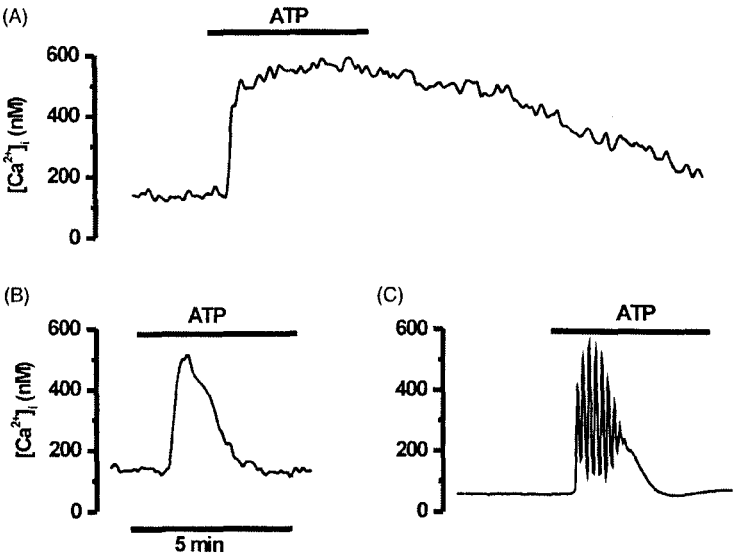

Fig. 1. ATP induces a $[Ca^{2+}]_i$ increase in human prostate cancer DU-145 cells. (A) A typical biphasic $[Ca^{2+}]_i$ transient induced by an extracellular application of ATP (100 μM) was recorded in fura-2-loaded cells in a medium containing 2 mM $CaCl_2$. In a Ca^{2+}-free medium, ATP could still induce either a single Ca^{2+} peak (B) or a series of Ca^{2+} oscillations (C).

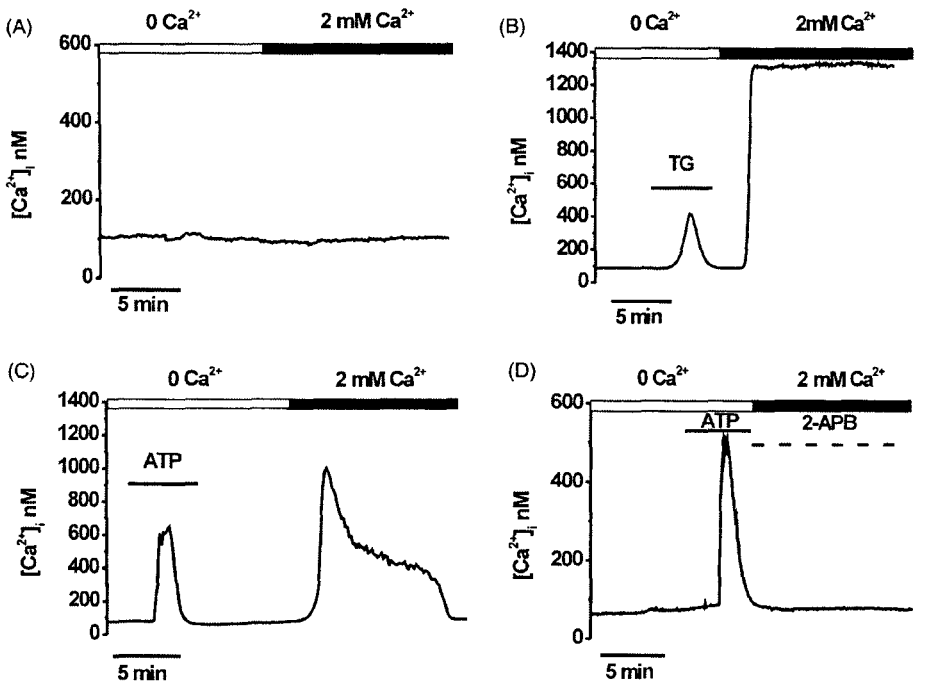

Fig. 2. ATP causes a capacitative calcium entry subsequently to the mobilization of Ca^{2+} from internal stores. (A) Changing the external calcium concentration from 0 to 2 mM does not induce any $[Ca^{2+}]_i$ increase. (B) Thapsigargin (0.1 μM) stimulates a Ca^{2+} release in Ca^{2+}-free HBSS with a consecutive Ca^{2+} entry when Ca^{2+} is readmitted. (C) An application of 100 μM ATP causes a mobilization of Ca^{2+} from internal stores in Ca^{2+}-free HBSS medium, followed by a capacitative Ca^{2+} entry when Ca^{2+} is readmitted. (D) In a medium containing 100 μM 2-APB, the capacitative Ca^{2+} entry induced by the application of ATP (100 μM) is abolished.

sure of cells to 0.1 μM TG in a calcium-free buffer initially produced a transient calcium peak ($\Delta[Ca^{2+}] = 233 \pm 15$ nM, $n = 192$). When calcium was readmitted to the bathing solution, a calcium plateau ($\Delta[Ca^{2+}] = 1045 \pm 35$ nM, $n = 192$) was observed. In the absence of TG, changing the extracellular calcium concentration did not affect the $[Ca^{2+}]_i$ (Fig. 2A). This demonstrates the existence of a CCE mechanism in DU-145 cells.

In order to assess whether Ca^{2+}-store depletion induced by ATP caused CCE, the same protocol was used. In this

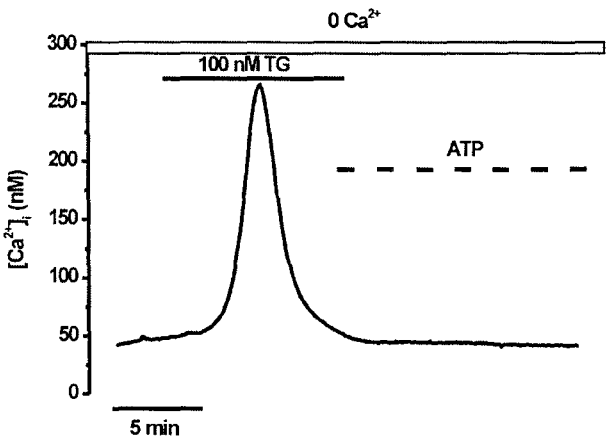

Fig. 3. Involvement of the endoplasmic reticulum Ca^{2+} store in the ATP-induced Ca^{2+} release. In Ca^{2+}-free HBSS, the Ca^{2+} response of fura-2-loaded cells to ATP (100 μM) is abolished when the endoplasmic reticulum Ca^{2+} content is previously depleted by thapsigargin (0.1 μM).

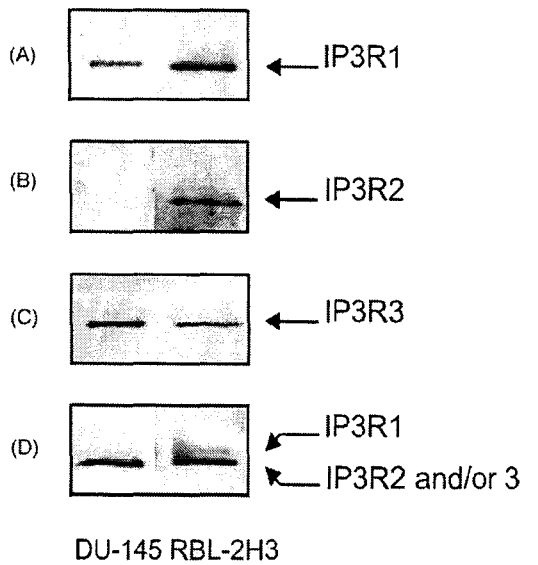

Fig. 4. IP_3R isoforms analysis. Antibody detection of IP_3R1 (A), IP_3R2 (B), IP_3R3 (C) and simultaneous detection of IP_3R1 and IP_3R2/IP_3R3 (D) in DU-145 (left lanes) and RBL-2H3 cells (right lanes). Antibodies used were Rbt031/2000 (A), Rbt2261/250 (B), MMAtype31/1000 (C), and Rbt475 (1/2000). Each lane was loaded with 20 μg (DU-145) or 50 μg proteins (RBL-2H3). Only the relevant parts of the gels are shown. Arrows indicate the position of the various IP_3R isoforms. Typical for four to seven experiments.

case, exposing cells to 100 μM ATP first led to a transient calcium peak followed by a reversible calcium rise with a mean $[Ca^{2+}]_i$ increment of 1230±28 nM, $n = 127$ (Fig. 2C) when calcium was added to the external buffer.

We also studied the effect of diphenylboric acid 2-aminoethyl ester (2-APB), commonly used as CCE inhibitor, on calcium entry. Fig. 2D shows that, in the presence of 100 μM 2-APB ($n = 65$), the Ca^{2+} release induced by ATP was not followed by CCE. In DU-145 cells, CCE was not inhibited by econazole, which inhibits CCE in other cell models (data not shown).

3.4. Nature of the second messengers involved in ATP-induced calcium signaling

We next examined whether the ATP-induced calcium increase was mediated by a Ca^{2+} release from the ER. To investigate the involvement of ER stores in the ATP-induced calcium peak, we exposed DU-145 cells to TG in a Ca^{2+}-free buffer, which induces the depletion of calcium stores contained in the ER [30]. Fig. 3 shows that applying TG to DU-145 cells in the absence of external calcium caused a transient calcium increase. However, when ATP was applied to the cells few minutes later, no ATP-induced calcium signal was evoked ($n = 25$). The ability of TG to inhibit the ATP-induced $[Ca^{2+}]_i$ response indicates that ER Ca^{2+} stores are effectively involved in the effect of ATP.

We have shown above that the initial rapid rise in $[Ca^{2+}]_i$ is due to Ca^{2+} release from the ER, while the sustained increase in $[Ca^{2+}]_i$ requires a Ca^{2+} influx. It has also been shown that DU-145 express P2Y receptors, which are usually coupled to phospholipase C (PLC) [5]. Therefore, we suggested that extracellular ATP activates PLC, thus leading to the generation of IP_3. To test for this possibility, we examined IP_3Rs expression.

The use of isoform-specific antibodies indicated that microsomal preparations of DU-145 cells contained both IP_3R1 and IP_3R3 (Fig. 4A and C). Despite the use of two different antibodies against IP_3R2, no specific signal was resolved above background, indicating that IP_3R2, if any, would in any case only be present at very low density (Fig. 4B). To quantitatively analyze the amount of each IP_3R isoform, values were compared to those measured in microsomes of RBL-2H3 cells, which contain the three IP_3R isoforms at a ratio of 10:70:20% [26]. In comparison with RBL-2H3 cells, DU-145 cells contained only 0.8 ± 0.1 ($n = 7$) times the amount of IP_3R1 but 4.8±0.4 ($n = 4$) the amount of IP_3R3. These results indicate that the IP_3R1:IP_3R3 ratio in DU-145 cells is 8:92%. This value was verified independently by using the Rbt475 antibody, that recognizes all three IP_3R isoforms with equal affinity (Fig. 4D). Direct comparison of the high molecular weight band, corresponding to IP_3R1, and the low molecular weight band, corresponding exclusively to IP_3R3, showed a nearly exclusive expression of IP_3R3. After quantification of both bands, it appeared that the strength of the IP_3R1 signal was only 0.12 ± 0.01 of the value observed for IP_3R3 ($n = 5$) indicating an IP_3R1:IP_3R3 ratio of 11:89%. In conclusion, DU-145 cells contain about 10% IP_3R1 and 90% IP_3R3.

We next inhibited the PLC pathway by pre-incubating the cells for 1 h with U73122 (20 μM), a PLC inhibitor, before applying ATP. U73122 abolished both the calcium mobilization and calcium influx ($n = 30$, Fig. 5A) whereas

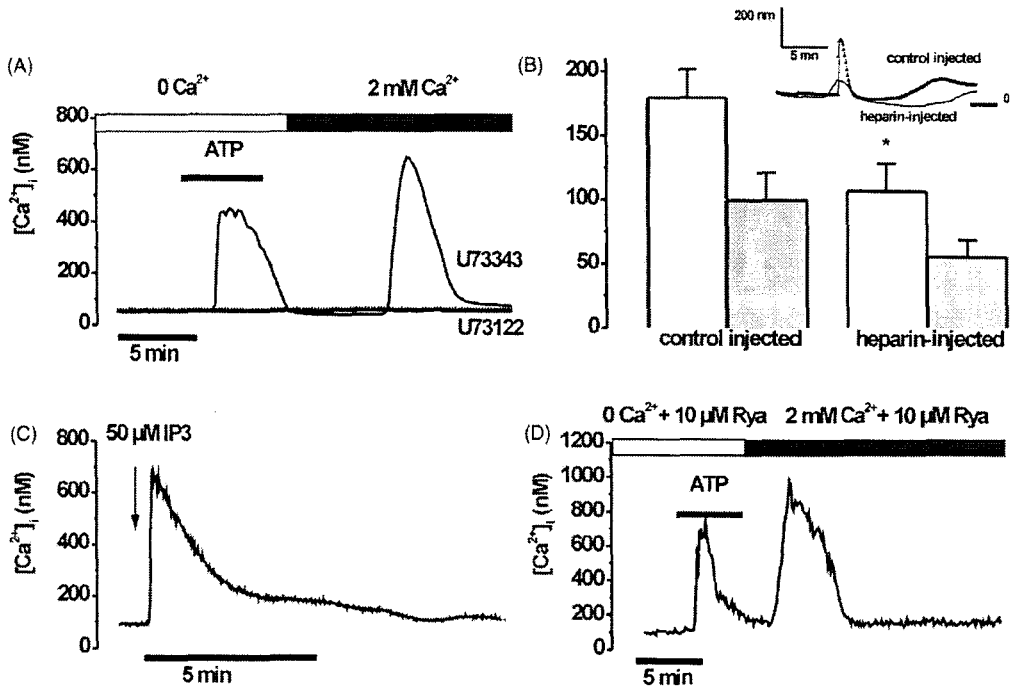

Fig. 5. Involvement of the PLC pathway in ATP-induced intracellular calcium increase. (A) The effect of extracellular ATP (100 μM) is abolished in presence of the PLC inhibitor U73122 (20 μM) and is maintained in presence of the inactive analogue U73343 (20 μM). (B) The ATP-induced Ca^{2+} response is reduced in cells previously microinjected with heparin (1 mg/ml) (□, Ca^{2+} peak (ATP, 0 Ca^{2+}); ▨, Ca^{2+} plateau (2 mM Ca^{2+})), inset: typical Ca^{2+} responses to ATP in both control and heparin-injected cells. (C) Cytosolic microinjection of IP_3 (50 μM) in fura-2-loaded cells produces an increase in $[Ca^{2+}]_i$. (D) DU-145 cell response to ATP (100 μM) is not modified when cells are incubated with ryanodine (10 μM) during the time of the experiment.

the same concentration of the inactive analogue, U73343, did not alter the ATP-induced calcium signals ($n = 30$).

The involvement of IP_3Rs in ATP-induced Ca^{2+} signaling was confirmed using heparin which inhibits the IP_3Rs of the ER. Heparin was microinjected into DU-145 cells to reach its target receptors before applying ATP. In order to localize heparin-injected cells, 100 μM fura-2 free acid was co-injected. Control cells were only injected with 100 μM fura-2 free acid. As shown in Fig. 5B, ATP was still able to induce both calcium mobilization and calcium influx, though with a lesser magnitude (calcium peak: $\Delta[Ca^{2+}] = 179 \pm 22$ nM, calcium plateau: $\Delta[Ca^{2+}] = 99 \pm 21$ nM, $n = 34$) than in non-injected fura-2-loaded cells (see Fig. 2C for comparison). In injected cells ($n = 29$), heparin (1 mg/ml) significantly reduced the amplitude of both calcium peak ($\Delta[Ca^{2+}] = 106 \pm 21$ nM) and calcium plateau ($\Delta[Ca^{2+}] = 55 \pm 13$ nM, Fig. 5B), showing that IP_3Rs are involved in ATP signaling. We also studied the functionality of IP_3Rs in DU-145 cells. As demonstrated in Fig. 5C, 50 μM of IP_3 introduced into the cytosol via a patch-pipette induced a transient calcium mobilization (506 ± 108 nM, $n = 6$) in the absence of external calcium, confirming that IP_3Rs are functional in DU-145 cells.

We also investigated the potential role of ryanodine receptors (RyRs) in ATP-induced Ca^{2+} release from the ER. For this, ryanodine, which at a concentration higher than 10 μM inhibits RyRs [31] was used. We show (Fig. 5D) that 20 μM ryanodine had no effect on either Ca^{2+} mobilization from intracellular stores or Ca^{2+} influx. The mean increase in $[Ca^{2+}]_i$ during calcium mobilization was $\Delta[Ca^{2+}] = 569 \pm 67$ nM, $n = 15$, compared to $\Delta[Ca^{2+}] = 528 \pm 54$ nM, $n = 42$ in control cells (Fig. 2C).

Activation of the PLC pathway results in the generation of IP_3, which releases Ca^{2+} from internal stores, and the production of diacylglycerol, the natural activator of protein kinase C (PKC). The possible involvement of PKC in ATP-induced CCE in DU-145 cells was therefore examined. Two experimental approaches were used to determine whether PKC was involved in the enhancement of $[Ca^{2+}]_i$ by extracellular ATP. First, cells were exposed to PMA (1 μM), a direct activator of PKC. Second, cells were pre-incubated with GÖ6976 (50 nM) or sphingosine (10 μM), two PKC inhibitors. PMA had no effect on calcium entry in the absence of ATP (see inset Fig. 6A). In the presence of PMA, calcium entry induced by extracellular application of ATP was 36% higher than in control cells. Inhibition of PKC by GÖ6976 and sphingosine ($n = 116$) decreased the calcium influx as measured during the Ca^{2+} plateau phase by 74 and 41%, respectively, compared to control (Fig. 6B). As shown in Fig. 6B, none of these pharmacological agents had any significant effect on ATP-induced Ca^{2+} release from the ER, induced by extracellular ATP, showing that they did not alter

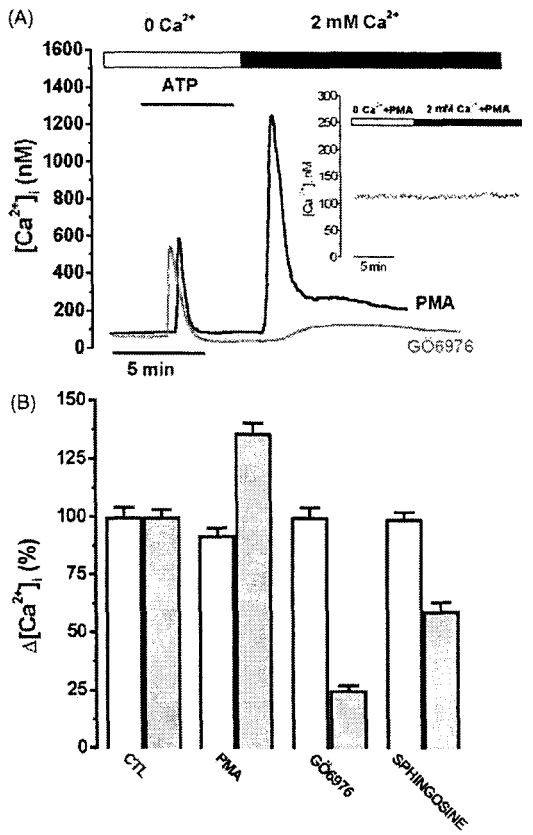

Fig. 6. Protein kinase C is involved in the capacitative calcium entry induced by extracellular ATP. Representation of typical calcium responses to ATP stimulation (A) and average values of $\Delta[Ca^{2+}]_i$ (B) (□ , Ca^{2+} peak (ATP, 0 Ca^{2+}); ▨ , Ca^{2+} plateau (2 mM Ca^{2+})) of fura-2-loaded DU-145 cells in the presence of the PKC activator PMA (1 μM) or of the PKC inhibitors GÖ6976 (50 nM) or sphingosine (10 μM). The inset on (A) represents the action of PMA on $[Ca^{2+}]_i$ in absence of TG or ATP.

the initial transduction events, such as ATP binding to its receptor or G-protein coupling. The fact that PMA increased the calcium influx while GÖ6976 and sphingosine decreased it suggests that PKC is involved in regulating ATP-induced CCE in DU-145 cells.

3.5. Long-term ATP treatment decreases the ER intraluminal Ca^{2+} concentration $[Ca^{2+}]_{ER}$

We further studied the long-term effects of ATP on $[Ca^{2+}]_i$ and $[Ca^{2+}]_{ER}$. For this, cells were cultured for 2 days in the presence of 100 μM extracellular ATP. After 2 days of culture, ER Ca^{2+} content was first estimated in fura-2 loaded cells by measuring the difference between the basal $[Ca^{2+}]_i$ and the Ca^{2+} peak induced by 0.1 μM TG in a Ca^{2+}-free medium, since TG only induces release from the ER under these conditions. The $[Ca^{2+}]_i$ itself was 123 ± 3.3 nM, n = 73. The amplitude of the TG-induced Ca^{2+} release from the endoplasmic reticulum was reduced by 68% in DU-145 cells treated with 100 μM ATP (268 ± 18 nM, n = 283 versus 86 ± 4 nM, n = 290). This observation was confirmed using the fluorescent Ca^{2+} indicator Mag-fura-2/AM. In this condition, luminal $[Ca^{2+}]_{ER}$ was significantly lower ($[Ca^{2+}]$ = 249 ± 6 μM, n = 28) in ATP-treated DU-145 cells than in control cells ($[Ca^{2+}]$ = 770 ± 30 μM, n = 25) (Fig. 7B).

3.6. Role of the sustained increase in $[Ca^{2+}]_i$ in the growth arrest of DU-145 cells by ATP

To study the relationship between sustained elevated $[Ca^{2+}]_i$ and ATP-induced growth arrest in DU-145 cells, the cells were cultured in RPMI-1640 media containing varying Ca^{2+} concentrations for 4 days.

Fig. 7 shows that extracellular calcium did not modify the ATP-dependent growth inhibition of DU-145 cells since ATP provoked 83% growth inhibition in 0 mM $CaCl_2$ (Fig. 7A) and 75% in 2 mM $CaCl_2$ (Fig. 7B) compared with control (67% in 0.4 mM $CaCl_2$, Fig. 7C). This growth-rate inhibition cannot be explained by an increase in apoptosis, since no stimulation of apoptosis was observed in our experiments as determined by Hoechst staining (data not shown). In addition, the decrease in CCE after treatment with GÖ6976 did not influence the growth inhibitory effect of ATP on DU-145 cells (inhibition of 67%, Fig. 7D). It is important, however, to note that the Ca^{2+}-free medium by itself decreased the growth of DU-145 cell by 40%. This is not surprising since a similar effect was previously observed in a large variety of cell models [32,33]. We checked if the Ca^{2+}-free medium could modify the $[Ca^{2+}]_i$. Our results show that after 4 days of treatment in a Ca^{2+}-free medium, the $[Ca^{2+}]_i$ was not significantly changed (data not shown). Altogether, these results suggest that a variation in $[Ca^{2+}]_i$ seems not to be a major factor involved in the effect of ATP on cellular proliferation.

3.7. A decrease in DU-145 cell growth rate is correlated with a decrease in Ca^{2+} pool content

As maintenance of luminal Ca^{2+} within the ER has been demonstrated to be essential for cell growth in some cell lines [8,34] including prostate cancer cells [14] and since we observed that long treatments with ATP reduced the intracellular calcium store content, we investigated whether the growth inhibitory effect of ATP could be related to a decrease in the ER Ca^{2+}-pool content.

We first determined a concentration of TG which did not induce apoptosis (verified by Hoechst staining) but sufficient to deplete the ER Ca^{2+}-pool content. The depletion of ER Ca^{2+}-pool content was confirmed using the fluorescent Ca^{2+} indicator Mag-fura-2. We observed (Fig. 8A) that culture with 1 nM TG for 2 days reduced the ER Ca^{2+}-pool content to 309 ± 16 μM (n = 30), compared to control ($[Ca^{2+}]_{ER}$ = 728 ± 28 μM, n = 24), and decreased the growth rate by 6% without inducing apoptosis. We then treated the cultures with 1 nM TG 15 min before ATP application to deplete

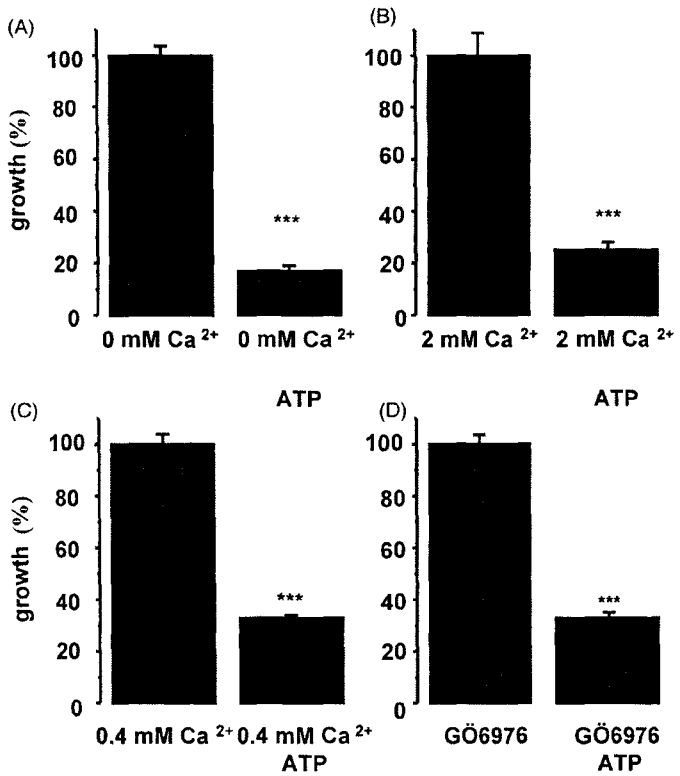

Fig. 7. Assessment of the role of the $[Ca^{2+}]_i$ increase in the ATP-induced growth arrest. Percentage of growth is estimated in culture media containing 0 mM Ca^{2+} (A), 2 mM Ca^{2+} (B), 0.4 mM Ca^{2+} (C), or the PKC inhibitor GÖ6976 (50 nM) (D) during 4 days of culture, with or without extracellular ATP (100 μM).

ER Ca^{2+}-pool content. Cells were cultured for 2 days in four conditions: control, 1 nM TG, 100 μM ATP, 1 nM TG plus100 μM ATP. The media was changed every day. Under these conditions, whatever the concentration of calcium was in the culture media (0.4 mM $CaCl_2$ and Ca^{2+}-deprived), no significant effect of ATP on the growth rate was detectable after TG pretreatment (Fig. 8B).

4. Discussion

In this study, we have identified and characterized the intracellular Ca^{2+} homeostasis mechanisms involved in ATP-induced inhibition of androgen-independent human prostate carcinoma cell growth. We have demonstrated that extracellular ATP exerts an inhibitory action on the growth of DU-145 cells. We have also shown that ATP-induced cell growth inhibition is partly due to a reduction in ER calcium-store content.

The extracellular effects of nucleotides like ATP are mediated by P2 receptors, subdivided into ligand-gated P2X and G-protein-coupled P2Y families [35]. The ATP-induced $[Ca^{2+}]_i$ response is mainly mediated by P2Y purinergic receptors via the formation of IP_3 and the subsequent release of Ca^{2+} from intracellular stores [6]. The $[Ca^{2+}]_i$ response of DU-145 cells induced by extracellular ATP was first evoked by Fang et al. [5]. These authors showed that P2 purinergic receptor agonists, including ATP, induced a rapid and transient increase in cytoplasmic free Ca^{2+}.

It has also been demonstrated in a variety of other non-excitable cells like parotid acinar cells [36], normal human airway epithelial cells [37], and human breast tumor cells MCF7 [38], that ATP induces a biphasic increase in $[Ca^{2+}]_i$. This type of response is due to the depletion of internal Ca^{2+} stores, which activates CCE, leading to an influx of Ca^{2+} from the extracellular space [18]. The initial rise in $[Ca^{2+}]_i$ occurs as a direct effect of IP_3 binding to IP_3Rs in the ER. In our study, we show the presence of IP_3R3 in DU-145 cells for the first time. The fact that IP_3R3 is expressed at 90% compared to the 10% of IP_3R1 suggests that the type 3 receptor plays a key role in Ca^{2+} signaling in these cells. As shown by many authors, type 1 IP_3R might be capable of generating oscillatory Ca^{2+} release [39,40] whereas the type 3 IP_3R is implicated in Ca^{2+}-store release followed by CCE and may even operate as a CCE channel in some cell types [41]. Here, the type 1/type 3 ratio may explain why we infrequently observe an oscillatory calcium response to ATP. Since the use of inhibitors of the ryanodine receptors did not affect the calcium release from the ER, while it was abolished when PLC was inhibited by U73122, we suggest

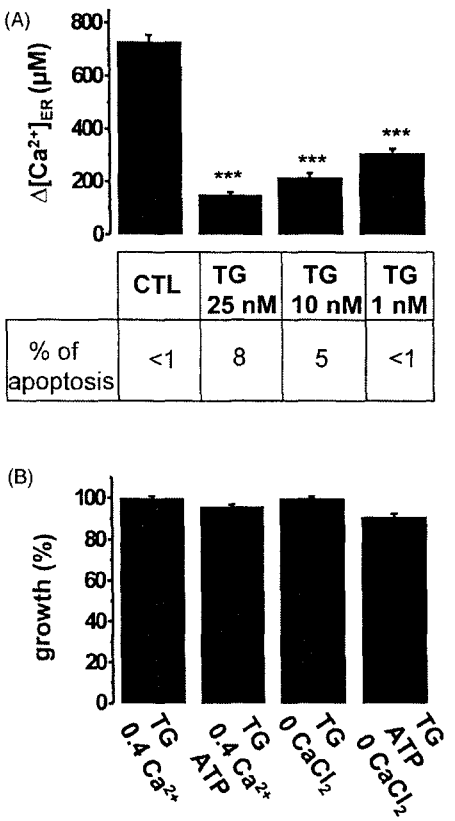

Fig. 8. Calcium-store content is associated with ATP-induced growth arrest. (A) Cells are treated for 2 days with different concentrations of thapsigargin. Ca^{2+}-pool contents are estimated with the Mag-fura-2 probe and the percentage of apoptotic cells is assessed by Hoechst staining. (B) Determination of ATP action on the growth of DU-145 cells after the Ca^{2+} stores depletion induced by a non-apoptotic concentration of thapsigargin as determined (1 nM) after 2 days of culture.

that the PLC/IP3 pathway is certainly the main intracellular transduction pathway involved in ATP signaling in DU-145 cells.

PLC stimulation results in the production of diacylglycerol, a natural activator of PKC. ATP-induced $[Ca^{2+}]_i$ increase was attenuated by inhibiting PKC with sphingosine or GÖ6976. These results suggest that the ATP-induced $[Ca^{2+}]_i$ increase (and especially the CCE mechanism) is a PKC-regulated event. The relation between PKC and CCE seems to be dependent on the cell model since in rabbit airway ciliated cells, the ATP-induced CCE was not altered when PKC was inhibited by chelerythrine [42]. These opposite modulations of CCE are most probably related to the fact that regulatory and pharmacological properties of the endogenous channels responsible for CCE depend on the cell type [43,44]. Indeed, it is now clearly demonstrated that the expression of the transient receptor potential (TRP) proteins, the most likely candidates for store-operated calcium channels, varies quantitatively and qualitatively in different cell types. PKC activation could have multiple actions on the calcium storage capacity, and on the calcium signaling function by its participation in the modulation of CCE. On the one hand, depending on the cell type and on the exact conditions, PKC activation can potentiate [45] or inhibit CCE [46]. On the other hand, as in both NIH3T3 and HEK293 cells, PKC reduces intracellular Ca^{2+}-storage capacity and can protect the ER against the detrimental effects of high $[Ca^{2+}]_i$ on ER structure [45,46]. These actions indicate a complex and potentially important role for the PKC system in calcium homeostasis.

The last aspect of this paper was to study the source of Ca^{2+} involved in growth arrest induced by extracellular ATP. Indeed, extracellular ATP has been reported to stimulate [47] or to inhibit [48] cell growth, depending on the cell type and the composition of the culture medium. It is now known that ATP inhibits the growth of androgen-independent prostate cancer cells such as DU-145 and PC3 [5,6]. Furthermore, it is well-documented that Ca^{2+} controls numerous cell functions, including protein synthesis and cell proliferation [49]. Alterations in cytoplasmic free Ca^{2+} are important for cell proliferation and some groups reported that a sustained increase in cytoplasmic free Ca^{2+} was necessary for growth arrest and cell death [12]. Nevertheless, no relation has been established between the calcium response and cell growth arrest induced by ATP. Therefore, our aim was to demonstrate the role of calcium in the modulation of proliferation by extracellular ATP. Increases in $[Ca^{2+}]_i$ have been suggested, but not demonstrated, to play a role in extracellular ATP-induced growth inhibition [5,6,50]. Our results provide the first direct demonstration that the $[Ca^{2+}]_i$ increase is not implicated in the physiological role of ATP. Indeed, we show that whatever the extracellular concentrations of Ca^{2+} are, no modulation in ATP-induced growth arrest was observed. Moreover, cell growth arrest was not due to reduced cytosolic Ca^{2+} concentration since no significant variation in basal Ca^{2+} levels was observed after long-term treatment with ATP. Therefore, our findings suggest that a decrease in Ca^{2+} pool content participates in the ATP-induced growth arrest in the DU-145 cells. This hypothesis was confirmed by the experiment where a decrease in the Ca^{2+} pool content using 1 nM TG prevented the growth inhibitory effect of ATP. Here, we observed that although 1 nM TG induced a fall in Ca^{2+} pool content similar to that induced by ATP, no significant inhibitory effect on cell growth was observed.

ATP and TG are two agents that cause depletion of ER calcium-store content by clearly distinct mechanisms: IP_3R activation and inhibition of SERCA pumps that accumulate Ca^{2+} in the ER, respectively. Moreover, it has been suggested that IP_3R and SERCA pumps are differently localized on the ER [51]. The nature and location of the channels are supposed to be implicated in the spatio-temporal profile of the Ca^{2+} release [52,53]. As suggested by these studies, the spatio-temporal profile could be determined by the flux of calcium ions across the ER as well as the diffusion mobility of Ca^{2+} and Ca^{2+} buffers in the cell. This could explain how agents which seem to have identical action on Ca^{2+} signal,

have distinct biological effects. Indeed, Huang and Putney [54] show that on rat basophilic leukemia cells, the kinetics of calcium release from the ER differs between IP_3 agonist and TG, suggesting that a specific subfraction of the ER was more slowly depleted by IP_3 agonists than the majority of the ER by TG. Other authors noticed that signaling systems with distinct biological effects and operating within different temporal and spatial domains, can depend on Ca^{2+}-free concentration within the lumen of the ER [55]. Consequently, we conclude that a decrease in Ca^{2+} pool content by ATP is necessary but not sufficient to induce growth arrest. This suggests that the acceleration of Ca^{2+} recycling process by ATP mediated IP_3 function may be responsible for the inhibitory effect of ATP on prostate cancer cell growth. TG, on its own, only induces an irreversible emptying of ER Ca^{2+} store. In addition, ATP may involve other signaling mechanisms which are independent on calcium and interfere with cell growth. These Ca^{2+}-independent transduction pathways are probably different or not activated by TG.

In summary, our work establishes a link between PtdIns turnover, Ca^{2+} mobilization and growth inhibition. For the first time, we have characterized some of the Ca^{2+}-regulated mechanisms involved in ATP-induced growth arrest in androgen-insensitive human prostate cancer DU-145 cells. We suggest that $[Ca^{2+}]_{ER}$ exerts a profound control over cell growth and progression through the cell cycle and that a decrease in the level of the ER Ca^{2+} stores plays a central role in the growth control of androgen-independent human prostate cancer cells.

Acknowledgements

The excellent technical assistance of Ms. I. Willems is highly appreciated. This work was in part supported by the Institut National de la Santé et de la Recherche Médicale (INSERM), the Association pour la Rrecherche contre le Cancer (ARC), the Ligue Nationale contre le Cancer, the Association pour la Recherche sur les Tumeurs de la Prostate (ARTP) and by grant 99/08 of the Concerted Actions of the K.U. Leuven (J.B.P.).

References

[1] S.L. Parker, T. Tong, S. Balden, P.A. Wingo, Cancer statistics, CA Cancer J. Clin. 47 (1997) 5–27.
[2] R. Horton, Benign prostatic hyperplasia: new insights, J. Clin. Endocrinol. Metab. 74 (1994) 504A–504C.
[3] E.D. Crawford, M.A. Eisenberger, D.C. McLead, J. Spaulding, et al., A controlled trial of leuprolide with and without flutamide in prostate carcinoma, New Engl. J. Med. 321 (1989) 419–424.
[4] I. Friedberg, I. Belzer, O. Oged-Plesz, D. Kuebler, Activation of cell growth inhibitor by ectoprotein kinase-mediated phosphorylation in transformed mouse fibroblasts, J. Biol. Chem. 270 (1995) 20560–20567.
[5] W.G. Fang, F. Pirnia, Y.J. Bang, C.E. Myers, J.B. Trepel, P2-purinergic agonists inhibit the growth of androgen-independent prostate carcinoma cells, J. Clin. Invest. 89 (1992) 191–196.
[6] R. Janssens, J.M. Boeynaems, Effects of extracellular nucleotides and nucleosides on prostate carcinoma cells, Br. J. Pharmacol. 132 (2001) 536–546.
[7] A.R. Means, Calcium calmodulin and cell cycle regulation, FEBS Lett. 347 (1994) 1–4.
[8] A.D. Short, J. Bian, T.K. Gosh, R.T. Waldron, S.L. Rybak, D.L. Gill, Intracellular Ca^{2+} pool content is linked to control of cell growth, Proc. Natl. Acad. Sci. U.S.A. 90 (1993) 4986–4990.
[9] D.M.F. Savarese, J.T. Russel, A. Fatatis, L.A. Liotta, Type IV collagen stimulates an increase in intracellular calcium: potential role in tumor cell motility, J. Biol. Chem. 267 (1992) 21928–21935.
[10] E. Kohn, R. Allessandro, J. Spoonster, R. Wersto, L. Liotta, Angiogenesis: role of calcium-mediated signal transduction, Proc. Natl. Acad. Sci. U.S.A. 92 (1995) 1307–1311.
[11] P. Nicotera, B. Zhivotovsky, S. Orrenius, Nuclear calcium transport and the role of calcium in apoptosis, Cell Calcium 16 (1994) 279–288.
[12] M.J. Berridge, Calcium signalling and cell proliferation, Bioessays 17 (1995) 491–500.
[13] M.J. Berridge, Elementary and global aspects of calcium signalling, J. Physiol. 499 (1997) 291–306.
[14] G. Legrand, S. Humez, C. Slomianny, E. Dewailly, F. Vanden Abeele, F. Wuytack, N. Prevarskaya, Evidence for sarcoendoplasmic Ca^{2+}-ATPase 2B involvement in human prostate cancer, J. Biol. Chem. 276 (2001) 47608–47614.
[15] R. Skryma, P. Mariot, X. Lebourhis, et al., Store depletion and store-operated Ca^{2+} current in human prostate cancer LNCaP cells: involvement in apoptosis, J. Physiol. 527.1 (2000) 71–83.
[16] F. Vanden Abeele, R. Skryma, Y. Shuba, et al., Bcl-2-dependent modulation of Ca^{2+} homeostasis and store-operated channels in prostate cancer cells, Cancer Cell 1 (2002) 169–179.
[17] J.W. Putney Jr., Capacitative calcium entry revisited, Cell Calcium 11 (1990) 611–624.
[18] M.J. Berridge, Capacitative calcium entry, Biochem. J. 312 (1995) 1–11.
[19] G. Powis, D. Phil, Inhibitors of phosphatidylinositol signalling as antiproliferative agents, Cancer Metast. Rev. 13 (1994) 91–105.
[20] K. Cole, E. Kohn, Calcium-mediated signal transduction: biology, chemistry, and therapy, Cancer Metast. Rev. 13 (1994) 31–44.
[21] G. Grynkiewicz, M. Poenie, R.Y. Tsien, A new generation of Ca^{2+} indicators with greatly improved fluorescence properties, J. Biol. Chem. 260 (1985) 3440–3450.
[22] S. Vanlingen, J.B. Parys, L. Missiaen, H. De Smedt, F. Wuytack, R. Casteels, Distribution of inositol 1,4,5-trisphosphate receptor isoforms, SERCA isoforms and Ca^{2+} binding proteins in RBL-2H3 rat basophilic leukemia cells, Cell Calcium 22 (1997) 475–486.
[23] S. Vanlingen, H. Sipma, P. De Smet, G. Callewaert, L. Missiaen, H. De Smedt, J.B. Parys, Ca^{2+} and calmodulin differentially modulate *myo*-inositol 1,4,5-trisphosphate (IP_3)-binding to the recombinant ligand-binding domains of the various IP_3 receptor isoforms, Biochem. J. 346 (2000) 275–280.
[24] H.T. Ma, K. Venkatachalam, J.B. Parys, D.L. Gill, Modification of store-operated channel-coupling and $InsP_3$ receptor-function by 2-aminoethoxydiphenyl borate in DT40 lymphocytes, J. Biol. Chem. 277 (2002) 6915–6922.
[25] I.I. Mountian, F. Baba-Aissa, J.C. Jonas, H. De Smedt, F. Wuytack, J.B. Parys, Expression of Ca^{2+} transport genes in platelets and endothelial cells in hypertension, Hypertension 37 (2001) 135–141.
[26] B.S. Wilson, J.R. Pfeiffer, A.J. Smith, J.M. Oliver, J.A. Oberdorf, R.J.H. Wojcikiewicz, Calcium-dependent clustering of inositol 1,4,5-triphosphate receptors, Mol. Biol. Cell 9 (1998) 1465–1478.

[27] A.M. Hofer, I. Schultz, Quantification of intraluminal free [Ca^{2+}] in the agonist-sensitive internal calcium store using compartmentalized fluorescent indicators: some considerations, Cell Calcium 20 (1996) 235–242.
[28] G.A. Sarosi, D.C. Barnhart, D.J. Turner, M.W. Mulholland, Capacitative Ca^{2+} entry in enteric glia induced by thapsigargin and extracellular ATP, Am. J. Physiol. 275 (1998) G550–G555.
[29] B.A. Premack, T.V. McDonald, P. Gardner, Activation of the Ca^{2+} current in Jurkat T cells following the depletion of Ca^{2+} stores by microsomal Ca^{2+}-ATPase inhibitors, J. Immunol. 152 (1994) 5226–5240.
[30] G. Inesi, Y. Sagara, Thapsigargin, a high affinity and global inhibitor of intracellular Ca^{2+} transport ATPases, Arch. Biochem. Biophys. 298 (1992) 313–317.
[31] P.S. McPherson, K.P. Campbell, The ryanodin receptor/Ca^{2+} release channel, J. Biol. Chem. 268 (1993) 13765–13768.
[32] J. Martinez, J.F. Santibanez, Extracellular calcium modulates proliferation of factor dependent hemopoietic cells, Cell. Biochem. Funct. 11 (1993) 101–105.
[33] P. Pinton, D. Ferrari, P. Magalhaes, K. Schultze-Osthoff, F. Di Virgilio, T. Pozzan, R. Rizzuto, Reduced loading of intracellular Ca^{2+} stores and downregulation of capacitative calcium influx in Bcl2-overexpressing cells, J. Cell Biol. 148 (2000) 857–862.
[34] R.T. Waldron, A.D. Short, J.J. Meadows, T.K. Ghosh, D.L. Gill, Endoplasmic reticulum calcium pump expression and control of cell growth, J. Biol. Chem. 269 (1994) 11927–11933.
[35] M.P. Abbrachio, G. Burnstock, Purinoreceptors: are there families of P2X and P2Y purinoreceptors? Pharmacol. Ther. 64 (1994) 445–475.
[36] S.P. Soltoff, M.K. McMillian, E.J. Cragoe Jr., L.C. Cantley, B.R. Talamo, Effects of extracellular ATP on ion transport systems and $[Ca^{2+}]_i$ in rat parotid acinar cells. Comparison with the muscarinic agonist carbachol, J. Gen. Physiol. 95 (1990) 319–346.
[37] S.J. Mason, A.M. Paradiso, R.C. Boucher, Regulation of transepithelial ion transport and intracellular calcium by extracellular ATP in human normal and cystic fibrosis airway epithelium, Br. J. Pharmacol. 103 (1991) 1649–1656.
[38] M. Flezar, S. Heisler, P2-purinergic receptors in human breast tumor cells: coupling of intracellular calcium signaling to anion secretion, J. Pharmacol. Exp. Ther. 265 (1993) 1499–1510.
[39] I. Bezprozvanny, J. Watras, B.E. Ehrlich, Bell-shaped calcium-response curves of Ins(1,4,5)P_3 and calcium-gated channels from endoplasmic reticulum of cerebellum, Nature 351 (1991) 751–754.
[40] C.C. Petersen, E.C. Toescu, B.V.L. Potter, O.H. Petersen, Inositol triphosphate produces different patterns of cytoplamic Ca^{2+} spiking depending on its concentration, FEBS Lett. 293 (1991) 179–182.
[41] J.W. Putney Jr., TRP, inositol 1,4,5-trisphosphate receptors, and capacitative calcium entry, Proc. Natl. Acad. Sci. U.S.A. 96 (1999) 14669–14671.
[42] N. Uzlaner, Z. Priel, Interplay between the NO pathway and elevated [Ca^{2+}] enhances ciliary activity in rabbit trachea, J. Physiol. 516.1 (1999) 179–190.
[43] A.C. Elliott, Recent developments in non-excitable cell calcium entry, Cell Calcium 30 (2001) 73–93.
[44] C. Montell, L. Birnbaumer, V. Flockerzi, The TRP channels, a remarkably functional family, Cell 108 (2002) 595–598.
[45] C.M. Ribeiro, J.W. Putney, Differential effects of protein kinase C activation on calcium storage and capacitative calcium entry in NIH3T3 cells, J. Biol. Chem. 35 (1996) 21522–21528.
[46] C.M. Ribeiro, R.R. McKay, E. Hosoki, G.S. Bird, J.W. Putney Jr., Effects of elevated cytoplasmic calcium and protein kinase C on endoplasmic reticulum structure and function in HEK293 cells, Cell Calcium 27 (2000) 175–185.
[47] N. Huang, D.J. Wang, L.A. Heppel, Extracellular ATP is a mitogen for 3T3, 3T6, and A431 cells and acts synergistically with other growth factors, Proc. Natl. Acad. Sci. U.S.A. 86 (1989) 7904–7908.
[48] A. Fillipini, R.E. Taffs, M.V. Sitkovsky, Extracellular ATP in T-lymphocyte activation: possible role in effector functions, Proc. Natl. Acad. Sci. U.S.A. 87 (1990) 8267–8271.
[49] D.L. Gill, R.T. Waldron, K.E. Rys-Sikora, C.A. Ufret-Vincenty, M.N. Graber, C.J. Favre, A. Alfonso, Calcium pools, calcium entry, and cell growth, Biosci. Rep. 16 (1996) 139–157.
[50] B. Vandewalle, L. Hornez, F. Revillion, J. Lefebvre, Effect of extracellular ATP on breast tumor cell growth, implication of intracellular calcium, Cancer Lett. 85 (1994) 47–54.
[51] G.J. Barritt, Does a decrease in subplasmalemmal Ca^{2+} explain how store-operated Ca^{2+} channels are opened? Cell Calcium 23 (1998) 65–75.
[52] M.J. Berridge, M.D. Bootman, P. Lipp, Calcium—a life and death signal, Nature 396 (1998) 645–649.
[53] D.E. Clapham, Calcium signaling, Cell 80 (1995) 259–268.
[54] Y. Huang, J.W. Putney Jr., Relationship between intracellular calcium store depletion and calcium-release activated calcium current in mast cell line (RBL1), J. Biol. Chem. 273 (1998) 19554–19559.
[55] A. Verkhratsky, O.H. Petersen, The endoplasmic reticulum as an integrating signalling organelle: from neuronal signalling to neuronal death, Eur. J. Pharmacol. 447 (2002) 141–154.

Calcium et différenciation neuroendocrine

Article 7.

Overexpression of an alpha 1H (Cav3.2) T-type calcium channel during neuroendocrine differentiation of human prostate cancer cells.

Mariot P, Vanoverberghe K, Lalevée N, Rossier MF, Prevarskaya N (2002) **J. Biol. Chem.** 277 : 10824-10833

Article 8.

Ca^{2+} homeostasis and apoptotic resistance of neuroendocrine-differentiated prostate cancer cells.

Vanoverberghe K,Vanden-Abeele F, Mariot P, Lepage G, Roudbaraki M, Bonnal JL, Mauroy B, Shuba Y, Skryma R, Prevarskaya N (2003) **En révision pour Cell. Death and Differentiation**

I. Position du problème

La prostate saine exprime différents types cellulaires dont les cellules épithéliales luminales et basales, ces dernières pouvant servir de cellules souches, ainsi que des cellules neuroendocrines dispersées dans l'organe provenant soit de la crête neurale au cours de l'embryogénèse soit de la différenciation des cellule souches basales. Le cancer de la prostate, généralement dans les stades avancés, présente des foyers de cellules neuroendocrines, d'où la terminologie de "différenciation neuroendocrine". La différenciation neuroendocrine pourrait regrouper plusieurs phénomènes dont : une transformation maligne d'une cellule souche prostatique, une transformation d'une cellule neuroendocrine, ou une dédifférenciation d'une cellule épithéliale accompagnée d'un nouveau programme d'expression de gènes.

Les cellules de la prostate expriment des récepteurs à des hormones peptidiques comme la prolactine et aux neuropeptides tels que le GnRH, le VIP, la somatostatine ou la calcitonine, qui ont une importance fondamentale puisque leur stimulation peut activer ou bloquer la prolifération ou le caractère invasif des tumeurs (Wasilenko et al 1997, Limonta et al 1992, Hoosein et al 1993, Shah et al 1994). De plus, on sait maintenant que les cellules de la prostate sécrétent de la prolactine et de nombreux neuropeptides (TSH, calcitonine, somatostatine, GRP...). **La présence de récepteurs à des hormones et des neuropeptides émis localement a permis l'émergence du concept selon lequel le fonctionnement physiologique et pathologique des cellules de la prostate pourrait**

être régulé par des boucles autocrines/paracrines.

Un intérêt considérable s'est porté depuis plusieurs années sur la différenciation neuroendocrine dans le cancer de la prostate car celle-ci semble être associée à un pronostic clinique très défavorable. Cette terminologie est déterminée par les caractéristiques histologiques (immunoréactivité aux marqueurs neuronaux (Neuron Specific Enolase (NSE), chromogranine A, synaptophysine)) et regroupe aussi bien les carcinomes neuroendocrines, tels que carcinomes à petites cellules et tumeurs carcinoïdes ou apparentées, que les adénocarcinomes classiques avec différenciation neuroendocrine focalisée. Cette terminologie inclut également les carcinomes prostatiques avec présence de sécrétion ectopique (par exemple, ACTH, β–endorphine, PTH, glucagon, α– and β–HCG) ou eutopique de neurohormone (sérotonine, TSH-like peptides, somatostatine, calcitonine, bombesine-like peptides) et/ou la présence d'un marqueur neuroendocrinien (chromogranine A) dans le sérum, les urines ou la tumeur. La pathologie la plus commune reste l'adénocarcinome avec différenciation neuroendocrine focalisée. La différenciation neuroendocrine focalisée est caractérisée par la présence de foyers d'amas de cellules neuroendocrines dans un environnement de cellules non neuroendocrines en division (Bonkhoff 1998). Les méthodes de détection s'affinant de plus en plus, il est devenu évident qu'une différenciation neuroendocrine dans des adénomes prostatiques conventionnels était certainement très fréquente (diSant'Agnese and de Mesy Jensen 1987, Abrahamsson et al 1986). Le pronostic clinique semble être influencé par la différenciation neuroendocrine de la tumeur. Les carcinomes neuroendocrines à petites cellules, poursuivent une progression rapide et sont insensibles à une thérapie hormonale. Les tumeurs carcinoïdes, ou apparentées, sont également très agressives lorsqu'elles surviennent dans la prostate. Les carcinomes prostatiques avec différenciation neuroendocrine, enfin, ont également un mauvais pronostic clinique et sont associés à une survie considérablement réduite à 6 ans (Cohen et al 1990, Glezerson and Cohen 1991).

Plusieurs hypothèses sont avancées pour tenter d'expliquer pourquoi les cancers prostatiques présentant une différenciation neuroendocrine ont un mauvais pronostic clinique. D'une part, les cellules neuroendocrines sont réfractaires aux traitements anti-androgéniques car elles n'expriment généralement pas le récepteur aux androgènes. Ceci est cohérent avec le fait que les tumeurs présentant une différenciation neuroendocrine sont androgéno-indépendantes. Les tumeurs deviennent alors hormono-indépendantes lors d'une thérapie antiandrogénique, les cellules neuroendocriniennes tumorales remplaçant les cellules tumorales androgéno-dépendantes au fur et à mesure du traitement. D'autre part, les cellules neuroendocrines ne prolifèrent pas (Bonkhoff 1998) mais pourraient être impliquées dans le cancer de la prostate en sécrétant des facteurs paracrines/autocrines à activité mitogénique tels que la bombésine, la calcitonine ou les peptides

apparentés à l'hormone parathyroidienne. Ceci pourrait entraîner ou faciliter la prolifération des cellules épithéliales avoisinantes ou leur différenciation vers un phénotype neuroendocrine (Abrahamsson 1999). Ces actions paracrines pourraient aboutir à une croissance non controlée de la prostate. Ainsi, un dysfonctionnement de sécrétion de neuropeptides (défaut ou hypersécrétion), ainsi qu'un défaut d'expression de récepteurs à des neuropeptides et/ou une altération de la transduction intracellulaire par exemple, pourraient être responsables d'une croissance tumorale.

Les mécanismes impliqués dans la différenciation neuroendocrine des cellules de la prostate ne sont pas pour l'instant élucidés mais grâce aux modèles de lignées de cellules tumorales humaines (LNCaP et DU145), il semblerait que les cellules épithéliales pourraient se différencier en cellules neuroendocrines notamment sous l'effet de cytokines (interleukines 1 et 6) (Diaz et al 1998) ou de second messagers tels que l'AMPc (Bang et al 1994, Cox et al 2000) et les voies impliquant les p38MAP kinases (Kim et al 2002), la phosphatidylinositol 3'-kinase et les tyrosines kinases de type Btk (Qiu et al 1998).

II. But du travail

Le but de ces travaux était de déterminer les altérations des mécanismes d'homéostasie calcique lors du processus de différenciation neuroendocrine dans les cellules prostatiques.

Nous avons voulu déterminer dans un premier temps (**article 7**) si le processus de différenciation neuroendocrine était associé à une expression de canaux calciques voltage-dépendants. En effet, d'une manière générale, les cellules neuronales ou neuroendocrines (cellules hypophysaires, pancréatiques ou médullosurrénaliennes par exemple) sont associées à l'expression de ce type de canaux. D'autre part, dans certains modèles cellulaires, neurones ou cellules neuroendocrines (PC12), la différenciation est associée à une expression différentielle des canaux calciques voltage-dépendants.

Dans un second temps (**article 8**), nous avons poursuivi le travail précédent en ce qui concerne les altérations de l'homéostasie calcique lors du phénomène de différenciation neuroendocrine et avons voulu détérminé si ces altérations concernaient d'autres canaux que les canaux voltage-dépendants et si ces altérations jouaient un rôle dans la résistance à l'apoptose des cellules différenciées.

III. Résultats et discussion

Notre travail a montré, par des mesures électrophysiologiques et des approches de biologie moléculaire, que la différenciation neuroendocrine des cellules cancéreuses prostatiques LNCaP,

induite soit par la stimulation de la voie de l'adénylate cyclase, soit par une déplétion en stéroïdes, provoquait une surexpression d'un seul type de canal calcique voltage-dépendant, un canal calcique de type T, la sous-unité surexprimée étant la sous-unité pore α1H. Ce travail a été notamment possible grâce à une collaboration avec les Drs. M. Rossier et N. Lalevée, qui ont effectué les mesures de RT-PCR quantitative par Sybergreen. Nous avons de plus montré dans ce travail que ce canal était probablement impliqué dans le processus d'élongation neuritique, soit directement en augmentant le calcium cytosolique *via* une entrée à un potentiel membranaire de fenêtre, soit indirectement en stimulant la sécrétion de facteurs paracrines à activité neurotrophique (**article 7**).

Nous montrons d'autre part dans **l'article 8** que la différenciation neuroendocrine est associée à une diminution de la concentration calcique du réticulum endoplasmique et à une diminution de l'entrée capacitative et du courant SOC. La diminution de la concentration calcique des réserves intracellulaire est corrélée à une diminution du taux d'expression des SERCA2B, qui sont des isoformes ubiquitaires des pompes calciques ATPases responsables du remplissage du réticulum endoplasmique, et de la calréticuline, protéine chaperone de liaison au calcium.

D'autre part, nous montrons dans **l'article 8** que les cellules différenciées acquièrent une résistance à l'apoptose induite par la thapsigargine ou le TNFα. Les modifications d'homéostasie calcique étant similaires dans les cellules différenciées et dans les cellules transfectées avec bcl-2, nous suggérons que ces modifications pourraient être impliquées dans le processus de résistance à l'apoptose. Cependant, cette résistance à l'apoptose ne semble pas impliquer bcl-2 car celle-ci est sous-exprimée lors du processus de différenciation.

Ainsi, la différenciation neuroendocrine des cellules prostatiques est associée à une expression différentielle de mécanismes d'homéostasie calcique correspondant effectivement à ceux de cellules neuroendocrines :

- Expression plus importante de canaux calciques voltage-dépendants
- Expression plus faible d'une entrée de type SOC

Un des enjeux importants consiste à déterminer quel peut être l'influence sur la physiopathologie cellulaire de cette expression différentielle de canaux calciques dans les cellules cancéreuses.

THE JOURNAL OF BIOLOGICAL CHEMISTRY
Vol. 277, No. 13, Issue of March 29, pp. 10824–10833, 2002
Printed in U.S.A.

Overexpression of an α_{1H} ($Ca_v3.2$) T-type Calcium Channel during Neuroendocrine Differentiation of Human Prostate Cancer Cells*

Received for publication, September 11, 2001, and in revised form, January 14, 2002
Published, JBC Papers in Press, January 17, 2002, DOI 10.1074/jbc.M108754200

Pascal Mariot‡§, Karine Vanoverberghe‡, Nathalie Lalevée¶, Michel F. Rossier¶‖, and Natalia Prevarskaya‡

From the ‡Laboratoire de Physiologie Cellulaire, INSERM EPI9938, Bâtiment SN3, Université des Sciences et Technologies de Lille, 59655 Villeneuve d'Ascq Cédex, France and the ¶Division of Endocrinology & Diabetology, Department of Internal Medicine, ‖Laboratory of Clinical Chemistry, Department of Pathology, University Hospital, CH-1211 Geneva 14, Switzerland

Neuroendocrine differentiation of prostate epithelial cells is usually associated with an increased aggressivity and invasiveness of prostate tumors and a poor prognosis. However, the molecular mechanisms involved in this process remain poorly understood. We have investigated the possible expression of voltage-gated calcium channels in human prostate cancer epithelial LNCaP cells and their modulation during neuroendocrine differentiation. A small proportion of undifferentiated LNCaP cells displayed a voltage-dependent calcium current. This proportion and the calcium current density were significantly increased during neuroendocrine differentiation induced by long-term treatments with cyclic AMP permeant analogs or with a steroid-reduced culture medium. Biophysical and pharmacological properties of this calcium current suggest that it is carried by low-voltage activated T-type calcium channels. Reverse transcriptase-PCR experiments demonstrated that only a single type of LVA calcium channel mRNA, an α_{1H} calcium channel mRNA, is expressed in LNCaP cells. Quantitative real-time reverse transcriptase-PCR revealed that α_{1H} mRNA was overexpressed during neuroendocrine differentiation. Finally, we show that this calcium channel promotes basal calcium entry at resting membrane potential and may facilitate neurite lengthening. This voltage-dependent calcium channel could be involved in the stimulation of mitogenic factor secretion and could therefore be a target for future therapeutic strategies.

Prostate cancer is a slowly evolutive cancer which, in the first stages, is dependent on androgens. Treatments designed to kill the tumors, based on androgen depletion, become eventually ineffective, this being probably due to the selection of resistant cells. One hypothesis is that androgen-insensitive cells resistant to anti-androgen therapies would be neuroendocrine cells lacking the androgen receptor (1). Extensive and focal neuroendocrine features, determined by cell immunoreactivity to different neuronal markers (neuron-specific enolase (NSE),[1] chromogranin A, synaptophysin), are evidenced in most prostate carcinoma in their late stages (for review, see Refs. 2 and 3). This focal neuroendocrine differentiation is characterized by the presence of dispersed clusters of neuroendocrine cells in a neighboring of non-neuroendocrine dividing cells (1) and is usually associated with an increased aggressivity and invasiveness of the tumors and a poor prognosis (4). Neuroendocrine cells do not proliferate (1) but could be involved in prostate cancer relapse by secreting mitogenic autocrine/paracrine factors like bombesin, calcitonin, and parathyroid hormone-related peptides in their vicinity (3). This could in turn promote either the proliferation of adjacent epithelial cells or their differentiation toward a neuroendocrine phenotype (2). Altogether, these autocrine/paracrine actions could lead to the uncontrolled growth of the prostate.

Some of the signals involved in neuroendocrine differentiation of the prostatic epithelium have been unraveled. Activation of membrane receptors coupled to adenylyl cyclase which leads to an increase in cytosolic cyclic AMP, as well as interleukins 1 and 6 induce the expression of neuroendocrine markers like NSE, secretory granules, and neurite extension (5–9). The stimulation of neuroendocrine differentiation by interleukin 6 has been shown to involve the induction of cyclin-dependent kinase inhibitor $p27^{Kip1}$ (7), as well as the tyrosine phosphorylation of epithelial and endothelial tyrosine kinase Etk/Bmx through the activation of phosphatidylinositol 3′-kinase (6). Steroid removal from the culture medium was also shown to induce neuroendocrine differentiation (10, 11).

Calcium entry through voltage-gated calcium channels is reported to be involved in differentiation and neurite outgrowth in other cells (12–15). It has been shown, for example, in the pheochromocytoma cell line (PC12 cells) that neuroendocrine differentiation is accompanied by an increased expression of voltage-dependent channels like low-voltage activated (LVA) (12) and high-voltage activated (HVA) calcium channels (14, 16). To our knowledge no functional voltage-dependent calcium channels have been clearly demonstrated in prostate cancer cells. We have investigated in this study the possible expression of voltage-gated calcium channels in human prostate cancer LNCaP cells and their modulation during neuroendocrine differentiation induced by increasing cytosolic cAMP or by reducing steroids in the culture medium. We show that a

* This work was supported by the INSERM, Ligue Nationale contre le Cancer, Association pour la Recherche contre le Cancer, Fondation pour la Recherche Médicale, and Swiss National Science Foundation Grant 32-58948.99 (to M. F. R. and N. L.). The costs of publication of this article were defrayed in part by the payment of page charges. This article must therefore be hereby marked "*advertisement*" in accordance with 18 U.S.C. Section 1734 solely to indicate this fact.

§ To whom correspondence should be addressed: Laboratoire de Physiologie Cellulaire, INSERM EPI9938, Bâtiment SN3, Université des Sciences et Technologies de Lille, 59655 Villeneuve d'Ascq Cédex, France. Tel.: 33-3-20-43-40-77; Fax: 33-3-20-43-40-66; E-mail: Pascal.Mariot@univ-lille1.fr.

[1] The abbreviations used are: NSE, neuron-specific enolase; LVA, low-voltage activated; HVA, high-voltage activated; RT, reverse transcriptase; IBMX, isobutylmethylxanthine; GAPDH, glyceraldehyde-3-phosphate dehydrogenase; $[Ca^{2+}]_i$, intracellular Ca^{2+}; Bt_2cAMP, dibutyryl cAMP.

small proportion of LNCaP cells displays an inward calcium current of weak amplitude and that this proportion and the calcium current density are increased during neuroendocrine differentiation. Biophysical and pharmacological properties of this calcium current show that it is carried by a LVA T-type calcium channel. RT-PCR experiments demonstrate that only an α_{1H} voltage-dependent calcium channel mRNA is expressed in LNCaP cells. Quantitative real-time RT-PCR reveals that α_{1H} mRNA is overexpressed during neuroendocrine differentiation induced by various stimuli increasing cytosolic cAMP. Finally, our results suggest that although they are not involved in triggering neurite elongation, T-type calcium channels participate to a "window" calcium current active at resting membrane potential and may be implicated in facilitating the extension of neuritic processes. In addition, we propose that this voltage-dependent calcium channel could participate to the stimulation of mitogenic factors secretion by neuroendocrine prostate cells and could therefore be a target for future therapeutic strategies.

EXPERIMENTAL PROCEDURES

Cell Culture and Treatments

LNCaP cells were purchased from the American Type Culture Collection and grown as recommended in RPMI 1640 (Biowhittaker, Fontenay sous Bois, France) supplemented with 10% fetal bovine serum (Seromed, Poly-Labo, Strasbourg, France) and 5 mM L-glutamine (Sigma, L'Isle d'Abeau, France). Cells were routinely grown in 50-ml flasks (Nunc, Poly-Labo) in a humidified atmosphere at 37 °C (95% air, 5% CO_2). To study the role of steroids in the expression of voltage-dependent calcium channels, cells were grown in phenol red-free RPMI 1640 supplemented with 10% charcoal-stripped fetal bovine serum (culture medium thereafter referred to as steroid-reduced medium). For electrophysiological studies, cells were subcultured in Petri dishes (Nunc) using trypsin. The culture medium was then changed every 3 days. Five days after trypsinization, the treatment was initiated and the culture medium containing the treatments (Bt_2cAMP, IBMX) was changed every day. Cells were then tested within 8 days.

Western Blot Analysis

Following treatments, LNCaP cells were lyzed in an ice-cold homogenizing buffer (pH 7.4) containing 20 mM HEPES, 50 mM NaCl, 0.5% Nonidet P-40 (v/v), 1 mM EGTA, 10 mM EDTA, 1 mM phenylmethanesulfonyl fluoride, 2 μg/ml aprotinin, 2 μg/ml pepstatin A, and 10 μg/ml leupeptin. The homogenates were cleared by a centrifugation at 900 × *g* for 10 min and the protein content in the supernatants was determined using a Bradford assay. 50 μg of total proteins of each sample were analyzed on a 10% SDS-polyacrylamide gel electrophoresis. After transfer, the blots were blocked in 5% non-fat dry milk in TBST (15 mM Tris buffer (pH 8), 140 mM NaCl, 0.05% Tween 20) before the mouse anti-NSE monoclonal antibody (1/100, M0873 DAKO) was added in TBST-3% non-fat dry milk for 1 h at room temperature. After washing, blots were incubated for 1 h with an horseradish peroxydase-linked secondary antibody (1/5000, Zymed Laboratories Inc., San Francisco, CA) and processed for chemiluminescent detection using Supersignal West Pico chemiluminescent substrate (Pierce, Chemical Co., Rockford, IL) according to the manufacturer's instructions. The blots were then exposed to X-Omat AR films (Eastman Kodak Co., Rochester, NY).

Qualitative and Quantitative RT-PCR

RNA Extraction—Total RNA isolation from 5 million cells in culture was performed using the RNeasy™ Total RNA isolation System kit (Quiagen AG, Basel, Switzerland), as indicated in the manufacturer's instructions. Dry RNA pellets were dissolved in nuclease-free water and stored frozen at a concentration of 500 ng/μl.

RT-PCR Procedure—Conventional RT-PCR was performed using the "GeneAmp™ Gold RNA PCR Reagent Kit" from PE-Biosystems following manufacturer's instructions. Briefly, first strand cDNA was generated by loading 300 ng of extracted RNA in the master mixture (50 μl) containing 500 nM specific primers for calcium channels (see Table I) and other reagents, as specified by the manufacturer. GAPDH (glyceraldehyde-3-phosphate dehydrogenase) transcripts were reverse transcribed and analyzed in parallel to evaluate RNA integrity. Reverse transcription was achieved by incubation at 42 °C for 12 min. A 10-min denaturation step at 95 °C then preceded 32 PCR cycles according to the following protocol: denaturation at 94 °C (20 s), annealing/elongation at 62 °C (1 min), and a final elongation step at 72 °C (7 min). Amplified fragments were then resolved on a 2% agarose gel.

Quantification by Real-time RT-PCR on LightCycler™—A one-step conventional RT-PCR protocol has been adapted for the LightCycler (Roche Molecular Diagnostics AG, Rotkreuz, Switzerland). Individual glass capillaries were filled with a solution containing 18 μl of RT-PCR mixture and 2 μl of total RNA template (250 ng). The reaction mixture was composed of primer oligonucleotides (250 nM), $Mn(OAc)_2$ (3.5 mM), and LightCycler RNA Master SYBR Green I, itself containing reaction buffer, dNTP, Tth DNA polymerase, and SYBR Green I dye at concentrations optimized by the manufacturer. The reverse transcription of the RNA template lasted 20 min at 61 °C and was followed by a 2-min denaturation of cDNA at 95 °C. The amplification of target cDNA was then performed for 45 cycles according to the following steps: denaturation, 95 °C (5 s); annealing, 54 °C (5 s); and elongation, 72 °C (8 s). The SYBR Green fluorescence was measured after each elongation step. At the end of the PCR, a melting curve analysis was performed by gradually increasing temperature from 60 to 95 °C (0.1 °C/s). Moreover, at the end of experiments, RT-PCR products were removed from capillaries and analyzed by gel electrophoresis to confirm the presence and assess the purity of the amplicons of interest.

After PCR was completed, the SYBR Green fluorescent signal was analyzed and converted into a relative number of copies of target molecules. For this purpose, the results of a series of standards prepared by successive dilutions and plotted against the logarithm of the concentration were used to estimate the relative amount of specific mRNA initially present in the various samples. Each sample was analyzed in triplicate.

Recording Solutions

Bath medium used for calcium imaging or current-clamp experiments consisted in Hank's balanced salt solution containing 142 mM NaCl, 5.6 mM KCl, 1 mM $MgCl_2$, 2 mM $CaCl_2$, 0.34 mM Na_2HPO_4, 0.44 mM KH_2PO_4, 10 mM HEPES, and 5.6 mM glucose. For measuring calcium currents in patch-clamp experiments, the external buffer contained 142 mM NaCl, 1 mM $MgCl_2$, 10 mM HEPES, 5.6 mM glucose, 10 mM TEA-Cl (tetra-ethyl ammonium chloride), and 10 mM $CaCl_2$ or $BaCl_2$. All the data shown in this study were obtained with a bath medium containing 10 mM $BaCl_2$. The osmolarity and pH of external buffers were adjusted to 310 mOsm liter^{-1} and 7.4, respectively.

For current-clamp experiments, the pipette solution contained 140 mM K-glutamate, 1 mM EGTA, 1 mM $MgCl_2$, 5 mM HEPES. For voltage-dependent calcium current studies, recording pipettes were filled with a solution containing 140 mM n-methylglucamine, 110 mM L-glutamic acid, 30 mM HCl, 5 mM HEPES, 1 mM $MgCl_2$, 1 mM EGTA. Osmolarity and pH were adjusted to 290 mOsm liter^{-1} and 7.2, respectively.

Electrophysiological Recordings

Patch-clamp recordings were performed in the whole cell configuration (17) using a RK-300 patch-clamp amplifier (Biologic, Grenoble, France). The patch-clamp amplifier was driven by Pulse 8.30 software (HEKA Elektronik, Lambrecht, Germany). Membrane currents were digitized at 20 kHz using a ITC16 computer interface (Instrutech Corp., Long Island, NY, low-pass filtered at 3 kHz and stored on-line on the hard-drive of the computer. Electrodes were pulled on a PIP5 puller (HEKA, Germany) in two stages from borosilicate glass capillaries (PG52151, World Precision Instruments, Aston, UK) to a tip diameter giving a pipette resistance of 5 MΩ. For each cell, the membrane potential was clamped initially at −80 mV and the passive membrane components (membrane resistance and capacitance) were determined immediately after the establishment of the whole cell configuration. A protocol to assess the current/voltage (I/V) relationship was then initiated. For such experiments, a p/n protocol (8 negative prepulses a 1/10th of the pulse magnitude) was used to correct for the background leak and capacitive membrane currents.

Calcium Imaging

LNCaP cells were grown on glass coverslips to carry out calcium imaging experiments. Cytosolic calcium concentration was measured using Fura-2-loaded cells (18). LNCaP cells were loaded for 45 min at room temperature with 2 μM Fura-2/AM prepared in Hank's balanced salt solution and subsequently washed three times with the same dye-free solution. The coverslip was then transferred onto a perfusion chamber on a Olympus IX70 microscope equipped for fluorescence. Fluorescence was alternatively excited at 340 and 380 nm with a monochromator (Polychrome IV, TILL Photonics GmBh, Planegg, Ger-

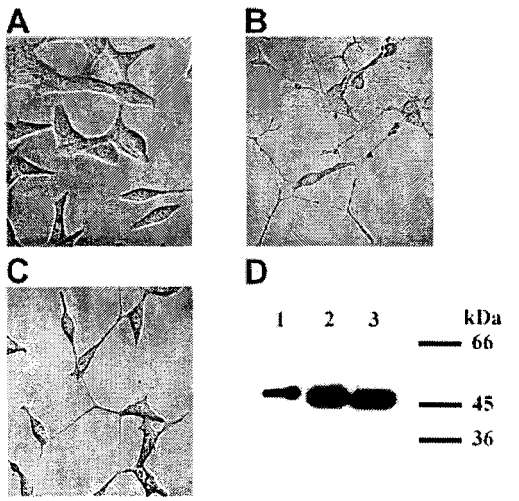

FIG. 1. **Treatments for 3 days with Bt_2cAMP or IBMX induce neuroendocrine differentiation of LNCaP cells.** *A*, untreated cells. *B*, cells treated with 1 mM Bt_2cAMP. *C*, cells treated with 100 μM IBMX. *D*, Western blot analysis of neuron-specific enolase expression. *Lane 1*, control cells. *Lane 2*, Bt_2cAMP. *Lane 3*, IBMX

many) and was captured after filtration through a long-pass filter (510 nm) by a MicroMax 5MHz CCD camera (Princeton Instruments, Evry, France). Acquisition and analysis was performed with the Metafluor 4.5 software (Universal Imaging Corp., West Chester, PA). The intracellular calcium concentration was derived from the ratio of the fluorescence intensities for each of the excitation wavelengths (F340/F380) and from the equation of Grynkiewicz *et al.* (18). All recordings were carried out at room temperature. The cells were continuously perfused with the Hank's balanced salt solution and chemicals were added via the perfusion system. The flow rate of the whole chamber perfusion system was set to 1 ml/min and the chamber volume was 500 μl.

Morphometric Analysis

Pictures of cultured LNCaP cells were recorded with a MicroMax 5 MHz CCD camera (Princeton Instruments, Evry, France). For each condition, at least 10 fields of cells were analyzed from two different batches of culture (total number of cells between 345 and 826). Images (1380 × 1030 pixels) were then analyzed and neurite processes were measured using an imaging software.

Chemicals

All chemicals were purchased from Sigma except for Fura-2 which was bought from Calbiochem (France Biochem, Meudon, France).

Statistical Analysis

Plots were produced using Origin 5.0 (Microcal Software, Inc., Northampton, MA). Results are expressed as mean ± S.E. Statistical analysis were performed using unpaired *t* tests or ANOVA tests followed by either Dunnett (for multiple control *versus* test comparisons) or Student-Newman-Keuls post-tests (for multiple comparisons).

RESULTS

Neuroendocrine Differentiation Induced by cAMP Permeant Analogs Is Associated with an Increased Inward Current—We first assessed by morphometric assays and Western blotting that culturing LNCaP cells for 3–5 days with cAMP permeant analogs (dibutyryl cAMP (Bt_2cAMP), 8-bromo-cAMP (8-Br-cAMP), 1 mM) or a phosphodiesterase inhibitor (isobutylmethylxanthine, IBMX, 100 μM) induced neuroendocrine differentiation. Treatment with Bt_2cAMP or IBMX (Fig. 1, *A–C*) or 8-Br-cAMP (not shown) led to neurite extension. In addition, treatments with Bt_2cAMP or IBMX enhanced the expression of a neuroendocrine marker, neuron-specific enolase (Fig. 1*D*). Morphological differentiation assessed by the presence of neurite extension was initiated as soon as 2 h after the onset of the treatment with Bt_2cAMP, 8-Br-cAMP, or IBMX.

Voltage-dependent calcium currents were then investigated in non-treated (control) and treated LNCaP cells in conditions where voltage-dependent potassium channels were eliminated (see "Experimental Procedures"). Fig. 2*A* represents a typical experiment performed on a control cell. No significant voltage-dependent inward current was observed on this control cell. On the opposite, a cell treated with Bt_2cAMP for 3 days displayed an inward current activating at membrane potentials positive to −40 mV and peaking around −10 mV (Fig. 2*B*). The inward current reached its peak value 15 ms after the beginning of the voltage step to −10 mV and then exponentially decayed with a time constant of 20.3 ms (Fig. 2*C*). On average, the transient inward current activated and inactivated with exponential time constants of 11.6 ± 0.9 and 23.9 ± 1.5 ms, respectively.

After normalization of the peak inward current to the membrane capacitance (indicative of the cell surface area) for each cell, we observed that after 3–5 days of treatment, the average current density was significantly increased in cells treated with Bt_2cAMP at all membrane potentials between −40 and +20 mV (Fig. 2*D*, control cells: $n = 96$; 9 batches of cells, Bt_2cAMP-treated cells: $n = 119$; 11 batches of cells). The maximum current density was −0.81 ± 0.07 pA/pF at −10 mV for Bt_2cAMP-treated cells *versus* −0.35 ± 0.05 pA/pF for control cells, this corresponding to a 2.3-fold increase. The voltage-dependent transient current was only occasionally present in control cells (22 ± 6%), this proportion being enhanced (Fig. 2*E*) after treatment with Bt_2cAMP (62 ± 8%). Fig. 2*F* shows that the distribution of the current amplitude (at −10 mV) in control cells follows a normal curve but that there is a multipeak distribution following treatment with Bt_2cAMP during 3–5 days with the emergence of a cell population with larger current densities (19% of treated cells with a current density larger than 1.5 pA/pF *versus* 3% for control cells).

The enhancement of this voltage-dependent transient inward current followed a slow kinetics. A 5-min application of Bt_2cAMP (1 mM) did not induce or increase such a current on control LNCaP cells (Fig. 2*G*, $n = 9$). Whereas a 1-day Bt_2cAMP treatment was ineffective, a 3-day treatment led to a significant and almost maximal increase in the transient current density (Fig. 2*H*). A 3-day treatment with another cAMP permeant analog, 8-Br-cAMP (1 mM), also raised the transient current density (−0.7 ± 0.08 pA/pF, $n = 26$, Fig. 2*I*). In addition, Bt_2cAMP action was potentiated by about 35% (Fig. 2*I*) by inhibiting the degradation of cAMP using IBMX (transient current density after Bt_2cAMP + IBMX (100 μM) = −1.09 ± 0.11 ($n = 29$)).

Biophysical and Pharmacological Characterization of the Inward Current Stimulated during Neuroendocrine Differentiation—We then investigated the ionic nature of this transient current observed in Bt_2cAMP-treated cells. As shown in Fig. 3, *A* and *B*, changing the external Na-containing solution to a Na-deprived solution (sodium being replaced by choline) did not significantly affect, whereas eliminating external calcium (calcium free solution and 0.1 mM EGTA) completely abrogated the transient inward current ($n = 8$). This shows that the ion channel evidenced in our studies belongs to the family of voltage-gated calcium channels which can be further distinguished by their kinetics and voltage dependence of activation, inactivation and deactivation in LVA and HVA calcium channels (19).

As shown above (Fig. 2), the inward current inactivated rapidly after the beginning of the depolarization. Since kinetics and voltage dependence may be indicative of the calcium channel nature, we have investigated its voltage-dependent inactivation (Fig. 3, *C* and *D*). This showed that the current during the test pulse followed a voltage-dependent inactivation. The inactivation began to occur for a membrane potential of −60

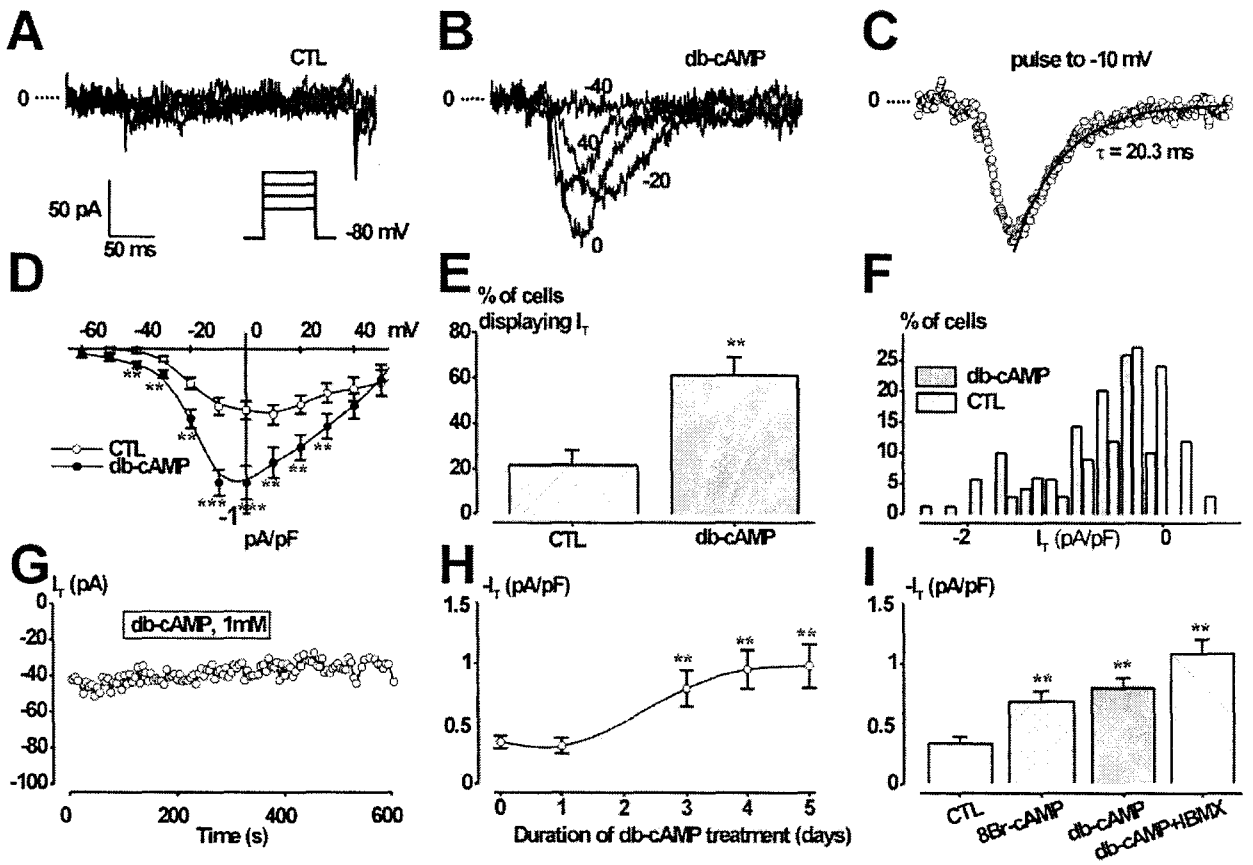

FIG. 2. **Overexpression of a voltage-dependent inward current during neuroendocrine differentiation of LNCaP cells.** *A–C*, examples of membrane currents in an untreated cell (*A*, CTL: control) and in a cell treated with Bt_2cAMP (*db-cAMP*) (*B–C*, 1 mM) for 3 days. Membrane potential was depolarized for 100 ms from −80 mV to different values shown next to the respective current recordings. The voltage pulse protocol is shown in *A* (*inset*). *C*, membrane current elicited by a depolarization from −80 to −10 mV in a Bt_2cAMP-treated cell (same as in *B*). For clarity, only one membrane current value (*open circle*) out of 10 was plotted. The current was fitted to an exponential function and displayed a time-dependent inactivation following a single exponential time constant (20.3 ms). *D*, average current/voltage (I/V) relationships for control (*open circle*) and Bt_2cAMP-treated cells (*solid circles*). *E*, proportion of cells displaying an inward current (I_T, T standing for transient) following an I/V curve similar to the one shown in *D*. *F*, membrane current density histogram showing that Bt_2cAMP treatments induced the emergence of a cell population with larger current densities. *G*, a 5-min bath application of 1 mM Bt_2cAMP did not alter the inward transient current observed in a control cell. *H*, whereas a 1-day treatment with Bt_2cAMP (1 mM) was ineffective, a 3–5-day treatment increased the transient current density. *I*, the transient current density was increased by a 3-day treatment with Bt_2cAMP (1 mM), 8-Br-cAMP (1 mM) or Bt_2cAMP and IBMX (100 μM). **, $p < 0.01$; ***, $p < 0.001$. Comparisons were performed using an unpaired *t* test (*panel E*) or an ANOVA followed by a Dunnett post-test (*panels H* and *I*).

mV during the prepulse and was complete at −10 mV. Fig. 3*D* (*inset*) shows that the transient inward current was not completely abolished at −40 mV. To determine precisely the nature of the channel involved in the transient calcium current, we measured the deactivation kinetics of the calcium current. A characteristic feature of the T-type calcium channel is its slow deactivation: these channels deactivate with an exponential time constant of about 2 ms at −80 mV when compared with other voltage-dependent calcium channels (19, 20) which deactivate more than 10 times faster. The kinetics of deactivation during the tail current measured after a test pulse (Fig. 3*E*) was fitted to a single exponential and a time constant τ was computed and plotted as a function of the membrane potential during repolarization (Fig. 3*F*). As illustrated by the Fig. 3*F*, the time constant τ varied with the repolarization potential and was comprised between 2 ± 0.16 and 10.8 ± 1 ms for −120 and −40 mV, respectively.

The overall biophysical characteristics of the calcium current expressed in differentiated LNCaP cells suggest that this current belongs to the LVA-T type family of calcium currents. This was confirmed by an absence of action of HVA calcium channel antagonists (nifedipine (0.5 μM) for L-type, ω-conotoxine GVIA (50 nM) for N-type, ω-agatoxine (20 nM) for P/Q type calcium channels (not shown). We then assessed the sensitivities of the inward current to both nickel and cadmium since they vary according to the nature of the calcium channel, T-type calcium channels being more sensitive to nickel than to cadmium, on the contrary to HVA calcium channels (19, 21). Fig. 4 shows that $NiCl_2$ dose dependently inhibited the transient calcium current with an IC_{50} of 2.4 ± 0.4 μM and a maximal inhibition of 90.8 ± 3.4%, whereas $CdCl_2$ dose dependently abolished the calcium current with an IC_{50} of 58.8 ± 8.9 μM. We then used mibefradil (Ro 40-5967), the most selective antagonist to voltage-dependent T-type calcium channels (22, 23). As shown on Fig. 4, mibefradil (20 μM) induced a reversible and dose-dependent reduction of the transient calcium current at all membrane potentials. At −10 mV, mibefradil reduced the transient calcium current by 74 ± 4% (n = 8). The IC_{50} was found to be around 5 μM. Our experiments demonstrate that 5 μM flunarizin (a piperazine derivative previously shown to inhibit T-type calcium channels (24)) reversibly decreased by 62 ± 3% the transient calcium current (n = 3).

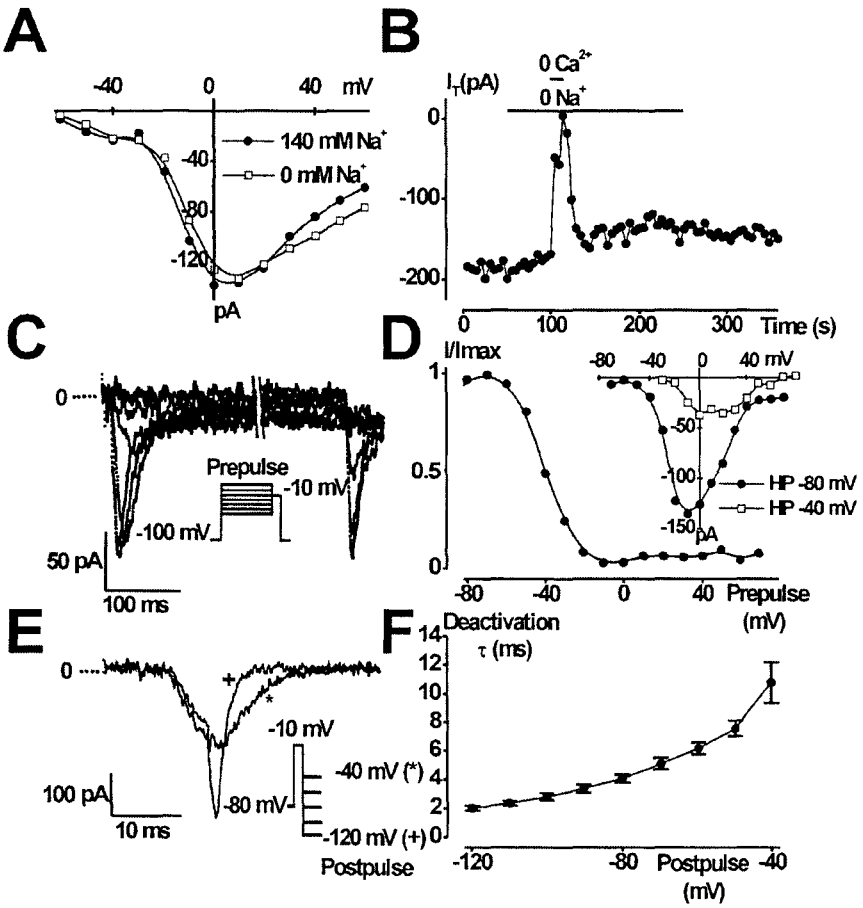

FIG. 3. **Biophysical properties of the transient inward current (I_T) expressed in differentiated LNCaP cells.** *A*, I/V curves in the presence and absence of sodium in the bath solution. *B*, changing the external sodium for choline did not inhibit whereas removing calcium (using a calcium-free solution and 0.1 mM EGTA) abolished the transient current. Voltage protocols for *A* and *B* were the same as in Fig. 2. *C*, the transient inward current displayed a voltage-dependent inactivation. Cells were submitted for 1 s to a prepulse from −100 mV to different membrane potential values and a test pulse was applied for 100 ms at −10 mV (protocol shown in *inset*). Traces were interrupted for clarity. *D*, plot of the membrane current during the test pulse as a function of the prepulse potential. The transient current was half-inactivated at −40 mV. *Inset*, I/V curves obtained for a holding potential of −40 mV or −80 mV. *E*, deactivation tail currents measured after a 10-ms prepulse for a repolarization potential (postpulse) of −40 mV (*) or −120 mV (+) (protocol shown in *inset*). *F*, plot of the deactivation time constant, τ, as a function of the repolarization potential.

The above results suggest that treatments with cAMP analogs increase the number of calcium channels in the plasma membrane. To study whether the T-type calcium current could be regulated in another way than an overexpression, we checked whether cAMP analogs induced a change in the characteristics of the T-type calcium current. Membrane currents obtained after a 3–5-day treatment with Bt_2cAMP, or Bt_2cAMP + IBMX, in addition to membrane currents recorded in control cells, were normalized to the maximum current. The treatments induced no shift in the voltage sensitivity of the calcium current as evidenced by the similarity of all the normalized I/V curves (Fig. 5*A*). A similar I/V curve was obtained for 8-Br-cAMP-treated cells (not shown). Activation and inactivation curves (Fig. 5, *B* and *C*) were computed for control cells (n = 5), Bt_2cAMP (n = 6, not shown), and Bt_2cAMP + IBMX-treated cells (n = 10). Data from each condition were fitted to a Boltzmann equation. These curves showed no significant differences in the mid-point of voltage dependence ($V_{0.5}$) nor in the slope factor (k). In both untreated and treated cells, the $V_{0.5}$ were close to −17 mV and −39 mV and the slope factors were close to 7 mV and −7 mV, for activation and inactivation, respectively. In addition, the kinetics of time-dependent activation and inactivation were not altered. Time constants of activation were 8.7 ± 0.8 *versus* 11.6 ± 0.9 ms and time constants of inactivation were 24.8 ± 2.4 *versus* 23.9 ± 1.5 ms, for control and treated cells, respectively.

Overexpression of an α_{1H} T-type Calcium Channel after Treatment by cAMP Permeant Analogs—To determine which subtypes of calcium channels are expressed in LNCaP cells, we elaborated one-step RT-PCR, using seven distinct sets of primers (Table I) designed according to the human sequence of specific regions (corresponding to the second large intracellular loop linking domains II and III, $L_{II\text{-}III}$) of the corresponding α_1 channel subunits. The three T-type channel isoforms (α_{1G}, α_{1H}, and α_{1I}) and the four L-type channel isoforms (α_{1C}, α_{1D}, α_{1S}, and α_{1F}) were tested. Analysis of RT-PCR products revealed the presence of one single fragment corresponding to the α_{1H} amplicon in control cells (Fig. 6*A*) while other channel isoforms were not detected. In LNCaP cells treated with Bt_2cAMP (1 mM, 1 or 3 days) and with IBMX (100 μM) + Bt_2cAMP (3 days), only the α_{1H} isoform was detected, as in control cells (figure not shown). Similarly, mRNA coding for the GAPDH, a housekeeping gene used for normalizing the initial amount of RNA, was reverse transcribed and amplified with specific primers in the same experiment.

To compare the mRNA coding for α_{1H} in control and treated cells, we used a real-time RT-PCR approach that combines the high sensitivity of the PCR technique with the accuracy supplied by a continuous monitoring of a fluorescent signal proportional to the accumulated PCR product, as previously described in detail by Lesouhaitier *et al.* (25). This analysis has been performed on a LightCycler system (Roche Molecular Diagnostics) with online detection of the fluorescent dye SYBR Green I, that is excitable only when inserted in double stranded DNA. The variation of mRNA coding for α_{1H} channel was studied in cells submitted to various treatments known to increase cytosolic cAMP concentration in prostate LNCaP cells, Bt_2cAMP (1 mM), 8-Br-cAMP (1 mM), or a combination of both Bt_2cAMP and IBMX (100 μM). Treatments were applied for 1 or 3 days. To minimize errors due to variations occurring during RNA extraction and quantification, the results were normal-

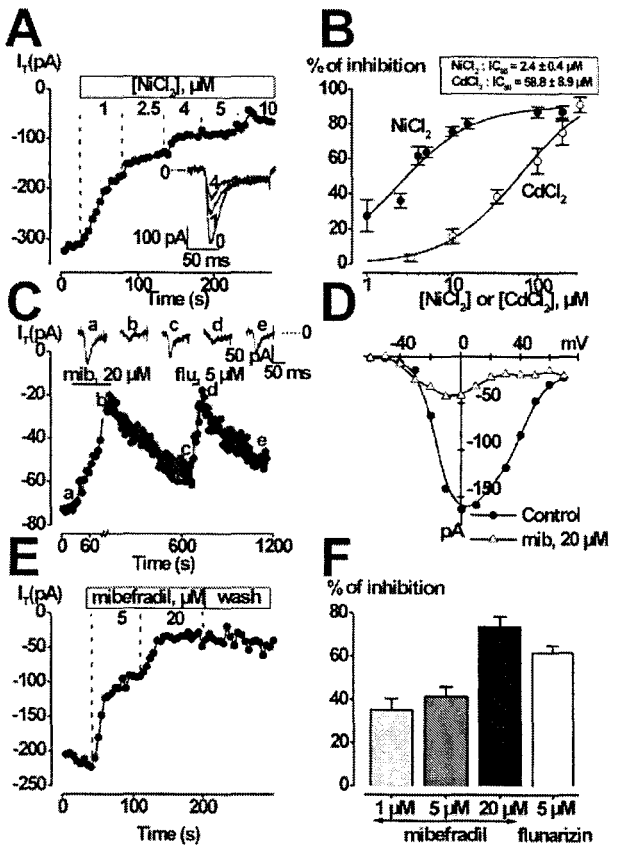

FIG. 4. **Pharmacological properties of the transient inward current (I_T) expressed in differentiated LNCaP cells.** *A*, increasing concentrations of $NiCl_2$ dose dependently inhibited I_T in a differentiated LNCaP cell. *Inset*, membrane currents for 3 concentrations of $NiCl_2$ (0, 1, and 4 μM). *B*, plot of the % of I_T inhibition as a function of $NiCl_2$ and $CdCl_2$ concentrations (n = 3 to 8 for each concentration). The curves were fitted to logistic dose-response functions, giving an IC_{50} of 2.4 μM for $NiCl_2$ inhibition and 58.8 μM for $CdCl_2$ inhibition. *C*, kinetics of mibefradil (*mib*)- and flunarizin (*flu*)-induced I_T inhibition. On the *top* of the *panel* is shown the membrane current at different times of the experiment (*a–e*). *D*, I/V curves in the absence (*solid circles*) and presence (*open triangles*) of 20 μM mibefradil. *E*, increasing concentrations of mibefradil dose-dependently inhibited I_T. *F*, *bar chart* summary of mibefradil- and flunarizin-induced I_T inhibitions (mibefradil 1 μM: n = 3; 5 μM: n = 16; 20 μM: n = 8; flunarizin: n = 3).

ized to the amount of mRNA coding in the same sample for GAPDH, the expression of which was unaffected by treatments. Analysis of GAPDH was also useful as quality control for the RNA extraction procedure. All the treatments led to an enhanced expression of the α_{1H} messenger after 3 days. A treatment for 3 days with Bt_2cAMP increased by 2.6-fold the ratio α_{1H}/GAPDH. The most efficient treatment was the combination of both Bt_2cAMP and IBMX which increased by 5-fold the α_{1H} mRNA expression. This increased expression of α_{1H} mRNA was time-dependent since no significant increase could be obtained after 1 day of treatment (Fig. 6*B*).

The α_{1H} T-type Calcium Channel Is Involved in a Window Calcium Current Promoting Calcium Entry at Resting Potentials—We then studied the involvement of the α_{1H} calcium channel in calcium homeostasis of LNCaP cells. T-type calcium channels generate transient inward currents which rapidly inactivate (exponential time constant 20 ms in our experiments). It was previously shown in other cell models that there may be a range of membrane potentials at which T-type calcium channels are activated, even partially, and at which inactivation is not complete (26). There should thus exist a window of potential allowing a sustained calcium current. From the inactivation curves and the current voltage relationship (Fig. 3), we computed the relative activation and inactivation conductance and fitted them to a Boltzmann equation. The window current was calculated by multiplying the normalized inactivation curve (Fig. 7*A*) by the non-normalized activation curve. As shown in Fig. 7*B*, the maximum predicted window current is significant from −40 to −20 mV with a peak at −30 mV. Therefore, there should be a sustained calcium entry at these membrane potentials occurring through T-type calcium channels. We measured the resting membrane potential of LNCaP cells and found it to be very close to −30 mV. Control cells had a resting membrane potential of −29.9 ± 1.4 mV (n = 10), whereas Bt_2cAMP-treated cells and Bt_2cAMP + IBMX-treated cells had a resting membrane potential of −35.3 ± 3.8 mV (n = 10) and −34 ± 4 mV (n = 5), respectively. These data show that T-type calcium channels may be open at resting potential in LNCaP cells. We carried out experiments to assess whether this putative window calcium current could lead to a basal sustained calcium entry and thus to higher cytosolic calcium levels in differentiated cells. Cells were loaded with 2 μM Fura-2/AM to measure cytosolic free calcium concentration. As shown in Fig. 8*A*, the basal calcium concentration of LNCaP cells was altered by a 3-day pretreatment with Bt_2cAMP, 8-Br-cAMP (Br-cAMP), or IBMX. In all cases, the average basal calcium concentration (n = 100 to 200 cells) was significantly higher in treated cells than in non-treated cells (46.2 ± 0.9, 61.4 ± 2.1, 55.7 ± 1.6, and 61.8 ± 1.8 nM for CTL, Bt_2cAMP, 8-Br-cAMP, and IBMX-treated cells, respectively). Differences were small (10–15 nM) but were significant and reproduced with 5 different batches of cells. We investigated the ability of $NiCl_2$ to decrease the basal-free calcium concentration in both control and treated cells. Mibefradil was not used in these experiments since it appeared to have side effects and in addition to block calcium entry, was also able to produce a calcium rise in some cells (not shown). Fig. 8, *B* and *C*, show the relative variation of $[Ca^{2+}]_i$ after the application of different concentrations of $NiCl_2$. As shown in Fig. 8*B*, $NiCl_2$ (20 μM) was much more effective to reduce $[Ca^{2+}]_i$ in cells treated 3–4 days with Bt_2cAMP or IBMX ($\Delta[Ca^{2+}]_i$ = −28.8 ± 2.9 and −21.6 ± 2.5 nM, respectively) than in control cells ($\Delta[Ca^{2+}]_i$ = −4 ± 0.9 nM). Cells treated with 8-Br-cAMP (1 mM) were also more sensitive to $NiCl_2$ than control cells (maximal $\Delta[Ca^{2+}]_i$ = −12.7 ± 2.3 nM). As shown in Fig. 8*C*, the reduction of $[Ca^{2+}]_i$ by $NiCl_2$ was dose-dependent with a concentration of 5 μM being only half effective as 20 μM in decreasing the basal cytosolic calcium concentration in Bt_2cAMP-treated cells. In addition, we observed that the basal calcium entry was inhibited by potassium depolarization (KCl, 100 mM) and that an application of $NiCl_2$ (20 μM) during depolarization, which should lead to full inactivation of T-type calcium channels, was not anymore able to reduce the cytosolic calcium concentration (not shown).

Physiological Implication of Voltage-dependent Calcium Channels—To identify the putative involvement of T-type calcium channels in prostate cell physiology, we first studied the influence, on voltage-dependent calcium currents, of steroid reduction, previously reported to induce neuroendocrine differentiation (10, 11). Indeed, LNCaP cells cultured in steroid-reduced conditions displayed a morphological differentiation as shown on Fig. 9 by the extension of neurites. In steroid-reduced conditions, most LNCaP cells (59.6 ± 7.7%, n = 44) displayed a voltage-dependent inward current similar to the Bt_2cAMP-induced current. Steroid reduction induced both an increase in the fraction of cells expressing the voltage-dependent current and the average current density (0.89 ± 0.1 pA/pF). However,

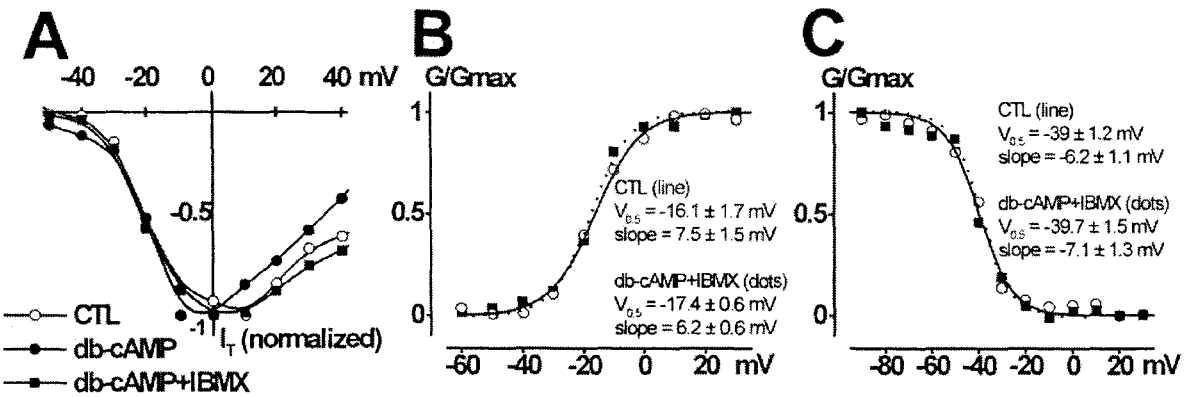

FIG. 5. **A 3–5 days treatment inducing neuroendocrine differentiation does not alter I_T properties.** *A*, normalized I/V curves for control cells (*CTL*), Bt_2cAMP (*db-cAMP*)-treated cells and Bt_2cAMP + IBMX-treated cells. For each curve, the current for each membrane potential was divided by the absolute value of the maximal current. *B*, activation; and *C*, inactivation curves for control cells and Bt_2cAMP + IBMX-treated cells (reversal potential = 80 mV).

TABLE I
Sequence of selected oligonucleotides used as RT-PCR primers

Target	Forward	Reverse	Product size
			bp
α_{1G}	5′-GAGCCCGATTTCTTCTCACC	5′-CGGTGACTTCATCTCGTGG	256
α_{1H}	5′-TCGAGGAGGACTTCCACAAG	5′-TGCATCCAGGAATGGTGAG	177
α_{1I}	5′-AGGATGAGCTATGACCAGCG	5′-CAGAGAGCAGGGACTCATGC	151
α_{1C}	5′-CAAGAGTTGGTGGAGAAGCC	5′-TGAAGCTCAGAGAGTGGTCG	236
α_{1D}	5′-AGCCAACAGTGACAACAAGG	5′-TTCAACTCCGAGATCCTTCG	169
α_{1S}	5′-GATGACGAGGAAGATGAGCC	5′-AAGATGAAGAAGGAGCTGGC	117
α_{1F}	5′-GAGCAGACATGGAGGAGGAG	5′-TGGCTGAGGCAGAAGAAGG	154
GAPDH	5′-GAAGGTGAAGGTCGGAGTC	5′-GAAGATGGTGATGGGATTTC	228

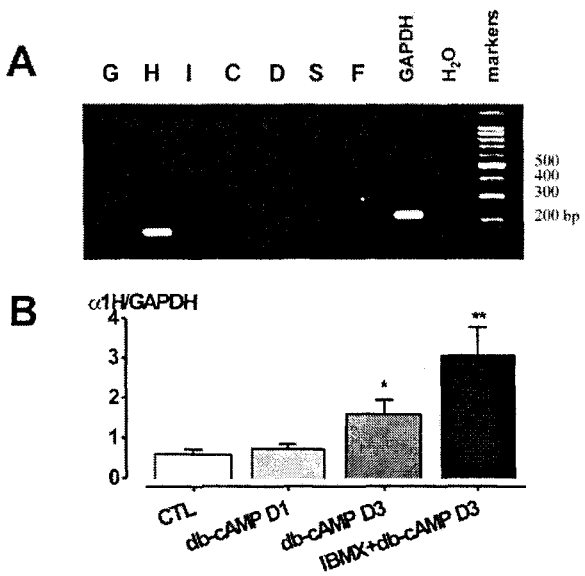

FIG. 6. **T-type α_{1H} calcium channel mRNA is overexpressed in LNCaP cells during neuroendocrine differentiation.** *A*, RT-PCR analysis reveals the presence of α_{1H} mRNA in control cells while other channel isoforms were not detected. mRNA coding for the GAPDH was present and amplified with specific primers in the same experiment. *B*, real-time SYBR Green RT-PCR reveals that all the treatments inducing neuroendocrine differentiation led to an enhanced expression of the α_{1H} messenger after 3 days (*D1* and *D3*, 1 or 3 days treatment, respectively). Results were normalized to the amount of mRNA coding in the same sample for GAPDH, a housekeeping gene, the expression of which was unaffected by treatments. *db-cAMP*, Bt_2cAMP.

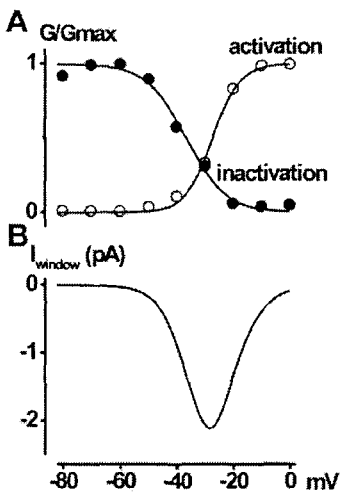

FIG. 7. **T-type calcium channels may carry a window calcium current in differentiated LNCaP cells.** *A*, normalized activation (*open circles*) and inactivation (*solid circles*) conductance curves (holding potential between steps was −100 mV). *B*, predicted window calcium current computed by multiplying the normalized inactivation conductance (*A*) by the activation conductance (not normalized).

the kinetics of both steroid-induced differentiation and the voltage-dependent calcium current induction were much slower than with cAMP permeant analog treatments since neurite extensions were evident after more than 3 days in the absence of steroids and since the calcium current was recorded only after a treatment period of 1 week (only 16.3 ± 3.8% of cells expressed the T-type calcium current after 3 days of treatment, n = 18, Fig. 9). As shown on Fig. 9*A* (*inset*), this calcium current displayed a slow deactivation.

We then investigated the implication of voltage-dependent calcium channels in neurite elongation. Neurite lengths were measured from digital pictures of LNCaP cells (see Fig. 10*A*) cultured for 1 or 5 days in either control or stimulated (1 mM

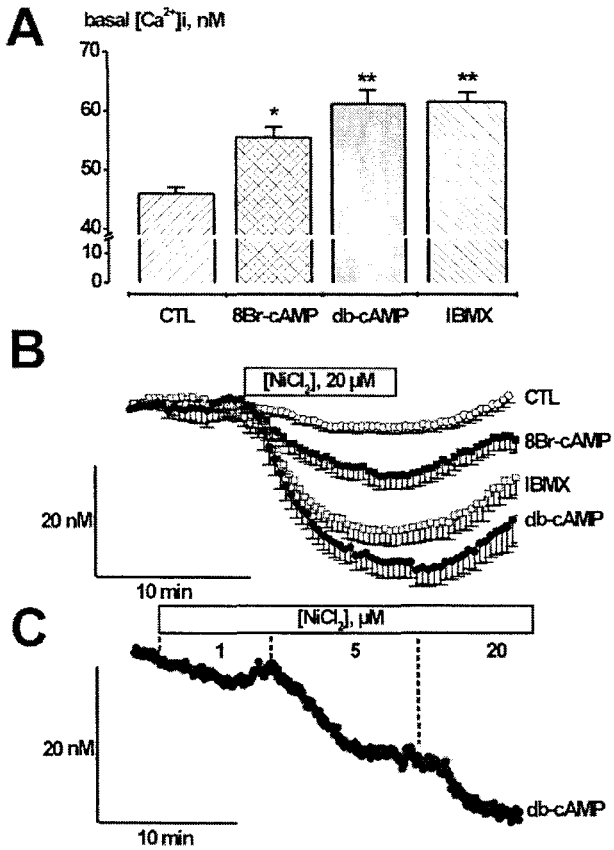

FIG. 8. **Calcium homeostasis is altered during neuroendocrine differentiation induced by increasing cytosolic cAMP concentrations.** *A*, resting calcium concentration ($[Ca^{2+}]_i$) in LNCaP cells after 3 days of treatment (1 mM 8-Br-cAMP, 1 mM Bt_2cAMP (*db-cAMP*), or 100 µM IBMX). *B* and *C*, dynamic $[Ca^{2+}]_i$ recording in Fura 2-loaded LNCaP cells. *B*, a bath application of 20 µM $NiCl_2$ decreases cytosolic resting calcium levels in LNCaP cells, this decrease being more pronounced in differentiated cells. Each trace represents the mean ± S.E. of 100–200 cells for each condition. All the traces were set to the same initial value at the beginning of the plot to compare the variation of $[Ca^{2+}]_i$. *C*, progressively increasing the bath concentration of $NiCl_2$ from 1 to 20 µM induces a staircase decrease in $[Ca^{2+}]_i$ in differentiated cells (the plot represents the mean of 150 cells). Comparisons were performed using an ANOVA followed by a Dunnett post-test.

Bt_2cAMP and 100 µM IBMX) conditions in the absence or presence of $NiCl_2$ (20 µM, 100 µM). cAMP-induced neurite lengthening was not statistically affected by the presence of 20–100 µM $NiCl_2$ if the treatment lasted only 1 day (not shown) but was reduced by 30–37% after a 5-day treatment (Fig. 10*B*). However, the increased expression of NSE induced by a treatment with both Bt_2cAMP and IBMX for 5 days was not modified by the presence of $NiCl_2$ (20 µM, not shown).

DISCUSSION

Neuroendocrine differentiation is a common feature of human prostate carcinoma (2, 3) and is considered to be associated with poor prognosis and reduced long-term survival (4). However, the molecular mechanisms linked to neuroendocrine differentiation development in the prostate epithelium are not fully understood. Therefore, their description are particularly relevant for the future development of therapeutical targets. To this end, different prostatic cell models have been developed, the most widely used being LNCaP prostate cells (5–9) expressing specific markers for neuroendocrine cells like NSE following treatment with cAMP permeant analogs (5, 8, 9). Neuroendocrine cells are generally characterized by the presence of voltage-gated calcium channels. We therefore carried out a study of the expression of such channels in LNCaP cells and followed their evolution during neuroendocrine differentiation. We report here for the first time the evidence of a basal expression of voltage-sensitive calcium channels in prostate cancer cells. Furthermore, and more importantly, we have demonstrated an up-regulation of voltage-gated calcium channels in prostate cancer cells during a treatment inducing a neuroendocrine differentiation as evidenced by a neurite extension and the overexpression of neuron-specific enolase.

The voltage-dependent current recorded in our study inactivates with time and potential and slowly deactivates. These properties are characteristic of T-type calcium currents since high-voltage activated L-, N-, P/Q-, and R-type calcium currents deactivate more rapidly (in less than 200 µs (19, 20)). The voltage-dependent calcium current we observed is certainly carried by a single type of voltage-dependent calcium channel expressed in LNCaP cells since we never observed a tail current deactivating with two exponential time constants. Furthermore, RT-PCR experiments showed the expression of only one subtype belonging to the α_1 subunit family which constitutes the pore subunit. To date, 10 different α_1 subunits have been cloned, among which three (α_{1G}, α_{1H}, and α_{1I}) have the biophysical and pharmacological properties of the native T-type calcium channels when overexpressed in *Xenopus* oocytes or HEK-293 cells (27–30). Our results indicate that prostate cancer cells only express the α_{1H} subunit. This is in good agreement with studies showing that the α_{1H} subunit is mostly distributed in peripheral tissues (28), on the contrary to α_{1G} and α_{1I} subunits expressed in the brain (29, 30). As recently shown (21), the α_{1H} subunit is highly sensitive to $NiCl_2$ (IC_{50} around 5 µM) and this sensitivity provides an assay for the expression of α_{1H} subunits (21, 29). Indeed, we observed that T-type calcium currents in LNCaP cells have a greater sensitivity to $NiCl_2$ (IC_{50} = 2.5 µM) over $CdCl_2$ (IC_{50} = 60 µM). Furthermore, in our study, the calcium current was inhibited by mibefradil, the best T-type calcium channel antagonist to date (22, 23, 31).

Our results clearly show that an α_{1H} T-type calcium channel is overexpressed during neuroendocrine differentiation of LNCaP cells. This was demonstrated by an increase in the average membrane current density paralleled by the overexpression of mRNA coding for the α_{1H} calcium channel isoform. The increase in membrane current was most unlikely due to a protein kinase A-dependent serine-threonine phosphorylation of the channels since changes in the calcium current density were not accompanied by any changes in the current characteristics, *i.e.* time and voltage-dependent activation and inactivation and since short-term applications of Bt_2cAMP were unable to increase the membrane current.

As previously demonstrated (10, 11), we confirm that steroid removal from the culture medium led to a morphological neuroendocrine differentiation with the appearance of neurite extensions after 3 days of culture, a delay much longer than with cAMP permeant analogs. This implies that neuroendocrine differentiation probably occurs through distinct intracellular pathways, as previously hypothesized (11), even if there are few evidences that depletion in androgens can increase intracellular cAMP (32) in prostate LNCaP cells. In addition, androgen removal increased the proportion of cells expressing the T-type calcium current and the overall calcium current density.

Recent studies have demonstrated that the α_{1H} subunit is involved in differentiation of myoblasts in myotubes (33) and that the α_{1G} subunit is differentially expressed during development (30). It seems unlikely that α_{1H} calcium channels are

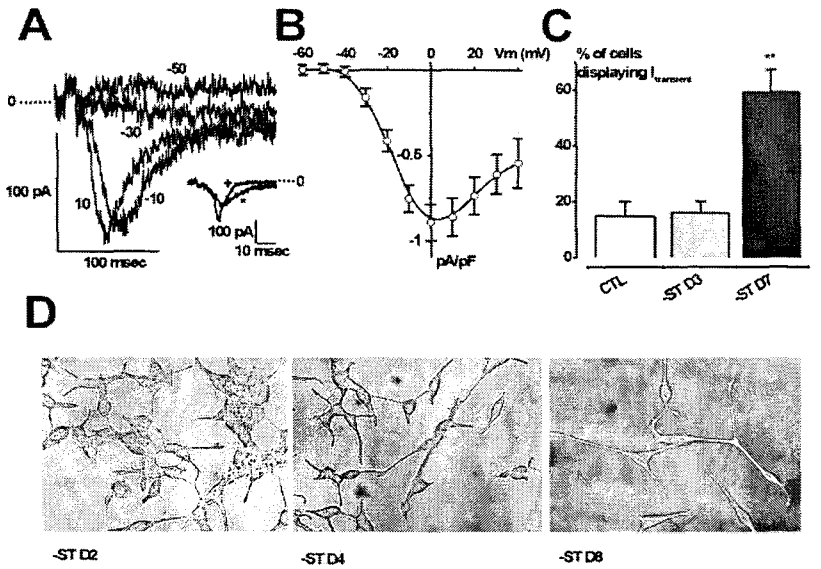

FIG. 9. **Steroid reduction promotes the overexpression of a T-type calcium current.** *A*, examples of membrane currents in a LNCaP cell treated with steroid-reduced medium for 7 days. Membrane potential was depolarized for 100 ms from −80 mV to different values shown next to the respective current recordings (protocol shown in Fig. 2*A*, *inset*). *Inset*, deactivation tail currents measured after a 10-ms prepulse for a repolarization potential (postpulse) of −40 mV (*) or −100 mV (+) (protocol shown in Fig. 3*E*, *inset*). *B*, average I/V relationship for LNCaP cells cultured in steroid-reduced medium. *C*, proportion of cells displaying an inward current following an I/V curve similar to the one shown in *B* after 3 days (−ST D3) and 7 days (−ST D7) of treatment. Comparisons were performed using an ANOVA followed by a Dunnett post-test. *D*, pictures of LNCaP cells after 2 (*left panel*), 4 (*middle panel*), or 8 (*right panel*) days of treatment.

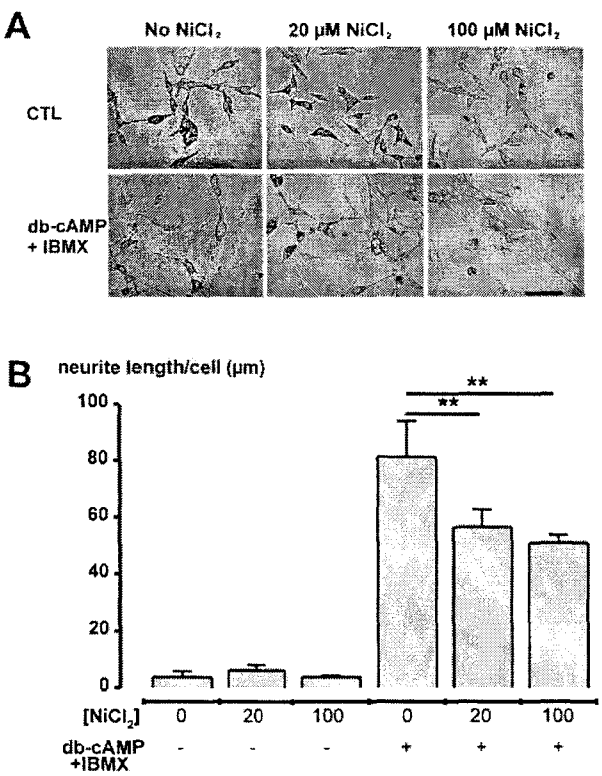

FIG. 10. **T-type calcium channel inhibition reduces the neurite elongation triggered by cAMP permeant analogs.** *A*, pictures of LNCaP cells without (*top panels*) or with 1 mM Bt_2cAMP (*db-cAMP*) and 100 µM IBMX (*bottom panels*). The action of different concentrations of $NiCl_2$ (20 µM, *middle panels*, and 100 µM, *right panels*) was compared with the control situation (*left panels*). *Scale bar*, 50 µm. *B*, bar chart summary of neurite lengths. Comparisons were performed using an ANOVA followed by a Student-Newman-Keuls post-test.

involved in triggering the neuroendocrine differentiation process itself since the morphological differentiation, induced by different stimuli, always preceded the overexpression of voltage-dependent calcium channels. Indeed, we have shown in this study that blocking T-type calcium currents with low concentrations of $NiCl_2$ (20–100 µM) did not impede the extension of neuritic processes triggered by cAMP permeant analogs. However, T-type calcium channels may have a potential role in maintaining neurite growth since long-term treatments (5 days) with $NiCl_2$ decreased cAMP-induced neurite lengthening by 30%. Further studies, using antisense and transfection strategies, will be necessary to delineate the involvement of α_{1H} calcium channels in prostate cancer cell physiopathology. Neuroendocrine differentiation is also associated with synchronization in phase G_1 of the cell cycle, cell growth arrest, and increased neuropeptide and prostate-specific antigen secretion in LNCaP cells (5, 8). Therefore, it will be of particular interest to assess α_{1H} calcium channels' role in cell growth and secretion. Indeed, T-type calcium channels have been suspected to be critical for cell cycle progression (34, 35) and were reported to be overexpressed in proliferating cells (36, 37). However, since transfection with different α_1 subunits corresponding to the LVA channel (G and H) does not modulate the proliferation HEK-293 cells, the evidence for a role of T-type calcium channels in cell proliferation are still very weak and remain debatable (38) and has to be determined in prostate cells. If this is the case, our data, when compared with the literature, would tend to attribute an inhibitory role for LVA calcium channels in cell growth.

We have shown that the T-type calcium channel continuous opening at resting membrane potential allows calcium entry, via a so-called calcium window current. We thus demonstrate that this α_{1H} calcium channel is involved in calcium homeostasis and that cytosolic calcium concentrations are modified during neuroendocrine differentiation, due to the overexpression of α_{1H} calcium channels, induced by permeant analogs of cAMP or IBMX. Such window currents occurring through T-type calcium channels have been reported in other cells (26, 29, 38). This slight increase in cytosolic calcium concentration may serve in facilitating neurite growth, as proposed in nerve cells (15). Furthermore, it is now well established that calcium homeostasis mechanisms are involved in the control of cell death (39). In prostate cancer cells, we have previously shown that altering intracellular calcium concentration may lead to apoptosis (40). It is therefore possible that calcium entry through α_{1H} calcium channels may be implicated in prostate cell death as it was described for T-type calcium channels in cytokine-induced cell death of pancreatic β cells (41) and in neuronal cells expressing expanded androgen receptors (42).

The role of T-type calcium channels may also be of great

importance in the control neuropeptide secretion by neuroendocrine prostate cells. Indeed, it was shown that secretion of mitogenic peptides by LNCaP cells is enhanced during neuroendocrine differentiation (5). Furthermore, it is known that calcium is the main ion involved in the control of exocytosis in many cell models and a fundamental role has been shown for L-type and N- and P/Q-type calcium channels in neuroendocrine cells (43). Few studies have demonstrated a direct role of T-type calcium channels in exocytosis (44). Since neuroendocrine differentiation of prostate cancer cells is associated with an increase in secretory granule number in the cytoplasm (8), an increase in serotonin immunofluorescence, in secretion of neurotensin and PTH-related peptides (5), it is conceivable that overexpression of α_{1H} T-type calcium channels would participate in triggering secretion in these cells. In relation to the role of α_{1H} T-type calcium channels in secretion, we cannot exclude that the reduction of neurite lengthening by $NiCl_2$ we have observed in our study may be due to the inhibition of secretion of paracrine factors having a growth/neurotrophic activity.

In summary, this study demonstrates for the first time the overexpression of voltage-gated T-type calcium channels in prostate cancer cells during neuroendocrine differentiation. Since neuroendocrine differentiation is a common feature of prostate cancer, the functional expression of these calcium channels could have fundamental consequences in understanding the etiology of prostate cancer. Future studies performed on prostate tissue obtained from surgery will be necessary to assess the expression of these channels, and particularly in the late stages of the disease when neuroendocrine differentiation develops.

Acknowledgments—We are particularly grateful to A. Chiappe for excellent technical assistance. We thank Drs. E.-M. Gutknecht and P. Weber for providing us with mibefradil (F. Hoffmann-La Roche, Basel, Switzerland).

REFERENCES

1. Bonkhoff, H. (1998) *Prostate Suppl.* **8,** 18–22
2. Abrahamsson, P. A. (1999) *Prostate* **39,** 135–148
3. di Sant'Agnese, P. A. (1992) *Cancer* **70,** 254–268
4. Cohen, R. J., Glezerson, G., Haffejee, Z., and Afrika, D. (1990) *Br. J. Urol.* **66,** 405–410
5. Cox, M. E., Deeble, P. D., Lakhani, S., and Parsons, S. J. (1999) *Cancer Res.* **59,** 3821–3830
6. Qiu, Y., Robinson, D., Pretlow, T. G., and Kung, H. J. (1998) *Proc. Natl. Acad. Sci. U. S. A.* **95,** 3644–3649
7. Mori, S., Murakami-Mori, K., and Bonavida, B. (1999) *Biochem. Biophys. Res. Commun.* **257,** 609–614
8. Bang, Y. J., Pirnia, F., Fang, W. G., Kang, W. K., Sartor, O., Whitesell, L., Ha, M. J., Tsokos, M., Sheahan, M. D., Nguyen, P., Niklinski, W. T., Myers, C. E., and Trepel, J. B. (1994) *Proc. Natl. Acad. Sci. U. S. A.* **91,** 5330–5334
9. Cox, M. E., Deeble, P. D., Bissonette, E. A., and Parsons, S. J. (2000) *J. Biol. Chem.* **275,** 13812–13818
10. Zi, X., and Agarwal, R. (1999) *Proc. Natl. Acad. Sci. U. S. A.* **96,** 7490–7495
11. Zelivianski, S., Verni, M., Moore, C., Kondrikov, D., Taylor, R., and Lin, M. F. (2001) *Biochim. Biophys. Acta* **1539,** 28–43
12. Garber, S. S., Hoshi, T., and Aldrich, R. W. (1989) *J. Neurosci.* **9,** 3976–3987
13. Solem, M., McMahon, T., and Messing, R. O. (1995) *J. Neurosci.* **15,** 5966–5975
14. Sherwood, N. T., Lesser, S. S., and Lo, D. C. (1997) *Proc. Natl. Acad. Sci. U. S. A.* **94,** 5917–5922
15. Spitzer, N. C., Lautermilch, N. J., Smith, R. D., and Gomez, T. M. (2000) *Bioessays* **22,** 811–817
16. Shitaka, Y., Matsuki, N., Saito, H., and Katsuki, H. (1996) *J. Neurosci.* **16,** 6476–6489
17. Hamill, O. P., Marty, A., Neher, E., Sakmann, B., and Sigworth, F. J. (1981) *Pflugers Arch.* **391,** 85–100
18. Grynkiewicz, G., Poenie, M., and Tsien, R. Y. (1985) *J. Biol. Chem.* **260,** 3440–3450
19. Randall, A. D. (1998) *J. Membr. Biol.* **161,** 207–213
20. Matteson, D. R., and Armstrong, C. M. (1986) *J. Gen. Physiol.* **87,** 161–182
21. Lee, J. H., Gomora, J. C., Cribbs, L. L., and Perez-Reyes, E. (1999) *Biophys. J.* **77,** 3034–3042
22. Rossier, M. F., Ertel, E. A., Vallotton, M. B., and Capponi, A. M. (1998) *J. Pharmacol. Exp. Ther.* **287,** 824–831
23. McDonough, S. I., and Bean, B. P. (1998) *Mol. Pharmacol.* **54,** 1080–1087
24. Dzhura, I., Kostyuk, P., Lyubanova, O., Naidenov, V., and Shuba, Y. (1994) *Neuroreport* **5,** 1960–1962
25. Lesouhaitier, O., Chiappe, A., and Rossier, M. F. (2001) *Endocrinology* **142,** 4320–4330
26. Rossier, M. F., Aptel, H. B., Python, C. P., Burnay, M. M., Vallotton, M. B., and Capponi, A. M. (1995) *J. Biol. Chem.* **270,** 15137–15142
27. Perez-Reyes, E., Cribbs, L. L., Daud, A., Lacerda, A. E., Barclay, J., Williamson, M. P., Fox, M., Rees, M., and Lee, J. H. (1998) *Nature* **391,** 896–900
28. Cribbs, L. L., Lee, J. H., Yang, J., Satin, J., Zhang, Y., Daud, A., Barclay, J., Williamson, M. P., Fox, M., Rees, M., and Perez-Reyes, E. (1998) *Circ. Res.* **83,** 103–109
29. Lee, J. H., Daud, A. N., Cribbs, L. L., Lacerda, A. E., Pereverzev, A., Klockner, U., Schneider, T., and Perez-Reyes, E. (1999) *J. Neurosci.* **19,** 1912–1921
30. Monteil, A., Chemin, J., Bourinet, E., Mennessier, G., Lory, P., and Nargeot, J. (2000) *J. Biol. Chem.* **275,** 6090–6100
31. Martin, R. L., Lee, J. H., Cribbs, L. L., Perez-Reyes, E., and Hanck, D. A. (2000) *J. Pharmacol. Exp. Ther.* **295,** 302–308
32. Burchardt, T., Burchardt, M., Chen, M. W., Cao, Y., de la Taille, A., Shabsigh, A., Hayek, O., Dorai, T., and Buttyan, R. (1999) *J. Urol.* **162,** 1800–1805
33. Bijlenga, P., Liu, J. H., Espinos, E., Haenggeli, C. A., Fischer-Lougheed, J., Bader, C. R., and Bernheim, L. (2000) *Proc. Natl. Acad. Sci. U. S. A.* **97,** 7627–7632
34. Day, M. L., Johnson, M. H., and Cook, D. I. (1998) *Pflugers Arch.* **436,** 834–842
35. Kuga, T., Kobayashi, S., Hirakawa, Y., Kanaide, H., and Takeshita, A. (1996) *Circ. Res.* **79,** 14–19
36. Xu, X. P., and Best, P. M. (1990) *Proc. Natl. Acad. Sci. U. S. A.* **87,** 4655–4659
37. Wang, Z., Estacion, M., and Mordan, L. J. (1993) *Am. J. Physiol.* **265,** C1239–1246
38. Chemin, J., Monteil, A., Briquaire, C., Richard, S., Perez-Reyes, E., Nargeot, J., and Lory, P. (2000) *FEBS Lett.* **478,** 166–172
39. Berridge, M. J., Bootman, M. D., and Lipp, P. (1998) *Nature* **395,** 645–648
40. Skryma, R., Mariot, P., Bourhis, X. L., Coppenolle, F. V., Shuba, Y., Abeele, F. V., Legrand, G., Humez, S., Boilly, B., and Prevarskaya, N. (2000) *J. Physiol.* **527,** 71–83
41. Wang, L., Bhattacharjee, A., Zuo, Z., Hu, F., Honkanen, R. E., Berggren, P. O., and Li, M. (1999) *Endocrinology* **140,** 1200–1204
42. Sculptoreanu, A., Abramovici, H., Abdullah, A. A., Bibikova, A., Panet-Raymond, V., Frankel, D., Schipper, H. M., Pinsky, L., and Trifiro, M. A. (2000) *Mol. Cell Biochem.* **203,** 23–31
43. Lukyanetz, E. A., and Neher, E. (1999) *Eur. J. Neurosci.* **11,** 2865–2873
44. Mansvelder, H. D., and Kits, K. S. (2000) *J. Physiol.* **526,** 327–339

Ca^{2+} homeostasis and apoptotic resistance of neuroendocrine-differentiated prostate cancer cells

K. Vanoverberghe[1], F. Vanden Abeele[1], P. Mariot, G. Lepage, M. Roudbaraki, J. L. Bonnal, B. Mauroy, Y. Shuba[2], R. Skryma, and N. Prevarskaya[3]

Laboratoire de Physiologie Cellulaire, INSERM EMI 0228, USTL Bât. SN3, 59655 Villeneuve d'Ascq, France

[1]These authors contributed equally to this work and should be considered co-first authors

[2]Permanent address: Bogomoletz Institute of Physiology NASU, Bogomoletz Str., 4, 01024 Kiev, Ukraine

[3]Corresponding author:

Laboratoire de Physiologie Cellulaire, INSERM EMI 0228
Université des Sciences et Technologies de Lille, Bât. SN3
59655 Villeneuve d'Ascq, France
Tel. (33) 3 20 33 60 18; Fax: (33) 3 20 43 40 66
Email: phycel@pop.univ-lille1.fr

Running title: Neuroendocrine differentiation and Ca^{2+} homeostasis

Key words: Endoplasmic reticulum - SERCA pump – Calreticulin – Store-operated Ca^{2+} current – Bcl-2

Number of characters: 46265

Abstract

Neuroendocrine (NE) differentiation is a hallmark of advanced, androgen-independent prostate cancer, for which there is no successful therapy. NE tumor cells are non-proliferating and escape apoptotic cell death, therefore an understanding of the apoptotic status of the NE phenotype is imperative for the development of new therapies for prostate cancer. Here, we report for the first time on alterations in intracellular Ca^{2+} homeostasis, whch is a key factor in apoptosis, caused by NE differentiation of androgen-dependent prostate cancer epithelial cells. NE-differentiating regimens, either cAMP elevation or androgen deprivation – resulted in a reduced endoplasmic reticulum Ca^{2+}-store content due both to SERCA 2b Ca^{2+} ATPase and luminal Ca^{2+} binding/storage chaperone calreticulin underexpression, and to a downregulated store-operated Ca^{2+} current. NE-differentiated cells showed enhanced resistance to thapsigargin- and TNF-α-induced apoptosis, unrelated to anti-apoptotic Bcl-2 protein overexpression. Our results suggest that targeting the key players determining Ca^{2+} homeostasis in an attempt to enhance the pro-apoptotic potential of malignant cells, may prove to be a useful strategy in the treatment of advanced prostate cancer.

Introduction

Neuroendocrine differentiation (NE) has been demonstrated in a variety of carcinomas arising in various tissues. Prostatic carcinoma, non-small-cell lung cancer, breast cancer, gastric carcinoma, and colorectal carcinoma are some of the tumors in which neuroendocrine differentiation has been described and suggested as an indicator of poor prognosis. However, the molecular and cellular mechanisms controlling NE differentiation are only partially understood.

Prostate cancer, one of the leading threats to men's health, is dependent on the androgens in the early stages. Consequently, androgen ablation therapies may, at this time, cause a tumor to regress. Nevertheless, these treatments do not prevent evolution to an androgen-independent stage, for which there is currently no successful therapy (1). Therefore, an understanding of what drives the progression to androgen independence is critical. It is well established that androgen-independence is associated with tumor enrichment in cell phenotypes, for which apoptosis inhibition rather than enhanced proliferation is the main feature (2, 3). Malignant neuroendocrine (NE) cells represent one of such phenotypes (4).

NE cells are fully differentiated cells that share structural, functional and metabolic properties with neurons (5). They are a normal component of both the developing and the mature prostate epithelium (4-6), although their origin and functional role is as yet, poorly elucidated. According to the existing hypotheses, NE cells are either derived from undifferentiated basal cells of the prostatic epithelium (7), or have a neurogenic origin (8). It is suggested that by releasing a variety of neurosecretory products, such as parathyroid hormone related peptides, neurotensin, serotonin, calcitonin and bombesin-related peptides (4-6), these cells participate in the regulation of normal development and secretory activity of the prostate in the endocrine/paracrine fashion.

NE cells lack nuclear androgen receptors (9-10) and thus represent an androgen

insensitive cell phenotype in the prostate. Expanding their population beyond normal proportions as a result of malignant transformation of epithelial/basal cells developing dormant NE features, is a common characteristic of prostate cancer progression (4). Tumor enrichment in NE cells and the consequent increase in neurosecretory products with growth-promoting properties, contribute to increases in malignancy and reduce responsiveness to androgen ablation therapy (4-6; 11).

An additional factor that greatly enhances the malignant potential associated with NE differentiation, is that of non-proliferating NE tumor cells escaping apoptotic cell death (3). The mechanisms of NE cells' apoptotis-resistance are still obscure, although existing evidence suggests that they are not associated with the common anti-apoptotic oncoprotein Bcl-2 (12), but are rather triggered by recently discovered survival proteins, such as survivin (13) and clusterin (14). It is obvious that further studies of all aspects of NE cells' apoptotis-resistance are imperative for the development of new therapeutic options in the treatment of advanced prostate cancer.

In a recent study (15) we demonstrated that the apoptotis-resistance of androgen-dependent LNCaP (Lymph Node Carcinoma of the Prostate (16)) prostate cancer epithelial cells, associated with Bcl-2 overexpression, results in a complex rearrangement of the whole intracellular Ca^{2+} homeostasis. The characteristics of this rearrangement are reduced filling of the endoplasmic reticulum (ER) Ca^{2+} store, a decreased expression of key ER Ca^{2+} handling proteins and a substantial down-regulation of store-operated Ca^{2+} current (I_{SOC}). Bcl-2 overexpression is known to transform androgen-dependent LNCaP cells into an androgen-independent phenotype (2). Since LNCaP cells can be differentiated into NE cells (e.g., 17-19) – which are qualitatively different from the Bcl-2-mediated mechanisms of apoptosis-resistance and androgen independence and as it is also known that Ca^{2+} signaling plays a key role in proliferation and

apoptosis (20, 21), we therefore sought in the present study, to examine the type and manner of NE differentiation-induced alterations in Ca^{2+} homeostasis. Our results show for the first time that NE differentiation of prostate cancer epithelial cells causes significant modifications in Ca^{2+} homeostasis, which in their major hallmark features (i.e. the reduced filling of the ER Ca^{2+} store, the decreased expression of both endolemmal SERCA 2b Ca^{2+} ATPase and the luminal Ca^{2+} binding/storage chaperone calreticulin, as well as a substantial I_{SOC} down-regulation) mimicked those associated with Bcl-2 overexpression. This would suggest the existence of common sites for Ca^{2+}-dependent triggering of various anti-apoptotic pathways in androgen-independent prostate cancer. We also show that NE-differentiated LNCaP cells become resistant to thapsigargin- (TG) and TNF-α-induced apoptosis.

Results

LNCaP cells rapidly acquire NE characteristics including the cessation of mitotic activity, the development of neuritic processes and an increased expression of neuron-specific enolase (NSE), under either pharmacological stimulation increasing intracellular cAMP levels, or under physiological stimulations using interleukines or long-term androgen deprivation (17-19; 22). In a previous work (23) we presented evidence of LNCaP cells' NE differentiation in response to interventions that increase intracellular cAMP ($[cAMP]_{in}$) levels. In the present study, we have used both $[cAMP]_{in}$ elevation and long-term androgen deprivation by means of charcoal stripped culture medium, in order to induce NE differentiation of LNCaP cells. The functional results obtained on NE-differentiated LNCaP cells were compared with regular androgen-dependent LNCaP cells, which served as a control.

Neuroendocrine differentiation decreases both ER free Ca^{2+} concentration and store-operated calcium entry. In terms of basic morphological NE characteristics, the two NE-differentiated cell types were similar to those described previously (23). Culturing LNCaP cells for 4 days with a cAMP permeant analog (dibutyryl cAMP, Bt2cAMP 1 mM) plus a phosphodiesterase inhibitor (isobutylmethylxanthine, IBMX 100 μM) or with an androgen-deprived culture medium, induced NE differentiation. In order to comprehend the possible alterations in overall Ca^{2+} homeostasis induced by NE differentiation of LNCaP cells, we used a widely used experimental protocol, which allows the dissection of intracellular Ca^{2+} release from Ca^{2+} entry in a single cell fluorometric measurement of cytosolic free Ca^{2+} concentration ($[Ca^{2+}]_c$). This protocol consisted in Fura-2-loaded cell exposure to a SERCA pump inhibitor, thapsigargin (TG), in nominally Ca^{2+}-free extracellular saline, which should thus reveal the

liberation of only intracellularly stored Ca^{2+}, with the subsequent re-addition of extracellular Ca^{2+} to initiate the influx via activated store-operated Ca^{2+} entry (SOCE). Fig. 1A compares the results of such an experiment in a representative control in LNCaP cell (ctrl-LNCaP) and LNCaP cells differentiated into NE phenotype by either $[cAMP]_{in}$ elevation (NE-cAMP-LNCaP, pre-treatment for 96 hours with 1 mM Bt_2cAMP plus 100 μM IBMX), or by androgen deprivation (NE-Andr(-)-LNCaP). An inspection of $[Ca^{2+}]_c$ traces in Fig. 1A suggests that NE differentiation, irrespectively of how it was achieved, did not affect basal $[Ca^{2+}]_c$ level ($[Ca^{2+}]_{c,\ basal}$), but decreases both the amounts of liberated Ca^{2+} ($[Ca^{2+}]_{c,\ lib}$) and of Ca^{2+} influx ($[Ca^{2+}]_{c,\ SOCE}$). The quantification of basal $[Ca^{2+}]_c$ and its rise due to store-operated Ca^{2+} influx, in up to 240 cells of each type (Fig. 1B), confirmed this conclusion and provided numerical values for $[Ca^{2+}]_{c,\ basal}$ of 52±1.7 nM, 49±1.5 nM and 45±1.6 nM and for $[Ca^{2+}]_{c,\ SOCE}$ of 757±22 nM, 462±34 nM and 509±21 nM in the ctrl-LNCaP, NE-cAMP-LNCaP and NE-Andr(-)-LNCaP cells, respectively. The reductions in $[Ca^{2+}]_{c,\ SOCE}$ were insignificant after 24 hours of initial NE differentiating treatment (irrespective of the nature of the treatment), and became maximal after 96 hours when NE morphological features were fully acquired (e.g., 23).

As $[Ca^{2+}]_{c,\ lib}$ apparently becomes notably lower in NE-differentiated cells too (Fig. 1A), this suggests that their ER Ca^{2+} store content ($[Ca^{2+}]_{ER}$) is lower than that of the control. However, the magnitude of the apparent $[Ca^{2+}]_{c,\ lib}$ signal may not directly reflect $[Ca^{2+}]_{ER}$, as it can be substantially affected by ER-independent Ca^{2+} uptake mechanisms, of the mitochondrial type in particular, which may undergo upregulation during NE differentiation. In order to obtain more direct evidence on the filling status of ER Ca^{2+} store, we performed two additional series of experiments. In the first, we used cell exposure to ionomycin (IM, 1 μM) – a Ca^{2+} ionophore that causes complete ER Ca^{2+} store depletion when incorporated into membranes (24). This was

carried out in nominally Ca^{2+}-free extracellular saline, supplemented with the mitochondrial inhibitors, oligomycin (40 μM) and rotenon (20 μM) (15), in order to provide conditions under which IM-induced $[Ca^{2+}]_{c,\,lib}$ would more fully reflect the actual $[Ca^{2+}]_{ER}$. In the second series, we directly monitored $[Ca^{2+}]_{ER}$ in digitonin-permeabilized cells by means of the compartmentalized fluorescent dye, Mag-fura 2-AM (15).

The summaries of the experiments on the effects of NE differentiation on ER Ca^{2+} store content are presented in Fig. 2. As is evident from individual traces (Fig. 2A), the IM-induced $[Ca^{2+}]_{c,\,lib}$ under inhibited mitochondrial uptake, is about 50% lower in NE-differentiated LNCaP cells than in control cells (i.e., 200±9 nM, n=176 vs. 413±29 nM, n=197). This suggests that their ER Ca^{2+} store content would also be lower by approximately the same percentage. This conclusion was generally confirmed by direct Mag-fura 2-AM $[Ca^{2+}]_{ER}$ measurements, although they provided a somewhat lower $[Ca^{2+}]_{ER}$ decrease (- 35%) following 96 hours of NE differentiation (from 540±35 μM, n=25 to 350±40 μM, n=29, Fig. 2C), whereas 24 hours appeared to be insufficient to produce a statistically significant $[Ca^{2+}]_{ER}$ decrease (Fig. 2B).

NE differentiation reduces a store-operated current. To determine whether or not the reduction in SOCE following NE differentiation, detected in fluorometric experiments, is indeed associated with a decrease in the store-operated membrane Ca^{2+} current (I_{SOC}), we proceeded to record the whole cell-patch clamp of this current both in the control and in the NE-differentiated LNCaP cells. In this series of experiments, we dialyzed cells with a high concentration of BAPTA, a highly potent Ca^{2+} chelator, which rapidly binds Ca^{2+} passively leaking from the ER, thereby causing its depletion, thereby activating I_{SOC} (e.g., 25).

Fig. 3A shows that progression of the dialysis with 10 mM BAPTA containing intracellular solution, caused the development of inward I_{SOC} in all three LNCaP cell types : control and NE-differentiated both by means of $[cAMP]_{in}$ elevation or androgen deprivation. The development of these currents followed comparable time courses, but the maximal densities, reached in about 4 min following the establishment of a whole-cell configuration, were different (Fig. 3A). The I-Vs of fully developed currents in all cell types showed a strong inward rectification and reversal potential at around +40 mV, which is typical of I_{SOC} (Fig. 3B). The quantification of maximal current density at 100 mV and 10 mM Ca^{2+} as a charge carrier, showed that it is the largest of the control LNCaP cells (1.4±0.2 pA/pF, n=12), which however decreases to 0.8±0.1 pA/pF and 0.6±0.1 pA/pF (n=8-9) following 96 hours of NE differentiation by $[cAMP]_{in}$ elevation or androgen deprivation, respectively (Fig. 3C). 24 hours of differentiation were insufficient to reveal statistically significant differences in current densities.

Thus, the data on direct I_{SOC} recordings indicate that the reduction in SOCE observed in NE-differentiated LNCaP cells by fluorometric means, is associated with a decrease in the density of store-operated current.

NE differentiation decreases SERCA 2b and calreticulin expression. One of the mechanisms by which NE differentiation may decrease the Ca^{2+} filling status of the ER, is by affecting the expression of ER-specific Ca^{2+}-handling proteins, such as the endolemmal SERCA pump and/or the luminal Ca^{2+} binding/storage chaperone, calreticulin. We therefore compared the expression of these proteins in both control and NE-differentiated cells, using a semi-quantitative Western blot analysis. We analyzed the expression pattern of three proteins, NSE, Bcl-2 and Bcl-xl. NSE, a neuroendocrine marker, is important in the appreciation of NE differentiation, whereas

the assessment of common anti-apoptotic oncoproteins Bcl-2 and Bcl-xl, may provide a clue about the mechanisms of NE cells' apoptotis-resistance.

Fig. 4A shows that androgen deprivation as well as the $[cAMP]_{in}$ elevation, increase NSE expression (1.84 vs. 1.74-fold respectively). This was also accompanied by a greater decrease in levels of SERCA 2b (0.52 vs. 0.69-fold) and calreticulin (0.48 vs. 0.61-fold). Such expression patterns pointed strongly to the fact that a reduction in both proteins, SERCA pump and calreticulin, constitute a major factor determining decreased ER Ca^{2+} filling status during NE differentiation. Surprisingly, androgen deprivation and $[cAMP]_{in}$ elevation resulted in a notable decrease in Bcl-2 levels (to 0.65 and 0.49 of the control value respectively) and in the Bcl-xl level (to 0.8 and 0.6, figure 4B), suggesting that an anti-apoptotic oncoprotein-independent mechanism contributes to NE cells' apoptotis-resistance.

Androgen deprivation confers resistance to thapsigargin and TNF-α-induced apoptosis. Possible alterations in the NE-differentiated LNCaP cells' potential to resist pro-apoptotic stimuli were assessed using thapsigargin (TG), which has was previously been shown to be an effective experimental inductor of apoptosis in LNCaP cells, through an ER depletion mechanism (26), as well as by using a physiological pro-apoptotic factor, namely TNF-α, acting via a surface membrane death receptor (27). These experiments were conducted on NE-differentiated LNCaP cells by androgen deprivation, as this regimen is more physiological and more relevant from a clinical perspective.

Fig. 5A shows that, in control LNCaP cells, treatment with TG for 48 h induced apoptosis in a dose dependent manner, with a maximal percentage of apoptotic cells observed for 1 μM TG (26±2.1%). Following NE differentiation, the fraction of apoptotic cells was reduced

approximately 2-fold both in the absence of TG, as well as for each TG dose (Fig. 5A), thereby suggesting enhanced apoptotis resistance. The treatment of NE differentiated cells with TG for 72 h did not increase the fraction of apoptotic cells (data not shown), consequently suggesting that the apoptosis in differentiated cells was not delayed.

Qualitatively similar results were obtained with TNF-α (10 ng). This pro-apoptotic factor increased control LNCaP cells' apoptosis nearly 10-fold (from 0.5±0.1% to 5.1±1.4%), but appeared to be completely ineffective in inducing apoptosis of NE-differentiated LNCaP cells (Fig. 5B). The typical apoptotic features induced by treatment with TG or TNF-α are shown in fig. 5C. Apoptosis resistance was also detected by the TUNEL technique (Fig. 6A), thus demonstrating the decrease in LNCaP differentiated cells' apoptosis. Moreover, our results are confirmed by the DNA ladder technique (Fig.6B).

Discussion

In the present study, we report two major findings characterizing NE differentiation in prostate cancer. Firstly, we describe the effect on Ca^{2+} homeostasis manifested through reduced filling of ER Ca^{2+} store, due to the under-expression of major Ca^{2+}-handling proteins, SERCA 2b and calreticulin and the downregulation of store-operated Ca^{2+} entry. Secondly, we demonstrate an enhanced resistance to apoptosis, which is not related to Bcl-2 and Bcl-xl, but, we believe, is a consequence of altered Ca^{2+} homeostasis.

Ca^{2+} homeostasis and apoptosis. The involvement of Ca^{2+}-dependent mechanisms in the induction and regulation of apoptosis is now generally accepted. Although interrelated, depending on the site of action, these mechanisms can be roughly subdivided into mitochondrial, cytoplasmic and ER-dependent types. Mitochondria may respond to high-matrix Ca^{2+}. This might be accumulated as a result of enhanced sequestration, either through a transition in permeability allowing the release of the following : Ca^{2+}, some matrix components as well as an apoptogenic factor, cytochrome c, or perhaps through an enhanced production of reactive oxygen species (28). A rise in cytosolic free Ca^{2+}, which has long been considered as a primary death signal, leads to the activation of the calpain family of Ca^{2+}-dependent proteases participating in apoptosis (e.g., 29), and to the increase in the activity of some caspases (30). Ca^{2+} homeostasis normally plays a pivotal role in the folding and processing of newly synthesized proteins as well as in maintaining the overall physiological state of the cell. When this decreases due to the depletion of ER Ca^{2+} stores, a stress response is activated, leading to growth arrest and cell death (31). It is therefore possible, that disrupting intracellular calcium homeostasis, by the alteration of the way in which

proteins regulating calcium homeostasis are expressed and function, will affect the cell's sensitivity to apoptosis. For example, it was shown that the over-expression of the intraluminal ER protein, calreticulin, increased cell sensitivity to TG- and staurosporine-induced apoptosis and, conversely, that cells lacking calreticulin showed considerable resistance to drug-induced apoptosis (32).

Androgen ablation therapy in prostatic adenocarcinoma induces an involution of prostate tissue mainly through the enhancement of cellular apoptosis (33), which necessarily involves a pro-apoptotic decrease in the ER Ca^{2+} filling status. A fraction of malignant cells withstanding such therapy, would emerge as new populations of apoptotis-resistant cells, for which underfilled ER represents another natural level of functional equilibrium. The enrichment of the prostate with such cell phenotypes eventually causes virtually all tumors to relapse into an androgen-independent, more aggressively growing type.

Apoptotis-resistance in prostate cancer following androgen ablation therapy may evolve through two major pathways: the over-expression of the anti-apoptotic Bcl-2 protein (2) or Bcl-2-independent NE differentiation (3). In a recent study we characterized Ca^{2+} homeostasis in a model system of LNCaP prostate cancer epithelial cells transfected with Bcl-2 (15), and showed that the Bcl-2-conferred apoptotis-resistance on these cells is associated with reduced ER Ca^{2+} content and the substantial downregulation of I_{SOC}. We also showed that reduced ER filling was a consequence of enhanced leakage and the lower expression of the key ER Ca^{2+}-handling proteins, SERCA 2b and calreticulin, whereas diminished I_{SOC} most probably reflected an adaptive decrease in the number of functional channels to the long-term reduction in the ER Ca^{2+} content (15).

The results of our present work show that alterations in Ca^{2+} homeostasis induced by the

NE differentiation of LNCaP cells, which are schematically represented in Fig. 7, basically mimic those of Bcl-2-overexpressing LNCaP cells, in terms of such hallmark features as an underfilled ER Ca^{2+} store, lower levels of ER SERCA 2b and calreticulin and reduced I_{SOC}.

Mechanisms of NE cells apoptotis-resistance. Apoptosis is an extremely rare event in prostate cancer cells with neuroendocrine features in primary, metastatic and recurrent disease (3). Recent studies suggest that the apoptotis-resistance of NE cells may be related to over-expression of new survival proteins, survivin (13) and/or clusterin (34, 14). The first of these is a member of the IAP (inhibitor of apoptosis) family with direct caspase-3 and caspase-7 inhibitory functions (35), whereas the second represents multifunctional glycoprotein, commonly involved in the transport of lipoproteins, the inhibition of complement-mediated cell lysis and the modulation of cell-cell interactions (36). The anti-apoptotic mechanisms of the latter remain to be clarified. Survivin is highly expressed in various common human cancers (e.g., 37-39), but not in normal tissues, and clusterin expression is strongly enhanced in tissues undergoing apoptosis (e.g., 40).

The fact that LNCaP cells undergo similar alterations in Ca^{2+} homeostasis, irrespective of whether their apoptotis-resistance was enhanced by Bcl-2 overexpression or as a result of NE differentiation, suggests that these alterations create a generally favorable environment for the functioning of mechanisms counteracting apoptosis. These alterations are therefore a necessary prerequisite for the cell's ability to successfully withstand pro-apoptotic stimuli. Our previous work showed that NE differentiation of LNCaP cells is also characterized by a strong over-expression of voltage-gated T-type Ca^{2+} channels (23), which seem to be involved in the formation of neuronal-like morphological features (i.e., neurite outgrowth). Whether or not these channels contribute to the enhanced anti-apoptotic potential of NE cells is not yet clear.

Implications for androgen-independent prostate cancer. Apoptosis is essential in maintaining tissue homeostasis. The acquisition of a resistance to apoptosis plays a pivotal role in tumor genesis by disrupting the balance between cell proliferation and cell destruction and also by allowing cancer cells to escape radiation and chemotherapy. Androgen-independent prostate cancer is characterized by tumor enrichment in apoptosis resistant cell phenotypes, which, although differing in specific anti-apoptotic mechanisms, nevertheless shares the same basic changes in intracellular Ca^{2+} homeostasis. It would therefore seem that targeting the key players involved in its maintenance, in an attempt to enhance the pro-apoptotic potential of malignant cells, may prove to be a useful strategy in the treatment of advanced prostate cancer.

In the present work we identify three molecular entities, the expression of which undergoes significant changes (reduction) during the NE differentiation of prostate cancer epithelial cells – calreticulin, SERCA 2b and store-operated channel (SOC). The molecular origin of SOCs is still unknown, but there is strong evidence that the most likely candidate proteins belong to the transient receptor potential (TRP) channel family (e.g., 41-43). Thus, the identification of the specific TRPs involved in endogenous I_{SOC} in prostate cancer cells acquires potentially great practical importance, as they may represent appropriate targets for influencing the apoptotic status of NE cells in advanced, androgen-independent prostate cancer.

Materials and Methods

Cell culture. The human prostatic carcinoma cell line, LNCaP, was obtained from the American Type Culture Collection (Rockville, MD, USA). Cells were grown in RPMI 1640 with 10% decomplemented fetal bovine serum (FBS, Deutcher, Brumath, France) at 37°C in a humidified atmosphere containing 5% CO_2. The medium was supplemented with 300 µg/ml L-glutamine, 100 U/ml penicillin and 100 µg/ml streptomycin. Tissue culture media and supplements were obtained from Life Technologies (Life Technologies, Cergy Pontoise, France). Cells were seeded in 75 cm^2 flasks and the growth medium was renewed every other day.

Prior to fluorescence measurements, the cells were removed from the culture flasks with 0.05% trypsin (Life Technologies, Cergy Pontoise, France), and cultured on glass cover slips in the same culture medium. Cells were then used 2 days after trypsinization.

Charcoal stripped medium. The tube containing charcoal 10% (w/v) and FBS was agitated for 16 hours at 4°C. Following 1 hour's centrifugation at 10000 g and 4°C, the supernatant was collected and centrifuged again for 30 min at 27000 g. The resultant supernatant was filtrated through 0.22 µm filters. Before use, the charcoal stripped FBS was decomplemented for 30 min at 56° C.

Fluorescence $[Ca^{2+}]_c$ measurements and Fluorescence $[Ca^{2+}]_{ER}$ measurements. For both the cytoplasmic and the ER Ca^{2+} imaging, the detailed procedure has been described previously (15, 23).

Electrophysiology and solutions. Membrane currents in LNCaP cells were recorded in the whole-cell configuration of the patch-clamp technique, using a computer controlled EPC-9 amplifier (HEKA Electronic, Germany) as described previously (44). Patch pipettes were made on a PIP- 5 puller (HEKA Electronic, Germany) from borosilicate glass capillaries (WPI, USA). The resistance of the pipettes filled with the basic intracellular pipette solution (in mM): CsCl – 120, $MgCl_2$ – 3, BAPTA – 10, HEPES – 10, pH – 7.3 (adjusted with Cs(OH)) varied between 4-6 MΩ.

The composition of the regular extracellular bath solution was (in mM): NaCl –120, KCl –5, $CaCl_2$ – 2, $MgCl_2$ – 2, glucose – 5, HEPES – 10, pH – 7.3 (adjusted with Na(OH)). The high-Ca^{2+}, Na^+-free extracellular solution used for store-operated Ca^{2+} current recordings contained (in mM): TEA-Cl – 120, $CaCl_2$ – 10, glucose – 5, HEPES – 10, pH – 7.3 (adjusted with TEA(OH)). External solutions were changed using a multibarrel puffing micropipette with common outflow, positioned in close proximity to the cell under investigation. During the experiment, the cell was continuously superfused with the solution *via* a puffing pipette to reduce possible artifacts related to the switch from static to moving solution and vice versa. Complete external solution exchange was achieved in less than 1 s.

Western-blot analysis. Cells were lysed in an ice-cold buffer (pH 7.4) containing (in mM) 20 HEPES, 50 NaCl, 10 EDTA, 1 EGTA, 1 PMSF, 1% NP40 and a mixture of protease inhibitors. After one hour on ice, the lysates were homogenized and centrifuged at 1500 rpm for 10 min at 4° C. The resulting supernatants were stored at -80°C until use. Samples were fractionated in a Laemmli-type SDS-PAGE (16%). The proteins were then transferred onto a nitrocellulose membrane using a semi-dry electroblotter (Bio-Rad). After transfer, the membrane was cut into

thin strips that were further processed for immunodetection. The strips were blocked in TNT (15 mM Tris buffer (pH 8), 140 mM NaCl, 0.05% Tween 20, 3% skimmed dry milk for 30 min at room temperature), washed in TNT 3 times, then incubated with mouse monoclonal antibodies for 1 h at room temperature. After 3 washes in TNT, the strips were treated with the corresponding horseradish peroxydase-linked secondary antibodies (Zymed Laboratoires Inc., San Francisco, CA), for 1 h. After washes in TNT without milk, the strips were processed for chemiluminescent detection using Supersignal West Pico chemiluminescent substrate (Pierce chemical Co., Rockfortd, IL) according to the manufacturer's instructions. Blots were then exposed to X-Omat AR films (Eastman KodakCo., Rochester, NY). Blot intensity was quantified by scanning densitometry (Bio-Rad).

Determination of apoptosis.

The Hoechst technique : The level of apoptosis was estimated from the number of apoptotic bodies visualized by Hoechst staining. The percentage of apoptotic cells was determined by counting at least 500 cells in random fields (the detailed procedure has been described previously (26).

The TUNEL technique : apoptosis was also detected by the TUNEL technique (terminal deoxynucleotide transferase-mediated dUTP-biotin nick-end labelling) using an apoptosis detection kit (Borhringer Mannheim).

DNA fragmentation analysis : Cells ($2x10^6$ cells per sample) were lysed in an extraction buffer (50 mM Tris pH 7.5, 10 mM EDTA, 1% sodium dodecyl sulfate (SDS) and 200 µg/ml proteinase K, 50 µg/ml RNase A) and incubated at 37°C for 6h. DNA was subsequently extracted with phenol/chloroform/isoamyl alcohol (25:24:1) and then precipitated with isopropyl alcohol,

pelleted and resuspended in TE with 20μg/ml Rnase. The DNA was quantitated spectroscopically, and 10 μg of DNA were analyzed for fragmentation on a 1.5 % agarose gel. The gel was stained with ethidium bromide and visualized using a UV light source.

Reagents and chemicals. All chemicals were from Sigma (l'Isle d'Abeau, France) except for fura-2/AM and thapsigargin which were purchased from France Biochem (Meudon, France).

Data analysis and statistics. Each experiment was repeated several times. The data were analyzed using PulseFit (HEKA Electrinics, Germany) and Origin 5.0 (Microcal Software Inc., Northampton, MA, USA). Results were expressed as mean ± standard error of the mean (s.e.m.). Statistical analysis was performed using the student's t test and ANOVA tests, followed by Tukey-Kramer post-tests ($P<0.05$ considered significant).

Acknowledgements

This work was supported by grants from INSERM, La Ligue Nationale Contre le Cancer and l'ARC (France), Association pour la Recherche sur les Tumeurs de la Prostate (ARTP), Fondation pour la Recherche Médicale (FRM), and INTAS-99-01248. Y.M. Shuba was supported by INSERM and the French Ministry of Science.

References

1. Feldman BJ and Feldman D (2001) The development of androgen-independent prostate cancer. Nat Rev Cancer. 1: 34-45.
2. Raffo AJ, Perlman H, Chen MW, Day ML, Streitman JS and Buttyan R (1995) Overexpression of Bcl-2 protects prostate cancer cells from apoptosis in vitro and confers resistance to androgen depletion in vivo. Cancer Res. 55: 4438-4445.
3. Fixemer T, Remberger K and Bonkhoff H (2002) Apoptosis resistance of neuroendocrine phenotypes in prostatic adenocarcinoma. Prostate. 53: 118-123.
4. Abrahamsson PA (1999) Neuroendocrine cells in tumour growth of the prostate. Endocr Relat Cancer. 6: 503-519.
5. di Sant'Agnese PA (1998) Neuroendocrine cells of the prostate and neuroendocrine differentiation in prostatic carcinoma: a review of morphologic aspects. Urology. 51: 121-124.
6. di Sant'Agnese PA (1992) Neuroendocrine differentiation in carcinoma of the prostate. Diagnostic, prognostic, and therapeutic implications. Cancer. 70: 254-268.
7. Bonkhoff H and Remberger K (1996) Differentiation pathways and histogenetic aspects of normal and abnormal prostatic growth: a stem cell model. Prostate. 28: 98-106.
8. Aumuller G, Leonhardt M, Janssen M, Konrad L, Bjartell A and Abrahamssonn PA (1999) Neurogenic origin of human prostate endocrine cells. Urology. 53: 1041-1048.
9. Krijnen JL, Janssen PJ, Ruizeveld de Winter JA, van Krimpen H, Schroder FH and van der Kwast TH (1993) Do neuroendocrine cells in human prostate cancer express androgen receptor? Histochemistry. 100: 393-398.
10. Bonkhoff, H. (2001) Neuroendocrine differentiation in human prostate cancer.

Morphogenesis, proliferation and androgen receptor status. Ann Oncol. 12: S141-144.

11. Ito T, Yamamoto S, Ohno Y, Namiki K, Aizawa T, Akiyama A and Tachibana M (2001) Up-regulation of neuroendocrine differentiation in prostate cancer after androgen deprivation therapy, degree and androgen independence. Oncol Rep. 8: 1221-1224.
12. Xue Y, Verhofstad A, Lange W, Smedts F, Debruyne F, de la Rosette J and Schalken J (1997) Prostatic neuroendocrine cells have a unique keratin expression pattern and do not express Bcl-2: cell kinetic features of neuroendocrine cells in the human prostate. Am J Pathol. 151: 1759-1765.
13. Xing N, Qian J, Bostwick D, Bergstralh E and Young CY (2001) Neuroendocrine cells in human prostate over-express the anti-apoptosis protein survivin. Prostate. 48: 7-15.
14. July LV, Akbari M, Zellweger T, Jones EC, Goldenberg SL and Gleave ME (2002) Clusterin expression is significantly enhanced in prostate cancer cells following androgen withdrawal therapy. Prostate. 50: 179-188.
15. Vanden Abeele F, Skryma R, Shuba Y, Van Coppenolle F, Slomianny C, Roudbaraki M, Mauroy B, Wuytack F and Prevarskaya N (2002) Bcl-2-dependent modulation of Ca(2+) homeostasis and store-operated channels in prostate cancer cells. Cancer Cell. 1: 169-179.
16. Horoszewicz JS, Leong SS, Kawinski E, Karr JP, Rosenthal H, Chu TM, Mirand EA and Murphy GP (1983) LNCaP model of human prostatic carcinoma. Cancer Res. 43: 1809-1818.
17. Bang YJ, Pirnia F, Fang WG, Kang WK, Sartor O, Whitesell L, Ha MJ, Tsokos M, Sheahan MD and Nguyen P (1994) Terminal neuroendocrine differentiation of human prostate carcinoma cells in response to increased intracellular cyclic AMP. Proc Natl Acad Sci U S A. 91: 5330-5334.

18. Burchardt T, Burchardt M, Chen MW, Cao Y, de la Taille A, Shabsigh A, Hayek O, Dorai T and Buttyan R (1999) Transdifferentiation of prostate cancer cells to a neuroendocrine cell phenotype in vitro and in vivo. J Urol. 162: 1800-1805.

19. Zelivianski S, Verni M, Moore C, Kondrikov D, Taylor R and Lin MF (2001) Multipathways for transdifferentiation of human prostate cancer cells into neuroendocrine-like phenotype. Biochim Biophys Acta. 1539: 28-43.

20. Berridge MJ, Bootman MD and Lipp P (1998) Calcium-a life and death signal. Nature. 395: 645-648.

21. McConkey DJ and Orrenius S (1997) The role of calcium in the regulation of apoptosis. Biochem Biophys Res Commun. 239: 357-366.

22. Deeble PD, Murphy DJ, Parsons SJ and Cox ME (2001) Interleukin-6- and cyclic AMP-mediated signaling potentiates neuroendocrine differentiation of LNCaP prostate tumor cells. Mol Cell Biol. 21: 8471-8482.

23. Mariot P, Vanoverberghe K, Lalevée N, Rossier MF and Prevarskaya N (2002) T-type calcium channel during neuroendocrine differentiation of human prostate cancer cells. J Biol Chem. 277: 10824-10833.

24. Huang Y and Jr Putney JW (1998) Relationship between intracellular calcium store depletion and calcium release-activated calcium current in a mast cell line (RBL-1). J Biol Chem. 273: 19554-19559.

25. Hoth M and Penner R (1993) Release-activated calcium current in rat mast cells. J Physiol. 465: 359-386.

26. Skryma R, Mariot P, Bourhis XL, Coppenolle FV, Shuba Y, Vanden Abeele F, Legrand G, Humez S, Boilly B and Prevarskaya N (2000) Store depletion and store-operated Ca2+

current in human prostate cancer LNCaP cells: involvement in apoptosis. J Physiol. 527: 71-83.

27. Ashkenazi A and Dixit VM (1998) Death receptors: signaling and modulation. Science. 281: 1305-1308.

28. Kass GE and Orrenius S (1999) Calcium signaling and cytotoxicity. Environ Health Perspect. 107: 25-35.

29. Mathiasen IS, Sergeev IN, Sergeev L, Bastholm F, Elling AW, Norman and Jaattela M (2002) Calcium and calpain as key mediators of apoptosis-like death induced by vitamin D compounds in breast cancer cells. J Biol Chem. 277: 30738-30745.

30. Juin P, Pelletier M, Oliver L, Tremblais K, Gregoire M, Meflah K and Vallette FM (1998) Induction of a caspase-3-like activity by calcium in normal cytosolic extracts triggers nuclear apoptosis in a cell-free system. J Biol Chem. 273: 17559-17564.

31. Paschen W and Doutheil J (1999) Disturbance of endoplasmic reticulum functions: a key mechanism underlying cell damage? Acta Neurochir Suppl. (Wien) 73: 1-5.

32. Nakamura K, Bossy-Wetzel E, Burns K, Fadel MP, Lozyk M, Goping IS, Opas M, Bleackley RC, Green DR, Michalak M (2000) Changes in endoplasmic reticulum luminal environment affect cell sensitivity to apoptosis. J Cell Biol. 150(4): 731-740.

33. Montironi R, Pomante R, Diamanti L and Magi-Galluzzi C (1998) Apoptosis in prostatic adenocarcinoma following complete androgen ablation. Urol Int. 60: 25-39.

34. Lee C, Janulis L, Ilio K, Shah A, Park I, Kim S, Cryns V, Pins M and Bergan R (2000) In vitro models of prostate apoptosis: clusterin as an antiapoptotic mediator. Prostate Suppl. 9: 21-24.

35. Yamamoto T and Tanigawa N (2001) The role of survivin as a new target of diagnosis and

treatment in human cancer. Med Electron Microsc. 34: 207-212.

36. Koch-Brandt C and Morgans C (1996) Clusterin: a role in cell survival in the face of apoptosis? Prog Mol Subcell Biol. 16: 130-149.

37. Takai N, Miyazaki T, Nishida M, Nasu K and Miyakawa I (2002) Expression of survivin is associated with malignant potential in epithelial ovarian carcinoma. Int J Mol Med. 10: 211-216.

38. Nasu S, Yagihashi A, Izawa A, Saito K, Asanuma K, Nakamura N, Kobayashi D, Okazaki M and Watanabe N (2002) Survivin mRNA expression in patients with breast cancer. Anticancer Res. 22: 1839-1843.

39. Kajiwara Y, Yamasaki F, Hama S, Yahara K, Yoshioka H, Sugiyama K, Arita K and Kurisu K (2003) Expression of survivin in astrocytic tumors. Cancer. 97: 1077-1083.

40. Viard I, Wehrli P, Jornot L, Bullani R, Vechietti JL, Schifferli JA, Tschopp J and French LE (1999) Clusterin gene expression mediates resistance to apoptotic cell death induced by heat shock and oxidative stress. J Invest Dermatol. 112: 290-296.

41. Clapham DE, Runnels LW and Strubing C (2001) The TRP ion channel family. Nat Rev Neurosci. 2: 387-396.

42. Minke B and Cook B (2002) TRP channel proteins and signal transduction. Physiol Rev 82: 429-472.

43. Venkatachalam K, van Rossum DB, Patterson RL, Ma HT and Gill DL (2002) The cellular and molecular basis of store-operated calcium entry. Nat Cell Biol. 4: E263-E272.

44. Vanden Abeele F, Roudbaraki M, Shuba Y, Skryma R and Prevarskaya N (2003) Store-operated Ca2+ Current in Prostate Cancer Epithelial Cells. ROLE OF ENDOGENOUS Ca2+ TRANSPORTER TYPE 1. J Biol Chem. 278: 15381-9.

Figure Legends

Figure 1. **NE differentiation of LNCaP cells reduces thapsigargin-induced Ca^{2+} influx, but does not affect basal Ca^{2+}.** (A) Representative experiments on thapsigargin- (TG, 1 μM) induced changes in cytoplasmic Ca^{2+} concentration ($[Ca^{2+}]_c$, measured using fura-2 fluorescence) in LNCaP control cells (ctrl-LNCaP) and NE-differentiated LNCaP cells by $[cAMP]_{in}$ elevation (NE-cAMP-LNCaP) or androgen deprivation (NE-Andr(-)-LNCaP); periods of TG application and extracellular Ca^{2+} elevation from 0 mM (0/Ca) to 2 mM (2/Ca) are marked by horizontal bars; see text for details. (B) Quantification of basal cytoplasmic Ca^{2+} concentration ($[Ca^{2+}]_{c,basal}$) and store-operated Ca^{2+} entry ($[Ca^{2+}]_{c,SOCE}$) in the control LNCaP cells (ctrl-LNCaP) and two types of NE-differentiated LNCaP cells (NE-cAMP-LNCaP and NE-Andr(-)-LNCaP); mean±s.e.m., n=173-239.

Figure 2. **NE differentiation of LNCaP cells reduces ER Ca^{2+} content.** (A) Representative experiments on ionomycin (1 μM) induced Ca^{2+} liberation ($[Ca^{2+}]_c$, which was measured using fura-2 fluorescence) from the ER in the LNCaP control cells (ctrl-LNCaP) and NE-differentiated LNCaP cells (NE-cAMP-LNCaP) bathed in nominally Ca^{2+}-free extracellular saline (0/Ca) supplemented with the mitochondrial inhibitors, oligomycin (40 μM) and rotenon (20 μM); mean±s.e.m., n=197-176; see text for details. (B) The quantification of the ER intraluminal Ca^{2+} concentration ($[Ca^{2+}]_{ER}$, measured in digitonin-permeabilized cells based on Mag-fura 2AM fluorescence) in the LNCaP control cells (ctrl-LNCaP) and LNCaP cells subjected to NE-differentiating treatment (NE-cAMP-LNCaP) with Bt_2cAMP (1 mM) plus IBMX (100 μM) 1 and

4 days after treatment initiation; mean±s.e.m., n=25-29; see text for details.

Figure 3. **NE differentiation of LNCaP cells reduces store-operated Ca^{2+} current.** (A) Representative time-courses of store-operated Ca^{2+} current development (I_{SOC}, normalized to membrane capacitance to yield current density) in response to 10 mM BAPTA infusion in the control LNCaP cells (ctrl-LNCaP) and NE-differentiated LNCaP cells by $[cAMP]_{in}$ elevation (NE-cAMP-LNCaP) or androgen deprivation (NE-Andr(-)-LNCaP) at 10 mM $[Ca^{2+}]_{out}$ and V_m=-100 mV; Inset shows example of original baseline (1) and fully developed (2) currents together with voltage-clamp protocol. (B) Representative I-V relationships of I_{SOC} in control (ctrl-LNCaP) and NE-differentiated (NE-cAMP-LNCaP and NE-Andr(-)-LNCaP) cells derived from currents in response to voltage ramps. (C) The quantification of maximal I_{SOC} density at −100 mV in the control LNCaP cells (ctrl-LNCaP) and LNCaP cells subjected to NE-differentiating treatments by $[cAMP]_{in}$ elevation (NE-cAMP-LNCaP) or androgen deprivation (NE-Andr(-)-LNCaP) 1 and 4 days after treatment initiation; mean±s.e.m., n=12-8-9 respectively; see text for details.

Figure 4. **NE differentiation of LNCaP cells alters the expression of the ER Ca^{2+}-handling proteins.** Semi-quantitative Western blots (after 30 μg per well of total protein extraction for Bt_2cAMP + IBMX treatment and 50 μg per well of total protein extraction for androgen deprivation) showing (A) increased expression of the NE marker neuron-specific enolase (NSE) and under-expression of the endolemmal SERCA 2b Ca^{2+} pump, the luminal Ca^{2+} binding/storage chaperone calreticulin, and the anti-apoptotic Bcl-2 and (B) Bcl-xl proteins in LNCaP cells subjected to 96 hours of NE-differentiating treatments by $[cAMP]_{in}$ elevation (NE-cAMP-LNCaP) or androgen deprivation (NE-Andr(-)-LNCaP) compared to the controls (ctrl-

LNCaP). Actin expression was assessed to ensure identical experimental conditions. All stains in Fig 4A were performed on a single membrane at the same time, except in the case of the Bcl-xl protein, where we have added the corresponding actin control (Fig 4B).

Figure 5. **NE differentiation of LNCaP cells enhances their anti-apoptotic potential.** (A) Bar graph showing the muchlower percentage of apoptotic NE-differentiated LNCaP cells (after 96 hours of androgen deprivation, NE-Andr(-)-LNCaP) in response to two concentrations of thapsigargin (TG, 0.1 μM and 1 μM) for 48 hours compared to the control LNCaP cells (ctrl-LNCaP); "***" denotes $P<0.01$. (B) Same as in (A), but for 10 ng/ml TNF-α. (C) Illustration of the typical apoptotic features with the hoechst technique in each condition, (a, b, c) are ctrl-LNCaP cells (a), LNCaP cells with TG 1 μM (b) or TNF-α 10 ng/ml (c) ; (d, e, f) represent NE-Andr(-)-LNCaP cells (d), NE-Andr(-)-LNCaP cells with TG 1 μM (e) or TNF-α 10 ng/ml (f).

Figure 6. **Apoptosis detection in control and differentiated LNCaP prostate cells using the TUNEL and the DNA ladder techniques.** (A) the TUNEL technique, a and d showing undifferentiated control cells and differentiated LNCaP cells respectively; (b, c) represent undifferentiated cells treated for 48 h with TG 1 μM or TNF-α 10ng/ml respectively ; (e, f) represent the same as in (b and c) but with differentiated cells. The DNA ladder technique (B) shows a reduction in the DNA fragmentation of differentiated LNCaP cells under TNF-α 10 ng/ml treatment for 48 hours.

Figure 7. **Schematic diagram showing the major effects of prostate cancer cells neuroendocrine differentiation on Ca^{2+} homeostasis.** The left-hand panel presents the control

conditions characterized by basal expression of the ER leak channels, the SERCA pump, the intraluminal calreticulin (CRT) and the plasma membrane SOCs, which when taken together, result in the background ER Ca^{2+} concentration and store-operated Ca^{2+} entry (I_{SOC}, see upper left graph) typical of control, androgen-dependent prostate cancer epithelial cells. Neuroendocrine differentiation (right-hand panel) results in an ER intraluminal Ca^{2+} concentration which had been lowered through the downregulated expression of SERCA pump and CRT, and decreased store-operated Ca^{2+} entry, which was most probably associated with the diminished density of functional SOCs.

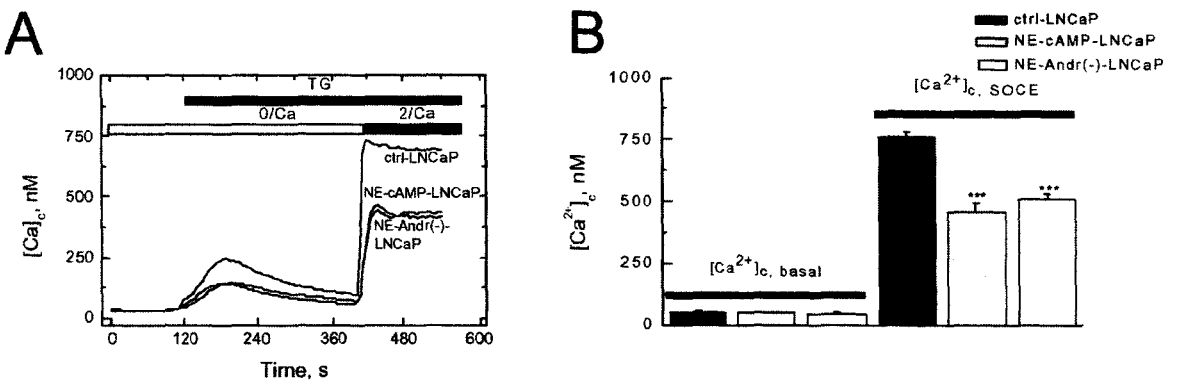

Figure 1

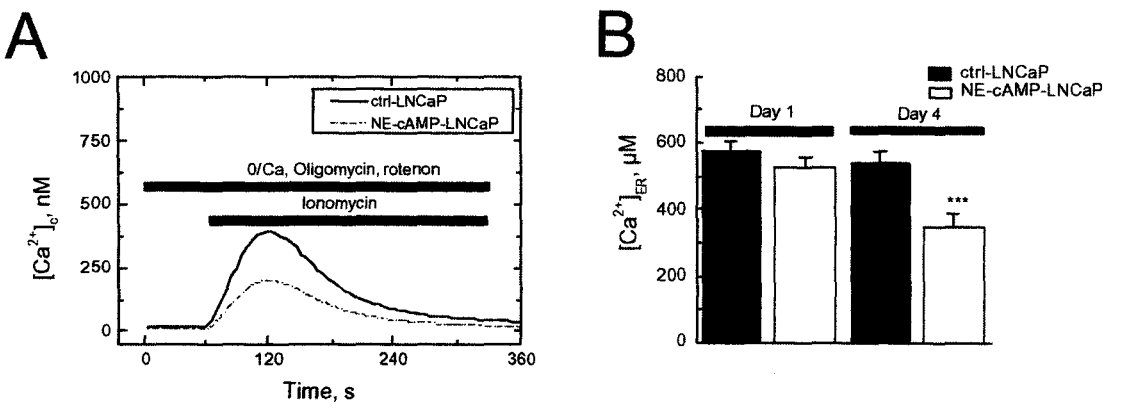

Figure 2

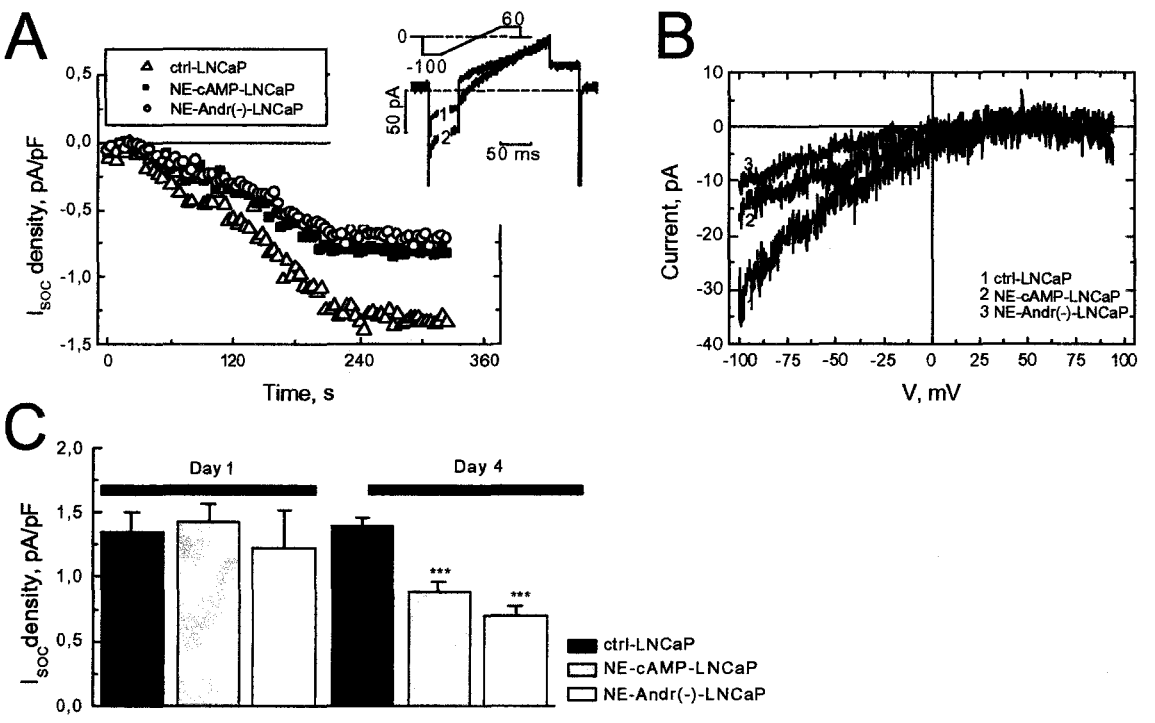
A
ctrl-LNCaP
NE-cAMP-LNCaP
NE-Andr(-)-LNCaP
0,5
0,0
-0,5
-1,0
-1,5
I_{soc} density, pA/pF
0
120
240
360
Time, s
60
0
-100
50 pA
50 ms
1
2
B
10
0
-10
-20
-30
-40
Current, pA
-100 -75 -50 -25 0 25 50 75 100
V, mV
1 ctrl-LNCaP
2 NE-cAMP-LNCaP
3 NE-Andr(-)-LNCaP
C
2,0
1,5
1,0
0,5
0,0
I_{soc} density, pA/pF
Day 1
Day 4
***
***
ctrl-LNCaP
NE-cAMP-LNCaP
NE-Andr(-)-LNCaP

Figure 3

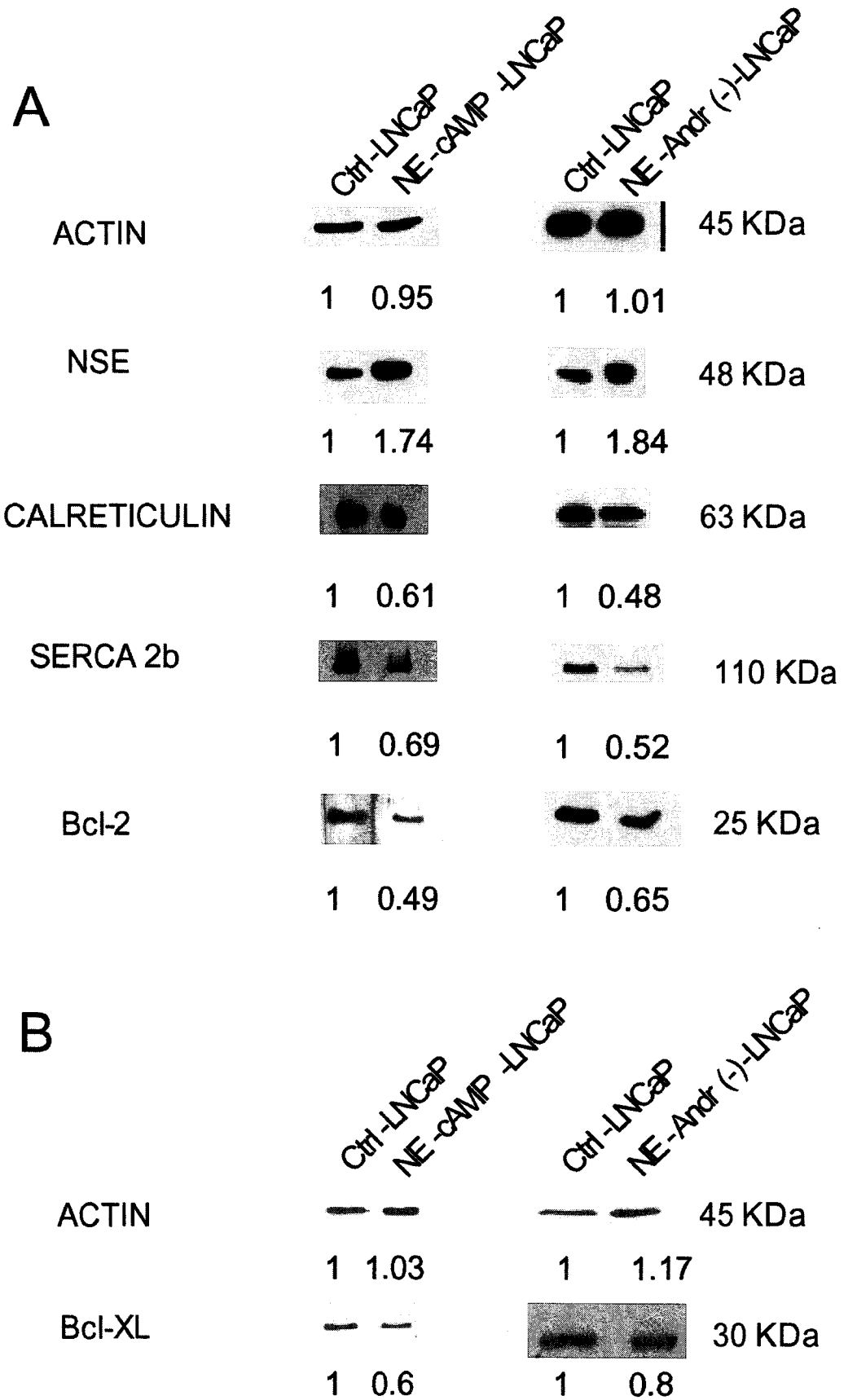
A
Ctrl-LNCaP
NE-cAMP -LNCaP
Ctrl-LNCaP
NE-Andr (-)-LNCaP
ACTIN
45 KDa
1 0.95
1 1.01
NSE
48 KDa
1 1.74
1 1.84
CALRETICULIN
63 KDa
1 0.61
1 0.48
SERCA 2b
110 KDa
1 0.69
1 0.52
Bcl-2
25 KDa
1 0.49
1 0.65
B
Ctrl-LNCaP
NE-cAMP -LNCaP
Ctrl-LNCaP
NE-Andr (-)-LNCaP
ACTIN
45 KDa
1 1.03
1 1.17
Bcl-XL
30 KDa
1 0.6
1 0.8

Figure 4

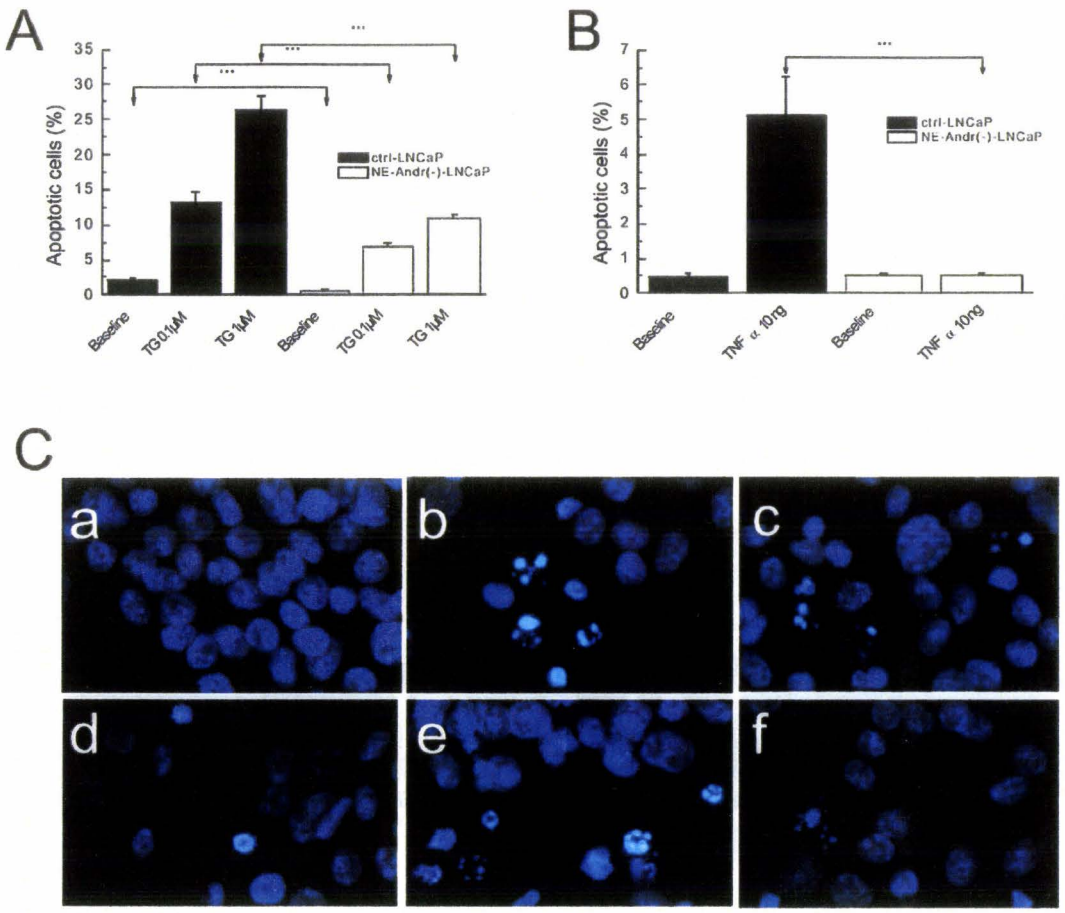
A
Apoptotic cells (%)
35
30
25
20
15
10
5
0
***
***
***
ctrl-LNCaP
NE-Andr(-)-LNCaP
Baseline
TG0.01μM
TG1μM
Baseline
TG0.01μM
TG1μM
B
Apoptotic cells (%)
7
6
5
4
3
2
1
0
***
ctrl-LNCaP
NE-Andr(-)-LNCaP
Baseline
TNF α 10ng
Baseline
TNF α 10ng
C
a
b
c
d
e
f

Figure 5

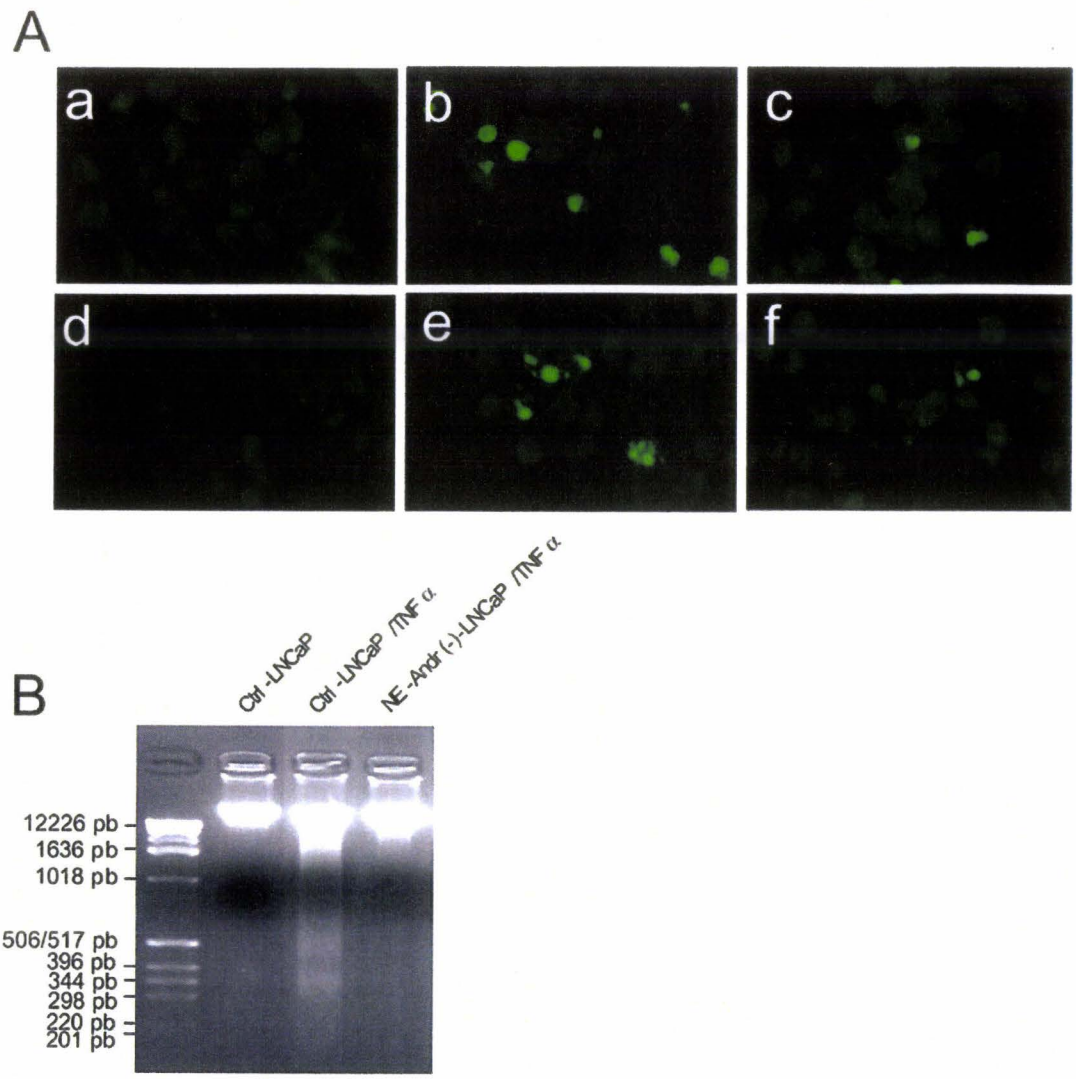
A
a
b
c
d
e
f
B
Ctrl-LNCaP
Ctrl-LNCaP /TNF α
NE-Andr (-)-LNCaP /TNF α
12226 pb
1636 pb
1018 pb
506/517 pb
396 pb
344 pb
298 pb
220 pb
201 pb

Figure 6

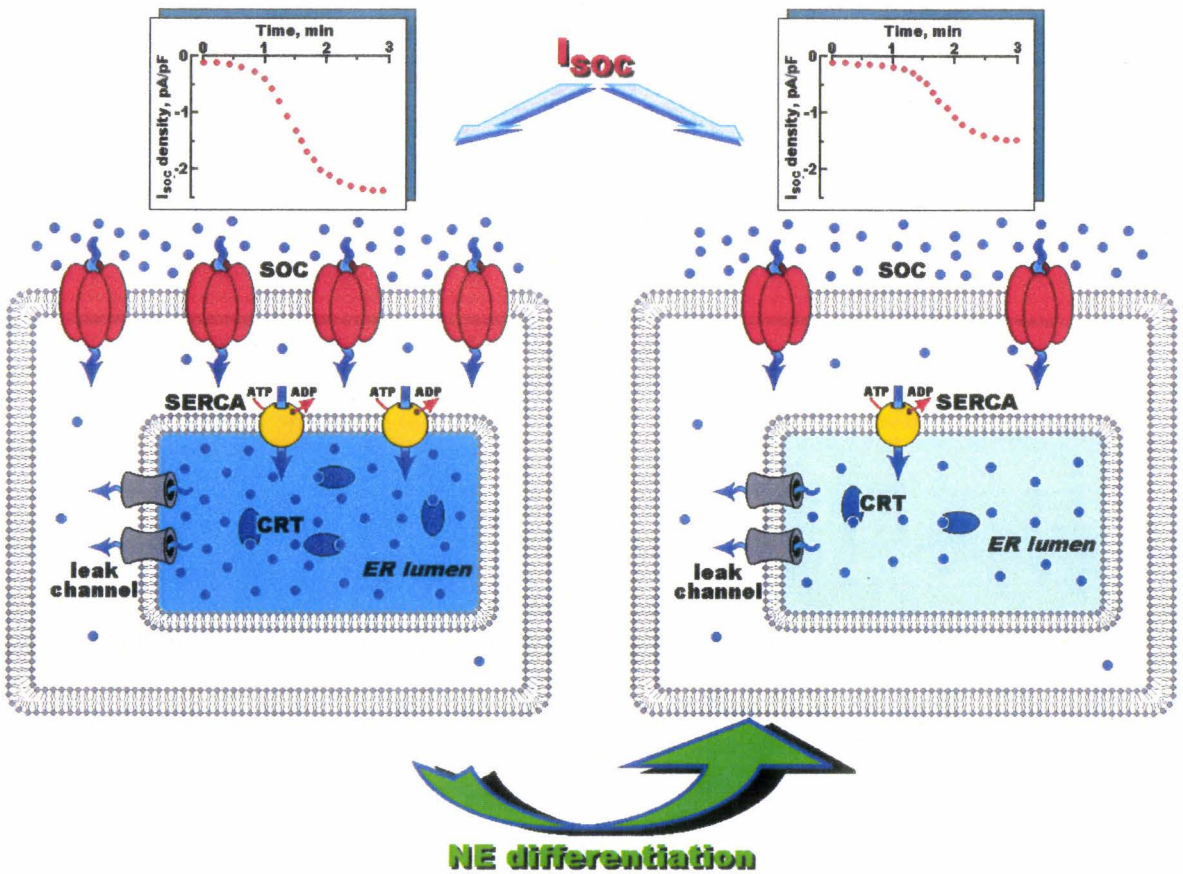
Time, min
0
1
2
3
I_{SOC} density, pA/pF
0
-1
-2
I_{SOC}
SOC
SERCA
ATP
ADP
CRT
ER lumen
leak channel
NE differentiation

Figure 7

Perspectives

Nous avons montré préalablement que les mécanismes d'homéostasie calcique ont un retentissement fondamental sur les processus physio-pathologiques cellulaires, apoptose, prolifération et différenciation cellulaire. Ainsi, non seulement les niveaux de calcium dans le cytosol sont importants à ce titre mais également la concentration en calcium dans le RE. Il est nécessaire de déterminer quel peut être le rôle d'une altération de l'expression des canaux calciques membranaires dans ces processus. Je m'intéresserai plus particulièrement au rôle et à la régulation des canaux calciques voltage-dépendants de type T.

I. Expression et régulation de canaux calciques voltage-dépendants

Comme nous l'avons montré dans ce manuscrit, nous avons commencé l'étude de la régulation du métabolisme calcique dans les cellules épithéliales prostatiques et son rôle dans les mécanismes de prolifération et mort cellulaire. Nous poursuivrons cette étude sur les cellules neuroendocrines prostatiques. Ce travail a déjà débuté et, à l'aide de la technique de patch-clamp, nous avons montré que des traitements induisant une différenciation neuroendocrine, entraînent dans les cellules LNCaP une surexpression de canaux calciques voltage-dépendants de type T (Mariot et al 2002). Les canaux calciques voltage-dépendants sont constitués de différentes sous-unités, $\alpha 1$ pour le pore et $\alpha 2$-δ, γ et β pour les sous-unités régulatrices. Pour chacune de ces sous-unités, il existe plusieurs isoformes et des produits d'épissage variable. Nous avons mis en évidence à l'aide de techniques de RT-PCR quantitative (SYBRGreen) que la sous-unité $\alpha 1H$ d'un canal calcique de type T était surexprimée au cours de la différenciation neuroendocrine de la prostate.

Nous possédons ici un modèle unique pour étudier la régulation physiologique d'un canal calcique voltage-dépendant de type T. En effet, on sait actuellement que ces canaux sont formés d'une sous-unité constituant le pore ($\alpha 1$) et qu'il en existe de trois types ($\alpha 1G$, H ou I), codés par 3 gènes différents (CACNA1G, CACNA1H, CACNA1I), qui possèdent les propriétés électrophysiologiques des canaux de type T. D'autre part, dans les différents tissus de l'organisme et dans les lignées cellulaires tumorales, les canaux T sont toujours coexprimés avec d'autres types de canaux calciques voltage-dépendants (canaux L, N, P et Q). Chacun de ces autres types de canaux peut être codé par 7 autres sous-unités $\alpha 1$ ($\alpha 1A$, B, E, C, D, S et F) dont l'activité peut être modulée par des sous-unités β, γ, et $\alpha 2$-δ (Randall and Benham 1999). On réalise ici le problème posé par

l'étude de canaux T qui ne sont jamais exprimés seuls dans les cellules. Pour cette raison, différentes équipes ont utilisé des modèles de surexpression de sous-unités α1G,H ou I conjointement à celle de sous-unités γ ou α2-δ. Cependant, ces situations ne reflètent pas l'expression naturelle de ces protéines dans les cellules. De plus, il est difficile de savoir dans ces conditions si les protéines sont co-adressées correctement.

Nous nous proposons ici d'étudier la régulation de l'expression et de l'activité d'un canal T (α_{1H}) dans un modèle cellulaire original (LNCaP différenciées) n'exprimant que ce canal calcique voltage-dépendant.

1) Régulation de l'expression de la sous-unité α_{1H}

Nous avons vu que la sous-unité α_{1H} est surexprimée au cours de la différenciation neuroendocrine. Nous savons actuellement que la surexpression de ce canal a lieu lors d'un traitement avec des analogues perméants de l'AMPc, ainsi que lors d'une réduction des taux d'androgènes dans le milieu de culture (Mariot et al, 2002). Il reste à déterminer si l'activation physiologique de l'adénylate cyclase par les neuropeptides (VIP et calcitonine) et neuromédiateur (nor-adrénaline), ou l'activation de la voie des tyrosines kinases Btk et de la PI3 kinase par des interleukines (IL6) induit également la surexpression de canaux calciques de type T. En d'autres termes, la surexpression de la sous-unité α1H est-elle un marqueur obligé de différenciation neuroendocrine terminale ? D'autre part, l'activation d'une voie de transduction telle que la voie adénylate cyclase entraîne une divergence d'informations cellulaires et une activation résultante de nombreuses autres voies de transduction telles que la voie des MAP kinase, connue pour être impliquée dans les processus de différenciation. Il est ainsi fondamental de déterminer de manière précise la chaîne de transduction aboutissant à la surexpression des canaux de type T.

Pour aborder cette étude, nous utiliserons des moyens physiologiques et pharmacologiques existant afin d'activer ou de bloquer les différentes voies de transduction menant à la différenciation neuroendocrine. Nous utiliserons également d'autres modèles cellulaires prostatiques androgéno-dépendants et indépendants ainsi que des tissus prostatiques humains obtenus par prélèvement chirurgical à différents stades de la maladie. Ceci nous permettra de déterminer si ce canal est toujours surexprimé dans les pathologies cancéreuses prostatiques et s'il existe une corrélation entre expression de la sous-unité α1H des canaux T et facteur pronostic.

Si ces hypothèses (le canal T est un marqueur obligatoire de la différenciation neuroendocrine et sa surexpression est associée avec un pronostic clinique défavorable) sont vérifiées, cela pourrait avoir des implications fondamentales en terme de diagnostic et possibilité thérapeutique.

2) Régulation de l'activité du canal T

La régulation des canaux de type T par les seconds messagers est pour l'instant très mal connue, ceci d'une part car ces canaux sont toujours co-exprimés avec d'autres types de canaux calciques et car les sous-unités α1G,H ou I, qui forment le pore, n'ont été clonées que récemment.

a) Régulation par les seconds messagers intracellulaires

La régulation des canaux de type T par des signaux intracellulaires est très mal connue. Bon nombre de travaux semblent contradictoires dans la mesure où des systèmes régulateurs, par exemple la protéine kinase C ou les sous-unités βγ des protéines G, peuvent être stimulateurs ou inhibiteurs selon le modèle cellulaire (pour revue voir Perez-Reyes 2002). En fait, ceci est probablement dû à la diversité moléculaire des canaux T, puisqu'ils sont codés par trois sous-unités α1 différentes. D'autre part, l'association des sous-unités α1 avec les sous-unités auxilliaires étant mal connue également, les diversités de régulation peuvent être dues à la présence de complexes moléculaires différents selon les tissous ou les cellules. Ainsi, il a été montré récemment que la sous-unité α1H, mais pas α1G, était inhibée spécifiquement par les sous-unités β2γ2 des protéines G (Wolfe et al 2003).

Il a été montré que l'activation de la CaM Kinase 2 potentialise l'activité des canaux T α1H (Wolfe et al 2002). Il a été également montré que les canaux T sont inhibés par une activité de type tyrosine kinase (Arnoult et al 1997). Nous tirerons partie de notre modèle unique qui nous permet d'étudier spécifiquement l'activité de ce canal dans des conditions "physiologiques". Il est possible que des facteurs modulant la croissance cellulaire tels que facteurs de croissance (EGF, IGF ou FGF), cytokines (interleukine 1β ou 6) ou des neuropeptides, tels que VIP ou calcitonine, modulent l'activité de ce canal. Ceci nous permettra de déterminer les mécanismes de transductions intracellulaires impliqués dans la régulation des canaux T α1H.

b) Régulation par les autres sous-unités

Il est pour l'instant supposé que l'activité des canaux de typeT est exclusivement dépendante de la sous-unité qui forme le pore (α1 G,H et I). Nous étudierons le rôle potentiel des sous-unités régulatrices dans le fonctionnement du canal. Nous avons observé que les sous-unités γ4 et α2δ2 sont exprimées dans les cellules prostatiques (figure 17).

D'autre part, des résultats préliminaires nous permettent de postuler un rôle fonctionnel de la sous-unité α2δ2 dans la régulation de la sous-unité α1H car l'inhibiteur pharmacologique des sous-unités α2δ, la gabapentine (utilisée comme thérapie anticonvulsivante dans les épilepsies), inhibe l'activité du courant T observé dans les cellules LNCaP différenciées (figure 18).

Nous étudierons leur rôle fonctionnel à l'aide de la stratégie anti-sens qui nous permettra d'abolir ou de diminuer l'expression de ces protéines. Nous avons déjà utilisé avec succès cette stratégie pour l'étude du rôle du canal calcique CaT1 et nous pensons ainsi que cette stratégie est applicable à cette étude.

D'autre part, en utilisant des anticorps contre les sous-unités γ4, α2δ2 et α1H, nous étudierons la colocalisation de ces sous-unités et la formation d'un complexe fonctionnel entre ces sous-unités par immunoprécipitation. Nous développerons également des modèles de cellules transfectées avec les sous-unités α1H, γ4 et α2δ2 couplées à des protéines reporteuses fluorescentes (GFP, BFP...) afin d'étudier leur interaction moléculaire fonctionnelle en microscopie confocale.

II. Etude du rôle des canaux calciques voltage-dépendants dans la physiopathologie de la prostate

Nous avons mis en évidence qu'un canal calcique de type T α1H était surexprimé au cours de la différenciation neuroendocrine de la prostate. Nos résultats montrent également que la différenciation neuroendocrine est associée à une modulation de l'expression des canaux calciques non voltage-dépendants. Nous étudierons le rôle des canaux T dans la physiopathologie de la prostate et nous nous intéresserons plus particulièrement :

-à leur implication fonctionnelle dans la régulation de l'homéostasie calcique.

Le rôle des canaux de type T est notamment à préciser en ce qui concerne la régulation du calcium intracellulaire. Son activité étant transitoire, il est réputé peu important dans le contrôle de l'homéostasie calcique. Nos travaux actuels montrent que son activité, même transitoire, est associée à une augmentation du calcium cytosolique (figure 20). Nous nous intéresserons particulièrement à son implication potentielle dans des mécanismes de « tunelling » entre différents compartiments et notamment entre le compartiment extracellulaire et réticulaire grâce à des associations moléculaires avec des canaux calciques du réticulum endoplasmique, comme cela a été montré pour les canaux calciques de types L et les récepteurs canaux RyR.

-à leur rôle dans la sécrétion de facteurs paracrines

Les cellules neuroendocrines de la prostate possèdent des granules de sécrétion contenant notamment de la sérotonine et plusieurs peptides. Bien que les fonctions de ces cellules ne soient pas encore bien établies, il est probable qu'elles aient un rôle important dans les phénomènes de croissance, de différenciation cellulaire et de sécrétion de la prostate. Il sera intéressant d'étudier

dans les tissus humains, pathologiques ou sains, prélevés par chirurgie, les propriétés des cellules neuroendocrines de la prostate. Afin de déterminer si lors de la différenciation neuroendocrine, il se produit une altération de la sécrétion de neuropeptides, entraînant par exemple une potentialisation de la sécrétion de prolactine par les cellules différenciées, ce qui pourrait par exemple expliquer un emballement du processus de croissance cellulaire, nous étudierons les altérations du processus de sécrétion lors de la différenciation neuroendocrine des cellules LNCaP induite par une augmentation des taux d'AMPc intracellulaire ou induite par des interleukines (IL 1 et 6). D'autre part, nous étudierons l'implication relative des différents mécanismes d'homéostasie calcique dans le processus d'exocytose et notamment le rôle des canaux de type T.

Nous aborderons cette problématique à l'aide des mesures électrophysiologiques de la capacité membranaire combinée à la mesure voltamétrique de sérotonine ainsi que grâce aux mesures de fluorescence utilisant un marqueur membranaire, le FM1-43, qui est une sonde capable de s'intégrer dans la membrane plasmique lors du processus d'exocytose, entraînant ainsi une augmentation de fluorescence lors de la sécrétion. Cette technique est mise au point au laboratoire. Des résultats préliminaires nous ont permis de montrer que les cellules LNCaP, différenciées ou non, possèdent une voie de sécrétion régulée, typique des cellules neuroendocrines, qui peut être activée par une augmentation de calcium cytosolique (Figure 19).

Nous avons pu également montrer par des expériences de mesures combinées des courants membranaires et de la sécrétion (FM1-43) que la sécrétion était stimulée par une activation du canal $T\alpha_{1H}$ (Figure 20).

Nous déterminerons d'autre part si les cellules différenciées sécrètent des facteurs à activité neurotrophique. En effet, le blocage de l'entrée de calcium par des moyens pharmacologiques se traduit par un ralentissement de l'extension des neurites. Cet effet pourrait être dû, soit à un rôle direct du calcium intracellulaire dans le processus d'extension neuritique, soit à une inhibition de la sécrétion de facteurs trophiques. Nous déterminerons par des études utilisant des milieux conditionnés si ces milieux provoquent une différenciation neuroendocrine.

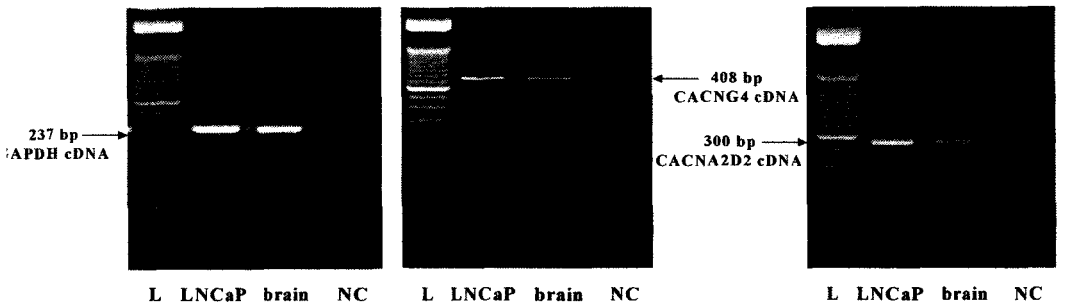

Figure 17 : Identification par RT-PCR des transcripts des sous-unités gamma4 et alpha2delta2 dans les cellules LNCaP.

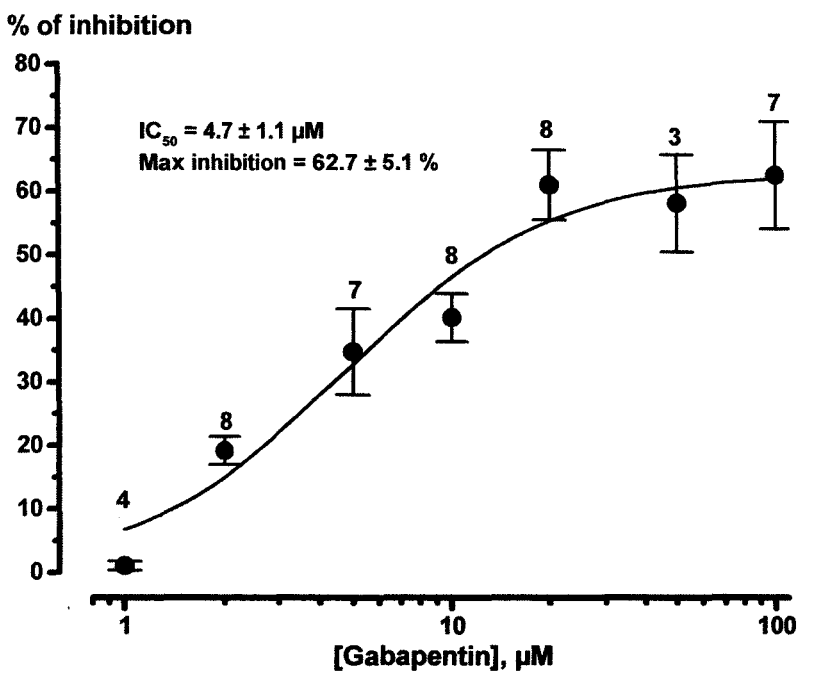

Figure 18 : Pourcentage d'inhibition du courant T dans les cellules LNCaP par la gabapentine.

-à leur rôle dans le processus de différenciation lui-même.

Il a en effet été montré dans d'autres modèles cellulaires (phéochromocytomes PC12) que la différenciation neuroendocrine était associée à une surexpression de canaux calciques voltage-dépendant et que l'activité de ces canaux participait au processus de différenciation. Nous avons observé qu'une diminution du calcium extracellulaire et que des inhibiteurs des canaux calciques ralentissaient le processus de différenciation neuroendocrine. Il reste à déterminer la nature des canaux mis en jeu. Le rôle des canaux T, outre notre travail, a été suggéré dans différentes études. Ainsi, la sous-unité α1H est particulièrement impliquée dans la différenciation des myoblastes en myotubes (Bijlenga et al 2000). La contribution des canaux T a été de plus démontrée dans les cellules d'une lignée de neuroblastome NG108-15 dont la différenciation neuroendocrine, caractérisée par une apparition de neurites et l'augmentation d'un courant calcique HVA, requiert l'activité fonctionnelle de la sous-unité α1H (Chemin et al 2002).

-à leur rôle dans la régulation du cycle cellulaire, de la prolifération cellulaire et de l'apoptose.

Pour ces études, nous mettrons au point des lignées cellulaires prostatiques surexprimant ces canaux calciques voltage-dépendants. Le rôle des différentes sous-unités sera envisagé.

III. Conclusion et perspectives

Par cette étude, nous espérons contribuer à une meilleure compréhension du rôle des canaux calciques dans la prostate. Nous espérons mieux comprendre notamment la régulation de la sécrétion des cellules neuroendocrines prostatiques et ses altérations éventuelles lors de la tumorisation. Si des boucles autocrines/paracrines existent au sein même du tissu, il est possible que lors de la tumorisation l'organe fonctionne en circuit fermé. Ainsi, des altérations de la sécrétion hormonale, notamment dues à une altération du fonctionnement des canaux calciques des cellules neuroendocrines de la prostate, auraient une importance fonctionnelle considérable. D'autre part, ce projet pourrait ouvrir des possibilités thérapeutiques. En effet, il faut souligner que les possibilités d'interventions pharmacologiques sur les canaux T existent et que différents médicaments ayant comme cibles ces canaux ont été (mibefradil, POSICOR, utilisé comme antihypertenseur, arrêt de commercialisation en 1998) ou sont sur le marché (gabapentine). Il reste évidemment à démontrer l'importance de ces canaux dans le développement, notamment à long terme, des tumeurs prostatiques.

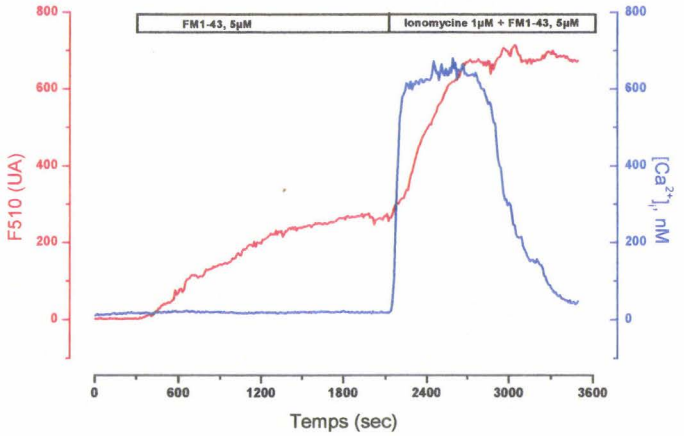

Figure 19 : L'exocytose (mesurée par la fluorescence du FM1-43) est stimulée par une augmentation de calcium cytosolique dans les cellules LNCaP
Courbe bleue : $[Ca^{2+}]i$
Courbe rouge : FM1-43

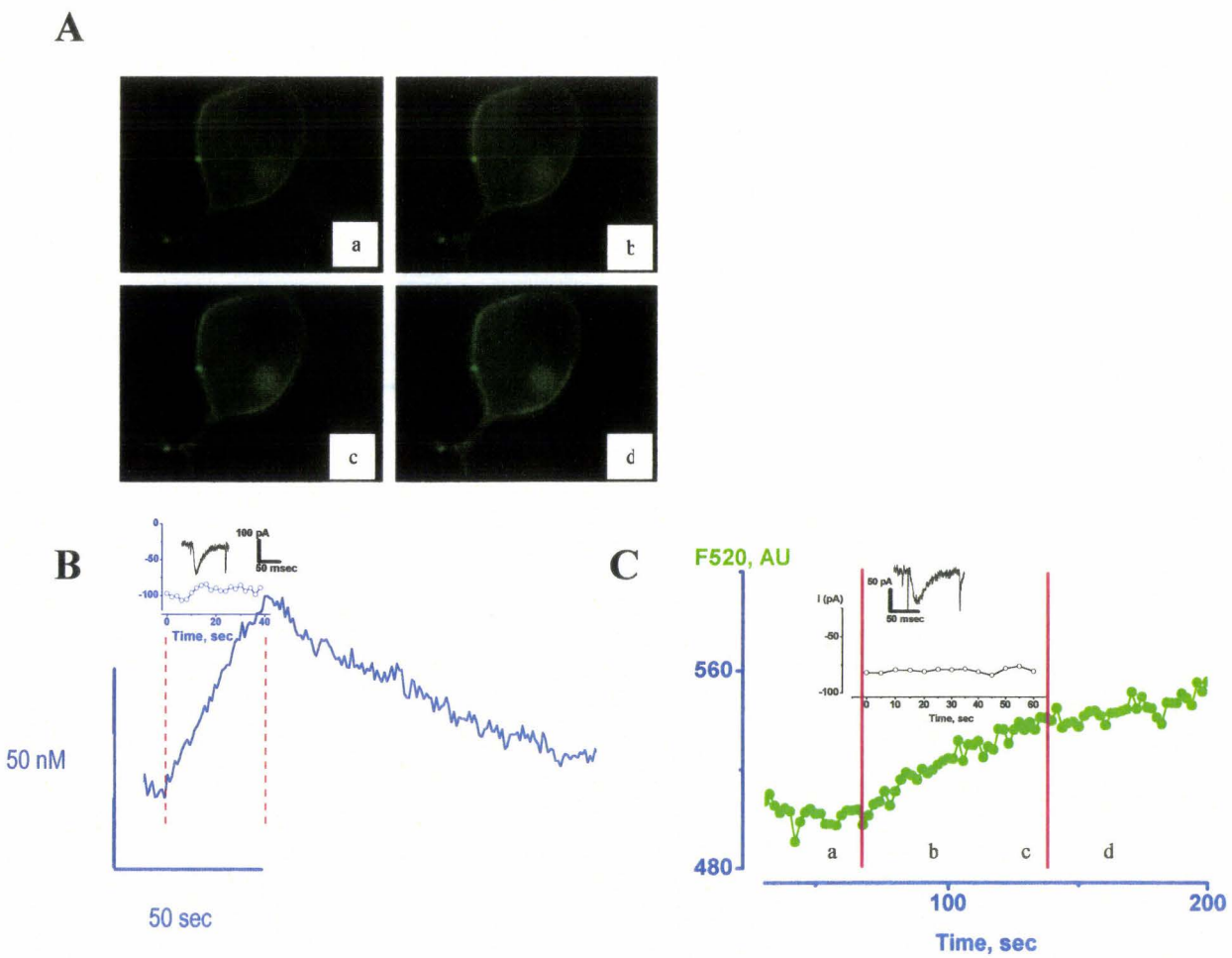

Figure 20 : L'exocytose (mesurée par la fluorescence du FM1-43) est stimulée par une augmentation de calcium cytosolique dans les cellules LNCaP due à une activation du canal T
A : Fluorescence du FM1-43 de la cellule correspondant à l'expérience C.
B : un train de stimulation de -80 à -10 mV (0.5 Hz) provoque une augmentation de la $[Ca^{2+}]i$ par les courants T.
C : un train de stimulation de -80 à -10 mV (0.5 Hz) provoque une augmentation de la fluorescence du FM1-43.

Références Bibliographiques

1. Abrahamsson P-A (1999) Neuroendocrine differentiation in prostatic carcinoma. Prostate 39 : 135-148

2. Abrahamsson P-A, Wadstrom LB, Alumets J, Falkmer S, Grimelius L (1986) Peptide-hormone and sertonin immunoreactive cells in normal and hyperplastic cells. Path.Res.Pract. 181 : 675-683

3. Ammon HPT, Heurich RO, Kolb HA, Lang F, Schaich R, drews G, Leiers T (1996) The phosphatase inhibitor okadaic acid blocks KCl-depolarization-induced rise of cytosolic calcium of rat insulinoma cells (RINm5F). Naunyn-Schmiedberg's Arch. Pharmacol. 354 : 95-101

4. Aridor M, Rajmilevich G, Beaven MA, Sagi-Eisenberg R (1993) Activation of exocytosis by the heterotrimeric G protein Gi3. Science 262 : 1569-1572

5. Arikkath J, Campbell KP (2003) Auxiliary subunits : essential components of the voltage-gated calcium channel complex. Current Opinion in Neurobiology 13 : 298-307.

6. Armstrong CM, Matteson DR. (1985) Two distinct populations of calcium channels in a clonal line of pituitary cells.Science. 227 : 65-67.

7. Arnoult C, Lemos JR, Florman HM (1997) Voltage-dependent modulation of T-type calcium channels by protein tyrosine phosphorylation. EMBO J. 16 : 1593-1599

8. Atlas D (2001) Functional and physical coupling of voltage-sensitive calcium channels with exocytotic proteins : ramifications for the secretion mechanism. J. Neurochem. 77 : 972-985

9. Augustine GJ (2001) How does calcium trigger neurotransmitter release ? Curr. Opin. Cell. Biol. 11 : 320-326

10. Bang YJ, Pirnia F, Fang WG, Kang WK, Sartor O, Whitesell L, Ha MJ, Tsokos M, Sheahan MD, Nguyen P, Niklinski WT, Myers CE, and Trepel JB (1994) Terminal neuroendocrine differentiation of human prostate carcinoma cells in response ton increased intracellular cyclic AMP. Proc.Natl.Acad.Sci USA, 90, 2559-2563

11. Barg S, Renstrom E, Berggren PO, Bertorello A, Bokvist K, Braun M, Eliasson L, Holmes WE, Kohler M, Rorsman P, Thevenod F (1999) The stimulatory action of tolbutamide on Ca2+-dependent exocytosis in pancreatic beta cells is mediated by a 65-kDa mdr-like P-glycoprotein. Proc Natl Acad Sci U S A. 96 : 5539-44.

12. Beech DJ, Xu SZ, McHugh D, Flemming R.(2003) TRPC1 store-operated cationic channel subunit. Cell Calcium. 33:433-40

13. Bennett DL, Bootman MD, Berridge MJ, Cheek TR. (1998) Ca2+ entry into PC12 cells initiated by ryanodine receptors or inositol 1,4,5-trisphosphate receptors. Biochem J. 329 : 349-57.

14. Bennett DL, Cheek TR, Berridge MJ, De Smedt H, Parys JB, Missiaen L, Bootman MD (1996) Expression and function of ryanodine receptors in nonexcitable cells. J. Biol. Chem. 271 : 6356-6362

15. Bennett MK and Scheller RH (1993) The molecular machinery for secretion is conserved from yeast to neurons. Proc.Natl.Acad.Sci USA, 91, 5330-5334

16. Berridge MJ, Bootman MD, Lipp P (1998) Calcium- A life and death signal. Nature 395 : 645-648

17. Berridge MJ, Lipp P, Bootman MD (2000) The versatility and universality of calcium signalling. Nature Rev. Mol. Cell. Biol. 1 : 11-21

18. Bian X, Hughes FM, Jr, Huang Y, Cidlowski Ja, Putney JW Jr (1997) Roles of cytoplasmic Ca^{2+} and intracellular Ca^{2+} stores in induction and suppression of apoptosis in S49 cells. Am. J. Physiol 272 : C1241-1249

19. Birnbaumer L, Yidirim E, Abramowitz J. (2003) A comparison of the genes coding for canonical TRP channels and their M, V and P relatives. Cell Calcium. 33 : 419-432.

20. Blackshaw S, Sawa A, Sharp AH, Ross CA, Snyder SH, Khan AA. (2000) Type 3 inositol 1,4,5-trisphosphate receptor modulates cell death. FASEB J. 14 : 1375-1379.

21. Bonkhoff H.(1998) Neuroendocrine cells in benign and malignant prostate tissue: morphogenesis, proliferation, and androgen receptor status.Prostate Suppl. 18:18-22.

22. Bootman MD, Lipp P, Berridge MJ (2001) The organization and functions of local Ca2+ signals. J. Cell Science. 114 : 2213-2222

23. Boynton AL, Whitfield JF, Isaacs RJ, Tremblay RG. (1977) Different extracellular calcium requirements for proliferation of nonneoplastic, preneoplastic, and neoplastic mouse cells.Cancer Res. 37 : 2657-61.

24. Brose N, Petrenko AG, Südhof TC, Jahn R (1992) Synaptotagmin: a calcium sensor on the synaptic vesicle surface. Science, 256, 1021-1025

25. Brown AM, O'Sullivan AJ, Gomperts BD. (1998) Induction of exocytosis from permeabilized mast cells by the guanosine triphosphatases Rac and Cdc42. Mol Biol Cell. 9 :1053-63.

26. Burgess DL, Gefrides LA, Foreman PJ, Noebels JL (2001) A cluster of three novel Ca2+ channel gamma subunit genes on chromosome 19q13.4: evolution and expression profile of the gamma subunit gene family. Genomics 71 : 339-350

27. Bush K, Strurat RO, Li SH et al (1994) Epithelial inositol 1,4,5 trisphosphate receptors. Multiplicity of localization, solubility and isoforms. J. Biol. Chem 28 : 23694-23699

28. Camello C, Lomax R, Petersen OH, Tepikin AV. (2002) Calcium leak from intracellular stores--the enigma of calcium signalling. Cell Calcium.32 : 355-361.

29. Cancela JM, Charpentier G, Petersen OH (2003) Co-ordination of Ca^{2+} signalling in mamallian cells by the new Ca^{2+}-releasing messenger NAADP. Pflügers Arch. 446 : 322-327

30. Cancela JM, Van Coppenolle F, Galione A, Tepikin AV, Petersen OH. (2002) Transformation of local Ca^{2+} spikes to global Ca2+ transients: the combinatorial roles of multiple Ca2+ releasing messengers. EMBO J. 21 : 909-19.

31. Carafoli E, Brini M (2000) Calcium pumps : structural basis for and mechanism of calcium transmembrane transport. Curr. Opin. Chem. Biol. 4 : 152-161

32. Carbone E, Lux HD.(1984) A low voltage-activated, fully inactivating Ca channel in vertebrate sensory neurones. Nature. 310 : 501-502.

33. Carrión AG, Link WA, Ledo F, Mellström B, Naranjo R, Mandel G, Goodman RH (1999) DREAM is a Ca^{2+}-regulated transcriptionnal repressor. DREAM on without calcium. Nature 398 : 80-84

34. Carroll AG, Rhoads AR, Wagner PD (1990) Hydrolysis-resistant GTP analogs stimulate catecholamine release from digitonin-permeabilized PC12 cells. J. Neurochem. 55 : 930-936

35. Chadwick CC, Saito A, Fleischer S, (1990) Isolation and characterization of the inositol trisphosphate receptor from smooth muscle. Proc. Natl. Acad. Sci. 87 : 2132-2136

36. Chard PS, Bleakman D, Christakos S, Fullmer CS, Miller RJ. (1993) Calcium buffering properties of calbindin D28k and parvalbumin in rat sensory neurones.J Physiol. 472 : 341-57.

37. Chawla S, Hardingham GE, Quinn DR, Bading H (1998) CBP : a signal-regulated transcriptional coactivator controlled by nuclear calcium and CaMKIV. Science 281 : 1505-1509

38. Chemin J, Nargeot J, Lory P. (2002) Neuronal T-type alpha 1H calcium channels induce neuritogenesis and expression of high-voltage-activated calcium channels in the NG108-15 cell line. J Neurosci. 22 : 6856-6862.

39. Chu PJ, Robertson HM, Best PM (2001) Calcium channel gamma subunits provide insights into the evolution of this gene family. Gene 280 : 37-48 (2001)

40. Clementi E, Meldolesi J (1996) Pharmacological and functional properties of voltage-independent Ca2+ channels. Cell Calcium 19 : 269-279

41. Cohen GM (1997) Caspases : the executioners of apoptosis. Biochem.J. 326 : 1-16

42. Cohen JJ, Duke RC (1984) Glucocorticoid activation of a calcium-dependent endonuclease in thymocyte nuclei leads to cell death. J. Immunol. 132 : 38-42

43. Cohen RJ, Glezerson G, Haffejee Z, Afrika D (1990) Prostatic carcinoma : histological and immunohistological factors affecting prognosis. Br.J. Urol. 66 : 405-410

44. Cox ME, Deeble PD, Bissonette EA, Parsons SJ (2000) Activated 3',5'-cyclic AMP-dependent protein kinase is sufficient to induce neuroendocrine-like differentiation of the LNCaP prostate tumor cell line. J. Biol. Chem 275 : 13812-13818

45. Cribbs LL, Lee JH, Yang J, Satin J, Zhang Y, Daud A, Barclay J, Williamson MP, Fox M, Rees M, Perez-Reyes E. (1998) Cloning and characterization of alpha1H from human heart, a member of the T-type Ca2+ channel gene family. Circ Res. 83 : 103-9.

46. Cristina Guatimosim,* Court Hull, Henrique von Gersdorff and Marco A. M. Prado*(2002) Okadaic acid disrupts synaptic vesicle trafficking in a ribbon-type synapse J. Neurochem. 82 : 1047

47. Crompton M. (1999) The mitochondrial permeability transition pore and its role in cell death. Biochem. J. 341 : 233-249

48. Csordás, Thomas AP, Hajnóczky G (1999) Quasi synaptic calcium signal transmission between endoplasmic reticulum and mitochondria. EMBO.J. 18 : 96-108

49. Csutora P, Su Z, Kim HY, Bugrim A, Cunningham KW, Nuccitelli R, Keizer JE, Hanley MR, Blalock JE, Marchase RB. (1999) Calcium influx factor is synthesized by yeast and mammalian cells depleted of organellar calcium stores. Proc Natl Acad Sci U S A. 96 : 121-6.

50. Daniel S, Noda M, Cerione RA, Sharp GWG (2002) A link between Cdc42 and syntaxin is involved in mastoparan-stimulated insulin release. Biochemistry 41 : 9663-9671

51. Dasgupta S, Dasgupta D, Chatterjee A, Biswas S, Biswas SBB (1997) Conformational changes ni plant Ins(1,4,5)P3 receptor on interaction with different myo-inositol trisphosphates and its effect on Ca2+ release from microsomal fraction and liposomes. Biochem. J. 321 : 355-360

52. De Koninck P, Schulman H (1998) Sensitivity of CaM Kinase II to the frequency of Ca2+ oscillations. Science 279 : 227-230

53. di Sant'Agnese PA, de Mesy Jensen KL (1987) Neuroendocrine differentiation in prostatic carcinoma. Hum. Path 18 : 849-856

54. Diaz M, Abdul M, Hoosein N (1998) Modulation of neuroendocrine differentiation in prostate cancer by interleukin-1 and -2. Prostate Suppl 8 : 32-36

55. Dolmetsch RE, Xu K, Lewis RS (1998) Calcium oscillations increase the efficiency and specificity of gene expression. Nature 392 : 933-936

56. Dolphin AC, Wyatt CN, Richards J, Beattie RE, Craig P, Lee JH, Cribbs LL, Volsen SG, Perez-Reyes E (1999) The effect of α2-δ and other accessory subunits on expression and properties of the calcium channel α1G. J. Physiol , 519 : 35-45

57. Doussau F, Augustine GJ (2000) The actin cytoskeleton and neurotransmitter release : an overview. Biochimie 82 : 353-363

58. Doussau F, Gasman S, Humeau Y, Vitiello F, Popoff M, Boquet P, Bader MF, Poulain B. A (2000) Rho-related GTPase is involved in Ca(2+)-dependent neurotransmitter exocytosis. J Biol Chem. 275 : 7764-70.

59. Dunne MJ, Cosgrove KE, Shepherd RM, Ämmälä C (1999) Potassium channels, sulphonylurea receptors and control of insulin release. TEM 10 : 146-152

60. Echevarria W, Leite MF, Guerra MT, Zipfel WR, Nathanson MH (2003) Regulation of calcium signals in the nucleus by a nucleoplasmic reticulum. Nature Cell Biol 5 : 440-446

61. Edmonds B, Reyes R, Schwaller B, Roberts WM. (2000) Calretinin modifies presynaptic calcium signaling in frog saccular hair cells. Nat Neurosci. 3 : 786-790.

62. Eliasson L., Renström E., Ämmälä C., Berggren P.O., Bertorello A.M., Bokvist K., Chibalin A., Deeney J.T., Flatt P.R., Gäbel J., Gromada J., Larsson O., Lindström P., Rhodes C.J., Rorsman P. (1996) PKC-Dependent Stimulation of Exocytosis by Sulfonylureas in Pancreatic Cells. Science 271 : 813-815.

63. Ellis SB, Williams ME, Ways NR, Brenner R, Sharp AH, Leung AT, Campbell KP, McKenna E, Koch WJ, Hui A, et al. (1988) Sequence and expression of mRNAs encoding the alpha 1 and alpha 2 subunits of a DHP-sensitive calcium channel. Science. 241 : 1661-4.

64. Etienne-Manneville S, Hall A (2002) RhoGTPases in cell biology Nature 420 : 629-635.

65. Fabiato A. (1983) Calcium-induced release of calcium from the cardiac sarcoplasmic reticulum. Am J Physiol. 245 : C1-14

66. Fang WG, Pirnia F, Bang YJ, Myers CE, Trepel JB (1992) P2-purinergic agonists inhibit the growth of androgen-independent oriostate carcinoma cells. J. Clin. Invest. 89 : 191-196

67. Fatt P, Katz B (1953) The electrical properties of crustacean muscle fibres. J. Physiol. 120 : 171-204

68. Fernandez JM, Neher E, Gomperts BD (1984) Capacitance measurements reveal stepwise fusion events in degranulating mast cells. Nature 312 : 453-455

69. Fernandez-Chacon R, Konigstorfer A, gerber SH, Garcia J, Matos MF, Stevens CF, Brose N, Rizo J, Rosenmud C, Südhof TC (2001) Synaptotagmin I functions as a calcium regulator of releasse probability. Nature 410 : 41-49

70. Ferris CD, Huganir RL, Suppattapone S, Snyder SH (1989) Purified inositol 1,4,5 trisphosphate receptor mediates calcium flux in reconstituted lipid vesicles. Nature 342 : 87-89

71. Fleischer S, Ogunbunmi EM, Dixon MC et al (1985) Localization of Ca2+ release channels with ryanodine in junctionnal terminal cisternae of sarcoplasmic reticulum of fast skeletal muscle. Proc. Natl. Acad. Sci. USA 82 : 7256-7259

72. Foyouzi-Youssefi R, Arnaudeau S, Borner C, Kelley WL, Tschopp J, Lew DP, Demaurex N, Krause KH. (2000) Bcl-2 decreases the free Ca^{2+} concentration within the endoplasmic reticulum.Proc Natl Acad Sci U S A. 97 : 5723-5728.

73. Furuichi T, Yoshikawa S, Miyawaki A, Wada K, Maeda M, Mikoshiba K (1989) Primary structure and functional expression of the inositol 1,4,5 trisphosphate-binding protein P400. Nature 342 : 32-38

74. Furuya Y, Lundmo P, Short AD, Gill DL, Isaacs JT (1994) The role of calcium, pH, and cell proliferation in the programmed (apoptotic) death of androgen-independant prostatic cancer cells induced by thapsigargin. Canc. Res. 54 : 6167-6175

75. Galli T, Martinez-Arca S, Paumet F (2002) Mécanisme de la fusion membranaire. Médecine Sciences 18 : 1113-1119

76. Gao B, Sekido Y, Maximov A, Saad M, Forgacs E, Latif F, Wei MH, Lerman M, Lee JH, Perez-Reyes et al (2000) Functional properties of a new voltage-dependent calcium channel alpha2delta auxiliary subunit gene (CACNA2D2). J. Biol. Chem. 275 : 12237-12242

77. Garcia-Barrado MJ, Jonas JC, Gilon P, Henquin JC. (1996) Sulphonylureas do not increase insulin secretion by a mechanism other than a rise in cytoplasmic Ca2+ in pancreatic B-cells.Eur. J. Pharmacol. 298 :279-286.

78. Geng X, Li L, Watkins S, Robbins PD, Drain P (2003) The insulin secretory granule is the major site of K(ATP) channels of the endocrine pancreas. Diabetes;52:767-76.

79. George CH, Higgs GV, Mackrill JJ, Lai FA.(2003) Dysregulated ryanodine receptors mediate cellular toxicity: restoration of normal phenotype by FKBP12.6. J Biol Chem. 278 :28856-64.

80. Gerasimenko OV, Gerasimenko JV, Tepikin AV, Petersen OH. (1995)ATP-dependent accumulation and inositol trisphosphate- or cyclic ADP-ribose-mediated release of Ca2+ from the nuclear envelope. Cell. 80 :439-444.

81. Ghosh TK, Bian JH, Short AD, Rybak SL, Gill DL. (1991) Persistent intracellular calcium pool depletion by thapsigargin and its influence on cell growth. J Biol Chem. 266 : 24690-24697.

82. Glezerson G, Cohen RJ (1991) Prognostic value of neuro-endocrine cells in prostatic carcinoma [Abstract]. J.Urol. 145 : 296

83. Golovian VA, Blaustein MP (1997) Spatially and functionally distinct calcium stores in sarcoplasmic and endoplasmic reticulum. Science 275 : 1643-1648

84. Gomperts BD (1990) GE : a GTP-binding protein mediating exocytosis. Annu Rev Physiol 52 :591-606

85. Gunteski-Hamblin AM, Clarke DM, Shull GE (1992) Molecular cloning and tissue distributionof alternatively apliced mRNAs encoding possible mammilian homologues of the yeast secretory pathway calcium pump. Biochemistry 31 : 760-7608

86. Guo L, Nakamura K, Lynch J, Opas M, Olson EN, Agellon LB, Michalak M. (2002) Cardiac-specific expression of calcineurin reverses embryonic lethality in calreticulin-deficient mouse. J Biol Chem. 277 : 50776-50779.

87. Guse AH (1999) Cyclic ADP-ribose : a novel Ca2+-mobilising second messenger. Cell. Signal. 11 : 309-316

88. Hajnócsky G, Csordás G, Madesh M, Pacher P (2000) Control of apoptosis by IP3 and ryanodine receptor driven calcium signals. Cell Calcium 28 : 349-363

89. Hajnócsky G, Davies E, Madesh M (2003) Calciu signaling and apoptosis. Biochem. Biophys. Res. Commun. 304 : 445-454

90. Hardie RC, Minke B.(1992) The trp gene is essential for a light-activated Ca2+ channel in Drosophila photoreceptors.Neuron. 8 : 643-651.

91. Hardingham GE, Chawla S, Cruzalegui FH, Bading H.(1999) Control of recruitment and transcription-activating function of CBP determines gene regulation by NMDA receptors and L-type calcium channels. Neuron. 22 : 789-98.

92. Hardingham GE, Chawla S, Johnson CM, Bading H (1997) Distinct functions of nuclear and cytoplasmic calcium in the control of gene expression. Nature 385 : 260-265

93. He H, Lam M, McCormick TS, Distelhorst CW (1997) Maintenance of calcium homeostasis in the endoplasmic reticulum by bcl-2. J. Cell. Biol. 138 : 1219-1228

94. Higashida H, Yokoyama S, Hashii M, Taketo M, Higashida M, Takayasu T, Ohshima T, Takasawa S, Okamoto H, Noda M. (1997) Muscarinic receptor-mediated dual regulation of ADP-ribosyl cyclase in NG108-15 neuronal cell membranes. J Biol Chem. 272 : 31272-7.

95. Hille B (2001) Ligand-gated channels of fast chemical synapses. In "Ion channels of excitable membranes". Third edition. pp 169-199

96. Hogan K, Powers PA, Gregg RG(1994) Cloning of the human skeletal muscle alpha1 subunit of the dihydropyridine-sensitive caclium channels (CACNL1A3). Genomics 24 : 608-609

97. Holst J, Sim AT, Ludowyke RI (2002) Protein phosphatases 1 and 2A transiently associate with myosin during the peak rate of secretion from mast cells. Mol Biol Cell. 13 :1083-98.

98. Hong-Geller E, Cerione RA. (2000) Cdc42 and Rac stimulate exocytosis of secretory granules by activating the IP(3)/calcium pathway in RBL-2H3 mast cells. J Cell Biol. 148 : 481-94.

99. Hoosein NM, Logothetis CJ, Chung IWK (1993) Differential effects of peptide hormones bombesin, vasoactive intestinal polypeptide and somatostatin analog RC-160 on the invasive capacity of human prostatic carcinoma cells. J.Urol 149 : 1209-1213

100.Hoth M, Penner R. (1992) Depletion of intracellular calcium stores activates a calcium current in mast cells. Nature. 355 : 353-356.

101.Hsu S, Ting AE, Hazuka CD, Davanger S, Kenny JW, Kee Y, Schuller RH (1996) The mammalian brain rsec6/8 complex. Neuron 17 : 1209-1219

102.Itagaki K, Hauser CJ.(2003) Sphingosine 1-phosphate, a diffusible calcium influx factor mediating store-operated calcium entry. J Biol Chem. 278 : 27540-7.

103.Jahn R, Lang T, Sudhof TC (2003) Membrane fusion. Cell 112 : 519-533

104.Jay SD, Ellis SB, McCue AF, Williams ME, Vedvick TS, Harpold MM, Campbell KP. (1990) Primary structure of the gamma subunit of the DHP-sensitive calcium channel from skeletal muscle. Science. 1990 248 : 490-2.

105.Jayaraman T, Marks AR (2000) Calcineurin is downstream of the inositol 1,4,5-trisphophate receptor in the apoptotic and cell growth pathways. J.Biol.Chem. 275 : 6417-6420

106.Jayaraman T, Marks AR. (1997) T cells deficient in inositol 1,4,5-trisphosphate receptor are resistant to apoptosis. Mol Cell Biol. 17 : 3005-3012.

107. Jensen P, Winger L, Rasmussen H, Nowell P. (1977) The mitogenic effect of A23187 in human peripheral lymphocytes. Biochim Biophys Acta. 49 : 374-83.

108.Jiang S, Chow SC, Nicotera P, Orrenius S. (1994) Intracellular Ca^{2+} signals activate apoptosis in thymocytes: studies using the Ca(2+)-ATPase inhibitor thapsigargin. Exp Cell Res. 212 : 84-92.

109.Jones PM, Persaud SJ (1998) Protein kinases, protein phosphorylation, and the regulation of insulin secretion from pancreatic B-cells. Endocrine reviews 19 : 429-461

110.Joutel A, Bousser MG, Biousse V, Labauge P, Chabriat H, Nibbio A, Maciazek J, Meyer B, Bach MA, Weissenbach J et al. (1993)A gene for familial hemiplegic migraine maps to chromosome 19. Nat. Genet. 5 : 40-45

111.Kao JPY, Alderton J, Tsien RY, Steinhardt RA (1990) Active involvment of Ca2+ in mitotic progression of Swiss 3T3 fibroblasts. J.Cell.Biol. 111 : 183-196

112.Kass GEN, Orrenius S (1999) Calcium signaling and cytotoxicity. Environ. Health. Perspect. 107 : 25-35

113.Keil EM, Sichel FJM (1936) The injection of aqueous solutions including acetylcholine into the isolated muscle fibre. Biol. Bull. 71 : 402

114.Kim J, Adam RM, Freeman MR (2002) Activation of the Erk mitogen-activated protein kinase pathway stimulates neuroendocrine differentiation in LNCaP cells independently of cell cycle withdrawal and STAT3 phosphorylation. Cancer Res. 62 : 1549-1554

115. Kiselyov K, Mignery GA, Zhu MX, Muallem S. (1999) The N-terminal domain of the IP3 receptor gates store-operated hTrp3 channels. Mol Cell. 4 : 423-429.

116. Kiselyov K, Xu X, Mozhayeva G, Kuo T, Pessah I, Mignery G, Zhu X, Birnbaumer L, Muallem S. (1998) Functional interaction between InsP3 receptors and store-operated Htrp3 channels.Nature. 396 : 478-482.

117. Kiselyov KI, Shin DM, Wang Y, Pessah IN, Allen PD, Muallem S. (2000) Gating of store-operated channels by conformational coupling to ryanodine receptors. Mol Cell. 6: 421-431.

118.Kits KS, Mansvelder HD (2000) Regulation of exocytosis in neuroendocrine cells : spatial organization of channels and vesicles, stimulus-secretion coupling, calcium buffers and modulation. Brain. Res.rev. 33 : 78-94

119.Klenchin VA, Martin TFJ (2000) Priming in exocytosis : attaining fusion-competence after vesicle docking. Biochimie 82 : 399-407

120.Klockner U, Lee JH, Cribbs LL, Daud A, Hescheler J, Pereverzev A, Perez-Reyes E, Schneider T. (1999) Comparison of the Ca2 + currents induced by expression of three cloned alpha1 subunits, alpha1G, alpha1H and alpha1I, of low-voltage-activated T-type Ca2 + channels. Eur J Neurosci. 11 : 4171-8.

121.Klugbauer N, Lacinova L, Marais E, Hobom M, Hofmann F (1999) Molecular diversity of the calcium channel alpha2delta subunit. J. Neurosci. 19 : 684-691

122.Koulen P, Cai Y, Geng L, Maeda Y, Nishimura S, Witzgall R, Ehrlich BE, Somlo S. (2002) Polycystin-2 is an intracellular calcium release channel.Nat Cell Biol. 4 : 191-197.

123.Kuno M, Gardner P (1987) Ion channels activated by inositol 1,4,5-trisphosphate in plasma membrane of human T-lymphocytes. Nature 326 : 301–304.

124.Lam M, Dubyak G, Distelhorst CW. (1993) Effect of glucocorticosteroid treatment on intracellular calcium homeostasis in mouse lymphoma cells.Mol Endocrinol. 7 : 686-693.

125.Lang J (1999) Molecular mechanisms and regulation of insulin exocytosis as a paradigm of endocrine secretion. Eur.J.Biochem. 259 : 3-17

126. Laplante JM, O'Rourke F, Lu X, Fein A, Olsen A, Feinstein MB. (2000) Cloning of human Ca2+ homoeostasis endoplasmic reticulum protein (CHERP): regulated expression of antisense cDNA depletes CHERP, inhibits intracellular Ca2+ mobilization and decreases cell proliferation. Biochem J. 348 : 189-199.

127. Lee HC,Walseth TF, Bratt GT, Hayes RN, Clapper DL (1989) Structural determination of a cyclic metabolite of NAD+ with intracellular Ca^{2+}-mobilizing activity. J. Biol. Chem. 264 : 1608-1615

128.Lee HC. (1997) Mechanisms of calcium signaling by cyclic ADP-ribose and NAADP.
Physiol Rev. 77 : 1133-64. Review.

129.Lee JH, Daud AN, Cribbs LL, Lacerda AE, Pereverzev A, Klockner U, Schneider T, Perez-Reyes E. (1999) Cloning and expression of a novel member of the low voltage-activated T-type calcium channel family. J Neurosci. 19 : 1912-21.

130.Lee MG, Xu X, Zeng W et al (1997) Polarized expression of Ca2+ channels in pancreatic and salivary gland cells. J. Biol. Chem. 272 : 15765-15770

131.Legrand G, Humez S, Slomianny C, Dewailly E, Abeele FV, Mariot P, Wuytack F, Prevarskaya N. (2001) Ca^{2+} pools and cell growth. Evidence for sarcoendoplasmic Ca^{2+}-ATPases 2B involvement in human prostate cancer cell growth control. J. Biol. Chem. 276 : 47608-47614.

132.Leite MF, Thrower EC, Echevarria W, Koulen P, Hirata K, Bennett AM, Ehrlich BE, Nathanson MH (2003) Nuclear and cytosolic calcium are regulated independently. PROC NATL ACAD SCI U S A 100 : 2975-2980

133. Leong P, MacLennan DH. (1998) The cytoplasmic loops between domains II and III and domains III and IV in the skeletal muscle dihydropyridine receptor bind to a contiguous site in the skeletal muscle ryanodine receptor. J. Biol. Chem.273(45):29958-64.

134.Letts VA, Felix R, Biddlecome GH, Arikkath J, Mahaffey CL,Valenzuela A, Bartlett FS II, Mori Y, Campbell KP, Frankel WN(1998) The mouse stargazer gene encodes a neuronal Ca2+-channel gamma subunit. Nat. Genet. 19 : 340-347

135. Li Q, Ho CS, Marinescu V, Bhatti H, Bokoch GM, Ernst SA, Holz RW, Stuenkel EL (2003) Facilitation of Ca^{2+}-dependent exocytosis by Rac1-GTPase in bovine chromaffin cells. J. Physiol. 550 : 431-445

136.Li W-H, Llopis J, Whitney M, Zlokarnik G, Tsien RY (1998) Cell-permeant caged InsP3 ester shows that Ca2+ spike frequency can optimize gene expression. Nature 392 : 936-941

137.Limonta, P., Dondi, D., Moretti, R.M., Maggi, R., Motta, M. (1992). Antiproliferative effects of luteinizing hormone-releasing hormone agonists on the human prostate cancer cell line LNCaP. Endocrinology 75 : 207-212.

138.Lipp P, Thomas D, Berridge MJ, Bootman MD. (1997) Nuclear calcium signalling by individual cytoplasmic calcium puffs. EMBO J. 16 : 7166-7173.

139.Lipschutz JH, Mostov KE (2002) Exocytosis : the many masters of the dispatch exocyst. Current Biology 12 : 212-214

140.Llinas R, Sugimori M, Lin JW, Cherksey B. (1989) Blocking and isolation of a calcium channel from neurons in mammals and cephalopods utilizing a toxin fraction (FTX) from funnel-web spider poison. Proc Natl Acad Sci U S A. 86 :1689-93.

141.Lu X, Xu L, Meissner G. (1994) Activation of the skeletal muscle calcium release channel by a cytoplasmic loop of the dihydropyridine receptor. J. Biol. Chem. 269 : 6511-6.

142.Lückhoff A, Clapham DE (1992) Inositol 1,3,4,5-tetrakisphosphate activates an endothelial Ca(2+) permeable channel. Nature 355 : 356-358

143.Ludowyke RI, Holst J, Mudge LM, and Sim ATR (2000) Transient Translocation and Activation of Protein Phosphatase 2A during Mast Cell Secretion. J. Biol. Chem., 275 : 6144-6152

144.Machesky LM, Insall RH. Signalling to actin dynamics. J. Cell. Biol. 1999. 146 : 267-272

145.Madden DR (2002) The structure and function of glutamate receptor ion channels. Nature. Rev. Neuro, 3 : 91-101

146.Mariot P, Prevarskaya N, Roudbaraki MM, Le Bourhis X, Van Coppenolle F, Vanoverberghe K, Skryma R. (2000) Evidence of functional ryanodine receptor involved in apoptosis of prostate cancer (LNCaP) cells. Prostate. 43: 205-214.

147.Mariot_P, Vanoverberghe K, Lalevée N, Rossier MF, Prevarskaya N (2002) Overexpression of an α1H (Ca_v3.2) T-type calcium channel during neuroendocrine differentiation of human prostate cancer cells. J. Biol. Chem. 277 : 10824-10833

148.Martikainen P, Kyprianou N, Tucker RW, Isaacs JT. (1991) Programmed death of nonproliferating androgen-independent prostatic cancer cells. Cancer Res. 51:4693-4700.

149.Maryleitner M, Schafer R, Fleischer S (1995) IP3 receptor purified from liver plasma membrane is an (1,4,5)IP3 activated and (1,3,4,5)IP4 inhibited calcium permeable channel. Cell Calcium 17 : 141-153

150.Matthew J. Donelan, Gerardo Morfini, Richard Julyan, Scott Sommers, Lori Hays, Hiroshi Kajio, Isabelle Briaud, Richard A. Easom, Jeffery D. Molkentin, Scott T. Brady, and Christopher J. Rhodes (2002) Ca2+-dependent Dephosphorylation of Kinesin Heavy Chain on -Granules in Pancreatic -Cells. Implications for regulated-granule transport and insulin exocytosis. J. Biol. Chem., 277 : 24232-24242

151. McConkey DJ, Hartzell P, Duddy SK, Hakansson H, Orrenius S. (1988) 2,3,7,8-Tetrachlorodibenzo-p-dioxin kills immature thymocytes by Ca2+-mediated endonuclease activation.Science. 242 : 256-259.

152.McPherson PS, Campbell KP (1993) The ryanodine receptor/Ca2+ release channel. J. Biol. Chem. 268 : 13765-13768

153.Michalak M, Robert Parker JM, Opas M. (2002) Ca2+ signaling and calcium binding chaperones of the endoplasmic reticulum. Cell Calcium. 32 : 269-278.

154.Minn AJ, Velez P, Schendel SL, Liang H, Muchmore SW, Fesik SW, Fill M, Thompson CB (1997) Bcl-x(l) forms an ion channel in synthetic lipid membranes. Nature 385 : 353-357

155.Missiaen L et al (1999) The bell shaped Ca2+ dependence of the inositol 1,4,5 trisphosphate induced Ca2+ release is modulated by Ca2+/Calmodulin. J. Biol. Chem. 274 : 13748-13751

156.Montell C. (2003) The venerable inveterate invertebrate TRP channels. Cell Calcium. 33 : 409-417.

157.Mori Y, Friedrich T, Kim MS, Mikami A, Nakai J, Ruth P, Bosse E, Hofmann F, Flockerzi V, Furuichi T et al. (1991) Primary structure and functional expression from complementary DNA of a brain calcium channel. Nature 350 : 398-402

158. Nakagawa T, Yuan J (2000) Cross-talk between two cyteine protease falmilies. Activation of caspase12 by calpain in apoptosis. J. Cell.Biol. 150 : 887-894

159.Nakagawa T, Zhu H, Morishima N et al. (2000) Caspase12 mediates endoplasmic reticulum specific apoptosis and cytotoxicity by amyloid-beta. Nature 403 : 98-103

160.Neher E, Zucker RS (1993) Multiple calcium dependent processes related to secretion in bovine chromaffin cells. Neuron 10 : 31-30

161.Neher E, Zucker RS (1993) Multiple calcium-dependent processes related to secretion in bovine chromaffin cells. Neurno 10 : 21-30

162.Nicotera P, Orrenius S, Nilsson N, Bergegren P. (1990) An inositol 1,4,5 trisphosphate sensitive calcium pool in liver nulei. Proc. Natl. Acad. Sci. 87 6858-6862

163.Niggli E (1999) Localized intracellular calcium signalling in muscle : calcium sparks and calcium quarks. Annu. Rev. Physiol. 61 : 311-335

164.Nishizaki T, Walent JH, Kowalchyk JA, Martin TF. (1992) A key role for a 145-kDa cytosolic protein in the stimulation of Ca(2+)-dependent secretion by protein kinase C.J. Biol. Chem. 267 : 23972-23981.

165.Norman JC, Price LS, Ridley AR, Hall A, Koffer A (1994) Actin filament organization in activated mast cells is regulated by heterotrimeric and small GTP-binding proteins. J. Cell. Biol 126 : 1005-1015

166.Nowycky MC, Fox AP, Tsien RW. (1985) Three types of neuronal calcium channel with different calcium agonist sensitivity. Nature. 316: 440-3.

167.Okano K, Monck JR, Fernandez JM (1993) GTPγS stimulates exocytosis in patch-clamped rat melanotrophs. Neuron 11 : 165-172

168.O'Rourke FA, LaPlante JM, Feinstein MB. (2003) Antisense-mediated loss of calcium homoeostasis endoplasmic reticulum protein (CHERP; ERPROT213-21) impairs Ca2+ mobilization, nuclear factor of activated T-cells (NFAT) activation and cell proliferation in Jurkat T-lymphocytes. Biochem J. 373 : 133-143.

169.Pacher P, Hajnoczky G.(2000) Propagation of the apoptotic signal by mitochondrial waves. EMBO J 20 : 4107-4021.

170.Pan Z, Damron D, Nieminen AL, Bhat MB, Ma J. (2000) Depletion of intracellular Ca^{2+} by caffeine and ryanodine induces apoptosis of chinese hamster ovary cells transfected with ryanodine receptor. J Biol Chem. 275 : 19978-19984.

171.Parekh AB, Penner R (1997) Store depletion and calcium influx. Physiol. Rev. 77 : 901-930

172.Patel R, Holt M, Philipova R, Moss S, Schulman H, Hidaka H, Whitaker M. (1999) Calcium/calmodulin-dependent phosphorylation and activation of human Cdc25-C at the G2/M phase transition in HeLa cells. J Biol Chem. 274 : 7958-7968.

173.Patel S, Joseph SK, Thomas AP (1999) Molecular prpoerties of inositol 1,4,5 trisphosphate receptors. Cell Calcium 25 : 247-264

174.Pessah IN, Waterhouse AL, Casida JE (1985) The calcium-ryanodine receptor complex of skeletal and cardiac muscle. Biochem. Biophys. Res. Commun 128 : 449-456

175.Petersen OH, Burdakov D, Tepikin AY (1999) Polarity in intracellular calcium signalling. Bioessays 21 : 851-860

176.Petterson RL, Van ossum DB, Gill DL (1999) Store-operated Ca2+ entry : evidence for a secretion-like coupling model. Cel 98 : 487-499

177.Pinton P, Ferrari D, Magalhaes P, Schulze-Osthoff K, Di Virgilio F, Pozzan T, Rizzuto R. (2000) Reduced loading of intracellular Ca(2+) stores and downregulation of capacitative Ca(2+) influx in Bcl-2-overexpressing cells. J Cell Biol. 148 : 857-862.

178.Pinton P, Pozzan T, Rizzuto R (1998) The Golgi apparatus is an inositol 1,4,5-trisphosphate-sensitive Ca^{2+}store, with functional properties distinct from those of the endoplasmic reticulum. EMBO J 17 : 5298–5308.

179.Pinton P, Pozzan T, Rizzuto R (1998) The Golgi apparatus is an inositol 1,4,5 trisphophate-sensitive Ca2+ store, with functional properties distinct from those of the endoplasmic reticulum. EMBO J 17 : 5298-5308

180.Pinxteren JA, O'Sullivan AJ, Tatham PER, Gomperts BD (1998) Regulation of exocytosis from rat peritoneal mast cells by G-proteins β sub-units. EMBO J 17 : 6210-6218

181.Pinxteren JA, O'Sullivan AJ, Larbi KY, Tatham PE, Gomperts BD .(2000) Thirty years of stimulus-secretion coupling: from Ca(2+) toGTP in the regulation of exocytosis. Biochimie. 2000 82 :385-93.

182.Powers PA, Liu S, Hogan K, Gregg RG (1993) Molecular characterization of the gene encoding the gamma subunit of the human skeletal muscle 1,4-dihydropyridine-sensitive Ca2+ channel (CACNLG), cDNA sequence, gene structure, and chromosomal location. J. Biol. Chem. 268 : 9275-9279

183.Pozzan T, Rizzuto R, Volpe V, Meldolesi J (1994) Molecular and cellular physiology of intracellular calcium stores. Physiol Rev 74 : 595–636

184.Pragnell M, De Waard M, Mori Y, Tanabe T, Snutch TP, Campbell KP (1994) Calcium channel β-subunit binds to a conserved motif in the I-II cytoplasmic linker of the α1-subunit. Nature 368 : 67-70

185.Prepens U, Just I, Von Eichel-Streiber C, Aktories K (1996) Inhibition of FcεRI-mediated activation of rat basophilic leukemia cells by Clostridium difficile toxine B (monoglucosyltransferase). J. Biol. Chem. 271 : 7324-7329

186.Proks P, Eliasson L, Ämmälä C, Rorsman P, Ashcroft F (1996) Ca2+ and GTPdependent exocytosis in mouse pancreatic beta cells involves both common and disctinct steps. J. Physiol. 496 : 255-264

187.Putney JW Jr. (1986) A model for receptor-regulated calcium entry. Cell Calcium. 7 : 1-12.

188.Putney JW Jr. Capacitative calcium entry revisited. Cell Calcium. 11 : 611-624

189.Putney JW, Broad LM, Braun FJ, Lievremont J-P, Bird GStJ (2001) Mechanisms of capacitative calcium entry. J. Cell Sci. 14 : 2223-2229

190.Qin N, Yagel S, Momplaisir ML, Codd EE, D'Andrea MR (2002) Mol. Pharmaco. 62 : 485-496

191.Qiu Y, Robinson D, Pretlow TG, Kung HJ (1998) Etk/Bmx, a tyrosine kinase with a pleckstrin-homology domain, is an effector of phosphatidylinositol 3'-kinase and is involved in interleukin 6-induced neuroendocrine differentiation of prostate cancer cells. Proc.Natl.Acad.Sci USA, 95 : 3644-3649

192.Raffo AJ, Perlman H, Chen MW, Day ML, Streitman JS, Buttyan R (1995) Overexpression of Bcl-2 protects prostate cancer cells from apoptosis in vitro and confers resistance to androgen depletion in vivo. Cancer Res. 55 : 4438-4445

193.Randall A, Benham CD (1999) Recent advances in the molecular understanding of voltage-gated calcium channels. Mol Cell. Neuroscience 14 : 255-272

194.Randall A, Tsien RW (1995) Pharmacological dissection of multiple Ca^{2+} channel currents in rat cerebellar granule neurons. J. Neuroscience 15 : 2995-3012

195.Randall Ad (1998) The molecular basis of voltage-gated Ca^{2+} channel diversity : is it time for T ? J. Membr. Biol. 161 : 207-213

196.Randriamampita C, Tsien RY. (1993) Emptying of intracellular Ca2+ stores releases a novel small messenger that stimulates Ca2+ influx. Nature. 364 : 809-14.

197.Renstrom E, Barg S, Thevenod F, Rorsman P (2002) Sulfonylurea-mediated stimulation of insulin exocytosis via an ATP-sensitive K+ channel-independent action. Diabetes : 51 Suppl 1: S33-6.

198.Ridley AJ (2001) Rho proteins : linking signaling with membrane trafficking. Traffic 2 : 303-310

199.Ringer S (1883) A further contribution regarding the influence of the different constituents of the blood on the contraction of the heart. J.Physiol. 4 : 29-42

200. Ringer S, Buxton LW (1887) Concerning the action of calcium, potassium and sodium salts upons the eel's heart and upon the skeletal muscles of the frog. J.Phsyiol. 8 : 15-19

201.Rizzuto R, Pinton P, Carrington W et al (1998) Close contacts with the endoplasmic reticulum as determinants of mitochondrial Ca2+ response. Science 280 : 1763-1766

202.Rossi D, Sorrentino V (2002) Molecular genetics of ryanodine receptors Ca^{2+}-releae channels. Cell Calcium 32 : 307-319

203.Rudolph HK Antebi A, Fink GR et al (1989) The yeast secretory pathwayis pertubed by mutations in PMR1, a member of a Ca2+ ATPAse family. Cell 58 : 133-145

204.Ruth P, Rohrkasten A, Biel M, Bosse E, Regulla S, Meyer HE, Flockerzi V, Hofmann F. (1989) Primary structure of the beta subunit of the DHP-sensitive calcium channel from skeletal muscle. Science. 245 : 1115-8.

205.Rzigalinski BA, Willoughby KA, Hoffman SW, Falck JR, Ellis EF. (1999) Calcium influx factor, further evidence it is 5, 6-epoxyeicosatrienoic acid.J.Biol. Chem. 274 : 175-82.

206. Santella L (1998) The role of calcium in the cell cycle : facts and hypotheses. Biochem. Biophys. Res. Comm. 244 : 317-324

207.Schanne FA, Kane AB, Young EE, Farber JL. (1979) Calcium dependence of toxic cell death: a final common pathway. Science. 206 : 700-702.

208.Schatzmann HJ (1966) ATP-dependent Ca^{2+} extrusion from human red cells. Experientia 22 : 364-365

209.Schendel SL, Xie Z, montal MO, Matsuyama S, Montal M, Reed JC (1997) Channel formation by antiapoptotic protein Bcl-2. Proc. Natl. Acad. Sci. USA 94 : 51113-5118

210.Schiavo G, Benfenati F, Poulain B, Rossetto O, Polverino de Laureto P, DasGupta BR, Montecucco C. (1992) Tetanus and botulinum-B neurotoxins block neurotransmitter release by proteolytic cleavage of synaptobrevin. Nature. 359 : 832-5.

211.Schollmeyer JE (1988) Calpain II involvement in mitosis. Science 240 : 911-913

212.Schultz D, Mikala G, Yatani A, Engle DB, Iles DE, Segers B, Sinke RJ, Weghuis DO, Klockner U, Wakamori M. et al. (1993) Cloning, chromosomal localization, and functional expression of the alpha 1 subunit of the L-type voltage-dependent calcium channel from normal human heart. Proc. Natl. Acad. Sci. U.S.A. 90 : 6228-6232

213.Scott CC, Furuya W, Trimble WS, Grinstein S.(2003) Activation of store-operated calcium channels: assessment of the role of snare-mediated vesicular transport. J Biol Chem. 278 : 30534-9

214.Shah GV, Rayford W, Noble MJ, Austenfeld M, Weigel J, Vamos S, Mebust WK (1994) Calcitonin stimulates growth of human prostate cancer cells through receptor-mediated increase in cyclic adenosine 3',5' - monophosphates and cytoplasmic Ca^{2+}transients. Endocrinology 134 :596-602

215.Sheng ME, Thompson MA, Greenberg ME (1991) CREB : a Ca^{2+} dependent transcription factor phosphorylated by calmodulin-dependent kinases. Science 252 : 1427-1430

216.Shibasaki F, Price ER, Milan D, McKeon F.(1996) Role of kinases and the phosphatase calcineurin in the nuclear shuttling of transcription factor NF-AT4. Nature. 382 : 370-3.

217.Shimazaki Y, Nishiki T, Omori A, Sekiguchi M, Kamata Y, Kozaki S, Takahashi M. (1996) Phosphorylation of 25-kDa synaptosome-associated protein. Possible involvement in protein kinase C-mediated regulation of neurotransmitter release. J Biol Chem. 271 : 14548-53.

218.Shorofsky SR, Balke CW (2001) Calcium currents and arrhythmias : insights from molecular biology. Am. J. Medecine 110 : 127-140

219. Short AD, Bian J, Ghosh TK, Waldron RT, Rybak SL, Gill DL. (1993) Intracellular Ca2+ pool content is linked to control of cell growth. Proc Natl Acad Sci U S A. 90:4986-4990.

220.Skryma R, Mariot P, Bourhis XL, Coppenolle FV, Shuba Y, Vanden Abeele F, Legrand G, Humez S, Boilly B, Prevarskaya N. (2000) Store depletion and store-operated Ca2+ current in human prostate cancer LNCaP cells: involvement in apoptosis. J Physiol. 527 : 71-83.

221.Smith J, hompson N, Thompson J, ArmstrongJ, Hayes B, Crofts A, Squire J, Teahan C, Upton L, Solari R. (1997) Rat basophilic leukemia (RBL) cells overexpressing Rab3A have a reversible block in antigen-stimulated exocytosis. Biochem J. 323 : 321-328

222.Smith PA, Proks P, Moorhouse A (1999) Direct effects of tolbutamide on mitochondrial function, intracellular Ca2+ and exocytosis in pancreatic beta-cells. Pflugers Arch. 437 : 577-88.

223. Soboloff J, Berger SA. (2002) Sustained ER Ca^{2+} depletion suppresses protein synthesis and induces activation-enhanced cell death in mast cells. J Biol Chem. 277 : 13812-13820.

224.Söllner T, Bennett MK, Whiteheart SW, Scheller RH, Rothman JE (1993) A protein assembly-disassembly pathway in vitro that may correspond to sequential steps of synaptic vesicle docking, activation and fusion. Cell 75 : 409-418

225.Soltoff SP, Avraham H, Avraham S, Cantley LC. (1998) Activation of P2Y2 receptors by UTP and ATP stimulates mitogen-activated kinase activity through a pathway that involves related adhesion focal tyrosine kinase and protein kinase C. J. Biol. Chem. 273 : 2653-2660.

226.Soong TW, Stea A, Hodson CD, Dubel SJ, Vincent SR, Snutch TP (1993) Structure and functional expression of a member of the low voltage-activated calcium channel family. Science 260 : 1133-1136

227.Starr TV, Prystay W, Snutch TP(1991) Primary structure of a calcium channel that is highly expressed in the rat cerebellum. Proc. Natl. Acad. Sci. U.S.A. 88 : 5621-5625

228.Stern MD (1992) Theory of excitation-contraction coupling in cardiac muscle. Biophys. J. 63 : 497-517

229.Stiles PG (1903) On the rhythmic activity of the oesophagus and the influence upon it of various media. Am. J. Physiol. 5 : 338-357

230.Strom TM, Nyakatura G, Apfelstedt-Sylla E, Hellebrand H,Lorenz B, Weber BH, Wutz K, Gutwillinger N, Ruther K, Drescher B, Sauer C, Zrenner E, Meitinger T, Rosenthal A, Meindl A (1998) An L-type calcium-channel gene mutated in incomplete X-linked congenital stationary night blindness. Nat. Genet. 19 : 260-263

231.Südhof TC (2000) The synaptic vesicle cycle revisited. Neuron 28 : 317-320

232.Sugarawa H, Kurosaki M, Takata M, Kurosaki T (1997) Genetic evidence for involvment of type1, type2 and type3 inositol 1,4,5-trisphosphate receptors in signal transduction through the B-cell antigen receptor. EMBO J. 16 :3078-3088

233.Suppattapone S, Worley PF, Baraban JM, Snyder SH (1988) Solubilization, purification, and characterization of an inositol trisphophate receptor. J. Biol. Chem. 263 : 1530-1534

234. Takai Y, Sasaki T, Matozaki T (2001) Small GTP-binding proteins. Physiol. Rev. 81 : 154-208

235.Takuwa N, Zhou W, Kumada M, Takuwa Y. (1993) Ca(2+)-dependent stimulation of retinoblastoma gene product phosphorylation and p34cdc2 kinase activation in serum-stimulated human fibroblasts. J Biol Chem. 268 : 138-45.

236.Tanabe T, Takeshima H, Mikami A, Flockerzi V, Takahashi H, Kangawa K, Kohima M, Matsuo H, Hirose T, Numa S (1987) Primary structure of the receptor for calcium channel blockers from skeletal muscle. Nature 32 : 313-318

237.Terbush DR, Maurice T, Roth D, Novick P (1996) The exocyst is a multiprotein complex required for exocytosis in Saccaromyces cerevisiae EMBO. J. 15 : 6483-6494

238.Thrower EC, Hagar RE, Ehrlich BE (2001) Regulation of Ins(1,4,5)P3 receptor isoforms by endogenous modulators. TIPS 22 : 580-586

239.Timmerman LA, Clipstone NA, Ho SN, Northrop JP, Crabtree GR.(1996) Rapid shuttling of NF-AT in discrimination of Ca2+ signals and immunosuppression. Nature 383 : 837-40.

240.Tinel H, Cancela JM, Mogami H, Gerasimenko JV, Gerasimenko OV, Tepikin AV, Petersen OH. (1999) Active mitochondria surrounding the pancreatic acinar granule region prevent spreading of inositol trisphosphate-evoked local cytosolic Ca(2+) signals. EMBO J. 18 : 4999-5008.

241.Ton VK, Mandal D, Vahadji C, Rao R (2002) Functional expression in yeast of the human secretory pathway Ca2+,Mn2+ATPase defective in Hailey-Hailey disease. J. Biol. Chem. 277 : 6422-6427

242.Trebak M, Vazquez G, Bird G St J, Putney JW Jr (2003) The TRPC3/6/7 subfamily of cation channels. Cell Calcium 33 : 451-461

243.Trepakova ES, Csutora P, Hunton DL, Marchase RB, Cohen RA, Bolotina VM.(2000) Calcium influx factor directly activates store-operated cation channels in vascular smooth muscle cells. J Biol Chem. 275 : 26158-63.

244.Turner H, Fleig A, Stokes A, Kinet JP, Penner R. (2003) Discrimination of intracellular calcium store subcompartments using TRPV1 (transient receptor potential channel, vanilloid subfamily member 1) release channel activity. Biochem J. 371 : 341-350.

245.Valentijn JA, Valentijn K, Pastore LM, Jamieson JD. (2000) Actin coating of secretory granules during regulated exocytosis correlates with the release of rab3D. Proc Natl Acad Sci U S A 97 : 1091-5.

246.Van Baelen K, Vanoevelen J, Missiaen L, Rayeymaekers L, Wuytack F (2001) The Gogi PMR1 P-type ATPase of *Caenorhabditis elegans*. Identification of the gene and demonstration of calcium and manganese transport. J. Biol. Chem. 276 : 10683-10691

247.Vanoverberghe K, Mariot P, Vanden Abeele F, Delcourt P, Parys JB, Prevarskaya N. (2003) Mechanisms of ATP-induced calcium signaling and growth arrest in human prostate cancer cells. Cell Calcium. 34 : 75-85.

248.Waldron RT, Short AD, Meadows JJ, Ghosh TK, Gill DL. (1994) Endoplasmic reticulum calcium pump expression and control of cell growth.J Biol Chem. 269:11927-11933.

249.Walker D, De Ward M (1998) Subunit interaction sites in voltage-dependent Ca2+ Channels : role in channel function. TINS 21 : 148-154

250.Wang HG, Pathan N, Ethel IM et al (1999) Ca2+-induced apoptosis through calcineurin dephosphorylation of BAD. Science 284 : 339-343

251.Wasilenko WJ, Cooper J, Palad AJ, Somers KD, Blackmore PF, Rhim JS, Wright GL Jr, Schellhammer PF (1997) Calcium signaling in prostate cancer cells : evidence for multiple receptors and enhanced sensitivuty to bombesin/GRP. Prostate 30 : 167-173

252.Wertz IE, Dixit VM (2000) Characterization of calcium-release activated apoptosis of LNCaP prostate cancer cells. J. Biol. Chem. 275 : 11470-11477

253.West AE, Chen WG, Dalva MB, Dolmetsch RE, Kornhauser JM, Shaywitz AJ, Takasu MA, Tao X, Greenberg ME(2001) Calcium regulation of neuronal gene expression. PROC NATL ACAD SCI U S A 98 : 11024-11031

254.Whitaker MJ, Patel R (1990) Calcium and cell-cycle control. Development 108 : 525-542

255.Wilden PA, Agazie YM, Kaufman R, Halenda SP. (1998) ATP-stimulated smooth muscle cell proliferation requires independent ERK and PI3K signaling pathways. Am J Physiol. 275 : H1209-1215

256.Williams ME., Brust PF, Feldman DH, Patthi S, Simerson S, Maroufi A, McCue AF, Velicelebi G, Ellis SB, Harpold MM (1992) Structure and functional expression of an omega-conotoxin-sensitive human N-type calcium channel. Science 257 : 389-395

257.Wolfe JT, Wang H, Howard J, Garrison JC, Barrett PQ (2003). T-type calcium channel regulation by specific G-protein βγ subunits Nature 424 : 209-213

258.Wolfe JT, Wang H, Perez-Reyes E, Barrett PQ (2002) Stimulation of recombinant $Ca_v3.2$, T-type, Ca^{2+} channel currents by $CaMKII\gamma_C$. J.Physiol. 538 : 343-355

259.Wu FS, Park YC, Roufa D, Martonosi A. (1981) Selective stimulation of the synthesis of an 80,000-dalton protein by calcium ionophores. J. Biol. Chem. 256 : 5309-12.

260.Wuytack F, Raeymaekers L, Missiaen L (2002) Molecular physiology of the SERCA and SPCA pumps. Cell Calcium 32 : 279-305

261.Wyllie AH, Beattie GJ, Hargreaves AD. (1981) Chromatin changes in apoptosis. Histochem J. 13 : 681-92.

262.Xie Q, Zhang Y, Zhai C, Bonnano JA (2002) Calcium influx factor from cytochrome P450 metabolism and secretion-like coupling mechanisms for capacitative calcium entry in corneal endothelial cells. J.Biol.Chem. 277 : 16559-16566

263.Yao Y, Ferrer-Montiel AV, Montal M, Tsien RY (1999) Activation of store-operated Ca2+ current in Xenopus Oocytes requires SNAP-25 but not a diffusible messenger. Cell 89 : 475-485

264.Yoo SH (2000) Coupling of the IP3receptor/Ca^{2+} channel with Ca2+ storage proteins chromogranins A and B in secretory granules.TINS 23 : 424-428

265. Zha J, Harada H, Yang E, Jockel J, Korsmeyer SJ. (1996) Serine phosphorylation of death agonist BAD in response to survival factor results in binding to 14-3-3 not BCL-X(L).Cell. 87 : 619-628.

266.Zhang JF, Randall AD, Ellinor PT, Horne WA, Sather WA, Tanabe T, Schwarz TL, Tsien RW (1993) Distinctive pharmacology and kinetics of cloned neuronal Ca^{2+} channels and their possible counterparts in mammalian CNS neurons. Neuropharmacology 32 : 1075-1088

267.Zhang S, Kim KH (1995) Glucose activation of acetyl-CoA carboxylase in association with insulin secretion in a pancreatic β-cell line. J Endocrinol. 147 : 33-41

268.Zimanyi I, Pessah IN. (1991) Comparison of [3H]ryanodine receptors and Ca^{2+} release from rat cardiac and rabbit skeletal muscle sarcoplasmic reticulum. J Pharmacol Exp Ther. 256 : 938-946.